

1. Report No. NASA CR-72899		2. Government Accession No.		3. Recipient's Catalog No.	
4. Title and Subtitle CYCLE-TESTING OF BORON-FILAMENT-WOUND TANKS				5. Report Date August 1971	
				6. Performing Organization Code	
7. Author(s) R. J. Alfring, E. E. Morris, and R. E. Landes				8. Performing Organization Report No.	
9. Performing Organization Name and Address Aerojet-General Corporation Structural Composites Industries Azusa, California				10. Work Unit No.	
				11. Contract or Grant No. NAS 3-12006	
12. Sponsoring Agency Name and Address National Aeronautics & Space Administration Washington, D. C. 20546				13. Type of Report and Period Covered	
				14. Sponsoring Agency Code	
15. Supplementary Notes Project Manager, R. F. Lark, Chemical Rocket Division, NASA Lewis Research Center, Cleveland, Ohio					
16. Abstract Filament tensile strengths and pressure-strain characteristics for a high-modulus, high-strength, boron-filament-wound/resin-composite pressure vessel were obtained at ambient and cryogenic temperatures, as were cyclic fatigue life relationships and strength retention after pressure cycling and long-term sustained pressurization. Filament tensile strengths as high as 354,000 psi (244,000 N/cm ²) were obtained in vessel burst testing; strains at vessel failure were about 0.4 to 0.5%.					
17. Key Words (Suggested by Author(s))				18. Distribution Statement Unclassified - unlimited	
19. Security Classif. (of this report) Unclassified		20. Security Classif. (of this page) Unclassified		21. No. of Pages 178	
				22. Price* \$3.00	

* For sale by the National Technical Information Service, Springfield, Virginia 22151

FOREWORD

This report is submitted by Aerojet-General Corporation, Structural Composites Industries Division, in fulfillment of the contract. It covers all work on the program, which was conducted from July 1968 to February 1971.

The work was done by the Structural Composites Industries Division of Aerojet under the cognizance of E. E. Morris, Manager of the Filament-Wound Tankage and Structures Department. R. J. Alfring was the Aerojet Program Manager and principal investigator, and was also responsible for vessel fabrication and test liaison. R. E. Landes and R. Molho conducted the pressure-vessel design analysis. N. R. Dunavant and M. Segimoto guided and assisted in winding and curing of the test tanks. Tank testing was conducted by R. F. Hayes, E. Jackson, and A. Taoyama of Aerojet's Mechanical Systems Operations and Quality Control and Test Department. Analysis of test data and all program results was done by E. E. Morris and R. E. Landes, who prepared this report.

Guidance and many helpful suggestions were provided throughout the program by the NASA Project Manager, Raymond F. Lark of the Liquid Rocket Technology Branch, Lewis Research Center.

CONTENTS

	<u>Page</u>
SUMMARY _____	1
I. INTRODUCTION _____	3
II. PRESSURE-VESSEL DESIGN _____	5
A. Design A Vessel Description and Analysis _____	5
B. Design B Vessel Description _____	15
III. FABRICATION	
A. Design A Metal Liner Fabrication _____	17
B. Boron-Filament/Epoxy Resin Preimpregnated Tape _____	18
C. Preparation For Winding _____	19
D. Vessel Winding _____	19
E. Curing _____	21
F. Inspection and Summary of Fabrication Data _____	21
G. Fabrication Problems and Techniques _____	22
IV. TEST PROGRAM	
A. Test Plan, Facility, and Instrumentation _____	27
B. Test Results _____	30
C. Evaluation of Test Results _____	36
V. CONCLUSIONS AND RECOMMENDATIONS _____	43
References _____	46

CONTENTS (cont.)

<u>Table</u>	<u>Page</u>
1 Pressure Vessel Design Criteria _____	47
2 Dimensional and Material Parameters _____	48
3 Weight Analysis _____	49
4 Fabrication Data _____	50
5 Results of Inspection of As-Received Boron/Epoxy Tape _____	54
6 Measurements of Boron Filament Diameters _____	56
7 Test Plan _____	57
8 Single Cycle Burst Test Data _____	58
9 Cyclic Fatigue Loading Test Data _____	60
10 Strength Retained After Sustained Loading Test Data _____	62
11 Pressure Vessel Performance Factors _____	64
 <u>Figure</u>	
1 Design A Pressure Vessel (Engineering Drawing) _____	65
2 Vessel Pressure vs Strain Relationships at Ambient Temperature _____	66
3 Vessel Pressure vs Strain Relationships at Liquid Nitrogen Temperature _____	67
4 Vessel Pressure vs Strain Relationships at Liquid Hydrogen Temperature _____	68
5 Pressure Vessel Stress-Strain Relationships, Longitudinal Direction of Cylinder _____	69
6 Pressure Vessel Stress-Strain Relationships, Hoop Direction of Cylinder _____	70
7 Pressure Vessel Boss (Engineering Drawing) _____	71
8 Design B Vessel (Engineering Drawing) _____	72

CONTENTS (cont.)

		<u>Page</u>
<u>Figure</u>		
9	Pressure Vessel Boss (Engineering Drawing) _____	73
10	Pressure Vessel Test Plug (Engineering Drawing) _____	74
11	Pressure Vessel Test Flange (Engineering Drawing) _____	75
12	Pressure Vessel Test Flange (Engineering Drawing) _____	76
13	Welded Liner (Engineering Drawing) _____	77
14	Pressure Vessel Boss (Engineering Drawing) _____	78
15	Pressure Vessel Doubler Ring (Engineering Drawing) _____	79
16	Metal Liner for Design A Vessels _____	80
17	Longitudinal Winding Boron Filament-Wound Vessel _____	81
18	Intersperced Longitudinal and Hoop Patterns, Boron Filament-Wound Vessel _____	82
19	Circumferential Winding Boron Vessel _____	83
20	Group of Completed Boron Filament-Wound Vessels _____	84
21	Design B Boron Filament-Wound Vessel _____	85
22	View of Head of Vessel B-1 _____	86
23	Boron Prepreg Tape Spool, Showing Poor Packaging _____	87
24	Boron Prepreg Tape Spool, Showing Typical Packaging _____	88
25	Liquid Cryogen Test Facility _____	89
26	Cryogenic Pressure-Test Facility _____	90
27	Location of Instruments on Test Vessels _____	91
28	Instrumentation and Cooling Coil on Pressure Vessel _____	92
29	Post Test Photograph of Tank B-1 _____	93
30	Pressure vs Strain for Tank B-1 _____	94

CONTENTS (cont.)

	<u>Page</u>
<u>Figure</u>	
31 Post Test Photograph of Tank B-3 _____	95
32 Pressure vs Strain for Tank B-3 _____	96
33 Post Test Photograph of Tank B-7 _____	97
34 Pressure vs Strain for Tank B-7 _____	98
35 Post Test Photograph of Tank B-12 _____	99
36 Pressure vs Strain for Tank B-12 _____	100
37 Post Test Photograph of Tank B-4 _____	101
38 Pressure vs Strain for Tank B-4 _____	102
39 Post Test Photograph of Tank B-2 _____	103
40 Pressure vs Strain for Tank B-2 _____	104
41 Post Test Photograph of Tank B-9 _____	105
42 Pressure vs Strain for Tank B-9 _____	106
43 Post Test Photograph of Tank B-5 _____	107
44 Pressure vs Strain for Tank B-5 _____	108
45 Post Test Photograph of Tank B-6 _____	109
46 Post Test Photograph of Tank B-13 _____	110
47 Pressure vs Strain for Tank B-6 _____	111
48 Pressure vs Strain for Tank B-13 _____	112
49 Post Test Photograph of Tank B-10 _____	113
50 Post Test Photograph of Tank B-11 _____	114
51 Pressure vs Strain for Tank B-10 _____	115
52 Pressure vs Strain for Tank B-11 _____	116
53 Post Test Photograph of Tank B-8 _____	117

CONTENTS (cont.)

	<u>Page</u>
<u>Figure</u>	
54 Pressure vs Strain for Tank B-8 _____	118
55 Post Test Photograph of Tank BB-1 _____	119
56 Pressure vs Strain for Tank BB-1 _____	120
57 Pressure vs Strain for Tank BB-2 _____	121
58 Post Test Photograph of Tank BB-2 _____	122
59 Post Test Photograph of Tank BB-11 _____	123
60 Pressure vs Strain for Tank BB-11 _____	124
61 Post Test Photograph of Tank BB-7 _____	125
62 Post Test Photograph of Tank BB-8 _____	126
63 Pressure vs Strain for Tank BB-7 _____	127
64 Pressure vs Strain for Tank BB-8 _____	128
65 Post Test Photograph of Tank BB-9 _____	129
66 Post Test Photograph of Tank BB-10 _____	130
67 Pressure vs Strain for Tank BB-9 _____	131
68 Pressure vs Strain for Tank BB-10 _____	132
69 Post Test Photograph of Tank BB-5 _____	133
70 Pressure vs Strain for Tank BB-5 _____	134
71 Post Test Photograph of Tank BB-6 _____	137
72 Pressure vs Strain for Tank BB-6 _____	138
73 Post Test Photograph of Tank BB-3 _____	141
74 Post Test Photograph of Tank BB-4 _____	142
75 Pressure vs Strain for Tank BB-3 _____	143
76 Pressure vs Strain for Tank BB-4 _____	146

CONTENTS (cont.)

<u>Figure</u>	<u>Page</u>
77 Boron Hoop Filament Stress at Filament-Wound Vessel Failure in Single Cycle Burst Tests vs Temperature _____	149
78 Boron Longitudinal Filament Stress at Filament-Wound Vessel Failure in Single Cycle Burst Tests vs Temperature _____	150
79 Hoop Filament Stress During Cycling vs Cycles to Boron Filament-Wound Vessel Failure _____	151
80 Longitudinal Filament Stress During Cycling vs Cycles To Boron Filament-Wound Vessel Failure _____	152
81 Cyclic Load Level vs Cycles to Boron Filament-Wound Vessel Failure _____	153
82 Strength Retention for Boron Filament-Wound Vessels Under Sustained Pressurization at 70% of Original Strength vs Time at Load _____	154
83 Post Test Vessel Showing Boron and Void Content Specimen Locations _____	155
APPENDIX A - SPECIFICATION FOR ORGANIC-RESIN-PREIMPREGNATED TAPE WITH CONTINUOUS BORON-FIBER BASE FOR USE IN FILAMENT WINDING _____	
	A-1
APPENDIX B - FABRICATION PROCEDURE FOR DESIGN A METAL-LINED BORON FILAMENT-WOUND PRESSURE VESSEL _____	
	B-1
APPENDIX C - FABRICATION PROCEDURE FOR DESIGN B BORON FILAMENT-WOUND PRESSURE VESSEL _____	
	C-1
APPENDIX D - CALCULATED DATA, METHODS AND PROCEDURES _____	
	D-1
Distribution List _____	

CYCLE-TESTING OF BORON-FILAMENT- WOUND TANKS

by R. J. Alfring, E. E. Morris, and R. E. Landes

Aerojet-General Corporation
Structural Composites Industries

SUMMARY

The principal program objective - development of mechanical property data at ambient and cryogenic temperatures for a high modulus boron-filament-wound/resin composite pressure vessel structure - was accomplished.

Designs were generated for 8-in.-(20.3-cm-) dia. by 13-in.-(33.0-cm-) long boron-filament-wound vessels for use as test specimens. Twenty-three vessels were fabricated and tested at ambient and cryogenic temperatures in burst tests, pressure cycling tests to failure, pressure cycling - plus burst tests, and sustained pressurization plus burst tests, with the following results:

- The average hoop filament strength at room temperature in single cycle burst tests was 220,000 psi or 152,000 N/cm² initially, increasing to 264,000 psi or 182,000 N/cm² as boron tape and vessel fabrication techniques improved. The strength level was further increased to 354,000 psi or 244,000 N/cm² at the end of the program, a 50% improvement over initial values.
- Strength increased 17% at liquid hydrogen temperature.
- Results from pressure cycling the vessels to failure seemed independent of test temperature. Fatigue life characteristics were similar to data for glass filament-wound vessels. Cyclic fatigue failures all occurred in the vessel longitudinal filaments, demonstrating the higher efficiency of the circumferential windings.
- A vessel pressure cycled 100 times to 55% of its estimated initial strength at liquid hydrogen temperature showed 84% strength retention when subsequently pressurized to its burst point.
- Sustained pressurization of vessels at 70% of initial strength for periods up to 90 days produced no strength loss.
- Good correspondence was obtained between the expected and measured pressure vs strain characteristics. Strains at burst were about 0.4 to 0.5%, one-tenth of the value for glass-filament-wound vessels.

- The boron vessels were more weight efficient than comparable graphite filament vessels, but of lower strength-to-weight performance than glass filament vessels. The low strain of the boron vessels, however, permits inner metal liners to operate below their yield strength, and thus minimizes problems existing in the higher strain glass filament vessels.

Boron prepreg tape integrity and packaging problems made vessel fabrication difficult initially. Subsequent improvements in tape manufacture, process controls, and packaging at the manufacturer resulted in substantial improvements in the tape processability and in vessel strength performance. Concurrent maturity of vessel winding techniques resulted in a 50% improvement in demonstrated vessel strength.

I. INTRODUCTION

Composite materials are replacing metals in many aerospace structures. Glass-filament-wound composites have already increased the performance of pressurized gas storage vessels and solid-rocket cases by providing significant weight savings. They now promise to extend this success to cryogenic tankage and vessels.

The use of such structures for cryogenic pressure vessels can yield considerable weight savings because composite filamentary materials have a much higher strength for their weight than do metal-tank materials. Test results for 50 metal-lined filament-wound tanks (under Contracts NAS 3-6287, 3-6292, and 3-6297 with the Lewis Research Center of the National Aeronautics and Space Administration) demonstrated the great potential for weight savings in cryogenic use (References 1, 2, and 3). Certain limitations may exist, however, in the application of glass-filament-wound vessels with very thin metal liners for service involving many cycles of pressure loading.

Glass-filament-wound vessels strain approximately 1 to 2% at the design operating pressure and cryogenic temperatures, because of the relatively low modulus and high strength of the glass filaments; when they are pressurized to the burst point at cryogenic temperatures, the ultimate strain is from 3 to 4%. For cryogenic service, metal liners are being used inside the tanks because polymeric materials cannot now provide the necessary leak tightness or required extensibility at low temperatures. Large strains of the glass-filaments at the operating stress, however, cause the thin, lightweight metallic liner to exceed its yield point and plastically deform. Repeated applications of such strains during pressure cycling have presented difficult problems in material selection and the design of compatible liners that can sustain extensive fatigue cycling.

Boron and graphite filaments have high strength-to-weight ratios and 4 to 5 times the tensile modulus of glass filaments, and provide a composite material uniquely suited for use with metal liners in pressure-vessel applications. The use of high-strength, high-modulus, filaments vs. glass filaments greatly reduces the large biaxial strains imposed on liners during vessel pressurization. This results in a high-performance structure. Efficient stress levels can be developed in the boron and graphite filaments at low strains below the elastic limit of high-strength metals. It is thus possible that the problems encountered with metal liners in glass-filament-wound vessels, which must plastically deform, could be alleviated with the use of boron and graphite filaments.

Boron-filament-wound vessels were fabricated and tested under Contract NAS 3-10282 with the Lewis Research Center of the National Aeronautics and Space Administration (Reference 4). The tests provided burst strength performance evaluations under biaxial loading conditions at ambient (75°F or 297°K) and liquid nitrogen (-320°F or 77°K) temperatures, and the data demonstrated the utility and advantages of boron filaments for low-strain service, as well as the desirability of additional development work aimed at generating performance data at ambient to liquid hydrogen -423°F or

20°K) temperatures for vessels subjected to burst, cyclic fatigue, and sustained loading tests.

Accordingly, the program covered by this report was undertaken to develop ambient and cryogenic-temperature mechanical fatigue-property data as well as burst strength and sustained pressure loading effects for high-modulus, high-strength, boron-filament-wound/epoxy-resin composite vessels. Performance evaluations under biaxial loading conditions were made at ambient, liquid nitrogen and liquid hydrogen temperatures using 8-in.-(20.3-cm-) dia. by 13-in.-(33.0-cm-) long vessels. A total of 24 vessels consisting of two configurations were fabricated and tested. Each vessel was instrumented to record, continuously, hoop and longitudinal deflection versus pressure and temperature versus pressure.

II. PRESSURE-VESSEL DESIGN

Test vessels of two slightly different configurations were utilized. The initial configuration had a thin metal liner and was designated as Design A vessels. A later configuration, designated as Design B vessels, was very similar to the Design A vessels except that the membrane liner inside the windings was of elastomeric material. The Design A vessels were tested over a cryogenic temperature range while the Design B vessels were tested at ambient temperature only. The structural analysis and design of these test vessels are described below.

A. DESIGN A VESSEL DESCRIPTION AND ANALYSIS

The metal-lined filament-wound composite structure employed as the test specimen was the 8-in.-(20.3-cm-) dia. by 13-in.-(33.0-cm-) long closed-end cylindrical vessel shown in Figure 1. This type of vessel, fabricated from longitudinally and circumferentially oriented filaments wound over a 0.006-in.-(0.152-mm-) thick Type 304 stainless steel (SS) foil liner, was selected on the basis of experience acquired in previous development efforts (References 1, 3, 4, and 5). The vessel was designed to have a burst pressure of 2500 to 2750 psig (1720 to 1900 N/cm²), considerably higher than the 740 to 915 psig (510 to 630 N/cm²) of the Reference 4 program, which dictated a three-fold increase in vessel filament-wound composite wall thickness. The composite structure was adhesively bonded to the liner to minimize compressive liner buckling during cryogen propellant fill and during strain cycling in the plastic range of the liner. The vessels were designed to achieve a longitudinal-to-circumferential strain ratio of approximately 1 to 1. The design and structural verification of the various vessel components are summarized in the following paragraphs.

1. Design-Allowable Strength

Boron monofilaments are currently exhibiting strengths of about 400,000 to 450,000 psi (276,000 to 310,000 N/cm²); boron-filament strengths determined from testing Naval Ordnance Laboratory (NOL) rings range from 275,000 to 390,000 psi (190,000 to 269,000 N/cm²), depending on ring diameter and thickness, and the test techniques used. The average ultimate boron-filament strength at ambient temperature was 236,000 psi (163,000 N/cm²) in 8-in.-dia. by 13-in.-long (20.3-cm-dia. by 33.0-cm-long) vessels fabricated and tested by Aerojet under Contract NAS 3-10282 (Reference 4). The values obtained were highly consistent (varying only 1.9% from the average) and provide the best basis for vessel design. It was anticipated that improvements in materials and fabrication procedures would increase the filament strength by 10% over these reported values. On this basis, the ambient temperature boron-filament strength level selected for the vessel design was 260,000 psi (179,000 N/cm²) for single-cycle burst conditions.

It is noted here and clarified in greater detail below that the 260,000 psi (179,000 N/cm²) stress value was first applied to the longitudinal filaments as part of the input data in the computer analysis. Since the vessel was designed to fail in the hoop filaments, this value was

subsequently applied to the hoop-filament stress level and the longitudinal-stress level was decreased proportionately.

Two boron-filament-wound vessels at liquid nitrogen temperature under the Reference 4 program exhibited hoop filament stresses of 256,500 and 291,200 psi (176,900 and 200,800 N/cm²) or an average value of 273,800 psi (189,000 N/cm²) (15% higher than the ambient temperature strength level). By applying the 15% increase to the 260,000 psi (179,000 N/cm²) at ambient temperature, a cryogenic design allowable strength of 300,000 psi (207,000 N/cm²) was utilized in the design analysis for the boron filaments under biaxial loading conditions. No design factors were applied in designing the vessels for cyclic loading or for the increased vessel wall thickness requirement. It was expected that these would be determined from the tests and subsequently applied to future vessels designed for cyclic-loading conditions.

2. Computer Programming

Dimensional coordinates of the pressure-vessel heads and other vessel characteristics were defined with the aid of a computer program that analyzed and designed the vessels. Input variables were based on design criteria presented in Table 1. Other dimensional and material parameters are presented in Table 2. The computer program, developed by Aerojet under Contract NAS 3-6292 (Reference 2), analyzed the filament shell by means of a netting analysis, which assumed that stresses are constant along the path of the filaments and that the structural contribution of the resin matrix is negligible. The filament shell and metal shell were combined in the analysis by equating strains in the longitudinal and hoop directions and by adjusting the radius of curvature of the shells to match the combined material strengths at the design pressure. In this case, flexibility in the computer program permitted input of longitudinal-and hoop-composite thickness values, thus obtaining the burst pressures and stress levels corresponding to these values. Adjustments were made in the design to encourage failure to occur in the hoop direction filaments of the cylinder by making the hoop filament stress 10% higher than the longitudinal filament stress. The computer program also defined the filament and metal-shell stresses and strains at zero pressure as well as at the burst pressure, the filament-path length, and the weight and volume of the components and complete vessel. A vessel-weight analysis is presented in Table 3.

Because the computer program contains optional input variables the design vessel-burst pressures at the ambient and cryogenic test temperatures were established on the basis of (1) a hoop-composite thickness of 0.061-in. (0.155-cm) for the boron-filament-wound structure, and (2) single-cycle design-allowable strengths for boron-filament at ambient and cryogenic temperatures. As previously discussed, these strengths were selected after a review of composite-property data for Contract NAS 3-10282

indicated that the strengths of the boron laminates could be increased 10% at ambient temperature by improvements in the processing techniques and that strength level increases of 15% could be expected at liquid nitrogen temperature over the ambient temperature strengths. Filament strengths at liquid hydrogen temperature were assumed to be equivalent to strengths at liquid nitrogen temperature.

Computer outputs were also used in analyzing the liner and boron-composite pressure-strain and stress-strain relationships. Figures 2, 3, and 4 represent the pressure-strain curves of the hoop and longitudinal filaments in the cylindrical section at test temperatures of $+75^{\circ}\text{F}$ (297°K), -320°F (77°K) and -423°F (20°K). Although not clearly evident, it may be noted that the slope of the curves changes at approximately 700 to 800 psi (480 to 550 N/cm^2) because of the plastic strain in the metal liner occurring at this pressure. The initial slope is due to the load carrying capability of the metal liner. As the liner undergoes plastic deformation, the increasing load is supported by the high-modulus filament-wound composite. The two slopes are quite close because of the similarity in the moduli of the metal liner and the boron-composite structure.

Figures 5 and 6 present the stress-strain relationships for the hoop and longitudinal directions in the cylindrical portion of the vessel at test temperatures of $+75^{\circ}\text{F}$ (297°K), -320°F (77°K) and -423°F (20°K).

Although the pressure vessel approaches a balanced design, the computer output shows that stress is slightly higher in the hoop direction of the cylinder in comparison to the stress in the longitudinal direction in the same area; this is the desired condition.

3. Winding-Pattern-Determination

The winding pattern developed for a glass filament-wound pressure vessel requires the application of a specific quantity of glass in a predetermined orientation in order to obtain the desired burst pressure. Within limitations, the number of turns of glass filaments per layer can be increased or decreased with little effort since the individual fibers possess a very small diameter (in the order of 0.0004 in. or 0.010 mm) and can be easily blended or "packed" into adjacent fibers to provide controlled variations in thicknesses for each layer applied.

Each individual high modulus boron fiber possesses a diameter of 0.004 in. (0.10 mm) which makes it rather difficult to pack with adjacent fibers and fabrication is time consuming if a vessel is wound with one fiber. In contrast to the glass fiber-reinforced vessels, the boron-fibers cannot be crowded in a tighter pattern as easily to increase burst pressure. A commercially available preimpregnated tape, 29 filaments in width and one filament in height, was selected to wind the boron-reinforced

vessels. The tape width has a specific finite dimension of 0.125 ± 0.003 in. (0.318 ± 0.008 cm) and subsequent turns are wound exactly adjacent to previously applied turns. The thickness is also a finite dimension (as calculated below) and as a result the vessel burst pressure is a function of the number and orientation of applied boron layers and the geometry of the vessel.

The boron filament-wound vessel had two primary winding patterns: (a) a planar or end-for-end pattern wherein tapes are applied along the cylinder and over the end domes, designed to provide the total strength in the heads and longitudinal strength in the cylindrical section, and (b) a circumferential pattern of tape in the cylindrical section for hoop strength. Longitudinal and hoop winding thicknesses, although more pertinent to the computer programming, are determined below in addition to the longitudinal and hoop winding patterns.

a. Longitudinal Thickness

The longitudinal-composite thickness (t_l) at the equator and in the cylinder of the boron-filament-wound vessel was calculated from an equivalent filament thickness per layer in the direction of the filaments (t_e) for the boron tape. This value was determined by the relation

$$t_e = \frac{A_f N_1 N_2}{w}$$

where

$$A_f = \text{area of single filament} = \pi D_f^2 / 4 \text{ in}^2 \text{ (mm}^2\text{)}$$

$$D_f = \text{diameter of single filament} = 0.004 \text{ in. (0.10 mm)}$$

$$N_1 = \text{number of filaments per tape} = 29$$

$$N_2 = \text{number of tapes per layer} = 1$$

$$w = \text{width of tape} = 0.125 \text{ in. (0.318 cm)}$$

Therefore,

$$t_e = \frac{\pi (0.004)^2 (29) (1)}{(4) (0.125)}$$

$$= 0.00292 \text{ in./layer} \quad (0.074 \text{ mm/layer})$$

The composite thickness per layer was determined from the relationship

$$t_o = t_e / P_{vg}$$

where

$$P_{vg} = \text{amount of boron filament in composite, volume fraction} = 0.535 \text{ (based on desired resin content of 29 wt \%)}$$

Therefore,

$$t_o = 0.00292 / 0.535$$

$$= 0.0055 \text{ in./layer} \quad (0.138 \text{ mm/layer})$$

Knowing that a burst pressure between 2500 and 2750 psi (1720 to 1900 N/cm²) was desired and that previous balanced designed boron vessels with one revolution of longitudinal windings (2 layers) had burst at approximately (750 psi or 517 N/cm²) (Reference 4), it was decided to fabricate the vessels with 3 revolutions (6 layers) with burst pressures approaching the desired 2500 psi (1720 N/cm²) burst value as closely as possible. Therefore, the total longitudinal composite thickness (t_ℓ) was determined as follows

$$t_\ell = N_3 \quad t_o$$

where

$$N_3 = \text{number of longitudinal layers} = 6$$

$$\alpha = \text{angle between filament and meridional direction} = 13 \text{ degrees } (0.227 \text{ rad})$$

Therefore,

$$\begin{aligned} t_\ell &= (6) (0.0055) \\ &= 0.033 \text{ in. } (0.838 \text{ mm}) \end{aligned}$$

b. Hoop Thickness

Based on the previous analyses which indicated that the equivalent composite thickness per layer (t_o) for the boron filament tape was (0.0055 in. or 0.138 mm) then the total hoop composite thickness (t_h) is then

$$t_h = N_4 t_o$$

where

$$N_4 = \text{number of hoop layers} = 11$$

Solving for t_h ,

$$\begin{aligned} t_h &= (11) (0.0055) \\ &= 0.061 \text{ in. } (1.518 \text{ mm}) \end{aligned}$$

c. Longitudinal Winding Pattern

The longitudinal winding pattern was determined by equating the chamber circumference (C) of the longitudinal composite thickness at the neutral axis to the number of side-by-side tape widths required to wind a complete revolution.

Therefore

$$C = \pi D_c \cos \alpha$$

$$= N_5 w$$

where

$$D_c = \text{vessel diameter at longitudinal neutral axis} = 7.879 \text{ in. (20.01 cm)}$$

$$N_5 = \text{number of turns per revolution}$$

Solving for N_5 ,

$$N_5 = \frac{\pi D_c \cos \alpha}{w}$$
$$= \frac{\pi(7.879)(0.974)}{(0.125)}$$

$$= 193 \text{ turns/revolution}$$

d. Hoop Winding Pattern

The hoop winding pattern was determined by the number of tape widths per layer (N_6) required in the cylindrical length (L_c) of the vessel.

Therefore,

$$L_c = N_6 w$$

Solving for N_6 ,

$$N_6 = \frac{L_c}{w}$$

$$= \frac{7.54}{0.125}$$

$$= 60 \text{ tapes per layer}$$

4. Metal Boss Analysis

The metal boss (Figure 7) was fabricated from annealed Type 304 stainless steel having a minimum ultimate strength (F_u) of 70,000 psi (48,000 N/cm²). The boss was to be capable of sustaining the design burst pressure (p_o) of 2500 psig (1720 N/cm²) at ambient temperature. Because the strength of the boss increases much more than the vessel strength at cryogenic temperatures, the design was not critical at the low temperatures.

The required margin of safety selected for the flange shear and bending was 0.25.

Only the most critical section of the boss, located at the base of the flange, was analyzed. Stresses there were determined by using the conservative assumption that the flange is a flat plate with a concentrated annular load and a fixed inner edge (the body). The end-for-end wrap pattern of the longitudinal filaments produces a rigid band around the boss that supports the flange. The load applied (W) is the reaction of the boss flange bearing against the composite structure. The total load is therefore equivalent to the pressure acting over the area within the reaction circle. The diameter at which the load is assumed to act (D_w) was (Reference 6).

$$D_w = (1 + \epsilon_{f,1}) D_o + 2.5 W_1$$

where

$$\epsilon_f = \frac{\sigma_{f,l}}{E_f} = \text{filament strain at ultimate stress, in./in.}$$

$$\sigma_{f,l} = \text{ultimate filament strength} = 260,000 \text{ psi} \\ (179,000 \text{ N/cm}^2)$$

$$E_f = \text{filament modulus} = 55 \times 10^6 \text{ psi} (379 \text{ GN/m}^2)$$

$$W_l = \text{filament winding tape width} = 0.125 \text{ in.} (0.318 \text{ cm})$$

$$D_o = \text{diameter at flange-to-body juncture} = 2.75 \text{ in.} \\ (6.99 \text{ cm})$$

The bending stress at the juncture of the flange and boss (σ_b) was calculated in accordance with formulas for loading on a flat plate (Reference 7).

$$\sigma_b = \beta \frac{22 W}{t^2}$$

where

$$W = \frac{\pi p_b D_w^2}{4}$$

$$\beta_{22} \approx \frac{D_w}{D_o} - 1$$

$$t = \text{flange thickness} = 0.190 \text{ in.} (0.483 \text{ cm})$$

Solving the relationships

$$\epsilon_{f,l} = \frac{\epsilon_{f,l}}{E_f} = \frac{260,000}{55 \times 10^6} = 0.0047 \text{ in./in.}$$

$$D_w = (1 + 0.0047) (2.75) + 2.5 (0.125)$$

$$= 3.063 \text{ in. (7.780 cm)}$$

$$\beta_{22} = \frac{3.063}{2.750} - 1 = 1.11 - 1 = 0.11$$

$$W = \frac{\pi p_b D_w^2}{4} = \frac{\pi (2500) (3.063)^2}{4} = 18,400 \text{ lbf (81,800 N)}$$

$$\sigma_b = \frac{\beta_{22} W}{t^2} = \frac{(0.11) (18,400)}{(0.190)^2} = 56,000 \text{ psi (38,600 N/cm}^2\text{)}$$

The margin of safety is given by

$$M.S. = \frac{F_{tu}}{\sigma_b} - 1 = \frac{70,000}{56,000} - 1 = \underline{\underline{+0.25}}$$

The shear stress in the boss flange is given by

$$\sigma_s = \frac{p_b D_w}{4 t} = \frac{(2500) (3.063)}{(4) (0.190)} = 10,000 \text{ psi (6,900 N/cm}^2\text{)}$$

with

$$F_{tu} = 70,000 \text{ psi (48,000 N/cm}^2\text{)}$$

$$\text{assume } F_{su} = \frac{70,000}{2} = 35,000 \text{ psi (24,000 N/cm}^2\text{)}$$

Then the margin of safety is

$$M.S. = \frac{F_{su}}{\sigma_s} - 1 = \frac{35,000}{10,000} - 1 = \underline{\underline{+2.5}}$$

B. DESIGN B VESSEL DESCRIPTION

The configuration of the Design B test vessel assembly is shown in Figure 8. The filament-wound composite structure design of these vessels, along with the outer diameter of the polar bosses was essentially identical to the Design A vessels; deviations consisted of a reduction in number of hoop layers from 11 to 9, and changes to the longitudinal and hoop layer interspersion sequence.

By use of an elastomeric liner, Design B vessel composite structures were filament-wound over a comparatively rigid plaster mandrel which was removed by an acetic acid washout after curing of the composite. Two types of elastomeric liners were considered. The first was a hand-lay-up of 0.060-in. (0.152-cm) thick uncured rubber over which the preimpregnated boron tape could be filament-wound and cured. The second type of elastomeric liner was an inflatable rubber bag, 0.025-in. (0.102-cm) thick which could be installed after the composite was wound and cured and the plaster mandrel washed-out. This later approach was selected because it allowed the preimpregnated-boron-tape to be wound directly on the plastic mandrel, thus providing a slightly more rigid mandrel than one with the hand-laid-up rubber liner. In the event that unforeseen problems were encountered with the bladder-type liner, the bosses had been designed to allow usage of a hand-laid-up rubber liner with only minor adjustment of the contour of the plaster mandrel to allow for the extra thickness of rubber.

The boss design was maintained externally the same as for Design A but the outer flange dimensions were adjusted to give an inner contour designed for elastomeric liner use rather than the thin flange utilized in the welding of the stainless steel liner assembly. The Design B boss shown in Figure 9 thus becomes a more lightly stressed component in all sections than the comparable Design A boss, which functioned satisfactorily on all Design A vessel tests.

Accordingly, no additional stress calculations were deemed necessary other than an evaluation of the loads on the bolted flange.

In the Design A boss the pressure load was taken by a special test plug which was electron-beam-welded into the boss, with the six screws used only during low pressure helium leak testing of the liner and for attachment of the winding shaft during vessel fabrication. The use of the

inflatable liner for the Design B vessels required different types of test plugs and flanges which are shown in Figures 10, 11, and 12 respectively. These components employ a bolted flange concept during the structural testing of the vessel and the number of bolts was increased from six to twelve.

The highest burst pressure encountered on Design A vessels at ambient temperature was 2000 psig (1380 N/cm^2). Using the "O" ring diameter of 2.246 inches (5.705 cm), the load at pressure was computed as 660 lbf (2900 N) per bolt. The breaking strength for the NAS 1351-3 alloy steel screws is 3110 lbf (13,800 N), giving a margin of safety of 3.71.

III. FABRICATION

Boron-epoxy filament-wound pressure vessels were fabricated generally in accordance with the designs just described. Metal liners of Design A configuration, shown in Figure 13, were made from AISI Type 304 stainless steel by pressure-forming the end domes, machining the polar bosses, rolling a cylindrical section and roll-resistance seam welding the components. These liners were pressurized and overwrapped with longitudinal and circumferential patterns of 0.125-in.-(0.318-cm-) wide boron-epoxy prepreg tape and cured to form the composite structure. Test closures were then electron beam welded into the metal polar bosses of the wrapped and cured vessels. Design B pressure vessels were wrapped directly over a plaster mandrel. An elastomeric bladder was later inserted after cure of the windings and plaster washout to provide the sealant liner to contain the pressurizing medium.

A total of thirteen Design A and eleven Design B pressure vessels were fabricated. All were subsequently tested to failure.

A. DESIGN A, METAL LINER FABRICATION

In pressure-forming the head sections of the liner, 0.006-in.-(0.152-mm-) thick 304 SS foil was sandwiched between multi-steel sheets and forced through a ring using a plug. After heat treatment to relieve stresses introduced in fabrication, the head was removed from the sandwich and trimmed, and the opening for the polar boss was punched.

The polar bosses were machined from 304 SS bar stock in accordance with Figure 14; particular care was exercised to maintain the thickness of the flange. Welding doublers used to join the head to the boss were fabricated from 0.010-in.-(0.254-mm-) thick stainless steel foil in accordance with Figure 15. A slight radius was rolled into each doubler to provide close contact between the head section and the boss flange.

The cylindrical section was rolled from 0.006-in.-(0.152-mm-) thick 304 SS foil and was roll-resistance seam welded to the required diameter.

The liner components were joined by roll-resistance seam welding after being fixed in position by spot welding. The bosses were first welded to the heads, as shown in Figure 13. The doubler (Figure 15) was used over the head to minimize damage to the thin liner and to assure weld integrity and, thus, prevent leakage. The heads were then joined to the cylinder with the aid of a curved electrode inserted through the boss opening. A completed liner is shown in Figure 16.

Two leak checks were made on each tank liner - the first a soap-solution leak test under an internal pressure of 7 psig (4.8 N/cm^2), and the second a helium-leak check with a mass spectrometer at a pressure differential of 20 psia (13.8 N/cm^2). All liners successfully passed the tests.

Following the helium-leak check, the liners were cleaned and etched in accordance with Aerojet Process Standard AGC 1221 which calls for cleaning in a strong solution of $63.0 \pm 6.0\%$ nitric acid and $0.4 \pm 0.001\%$ hydrofluoric acid. Each liner was dried and enclosed in a polyethylene bag until it was prepared for filament winding.

B. BORON-FILAMENT/EPOXY RESIN PREIMPREGNATED TAPE

Boron-epoxy tape 0.125-in.-(0.318-cm-) wide, consisting of 29 single 0.004-in.-(0.10-mm-) dia. filaments collimated in a side-by-side orientation and preimpregnated with epoxy resin was procured from the Narmco Materials Division of the Whittaker Corporation. The tape was made from monofilaments having a minimum average tensile strength of 400,000 psi ($276,000 \text{ N/cm}^2$) and an elastic modulus of 55×10^6 psi (379 GN/m^2).

Prior to selection of the resin matrix and establishment of a procurement specification for the boron-epoxy prepreg tape, a meeting was held with the supplier. The August 1968, state-of-the-art in resin content control, tape width control, and possible steps for tensile strength improvement were reviewed. Suppliers of the boron filament had improved their products strength reproducibility, and the multifilament tape resin impregnation process had been improved as regards resin content and tape width control, but no economical means had been found for obtaining prepreg tape with higher guaranteed tensile strength. Narmco indicated that resin content of the prepreg tape could be held $\pm 2 \text{ wt\%}$ of the nominal value specified.

Consideration was initially given to two prepreg tape materials systems. One of these, known as 5505, was a 26 boron filament, 0.125-in.-(0.318-cm-) tape preimpregnated with a proprietary epoxy resin system. The other, identified as 5501, was a 29 filament, 0.125-in.-(0.318-cm-) wide tape preimpregnated with 58-68R epoxy resin (consisting of Epon 828, Epon 1031, nadic methyl anhydride (NMA), and benzyldimethylamine (BDMA) in the ratio of 50/50/90/0.3 parts by weight). The 58-68R resin system has been widely used in filament-winding programs employing glass roving, and was used previously on the boron filament-wound vessel evaluation program reported in Reference 4 where five similar tanks were fabricated and single-cycle burst-tested at ambient and liquid nitrogen temperatures. The 5505 tape has a wider spacing of the 0.004-in.-(0.10-mm-) dia. boron filaments, and thus better control of the resin to boron filament spacing was claimed to be achievable. However, the 5505 system had not been evaluated cryogenically, and had a viscosity/temperature relationship which could possibly lead to excessive resin flow-out during curing (compared to 5501), which in turn raised the possibility of relaxation of winding tension during cure with attendant composite strength loss. Also, the reduced density of filaments per tape width and increased resin content would require a change in tank design toward more material (and weight) for the design burst pressure of the tank. Accordingly, a decision was made to use the 5501 system for vessel design and

fabrication.

Review of the results from the Reference 4 program lead to a selection of a nominal value for prepreg tape resin content of 29 ± 2 wt%.

Continuous filament splicing frequency control in the prepreg tape was discussed with Narmco to establish limits for material used in fabrication of vessels as follows: no more than three splices in 25 feet (7.62 meters) of tape and no splices closer than two feet (0.60 meter) to one another were adopted as target values.

The prepreg tape procurement specification (AGC-10585, Revision A) is presented in Appendix A. All material used on the program was procured in three lots: one lot (accepted January 1969) for the first thirteen vessels, a second lot (accepted January 1970) for the next ten vessels, and a third lot (accepted September 1970) for the last pressure vessel.

C. PREPARATION FOR WINDING

For the Design A vessels with the thin stainless steel liners, a resin adhesive system was applied to the liner prior to filament winding to insure a bond between the liner and high modulus boron overwrap and to uniformly distribute the biaxial strain from the thin metal liner to the overwrap. The process consisted of cleaning the liner with a paste cleaner, priming it, and applying the adhesive, using a thin nylon scrim cloth over the metal liner to provide a uniform cured adhesive thickness of approximately 0.003-in.(0.0762-mm). Details of the adhesive application process are given in Appendix B.

D. VESSEL WINDING

The tanks were filament-wound using combination longitudinal and hoop-winding machine, according to design requirements established in Task I and the procedures presented in Appendix B.

1. Trial Windings

Filament-winding experiments were performed using an old 8-in.-dia. by 13-in.-long (20.3-cm-dia by 33.0-cm-long) liner and 20-end dry glass roving with differing longitudinal wrap patterns and tape widths to optimize the pattern with respect to minimization of composite buildup in the area of the polar boss. Following this, experiments were conducted with surplus boron multifilament preimpregnated tape to further verify procedures. It was determined from these efforts that two 0.125-in.-(0.318-cm-) wide boron filament prepreg tapes longitudinally wound side-by-side reduced the composite thickness buildup at the polar boss and appeared to produce an acceptable wrap pattern.

2. Winding of Design A Vessels

Prior to vessel winding, the longitudinal pattern was checked out using 20-end glass roving and later boron-prepreg tape until final winding pattern adjustments were made. The winding shaft was installed in the liner, and the liner assembly was mounted in the machine. Two or three plies of No. 112 glass cloth fabric were applied to the liner-weld areas for the fairing in of the lap joints used in the roll-resistance seam welding. A hydraulic pressure technique was used for internal support of the liner during winding and curing.

The filament-wound tank wall consisted of six layers of longitudinal winding and eleven layers of hoop winding. In vessel winding, one revolution (two layers) of boron filament tape (consisting of two side-by-side prepreg tapes) was wound longitudinally along the cylinder and over the end domes, followed by three layers of hoop windings in the cylinder section, running between the tangency planes of the two heads; a single prepreg tape was used for hoop winding. Subsequently, two additional revolutions of longitudinal winding (four layers) were applied, followed by eight more layers of hoop winding to develop the total composite wall thickness. Temperature sensors were wrapped into the vessel at each end of the cylindrical section under the last two hoop layers. Extensometer attachment pins were wrapped into the composite near each end of the cylinder under the last hoop layer, to furnish attachment points for two longitudinal extensometers.

A tension of 6.5 lbf (28.9 N) per tape was used for longitudinal winding, and 10 lbf (44.5 N) per tape for circumferential winding. The finishing end of the hoop winding was tied off by passing it through two loops of 20-end glass-filament roving that was overwrapped with the last three turns of boron-filament tape. The two ends of each glass roving used for the tieoff loops were allowed to protrude, and the final hoop turn of boron was threaded through the glass loops. The final boron-tape turn was then drawn into place; the slack was carefully taken out of the loops by pulling on the protruding glass-roving ends.

Vessel winding is shown in Figures 17 to 19.

Problems encountered in filament-winding and curing of the relatively thick boron filament-wound composite are discussed in Section III-G.

3. Winding of Design B Vessels

Vessel fabrication was essentially as described above with two principal exceptions: (1) the boron filament-wound composite was applied over a plaster mandrel which was subsequently washed out from the wound and cured vessel; (2) two hoop layers were deleted, and the longi-

tudinal (L)/hoop (H) layer interspersion sequence was changed from 2L, 3H, 4L, 8H to 2L, 2H, 2L, 2H, 2L, 5H. Plaster mandrels were swept to contour, oven dried, and then coated to seal the surface. Prefabricated metal bosses, with a rubber layer bonded to the flange surfaces, were positioned on the plaster mandrel and winding shaft assembly. The prepared mandrel, boss, and shaft assembly were then positioned in the winding machine, and the vessel fabricated. The fabrication procedure is presented in Appendix C. Difficulties in fabrication are discussed in Section III-G.

E. CURING

After the last hoop layer was tied off, Design A vessels were cured in accordance with the following schedule:

<u>Part Temperature, °F (°K)</u>	<u>Curing Time, Hours</u>
150 (340)	4
200 (370)	4
250 (390)	2
300 (420)	6

After cure, the vessel was cooled to room temperature at approximately 100°F/hr (56°K/hr) and the finished vessel cleaned in preparation for testing. For the Design A vessels, test closures were electron-beam welded to the vessel polar bosses prior to testing.

Design B vessels were staged during winding, after the first longitudinal revolution, prior to application of the hoop windings and subsequent longitudinal windings.

F. INSPECTION AND SUMMARY OF FABRICATION DATA

All tanks were visually and dimensionally inspected internally and externally prior to testing. For Design A vessels, no liner debonding, wrinkling, or buckling was encountered, but definite diamond-shaped patterns were observed on the inside surface resulting from tension on the longitudinal filaments on the liner. This condition did not affect vessel performance. The Design B vessels had clean and smooth interior surfaces.

A group of completed Design A vessels is shown in Figure 20, and a Design B vessel in Figure 21.

Table 4 presents a summary of pertinent fabrication data obtained from evaluation and analysis of vessel log data sheets and obser-

uations made during tank fabrication. Included in the table are winding pattern details, weights, equivalent filament thicknesses, remarks on fabrication, as well as average filament and void contents in the wound boron-epoxy composite from samples taken from the tanks after testing.

G. FABRICATION PROBLEMS AND TECHNIQUES

1. Boron-Epoxy Prepreg Tape

Winding of initial tanks was delayed by an apparent boron multifilament tape processing problem at the filament supplier, Hamilton Standard Division of United Aircraft. The problem was explained by Narmco as follows:

"The basic cause of the problem is due to a twisting of the monofilaments which occurs during filament manufacture. The cognizant government agency, together with the filament manufacturer and the preimpregnation supplier, have worked several months at resolving the problem and believe that a resolution is near. However, due to the large demand backlog for boron filament and failure to obtain a final resolution to the problem as yet, no firm commitment can be made relative to the delivery of preimpregnated tape for use on this program. The twisted filament causes a concave shape in the cross-section of three-inch widths of tape (made from twenty-four 1/8 in. tapes), which subsequently causes problems in the layup of boron broad-goods. The bending is less severe in 1/8 in. tape and tends to disappear when the tape is tensioned. The 1/8 in. tape produced from the twisted filament probably does not yield degraded material properties and may not cause a major problem in subsequent filament-winding of the pressure vessel."

Further review of the potential problem area indicated that no adverse effects in winding of vessels or in their performance should be anticipated from the filament twist, and that no exceptions would have to be taken to the prepreg procurement specifications. Accordingly, the first lot of material was manufactured and accepted in January 1969 for use in the program for fabrication of Design A vessels.

The boron-epoxy tape used in the program deviated somewhat from objectives defined in the tape procurement specification as regards control of lineal footage in a roll, packaging of tape in a roll, and tape width. For example, the second lot of prepreg, used to fabricate ten of the Design B vessels, was delivered in January 1970 as rolls ranging in length from 700 to 1600 ft (210 to 490 m). The purchase order required the rolls to contain approximately 2000 ft (610 m) in order to eliminate tape splicing during winding and to minimize material waste at the end of the rolls. The shorter length rolls were useable, but required much more roll consumption planning in order to minimize tape splices during winding and to avoid wasting material. During tank winding, as tape was unwound from the roll,

some tape twisting was discovered as well as unexpected ending of the continuous tape and starting of a new end. Five of the 22 rolls were selected for specification verification. The resin content (specified to be 29 ± 2 wt%) averaged 27.7, 28.5, 28.1, 28.9, and 26.0 wt%; data are tabulated in Table 5. The width of the tape was specified to be 0.125 ± 0.003 -in. (0.318 ± 0.008 cm). As shown by the measurements presented in Table 5, the average tape width for each of the five rolls was 0.122 in. (0.310 cm), 0.112 in. (0.284 cm), 0.120 in. (0.305 cm), 0.120 in. (0.305 cm), and 0.127 in. (0.323 cm), and the deviations from specified values did present problems during vessel winding, as subsequently discussed. Some boron filament diameter data are given in Table 6, and were in accordance with the specified limit of 0.004 ± 0.0002 in. (0.102 ± 0.005 mm-) dia.

2. Vessel Winding

a. Design A Vessels

Tank B-1 was fabricated in accordance with the Appendix B fabrication specification. In applying the longitudinal tapes to the vessel heads, a nonuniformity in filament orientation and looseness resulted due to slight twisting and bowing of the width of the prepreg tape (discussed in Section III-G-1). This condition is shown in Figure 22.

Changes in winding technique were incorporated in Tank B-2 to overcome the tape twist problem. One of the two major changes was to invert the boron tape placing the resin rich tape surface against the vessel wall to allow the twisted contour to match, rather than conflict with the cylindrical and head surfaces of the tank. The other change was to apply heat to the tank during winding to cause softening of the prepreg resin and to allow the tape to conform more evenly to the vessel contour. Other minor modifications to the processing were to increase the stepping back of the hoop windings during layer interspersions and to add Cabosil filled 58-68R resin at the edges of the first three hoop wraps prior to application of the second longitudinal revolution to smooth and blend the hoop layer steps. These changes were used in fabrication of subsequent vessels. During vessel hoop winding some monofilament breakage occurred as did some gapping of the hoop winding at the center of the cylinder due to narrow tape width in the prepreg.

Tank B-3 was wrapped without problems.

During winding of the third longitudinal revolution of Tank B-4, the prepreg tape was found to be broken on the spool. A new roll was spliced in for continuing the winding. This was accomplished by backing up the winding pattern about six turns, and starting the winding with a new tape overlapping the last turns of the old tape. During vessel curing, the outer hoop windings at the head-to-cylinder juncture moved off the cylinder section onto the head knuckle area. After cure, the defective areas

were removed from the tank by use of a diamond wheel and a tool post grinder on a lathe. In this operation, the hoop windings were successfully machined away only in the defective area without any damage to the longitudinal windings. The areas were then successfully rewound locally with circumferential windings of boron and cured. Subsequent testing indicated the repair was a success since the failure did not occur in the repaired area.

Tank B-5 was wound without difficulty, except for doubling up of the prepreg tape for 6 to 8 turns in the middle of the fourth hoop layer, causing gapping in the winding pattern.

In winding of Tank B-6's tenth hoop layer, the prepreg tape spool ran out of material halfway across the cylinder section. A new tape was spliced into the winding by backing up the pattern about six turns, starting the new tape by overwinding the last six turns of the old tape, and then completing the winding.

Significant problems were encountered in winding Tank B-7 due to prepreg tape problems. First, in winding the second hoop layer, it was discovered that the boron tape was broken on its spool; a new tape was spliced in with a six turn overlap. During winding of the second longitudinal revolution, another break in the tape on the spool showed up, necessitating another six turn splice. In winding the fifth hoop layer, additional poorly packaged material was uncovered in the roll; see Figure 23. For comparison, typical appearance of the prepreg tape on the spool is shown in Figure 24. After replacement of the poor spool with better material, the tank winding was completed. After winding, the tank was held at room temperature over the weekend under pressure stabilization. On Monday, a bump about $\frac{1}{4}$ -in.-(0.63-cm-) high had formed on one end dome of the vessel from the head-to-cylinder juncture toward the boss area. The vessel was rotated under heat lamps to fully set up the resin prior to starting the final cure cycle. During test, the vessel failed in the locally bulged area. Further analysis indicated that two layers of longitudinal winding had been inadvertently omitted from the winding. Accordingly, the vessel was replaced by Aerojet/SCI at no additional cost to the program.

Tank B-8 was fabricated without incident except for breakage of a prepreg tape during winding of the second longitudinal layer; a six turn splice was used in the region of the broken tape.

Tank B-9 was wrapped without problems.

Tank B-10 had some necking and split tapes in the fourth hoop layers, and Tank B-11 had below average prepreg tape winding in three of its eleven hoop layers.

Tank B-12 had one tape splice in the third longi-

tudinal revolution. Due to short prepreg tape rolls, seven different rolls of tape had to be used in winding the eleven hoop layers; the ends of the tape occurred usually at the ends of the cylindrical section.

In winding of Tank B-13, longitudinal winding tension was reduced from 6.5 to 6.0 lbf (28.9 to 26.7 N) per tape, and hoop winding tension was reduced from 10 to 8 lbf (44.5 to 35.6 N) per tape.

b. Design B Vessels

After a review of the test results from the Design A vessels, it was decided to reduce the relative design stress in the longitudinal filaments and to increase the stress in the hoop filaments by reducing the number of circumferential filament layers from eleven to nine, while holding the number of longitudinal layers fixed at six. This resulted in a circumferential-to-longitudinal stress ratio of about 4:3, and it was believed that this change would result in a lower burst pressure but higher ultimate strength values in the circumferential filaments. In fact, the result of these changes was to cause failure to occur in the hoop filaments in the single cycle burst tests.

During winding of the first Design B tank, BB-1, a problem of loosely spooled prepreg tape was encountered with the second lot of boron-epoxy prepreg tape used on the program, causing damage (consisting side-wise slippage on the roll, overlap of the tape, and tape necking and twisting). The damaged turns of tape were stripped from the vessel and a new roll spliced in, using the technique previously described. The second and third longitudinal revolutions looked satisfactory when initially wrapped in place, but when covered with succeeding longitudinal turns, developed a looseness in the cylindrical section. The balance of the hoop winding was applied without incident. The looseness of the cylindrical section longitudinal windings was attributed to a gathering or "ironing" effect of subsequent revolutions of winding which gathered the looseness in that particular area. It was finally concluded that the reason that this problem did not occur on the Design A vessels was due to the tension created in the windings by the hydraulic support of the metal liner (pressure was increased incrementally as additional layers were wound over the liner). The Design B vessel was wound directly on a plaster mandrel which could not expand to give the tensioning provided by the hydraulic support. Since considerable boron tape had been deposited before the winding problem was encountered and since the amount of hoop windings had been reduced to encourage hoop filament failures, the vessel was completed.

A thorough review of the entire filament-winding process was conducted prior to further winding of Design B vessels. Narmco agreed to rewind with increased tension all rolls of loose prepreg tape to provide a firmer pack. In addition, a secondary capstan was placed in the

winding tension system to reduce the tape tension exerted on the prepreg tape roll during vessel winding. The longitudinal tape payoff system was changed to provide a single payoff roller at the tank for each of the two side-by-side tapes used for longitudinal winding; this change was to provide complete individual tape tension control as it payed off onto the tank. The layer interspersion sequence was changed from 2L, 3H, 4L, 6H to 2L, 2H, 2L, 2H, 2L, 5H. Hoop tension was reduced from 10 lbf (44.5 N)/tape to 6.5 lbf (28.9 N)/tape, the same as was used for the longitudinal tape. Each set of two layers of longitudinal windings plus two or five layers of hoop windings was staged and partially cured by rotating the tank under heat lamps overnight, prior to application of additional windings. The above procedures were used in winding Design B vessels BB-2 to BB-11.

Tanks BB-2, BB-3, and BB-4 were fabricated using the modified and improved processes. The end result of the changes incorporated was a much more uniform and compact wound composite and a considerable reduction in the buildup of the filament-wound composite around the polar bosses. Fabrication of tanks BB-5, BB-6, BB-7, BB-8, BB-9, and BB-10 was accomplished similarly without difficulty or problems. Significantly, the second lot of prepreg tape used, after reprocessing by Narmco, was of much better quality and consistency than the first lot. The improvement was so substantial that when coupled with the fabrication process improvements, no problems were encountered in fabrication of vessels BB-2 to BB-10.

Tank BB-11 was fabricated from a third lot of material, reflecting September 1970 state-of-the-art in boron-epoxy tape production. This vessel is discussed separately, because (1) it was fabricated from a boron-epoxy material two and three-quarter years more mature than the material used for initial vessel fabrication under the contract, (2) it was fabricated using the best processing parameters developed under the contract, (3) it was fabricated without any difficulty, and (4) it achieved the highest strength level obtained in the program.

IV. TEST PROGRAM

The boron filament-wound vessels were tested to determine their burst strengths, cyclic fatigue life, strength retention after cyclic loading, strength retention after sustained pressure loading, and strain vs pressure characteristics. Sixteen vessels were tested at ambient temperature (five of Design A and eleven of Design B). Three Design A tanks were tested at liquid nitrogen temperature (-320°F or 77°K), and five Design A tanks were tested at liquid hydrogen temperature (-423°F or 20°K).

A. TEST PLAN, FACILITY, AND INSTRUMENTATION

1. Test Plan

The test plan for the twenty-four boron filament-wound vessels is given in Table 5. Nine vessels were subjected to single-cycle burst tests: six were tested at ambient temperature, one at liquid nitrogen temperature, and two at liquid hydrogen temperature.

Three vessels were tested in cyclic fatigue to failure between 0 and 80% of single cycle burst pressure, one at ambient temperature, one at liquid nitrogen temperature, and one at liquid hydrogen temperature. Three vessels were tested in fatigue to failure between 0 and 60% of single cycle pressure, three at ambient temperature and one at liquid nitrogen temperature. One other vessel was given 100 pressure cycles to 60% of single cycle burst strength at liquid hydrogen temperature, followed by burst testing.

Two vessels were tested in sustained pressure loading at ambient temperature at 70% of single cycle burst pressure for 30 days and then pressurized to their burst points. Two other vessels were pressurized to the 70% load level for 90 days, and then burst tested.

For burst tests, cyclic fatigue tests, and sustained loading tests, a rate of pressurization that produced a strain of approximately 0.25%/minute in the longitudinal and circumferential directions was used.

Each vessel was equipped with extensometers for strain measurement and thermocouples for measurement of cryogenic temperatures. Data were recorded continuously during testing on internal pressure, exterior-surface temperature (cryogenic tests only), and deflection vs pressure relationships at three points distributed to provide hoop and longitudinal strains. One set of hoop-strain measurements was made at the vessel cylindrical-section center, and two sets of axial-strain measurements were made along the cylinder section.

2. Cryogenic Test Facility

Liquid nitrogen (LN_2) was used to pressurize the vessels

for the -320°F (77°K) tests, and liquid hydrogen (LH_2) for the -423°F (20°K) tests, with the pressurization rate regulated by gas-controlled valves. (Inhibited water was used for pressurization in the room-temperature tests.) The cryogenic-test facility is shown schematically on Figure 25. The test fixture (Figure 26) consisted of a vacuum chamber with provisions for instrument leads and vacuum-jacketed pressurization lines. The chamber interior and exterior were coated with aluminum paint, and a layer of aluminum foil was installed inside to provide additional insulation.

To aid in maintaining minimum test temperatures, the vessels installed in the vacuum chamber were equipped with external cooling coils through which liquid cryogen (nitrogen or hydrogen, as applicable) was flowed at essentially atmospheric pressure. A cylinder of reflective-type insulation was used around the exterior cooling coils. The vacuum chamber was pumped down to 4×10^{-4} mm Hg (5.3 cN/m^2) to assure the required temperatures. The tank temperatures were maintained as low as possible, and thermal equilibrium was obtained before testing was initiated. Thermal equilibrium for liquid nitrogen testing was defined as a vessel flange or skin temperature of -300°F (89°K), or less, with -310°F (83°K), or less, at the vessel outlet vent line. For liquid hydrogen testing, the two temperatures were -400°F (33°K) and -410°F (28°K), respectively.

3. Instrumentation

Temperatures, longitudinal and circumferential strains, and internal pressures were monitored throughout testing; Figure 27 shows the instrument locations.

The electronic and digital equipment used for these measurements was calibrated periodically, against standards traceable to the National Bureau of Standards, by the Metrology Department of Aerojet's Quality Control and Test Division. The calibration records are on file at Aerojet.

Platinum resistance thermometers and copper-constantan thermocouples were used in the LN_2 and LH_2 tests. The measurements were made on the exterior surface near the tangency at one end of the tank. In addition, the temperatures of the cryogenic fluids inside and outside the tank were recorded.

The Aerojet-developed "bow-tie" extensometers were used to make strain measurements. They consist of a piece of beryllium-copper sheet in a configuration that provides two cantilever beams fitted with bonded strain gages. Metal-foil strip, approximately 0.25 in. (0.63 cm) wide, was used to link the beam ends to the gage-length end points. Both the extensometers and the foil strips were positioned against the test-vessel surface. The small deflections of the high-modulus boron-filament-wound tanks required the development of a special bow-tie extensometer configuration that

would accurately measure the low strains encountered.

For girth (hoop) measurements, the thin metal strip was placed around the cylinder and secured to opposite ends of the extensometer; circumferential deflection resulted in a proportional output of the gages on the cantilever beams. For longitudinal-deflection measurements, metal strips were affixed to instrumentation-pin terminals wound into the tank near the ends of the cylindrical section. The strips were run along the cylinder longitudinally toward its center; the cantilever-beam ends were connected to the ends of the strips at the midsection of the tank. A longitudinal deflection produced a proportional strain-gage output. Figure 28 shows the extensometers installed on a test vessel.

The accuracy of the strain gages depends on the gage factor, which is extremely sensitive to cryogenic-temperature variations. To provide the required accuracy, the concept of controlled-temperature strain transduction was employed: Heaters were provided to maintain the gage temperatures within their compensation range, and a sensor was added to record the vessel-surface temperature in the vicinity of the extensometer. This sensor was used to verify that the heat input to the extensometer did not warm the tank surface in the region of the transducer. Thermal insulation was used under the heated extensometers to minimize heat transfer to the vessel. The test data showed that no significant vessel warming was produced.

Before testing, each extensometer was installed on the vessel and shunt calibrated under ambient conditions throughout its anticipated range of deflection. The gage factors did not vary under cryogenic conditions, because the heaters kept the gages essentially at the ambient temperature; monitoring during the cryogenic tests revealed that the gages were usually maintained at $75 \pm 20^\circ\text{F}$ ($297 \pm 11^\circ\text{K}$). Because the gage factor varies only 1% per 100°F (56°K) change in the 75°F (297°K) range, there was negligible loss in accuracy.

To calibrate for longitudinal displacements, the distance between the bow-tie attachment points or terminals (L_2) was carefully measured. The instrument and its metal-strip extensions were then stretched to the maximum expected deflection, using accurately determined positions (ΔL_2). The strain was calculated as $\Delta L_2/L_2$ to indicate the total between the two attachment points. To calibrate the girth extensometer, the tank circumference (L_1) was measured and the bow-tie attachment band was moved to produce the maximum expected deflection (ΔL_1). The girth strain was calculated as $\Delta L_1/L_1$. Calibration was performed under ambient conditions, and a shift in the zero point occurred due to thermal contraction when the tank was cooled to cryogenic levels. To correct for this shift it was only necessary to reset the recorder to zero, because the repeatability under ambient conditions was essentially linear and the heaters maintained ambient temperatures.

B. TEST RESULTS

Test results at ambient, liquid nitrogen, and liquid hydrogen temperatures are summarized in Tables 8, 9, and 10. The tables indicate the type of test each vessel was given, the test temperature, the load level used for fatigue and sustained loading, the pressure cycles achieved, the period of sustained pressurization, the burst pressures, the modes of failure, filament and composite ultimate stresses and strains, and pertinent remarks. Post test photographs and pressure vs strain characteristics are given in Figures 29 to 76. Comments on the individual vessel tests, amplifying data given in the tables and figures are given below.

1. Testing of Design A Vessels

a. Ambient Temperature Tests

(1) Single Cycle Burst

Tank B-1 was hydrostatically pressurized to its burst point of 1669 psig (1150 N/cm²). Failure appeared to originate in the longitudinal filaments of one head at the head-to-cylinder juncture and propagate onto the head. The failed tank is shown in Figure 29. At failure stresses were 200,000 psi (138,000 N/cm²) in the hoop filaments and 190,000 psi (131,000 N/cm²) in the longitudinal filaments. Pressure vs strain data are plotted in Figure 30.

As noted in Section III-G, fabrication difficulties encountered with Tank B-1 were corrected in winding Tank B-3. Tank B-3 was pressurized to its burst point of 1994 psig (1375 N/cm²), a 20% improvement over B-1. Failure was in the longitudinal filaments of the head at the boss and in the cylinder section as shown in Figure 31. At failure, the stresses were 240,000 psi (165,000 N/cm²) in the hoop filaments and 230,000 psi (159,000 N/cm²) in the longitudinal. Figure 32 shows the pressure vs strain data.

A third tank, B-7, was pressurized to its burst point of 1111 psig (766 N/cm²). As noted in Section III-G, significant difficulties were encountered in fabrication of this tank and two (out of six) layers of longitudinal winding were inadvertently omitted from the winding; these factors contributed to the low burst pressure. The failure occurred in the longitudinal filaments of the head (see Figure 33) in the locally bulged area, and extended on the head to the head-to-cylinder juncture. Stresses at failure were only 130,000 psi (90,000 N/cm²) in the hoop filaments and 182,000 psi (125,000 N/cm²) in the longitudinal. Strain data are presented in Figure 34, and reflect the higher longitudinal strains in the tank compared with hoop strains.

(2) Cyclic Fatigue Life

The above burst data were reviewed to establish a typical value for tank single cycle burst pressure which was needed to fix pressure levels for the pressure cycling tests to be conducted at approximately 80 and 60% of single cycle strength. Because the burst pressure for Tank B-7 was not representative, Tank B-1 and B-3's burst pressures of 1669 psig (1150 N/cm²) and 1994 psig (1375 N/cm²) were taken as a representative values of strength and averaged. Tanks were then cycled to failure at an 87% load level (1600 psi or 1100 N/cm²) and a 63% load level (1200 psi or 830 N/cm²).

Tank B-12 was set up for pressure cycling at the 87% level (1600 psig or 1100 N/cm²) and testing started. At the top of the second pressure cycle, the pressure of the tank was held by closing a manual valve in the high-pressure water supply line, in an impromptu attempt to determine if any liner leakage had started as a result of the previous pressure cycle. Another valve in the system was mistakenly opened, and a pressure surge of 1850 psig (1280 N/cm²) was recorded on the tank momentarily before the emergency vent valve was actuated. The tank subsequently failed on the 9th cycle between 0 and 1600 psig (1100 N/cm²) at what is believed to be a premature fatigue point resulting from the surge to 92.5% of the expected single cycle burst pressure. The test set up and procedure were subsequently revised to allow for a safe leak check during cycling for future vessels at 800 psig (550 N/cm²). Tank B-12 failed in the longitudinal filaments of the head at the boss, and the fracture extended to the dome head-to-cylinder juncture (see Figure 35). The peak stresses during cycling were 191,000 psi (132,000 N/cm²) in the hoop filaments and 182,000 psi (125,000 N/cm²) in the longitudinal. Pressure vs strain data are plotted in Figure 36. Strains measured during cycling were close to predicted values. The tank showed permanent set due to the first pressure cycle, and no increase in strain levels during the cycling.

Tank B-4 was fatigue cycled between 0 and the 63% load level until failure occurred in the 430th cycle in the same area of the vessel head as was noted for Tank B-12. During cycling, the peak stresses were 181,000 psi (125,000 N/cm²) in the hoop filaments and 133,000 psi (92,000 N/cm²) in the longitudinal. Figure 37 shows the failed tank, and Figure 38 presents the pressure vs strain data. Permanent set occurred in the tank after the first cycle. During cycling only minor increases in longitudinal strain occurred, while more significant increases occurred in hoop strain as the number of cycles increased. It is interesting to note that this tank had been previously repaired in the hoop winding by machining and locally rewinding and curing a local area of the vessels hoop wound composite cylindrical section, and that the failure did not occur in the repaired area.

b. Liquid Nitrogen Tests

(1) Single Cycle Burst

Tank B-2 was installed in the vacuum chamber and filled with liquid nitrogen. After steady-state conditions were attained, it was pressurized with liquid nitrogen to its burst point of 1760 psig (1210 N/cm^2). This value was lower than anticipated, since the ambient temperature results indicated a single cycle strength potential of about 2000 psig (1380 N/cm^2), and work on the Reference 4 program indicated that a 16% increase in strength should be expected at liquid nitrogen temperature. The failure appeared to originate in the longitudinal filaments of the head, as can be noted from Figure 39. Stresses at failure were 202,000 psi ($139,000 \text{ N/cm}^2$) in the hoop filaments and 183,000 psi ($126,000 \text{ N/cm}^2$) longitudinal. Data obtained on longitudinal and hoop strains are shown in Figure 40. Longitudinal strains were close to predictions, while the hoop strain was less than predicted, and lagged the longitudinal strains.

(2) Cyclic Fatigue Life

The liquid nitrogen single cycle burst strength value described above was reviewed to establish levels for liquid nitrogen temperature pressure cycling tests. After discussions with the NASA program manager, it was decided to use pressures for cycling of 1550 psi (1070 N/cm^2) and 1250 psi (860 N/cm^2) which equate to about 75 and 60%, respectively, of the estimated ultimate tensile strength of the boron-epoxy structure at -320°F (77°K), when previous related test results are considered.

Tank B-9 was prepared for liquid nitrogen testing as already described and pressure cycled between 0 and 1550 psig (1070 N/cm^2), approximately 75% load level, until failure on the 28th cycle, which consisted of general failure of the longitudinal filaments of one head; see Figure 41. Stresses during cycling were 176,000 psi ($121,000 \text{ N/cm}^2$) in the hoop filaments and 157,000 psi ($108,000 \text{ N/cm}^2$) in the longitudinal. Pressure vs strain data are plotted in Figure 42. Vessel permanent set occurred after the first cycle. Measured strains were very close to predictions.

Tank B-5 was pressure cycled between 0 and 1250 psi (860 N/cm^2) at liquid nitrogen temperature until structural failure on the 611th cycle. The failure was located in the longitudinal filaments at the head-to-cylinder juncture. The failed tank is shown in Figure 43 and the pressure vs strain data are given in Figure 44. Stresses during cycling were 139,000 psi ($96,000 \text{ N/cm}^2$) in the hoop filaments and 120,000 psi ($83,000 \text{ N/cm}^2$) in the longitudinal.

c. Liquid Hydrogen Tests

(1) Single Cycle Burst

Tanks B-6 and B-13 were installed in the vacuum chamber and burst tested by pressurizing with liquid hydrogen. Tank B-6 failed at 2305 psig, (1590 N/cm²) and Tank B-13 at 2175 psig (1500 N/cm²); the (130 psi or 90 N/cm²) difference amounts to a \pm 3% variation from the average value of the two burst tests. Tank B-6 stresses at failure were 263,000 psi (181,000 N/cm²) in the hoop filaments and 242,000 psi (167,000 N/cm²) in the longitudinal; stresses of 251,000 psi (173,000 N/cm²) in the hoop filament and 230,000 psi (159,000 N/cm²) in the longitudinal filament were achieved by Tank A-13. Both tanks failed in the longitudinal filaments of the head, with the entire head being blown off the vessel, as shown in Figures 45 and 46. Pressure vs strain data are given in Figures 47 and 48.

(2) Cyclic Fatigue Life

The average vessel burst pressure at liquid hydrogen temperature was 2222 psig, (1532 N/cm²), and Tank B-10 was cycled between 0 and 1880 psig (1300 N/cm²), an 85% load level, and Tank B-11 was cycled at 1580 psig (1090 N/cm²), a 71% load level. Tank B-10 sustained 41 full pressure cycles to the 85% load level before structural failure in the longitudinal filaments of the head (see Figure 49). Tank B-11 achieved 50 cycles at the 71% load level before longitudinal filament failure in one head (see Figure 50). Pressure vs strain data are presented in Figures 51 and 52.

(3) Strength Retention After Fatigue Cycling

Tank B-8 was pressure cycled between 0 and 1360 psi (940 N/cm²), a 61% load level, for 100 cycles, and then pressurized to its burst point of 1920 psig (1320 N/cm²). The vessel after test is shown in Figure 53. Failure occurred in the longitudinal filaments of one head. Peak stresses during cycling were 150,000 psi (103,000 N/cm²) in the hoop filaments and 130,000 psi (90,000 N/cm²) in the longitudinal. Stresses at failure were 220,000 psi (152,000 N/cm²) hoop and 199,000 psi (137,000 N/cm²) longitudinal. Pressure vs strain data are given in Figure 54. Strain values are in close accordance with predictions.

2. Testing of Design B Vessels

All Design B vessel tests were conducted at ambient temperature.

a. Single Cycle Burst

Tank BB-1 was hydrostatically pressurized to its burst point of 1825 psig (1258 N/cm^2). Failure appeared to originate in the hoop filaments of the cylinder, with the fracture extending onto the head area, as shown in Figure 55. At burst, stresses were 276,000 psi ($190,000 \text{ N/cm}^2$) in the hoop filaments and 224,000 psi ($154,000 \text{ N/cm}^2$) in the longitudinal. The strength achieved was 15% higher than for the best Design A vessel burst tested at ambient temperature, and 17% higher than for the thinner walled vessels fabricated and tested under the Reference 4 program. Pressure vs strain data for Tank BB-1 are plotted in Figure 56.

As noted in Section III-G, fabrication problems encountered with Tank BB-1 were minimized in winding subsequent tanks. Tank BB-2 was subjected to single-cycle burst testing and achieved an ultimate pressure of 1668 psig (1150 N/cm^2), which converts to ultimate filament stresses of 252,000 psi ($174,000 \text{ N/cm}^2$) in the hoop and 205,000 psi ($141,000 \text{ N/cm}^2$) in the longitudinal. Pressure vs strain data are given in Figure 57. This vessel also showed a classical hoop failure, with the failure extending into the head area as can be seen in Figure 58. Although Tank BB-2 appeared to be superior, more uniform, and structurally sound when compared to Tank BB-1 (due to the utilization of improved fabrication techniques), it had 9% less strength. The reason for the strength variation in the wrong direction between vessels BB-1 and BB-2 is not known, but can be attributed to strength variation in the preimpregnated boron tape, some adverse effect of the "improved" processing technique, or unknown occurrence during filament-winding and curing.

A third tank, BB-11, the last tank fabricated on the program, utilized prepreg tape of higher quality and more maturity than for the other Design A and Design B vessels. This tank failed at a burst pressure of 2342 psig (1615 N/cm^2) in the hoop filaments with failure extending into the heads (Figure 59), and demonstrated filament ultimate tensile strengths of 354,000 psi ($244,000 \text{ N/cm}^2$) in the hoop filaments and 288,000 psi ($199,000 \text{ N/cm}^2$) in the longitudinal. Pressure vs strain data are plotted in Figure 60.

b. Cyclic Fatigue Life

The single cycle burst pressures of tanks BB-1 (1825 psig or 1258 N/cm^2) and BB-2 (1668 psig or 1150 N/cm^2) were averaged to establish 1746 psig (1204 N/cm^2) as a typical ambient temperature vessel burst pressure. Cyclic fatigue life tests were then conducted at 70% (1225 psig or 845 N/cm^2) and 63% (1100 psig or 758 N/cm^2) load levels.

Tanks BB-7 and BB-8 were fatigue cycled at the 70% load level between 0 and 1225 psig (845 N/cm^2) until failure occurred in the 111th and 46th cycles, respectively. Both vessels failed in the longitudinal filaments of the head in a knuckle area; see Figures 61 and 62. During cycling, peak stresses were 185,000 psi ($128,000 \text{ N/cm}^2$) in the hoop filaments and 151,000 psi ($104,000 \text{ N/cm}^2$) in the longitudinal. Figures 63 and 64 present the vessel pressure vs strain characteristics.

Tanks BB-9 and BB-10 were pressure cycled between 0 and 1100 psig (758 N/cm^2) at the 63% load level. Failure occurred after 6659 and 4901 cycles respectively. Tank BB-9 failed at the tank head-to-cylinder juncture in the longitudinal filaments as can be seen in Figure 65; Tank BB-10 failed in the longitudinal filaments of the head in the dome knuckle area (see Figure 66). Peak stresses during the pressure cycling were 166,000 psi ($114,000 \text{ N/cm}^2$) in the hoop filaments and 135,000 psi ($93,000 \text{ N/cm}^2$) in the longitudinal. Pressure vs strain data are in Figures 67 and 68.

c. Strength Retention After
Sustained Loading

Four vessels, BB-3, BB-4, BB-5, and BB-6 were subjected to sustained pressure loading at 70% (1225 psig or 845 N/cm^2) of the typical ambient temperature ultimate strength level, and then burst tested. During sustained pressurization, stresses were 185,000 psi ($128,000 \text{ N/cm}^2$) in the hoop filaments and 150,000 psi ($103,000 \text{ N/cm}^2$) in the longitudinal.

Tanks BB-5 and BB-6 were pressurized to the 70% load level, which was maintained for 30 days. Only minor pressure fluctuations occurred during the sustained pressure loading, about $\pm 5 \text{ psi}$ ($\pm 3 \text{ N/cm}^2$). After the sustained loading, Tank BB-5 was pressurized to its burst point of 1825 psig (1258 N/cm^2); failure occurred in the hoop filaments of the vessels cylinder. Figure 69 shows the vessel after test. Burst strength of the vessel was equal to the best of the Design B series of vessels (BB-1) subjected to single cycle burst testing (excluding Tank BB-11, which is not considered typical of the Design B series vessels). Pressure vs strain data from the sustained loading and burst testing are given in Figure 70. At the burst pressure, stresses were 276,000 psi ($190,000 \text{ N/cm}^2$) in the hoop filaments and 224,000 psi ($154,000 \text{ N/cm}^2$) in the longitudinal.

Tank BB-6 burst at 2005 psig (1382 N/cm^2) in the hoop filaments of the cylinder after 30 days sustained pressurization at the 70% load level. This value was higher than any achieved with the Design B vessels (except B-11), and stresses were 303,000 psi ($209,000 \text{ N/cm}^2$) in the hoop filaments and 247,000 psi ($170,000 \text{ N/cm}^2$) in the longitudinal. Failure was in the hoop filaments of the cylinder (Figure 71). Pressure vs strain data are shown in Figure 72.

Tanks BB-3 and BB-4 were held at a pressure of 1225 psig (845 N/cm²), a 70% load level, for ninety days and then burst. Tank BB-3 had a burst pressure of 1420 psig (979 N/cm²) with corresponding hoop and longitudinal filament stresses of 214,000 psi (148,000 N/cm²) and 175,000 psi (121,000 N/cm²), respectively, and failed in the area of the knuckle of the head. Tank BB-4 had a burst pressure of 1875 psig (1293 N/cm²) with corresponding hoop and longitudinal filament stresses of 283,000 psi (195,000 N/cm²) and 231,000 psi (159,000 N/cm²), respectively, and failed in the hoop filaments of the cylinder. This result is also higher than for the single cycle burst strength results in BB-1 of 1825 psig (1258 N/cm²) and in BB-2 of 1668 psig (1150 N/cm²). Tanks BB-3 and BB-4 after test are shown in Figures 73 and 74, and pressure vs strain data are presented in Figures 75 and 76.

C. EVALUATION OF TEST RESULTS

1. Test Temperature Effect On Ultimate Filament Strength of Pressure Vessels

Appendix D presents the methods used to arrive at the filament stress equations. For calculations requiring the effect of the thin metal liner (Design A vessels), the liner stresses were assumed to be equal and slightly higher in magnitude than the yield strength of the material at the test temperature. It should be noted that the nonstructural liner used in Design B vessels causes filament stresses to be directly proportional to the applied load (pressure). Results of calculations based on the analysis of Appendix D are recorded in Tables 8 to 10 and evaluated in the discussion that follows.

Hoop and longitudinal filament stresses for all vessels subjected to single cycle burst tests are shown in Figures 77 and 78, respectively, as a function of the test temperature. Inspection of the "mode of failure" data for single cycle burst tests recorded in Tables 8 to 10 indicates that all Design A vessels were longitudinal filament failures, and all Design B vessels were hoop filament failures. Thus, Figure 78 defines the ultimate strength of Design A vessels as a function of temperature, whereas, Figure 77 defines the ultimate strength of Design B vessels (at ambient temperature only). Average ultimate hoop filament strength at ambient temperature in Design B vessels (264,000 psi or 182,000 N/cm²) was 20% higher than hoop filament stresses (220,000 psi or 152,000 N/cm²) at longitudinal filament failure in Design A vessels, due to reduced number of hoop layers, differences in failure modes, and improvements in prepreg tape quality and in vessel winding techniques (Figure 77). As shown in Figure 78, the average longitudinal filament stress of Design B vessels (215,000 psi or 148,000 N/cm²) remained in the same range as the Design A vessels (210,000 psi or 145,000 N/cm²).

One vessel (BB-11), constructed the same as other Design B vessels but of an improved lot of boron prepreg material, exhibited an ultimate filament strength (hoop stress) of 354,000 psi (244,000 N/cm²) with a corresponding longitudinal filament stress of 288,000 psi (199,000 N/cm²). These stress levels indicate a potential 33% increase in vessel strength due to improvements in fabrication raw material alone.

The single Design A data point at the liquid nitrogen (LN₂) test temperature shows a decrease in ultimate filament strength 183,000 psi (126,000 N/cm²) at LN₂ temperature vs 210,000 psi (145,000 N/cm²) at ambient temperature), but this data is definitely not indicative, since other test results (Reference 4) have shown an increase in strength at LN₂ temperature. The only conclusion is that some undetected defect existed in the test specimen.

At the liquid hydrogen (LH₂) test temperature, Figures 77 and 78 indicates a 17% increase in average hoop² filament-stress 257,000 psi (177,000 N/cm²) at LH₂ temperature vs 220,000 psi (152,000 N/cm²) at ambient temperature) and a 12% increase in average ultimate (longitudinal stress) strength 236,000 psi (163,000 N/cm²) at LH₂ temperature vs 210,000 psi (145,000 N/cm²) at ambient temperature. The potential increase in strength of a vessel at LH₂ temperature constructed according to Design B (20% increase) from a lot of material similar to that used in BB-11 (33% increase) is 60%; the corresponding hoop filament stress would be 410,000 psi (283,000 N/cm²).

2. Cyclic Fatigue Life

Hoop and longitudinal filament stresses for all single cycle and cyclic fatigue loading tests are shown in Figures 79 and 80 as a function of the number of cycles to cause failure. Semi-log paper was used to compress the data to one sheet and not necessarily to linearize the data. As noted in the figures all vessels failed in the longitudinal filaments except the three Design B single cycle burst vessels discussed previously. The cryogenic test data has been included with room temperature data resulting in a slight increase in data scatter.

In order to show general effects of cyclic load level on the fatigue life of all vessels tested, independent of design and test temperature, a normalization of the cycle stress levels recorded in Tables 8 and 9 was used. Since all cyclic fatigue failures originated in the longitudinal fibers (No. cycles >1), longitudinal filament stress was chosen as the normalization parameter for fatigue data presentation. Design A longitudinal filament stress normalization is based on average single cycle longitudinal filament failure stresses of 210,000 psi (145,000 N/cm²) at ambient, 183,000 psi (126,000 N/cm²) at LN₂ temperature, and 236,000 psi (163,000 N/cm²) at LH₂ temperature; Design B longitudinal filament stress normalization is based on an average single cycle longitudinal filament stress of 215,000 psi

(148,000 N/cm²) at ambient temperature.

Results of the normalization procedure are shown in Figure 81 which presents number of cycles to failure as a function of cyclic load level. The data appear to be independent of design or test temperature, and the data scatter falls within a cycle load level band width which is approximately $\pm 10\%$. The data trend and scatter is typical of fatigue life curves for both all-metal and filament-wound-composite pressure vessels. Assuming the lower limit of the bandwidth is valid, the minimum fatigue life of boron/epoxy pressure vessels can be established for selected load levels as follows:

<u>Load Level (%)</u>	<u>Minimum Number of Pressure Cycles to Failure</u>
70	40
65	100
60	250
53	1,000
50	1,600
40	10,000

3. Strength Retention After Cyclic Loading

One Design A vessel (B-8) was pressure cycled 100 times to a longitudinal stress level of 130,000 psi (90,000 N/cm²) at a test temperature of -423°F (20°K) and subsequently pressurized until failure occurred in the longitudinal filaments. Based on the average longitudinal single cycle burst strength of 236,000 psi (163,000 N/cm²) for vessels at LH₂ temperature, the normalized cyclic stress level was 55% and the strength retention at burst was 84%. Referring to Figure 81, it is interesting to note that had cycling continued at the 55% stress level the vessel could have sustained an additional minimum of 500 cycles and most probably an additional 4000 cycles.

4. Strength Retention After Sustained Loading

Four Design B vessels were maintained at a 70% of initial strength load level for two periods of time (30 and 90 days) and subsequently pressurized to failure. The hoop and longitudinal filament stresses at failure, recorded in Table 10, were normalized to the corresponding average room temperature single cycle burst filament stresses, thus providing the values for strength retention after sustained load conditions which are shown

in Figure 82. Since the values for strength retention of hoop and longitudinal filaments for each vessel varied only 0.5%, the plot is independent of filament failure mode. Although higher strength retentions are noted at the 30 day period than for the zero time period, all data shown in Figure 82 lies within the expected data scatter range. Thus, the specific load level sustained (70%) for periods up to 90 days appears to have little if any effect on the ultimate strength of vessels.

5. Pressure Vs Strain Characteristics

Vessel pressure vs strain data generally showed strains close to or slightly less than those predicted by the design analysis. Test data were carefully analyzed and checked, and it was concluded that the data were valid. The lower than anticipated strains are believed to be due to the orthotropic behavior of the boron/epoxy composite, and the fact that the netting type analysis used for vessel design analysis assumes no effect on strain from the resin matrix.

6. Pressure Vessel Performance

The pressure vessel performance factors ($p_b V_o / W_c$) shown in Table 11 were computed from measured values for both burst pressure (p_b) and composite weight (W_c) and a computer derived value for internal volume (V_o). As is noted, the units of performance factor were not reduced to the standard in.-lb notation, but instead were retained in the form in.-lb/1bm* to show vessel efficiency by relating the capability of the pressure vessel to store energy (in.-lb or joules) to the container wall weight penalty (1bm or grams).

Average room temperature filament-wound composite burst performance factors were 0.50×10^6 in.-lb/1bm (125 J/g) and 0.56×10^6 in.-lb/1bm (139 J/g) for Design A and Design B vessels, respectively; average performance factors at -320°F (77°K) and -423°F (20°K) were 0.47×10^6 in.-lb/1bm (117 J/g) and 0.63×10^6 in.-lb/1bm (157 J/g), respectively. The highest single value obtained in the program resulted from the room temperature burst of Design B vessel BB-11 which exhibited a performance factor of 0.72×10^6 in.-lb/1bm (179 J/g).

The average efficiency of boron/epoxy pressure vessels tested during this program are compared to the efficiencies of pressure vessels constructed from other composite materials in the table that follows:

* 1×10^6 (in.-lb)/1bm = 249 joules/gram (J/g)

AVERAGE FILAMENT-WOUND COMPOSITE PERFORMANCE FACTOR

Composite Wall Material	Test Temperature					
	Ambient		LN ₂		LH ₂	
	In.-lbf/lbm x 10 ⁻⁶	J/g	In.-lbf/lbm x 10 ⁻⁶	J/g	In.-lbf/lbm x 10 ⁻⁶	J/g
Boron/Epoxy	0.50-0.72	125-179	0.47	117	0.63	157
Graphite/Epoxy (Ref 5)	0.37-0.47	92-117	0.32-0.41	80-102	0.34-0.46	85-115
S-Glass/Epoxy (Ref 8)	0.94-0.96	234-239	1.34	333	-	-

The graphite/epoxy pressure vessels were of the same configuration and size as the boron/epoxy pressure vessels, whereas the S-glass/epoxy vessels had a larger size [12-in.-(30.5-cm-) dia. by 18-in.-(45.7-cm-) long] and corresponding greater internal volume. The performance and weight saving advantage of boron filaments over the various currently available forms of graphite filaments is evident from the table. S-glass filament construction clearly exhibits a marked improvement in efficiency over the temperature range when compared to boron and graphite. The primary disadvantage of S-glass filaments is the high strain levels associated with their high efficiency; these strains greatly tax the capability limits of the thin metal liners (necessary for containment of cryogenics) especially during fatigue cycling. Additionally, there is some evidence that graphite filament-wound composite vessels have relatively minor strength degradation due to fatigue cycling (Reference 9). Work is currently in progress to evaluate this in more detail (Reference 10).

A comparison of the three composite materials, in terms of vessel weight, was obtained by applying the corresponding maximum performance factors to a 500 in.³ (82.0 cm³) vessel (approx. 8-in.-(20.3-cm)-dia. by 12-in.-(30.5-cm)-long designed for a burst pressure of 3000 psig (2070 N/cm²) at room temperature. The resulting weight of the boron/epoxy composite was 2.1 lbm (950g) as compared to a graphite/epoxy composite weight of 3.2 lbm (1450g) and a S-glass/epoxy weight of 1.6 lbm (730 g). The required additional metal hardware weight would be the same for all three types of vessels.

7. Boron and Void Contents in Composite

Several 5/8 in. (1.59 cm) diameter specimens were cut with a hole-saw from the cylindrical section of each vessel subsequent to hydro-burst; Figure 83 shows a typical example of the location of the specimens. For vessels requiring a bond of the composite to the metal liner (Design A vessels), special care was taken to remove all scrim cloth and adhesive system prior to

laboratory analysis. The laboratory procedure and calculations specified in Appendix D were then used to arrive at the void contents and boron contents by weight and volume listed in Table 4.

In order to compare specific vessels within a design (A or B), mean values for boron and void contents were calculated and are shown below with corresponding values for standard deviation:

	<u>Boron Content</u>		<u>Void Content (%)</u>
	<u>Weight %</u>	<u>Volume %</u>	
Design A Vessels			
Mean	72.2	53.9	2.8
Standard Deviation	3.5	4.5	1.5
Design B Vessels			
Mean	68.6	47.7	6.3
Standard Deviation	2.3	2.7	3.3

Generally, Design B vessels exhibited higher void content than Design A vessels which accounts for the lower percentage of boron in Design B vessels. The apparent difference in void content between the two designs may have been caused, in part, by the use of CAB-O-SIL as a filler in Design B vessels.

Comparison of individual values of boron content to the mean value for Design A vessels does not reveal any additional significant information, but several Design B vessels do merit further examination. Vessel S/N BB-1 exhibited very low values for both boron content by weight and void content although the volume content of boron appears normal. Examination of Table 4 indicates a very high total composite weight, yet the amount of prepreg deposited was normal. These facts suggest that an excessive amount of filler material was added to the composite of this vessel, but the quality of the composite was good (well packed, low voids). Since the composite wall was thicker than normal, this caused the composite stresses (Table 8) and the performance factor (Table 11) to be lower than average.

Vessel S/N BB-5, a "30 day sustained load" test vessel, exhibited a high value for void content but normal values for boron content by weight and volume. These values imply a lower quality composite incorporating a normal amount of boron fibers. If void content effects the strength of vessels under sustained load, this particular vessel should have provided an indication of the loss in strength; Figure 82 shows it did not.

Vessel S/N BB-6, the second "30 day sustained load" test vessel, had high values for boron content by weight and by volume and a mean value for void content. Since both boron content values are much greater than the mean value, this implies a thinner (boron rich) composite wall which causes composite stress levels (Table 10) to be greater than the mean.

Vessel S/N BB-9 exhibited a low boron content by volume and a high void content, but the boron content by weight was close to the mean. This is a normal cause (high voids) and effect (low boron volume) condition. Thus, if void content effects the cycling capability of boron composite vessels, this vessel should have provided an indication of the loss; Figure 81 shows it did not.

V. CONCLUSIONS AND RECOMMENDATIONS

A. The principal objective of the program - the development of mechanical property data at ambient and cryogenic temperatures for a high-modulus boron-filament-wound/resin composite pressure vessel structure - was accomplished.

B. The twenty-three 8-in.-(20.3-cm-) dia. by 13-in.-(33.0-cm-) long pressure vessels that were fabricated and tested demonstrated the strength levels attainable with current state-of-the-art boron filament/epoxy resin preimpregnated tape and the strain-vs-pressure characteristics predicted by the design analysis. The following conclusions were drawn from these test results:

1. Vessels were fabricated from three lots of boron/epoxy tape which were procured as the work proceeded; vessel strength improved as subsequent lots of prepreg were used, reflecting both improvement in tape strength and quality, as well as improvement in vessel fabrication techniques.

2. The average hoop filament strength at room temperature in single cycle burst tests for initial vessels was 220,000 psi or 152,000 N/cm² which increased to 264,000 psi or 182,000 N/cm² with the second lot of prepreg tape and improved winding techniques. The single vessel fabricated from the third lot of tape at the conclusion of the program had a hoop filament strength of 354,000 psi or 244,000 N/cm²; this reflects a 50% increase in strength over vessel strength achieved with initial vessels.

3. At liquid hydrogen test temperature, vessel strength increased 17%, which is consistent with values obtained on previous evaluations.

4. In tests where vessels were pressure cycled to failure, the results appeared to be independent of test temperature (ambient, liquid nitrogen, and liquid hydrogen). The data trend was typical of fatigue life characteristics for both all-metal and glass filament-wound vessels, and load level (percentage of single cycle burst strength) vs cycles to failure plotted essentially as a straight line in semi-logarithmic coordinates. The minimum number of cycles to failure vs load level were 40 for 70%, 100 for 65%, 250 for 60%, 1600 for 50%, and 10,000 for 40%. The cyclic fatigue failures all occurred in the vessel longitudinal windings, usually in the vessel dome. It is anticipated that the hoop wound filament cyclic fatigue strength is significantly greater than determined in this program for the longitudinal filaments.

5. One vessel cycle tested 100 times to the 55% load level at liquid hydrogen temperature had a strength retention after cycling of 84% of the single cycle burst strength.

6. Vessels were maintained at 70% of single cycle strength under continuous sustained pressurization at ambient temperatures for periods up to 90 days, and showed no strength decrease (compared with initial single cycle strength) when subsequently pressurized to the burst point.

7. Vessel pressure vs strain characteristics generally were close to or slightly less than predicted behavior. Strains at burst were roughly one-tenth of the value for glass-filament-wound vessels.

8. Pressure vessel performance comparisons showed that the boron vessels had a higher demonstrated weight efficiency than similar graphite filament-wound vessels. Glass filament-wound vessels, however, clearly exhibited a marked weight efficiency improvement based on single cycle strength over boron vessels; the primary disadvantage of the glass filament vessels is the high strain associated with their high efficiency, and attendant problems in metal liner fatigue life capability.

C. Vessel strength improved significantly with improvements in material uniformity and fabrication techniques. Boron prepreg tape integrity and packaging problems made winding of the vessels difficult, and contributed to the lower-than-anticipated vessel quality and strength levels encountered early in the program with the first lot of boron tape used. Subsequent improvements in tape manufacture, process controls, and packaging at the manufacturer resulted in substantial improvements in tape and spool quality and processability, and in vessel strength performance. Additionally, as the prepreg tape quality matured, so did the vessel winding techniques, resulting in a 50% improvement in demonstrated vessel strength in the twenty-third vessel fabricated at the end of the program.

D. The vessels were much stronger in the circumferential windings than in the longitudinal windings. The higher strength efficiency of the hoop windings was demonstrated in both the single cycle burst testing and in the fatigue cycling.

E. The vessels displayed very low biaxial strains and high strength-to-weight ratios. The strains were sufficiently low to permit strong metal liners to work elastically up to the ultimate filament stress. The present strength and potential strength of boron are high enough to ensure that metal-lined, boron-overwrapped vessels will be lighter than competing homogeneous metal tanks for service at ambient to cryogenic temperatures. Additional studies of metal-lined boron filament-wound vessels are recommended to establish design, processing, and performance data. The areas of investigation should include:

1. Strength and cyclic-pressure testing of circumferential boron filament reinforced strong metal shells to demonstrate anticipated improvement in the pure hoop windings as regards strength and fatigue

performance.

2. Optimization studies of boron filament-winding fabrication process and design variables such as winding tension, curing technique (multishell fabrication, pressure curing, etc.) and wall thickness effects on strength.

REFERENCES

1. L. M. Soffer and R. Molho, Cryogenic Resins for Glass Filament-Wound Composites, NASA CR-72114 (Aerojet-General Report under Contract NAS 3-6287), January 1967
2. E. E. Morris, Glass-Fiber-Reinforced Metallic Tanks for Cryogenic Service, NASA CR-72224 (Aerojet-General Report under Contract NAS 3-6292), June 1967
3. A. Lewis and G. Bush, Improved Cryogenic Resin/Glass-Filament-Wound Composites, NASA CR-72163 (Aerojet-General Report under Contract NAS 3-6297), April 1967
4. E. E. Morris and R. J. Alfring, Cryogenic Boron-Filament-Wound Containment Vessels, NASA CR-72330 (Aerojet-General Report under Contract NAS 3-10282), November 1967
5. R. A. Simon and R. J. Alfring, Properties of Graphite Fiber Composites at Cryogenic Temperatures, NASA CR-72652 (NOL Report under NASA Defense Purchase Request C-10360B, dated May 1970)
6. E. E. Morris, Structural Materials Handbook, Aerojet-General Corporation, February 1964
7. R. J. Roark, Formulas for Stress and Strain, (Case 22, Page 201), McGraw-Hill, New York, 1954
8. Unpublished Data, "Cryogenic Filament-Wound Tank Evaluation", Contract NAS 3-10289, Aerojet-General Corporation (work in progress)
9. M. P. Hanson, Tensile and Cyclic Fatigue Properties of Graphite Filament-Wound Vessels at Ambient and Cryogenic Temperatures, NASA TM-X-52539, April 1969
10. "Cycle Testing of Graphite Filament-Wound Vessels", Contract NAS 3-13305, Martin-Marietta Corporation (work in progress)

TABLE 1

PRESSURE VESSEL DESIGN CRITERIA

BORON-FILAMENT-WOUND CRYOGENIC PRESSURE VESSELS FOR CYCLING

Diameter	7.766 in. (19.73 cm)
Length	12.250 in. (31.12 cm)
Polar-boss diameter	2.900 in. (7.37 cm)
Metal-liner thickness	0.006 in. (0.15 mm)
Longitudinal-filament-wound-composite thickness	0.036 in. (0.091 cm)
Hoop-filament-wound-composite thickness	0.061 in. (0.155 cm)
Design burst pressures	
At +75°F (297°K)	2250 psig (1550 N/cm ²)
At -320°F (77°K)	2660 psig (1830 N/cm ²)
At -423°F (20°K)	2700 psig (1860 N/cm ²)

Properties	Type 304 Stainless Steel, Annealed	Boron-Filament-Wound Composite
Density, lbm/in ³ (gm/cm ³)	0.289 (8.0)	0.068 (1.88)
Coefficient of thermal expansion, in/in/°F (μ/°K)	6.760 x 10 ⁻⁶ (12.68)	2.010 x 10 ⁻⁶ (3.618)
Tensile-yield strength, psi (N/cm ²)	38,000 (26,000)	-
Derivative of yield strength with respect to temperature, psi/°F (N/cm ² /°K)	-116.0 (-144.0)	-
Elastic modulus, psi (GN/m ²)	29.4 x 10 ⁶ (203)	55.0 x 10 ^{-6*} (379)
Derivative of elastic modulus with respect to temperature, psi/°F (GN/m ² /°K)	-8030 (-0.0997)	-
Plastic modulus, psi (GN/m ²)	800,000 (5.5)	-
Derivative of plastic modulus with respect to temperature, psi/°F (N/m ² /°K)	-0.1 (-1240)	-
Poisson's ratio	0.295	-
Derivative of Poisson's ratio with respect to temperature, 1/°F (1/°K)	0.0(0.0)	-
Volume fraction of filament in composite	-	0.52
Filament, design allowable stress, ksi (MN/m ²)	Hoop	Longitudinal
At +75°F (297°K)	260.0(1790)	235.0(1620)
At -320°F (77°K)	300.0(2070)	271.0(1870)
At -423°F (20°K)	300.0(2070)	271.0(1870)

* Filament modulus

TABLE 2
 DIMENSIONAL AND MATERIAL PARAMETERS
 BORON-FILAMENT-WOUND CRYOGENIC PRESSURE
 VESSELS FOR CYCLING

Internal Volume, cu. in. (cm ³)	511.3 (8380)
Outside Cylinder diameter, in. (cm)	7.960 (20.22)
Inside diameter of Metal Heads, in. (cm)	7.766 (19.73)
Inside diameter of Metal Cylinder, in. (cm)	7.754 (19.70)
Metal-Liner Thickness, in. (mm)	0.006 (0.15)
Total Composite Cylinder-wall Thickness, in. (cm)	0.097 (0.246)
Longitudinal Wound Composite, in. (cm)	0.036 (0.091)
Hoop Wound Composite, in. (cm)	0.061 (0.155)
Boss-to-Boss Length, in. (cm)	13.16 (33.40)
Cylinder Length (tangent to tangent), in. (cm)	7.23 (18.36)
Forward Boss Outside diameter, in. (cm)	2.90 (7.37)
Aft Boss Outside diameter, in. (cm)	2.90 (7.37)
Liner and Boss Material	Type 304 Stainless Steel (Annealed)
Boron Filaments	(0.004 in. or 0.10 mm) diameter
Tape Type	29-end Prepreg (0.125 in. or 0.318 cm) wide
Resin Matrix	Epon 1031/Epon 828/ MNA/BDMA (50/50/90/0.5)
Liner-to-Composite Adhesive	Adiprene L-100/ Epi-rez 5101/MOCA (80/20/17)

TABLE 3
WEIGHT ANALYSIS
BORON-FILAMENT-WOUND CRYOGENIC
PRESSURE VESSELS FOR CYCLING

	Component		Total	
	<u>lbm</u>	<u>grams</u>	<u>lbm</u>	<u>grams</u>
Composite Structure			1.86	844
Forward Head	0.30	136		
Aft Head	0.30	136		
Cylinder Section	1.26	572		
Metal Hardware			2.04	925
Forward Head	0.12	54		
Aft Head	0.12	54		
Cylinder Section	0.31	141		
Bosses (2)	1.46	662		
Doublers (2)	0.03	14		
Total Vessel			3.90	1769

TABLE 4
FABRICATION DATA
8-IN. DIA. BORON-EPOXY PRESSURE VESSEL

(a) Vessel Serial No.	(b) Winding Pattern	(c) Liner Material	(d) Ancillary Material					Weights (Grams)			(e) Boron Content (%)			Remarks
			(d) Ancillary Material	Prepreg Deposited		Cured Vessel	Composite Material	Weight	Volume	(e) Void Content (%)				
				Longi- tudinal	Hoop						Total			
B-1	A	1041	68	459	384	843	1906	797	66.0	44.4	7.5	Longitudinal winding not uniform due to twisting and bowing of prepreg tape.		
B-2	A	1043	65	650	448	1098	1972	864	71.3	53.0	2.1	Winding process modifications incorporated in this and subsequent tanks consisted of inverting prepreg tape and application of heat to tank during winding.		
B-3	A	1042	68	484	371	855	1994	784	77.0	59.5	3.0	-		
B-4	A	1039	63	522	365	887	1972	870	69.1	51.2	3.1	Hoop filament winding slipped at ends of cylinder during curing. Defective windings removed by machining and rewound with circumferential winding and cured.		
B-5	A	1049	67	518	375	893	1974	858	68.8	50.3	1.8	-		
B-6	A	1038	64	519	360	879	1885	779	74.9	57.4	2.2	-		
B-7	A	1037	76	359	385	744	1734	621	77.1	60.1	2.4	Area of head bulged prior to curing. Fabrication records indicate that two layers of longitudinal winding omitted in tank.		
B-8	A	1031	61	496	393	889	1908	816	72.6	53.6	3.8	-		

- (a) Metal lined pressure vessel fabricated according to Drawing No. 1269206.
 (b) Winding Patterns are described on Sheet 4 of this table.
 (c) Liner weight includes 2 metal bosses and a metal liner.
 (d) Ancillary weight includes bonding materials, extensometer pins, etc.
 (e) See Appendix D for methods of determining values.

TABLE 4 (cont.)

(a) Vessel Serial No.	(b) Winding Pattern	(c) Liner Material	(d) Ancillary Material	Weights (Grams)				(e) Boron Content (%)		(e) Void Content (%)	Remarks
				Prepreg Deposited		Cured Vessel	Composite Material	Weight	Volume		
				Longi- tudinal	Hoop						
B-9	A	1028	61	499	372	871	1859	74.6	56.9	2.3	-
B-10	A	1041	66	478	364	842	1876	75.2	57.5	2.5	
B-11	A	1032	68	500	388	888	1907	73.2	55.8	1.2	-
B-12	A	1032	64	532	378	910	1939	71.5	53.2	2.1	-
B-13	B	1041	73	488	388	876	1975	66.7	47.5	2.7	-

(a) Metal lined pressure vessel fabricated according to Drawing No. 1269206.

(b) Winding patterns are described on Sheet 4 of this table.

(c) Liner weight includes 2 metal bosses and a metal liner.

(d) Ancillary weight includes bonding materials, extensometer pins,

(e) See Appendix D for methods of determining values.

TABLE 4 (cont.)

(a) Vessel Serial No.	(b) Winding Pattern	(c) Liner	(d) Ancillary Material	Weights (Grams)				Composite Material	(e)Boron Content (%)		(e) Void Content (%)	Remarks
				Longi- tudinal	Prepreg Deposited		Cured Vessel		Weight	Volume		
					Hoop	Total						
BB-1	C	863	3	447	322	769	1778	912	64.4	46.0	0.5	Longitudinal filament tapes loose in cylindrical section compared with Design A vessels. Winding process modifications incorporated in subsequent vessels.
BB-2	D	872	2	470	312	782	1660	786	69.3	50.0	3.3	Fabrication process modifications incorporated in this and subsequent vessels consisted of longitudinal tape payoff system improvement, layer inspection sequence changes, winding tension changes, and partial staging of sets of winding during vessel winding.
BB-3	D	881	30	483	290	773	1660	749	68.9	48.9	4.5	-
BB-4	D	885	20	462	304	766	1681	776	66.1	45.3	5.8	-
BB-5	D	875	None	496	295	791	1684	809	69.0	45.1	12.3	-
BB-6	D	875	None	489	274	763	1646	771	73.0	53.1	5.5	-
BB-7	D	875	2	505	297	802	1700	823	71.7	50.1	8.3	-
BB-8	D	875	2	474	303	774	1660	786	68.1	47.2	6.1	-
BB-9	D	878	2	473	300	773	1700	824	66.6	43.4	10.8	-
BB-10	D	885	2	460	388	848	1719	832	68.2	46.3	8.3	-
BB-11	D	889	2	452	291	743	1646	755	69.2	49.8	3.5	Vessel fabricated from the third lot of prepreg material.

(a) Rubber bladder lined vessel fabricated according to Drawing No. 1269187.

(b) Winding patterns are described on Sheet 4 of this table.

(c) Liner weight includes 2 metal bosses.

(d) Ancillary weight includes 112 glass cloth and extensometer pins.

(e) See Appendix D for methods of determining values.

TABLE 4 (cont.)

FILAMENT WINDING PARAMETERS									
Pattern Designation	A		B		C		D		
Number of Layers									
Hoop	11		11		9		9		
Longitudinal	6		6		6		6		
Total	17		17		15		15		
(a) Layer Sequence	2L,3H,4L,8H		2L,3H,4L,8H		2L,3H,4L,6H		2L,2H,2L,2H,2L,5H		
(b) Equivalent Filament Thickness									
Hoop	in	cm	in	cm	in	cm	in	cm	
Longitudinal	0.0309	0.0785	0.0309	0.0785	0.0253	0.0643	0.0253	0.0643	
	0.0169	0.0429	0.0169	0.0429	0.0169	0.0429	0.0169	0.0429	
(c) Wrap Tension Per Tape	lbf/in		lbf/in		lbf/in		lbf/in		
Hoop	10.0		8		10.0		6.5		
Longitudinal	6.5		6		6.5		6.5		
	17.5		14.0		17.5		11.4		
	11.4		10.5		11.4		11.4		

(a) Refers to interspersions of hoop (H) and longitudinal (L) layers.

(b) Calculated values from Appendix D.

(c) Average tape width is 0.125 in (0.318 cm).

TABLE 5

RESULTS OF INSPECTION OF AS-RECEIVED BORON/EPOXY PREPREG TAPE

Roll Number	RESIN CONTENT			Specimen Number	TAPE WIDTH						
	Specimen Number	Resin Content, Wt%	Manufacturer's Measured Resin Content Wt%		Minimum		Average		Maximum		
					in	cm	in	cm	in	cm	
15	15-1	19.76		15-1	0.120	0.305	0.122	0.310	0.128	0.325	
	15-2	21.50		15-2	0.122	0.310	0.122	0.310	0.124	0.315	
	15-3	22.13		15-3	0.120	0.305	0.124	0.315	0.130	0.330	
	15-4	22.99									
	15-5	26.53									
	15-6	27.29									
	Average	23.36		30	Average	0.120	0.307	0.122	0.312	0.127	0.323
16	16-1	27.69		16-1	0.110	0.279	0.118	0.300	0.118	0.300	
	16-2	27.80		16-2	0.106	0.269	0.108	0.274	0.110	0.279	
	16-3	29.95		16-3	0.108	0.274	0.110	0.279	0.112	0.284	
	Average	28.48		31	Average	0.108	0.274	0.112	0.284	0.113	0.287
	17-1	28.54		17-1	0.122	0.310	0.122	0.310	0.124	0.315	
17	17-2	29.83		17-2	0.112	0.284	0.120	0.305	0.122	0.310	
	17-3	26.04		17-3	0.116	0.295	0.118	0.300	0.125	0.318	
	Average	28.13		28	Average	0.117	0.297	0.120	0.305	0.124	0.315

TABLE 5 (cont.)

Roll Number	RESIN CONTENT			TAPE WIDTH						
	Specimen Number	Resin Content, Wt%	Manufacturer's Measured Resin Content Wt%	Specimen Number	Minimum		Average		Maximum	
					in	cm	in	cm	in	cm
18	18-1	27.05		18-1	0.116	0.295	0.124	0.314	0.125	0.318
	18-2	30.53		18-2	0.116	0.295	0.118	0.300	0.128	0.325
	18-3	28.98		18-3	0.118	0.300	0.118	0.300	0.125	0.318
	<u>Average</u>	<u>28.85</u>	31	<u>Average</u>	<u>0.117</u>	<u>0.297</u>	<u>0.120</u>	<u>0.305</u>	<u>0.126</u>	<u>0.320</u>
20	20-1	26.28		20-1	0.125	0.318	0.126	0.320	0.138	0.351
	20-2	26.77								
	20-3	24.88		20-3	0.126	0.320	0.128	0.325	0.144	0.366
	<u>Average</u>	<u>25.97</u>	30	<u>Average</u>	<u>0.126</u>	<u>0.319</u>	<u>0.127</u>	<u>0.323</u>	<u>0.141</u>	<u>0.358</u>

TABLE 6
MEASUREMENTS OF BORON FILAMENT DIAMETERS TAKEN FROM
THREE ROLLS OF BORON/EPOXY PREPREG TAPE USED IN
WINDING TANK BB-2

Filament Sample Number	Filament Diameter					
	Roll Number 10		Roll Number 18		Roll Number 20	
	Mils	mm	Mils	mm	Mils	mm
1	3.90	0.099	3.90	0.099	3.90	0.099
2	4.00	0.102	3.85	0.098	3.75	0.095
3	3.80	0.097	3.85	0.098	4.05	0.103
4	4.00	0.102	3.80	0.097	3.80	0.097
5	4.00	0.102	3.85	0.098	4.05	0.103
6	3.80	0.097	3.95	0.100	4.00	0.102
7	3.90	0.099	4.00	0.102	4.00	0.102
8	3.85	0.098	4.05	0.103	4.00	0.102
9	3.90	0.099	3.90	0.099	3.95	0.100
10	3.85	0.098	4.10	0.104	3.85	0.098
Average	3.90	0.099	3.93	0.100	3.94	0.100

TABLE 7

TEST PLAN

Test Description	Vessel Serial Numbers For Each Design			
	+75°F (297°K) Design A	Design B	-320°F (77°K) Design A	-423°F (20°K) Design A
Single cycle burst	B-1, B-3, B-7	BB-1, BB-2, BB-11	B-2	B-6, B-13
Cyclic fatigue to failure at 80% of single cycle burst strength	B-12		B-9	B-10
Cyclic fatigue to failure at 70% of single cycle burst strength	-	BB-7, BB-8	-	B-11
Cyclic fatigue life to failure at 60% of single cycle burst strength	B-4	BB-9, BB-10	B-5	-
Cyclic fatigue for 100 cycles at 60% of single cycle burst strength, then pressurize to burst point	-		-	B-8
Sustained loading for 30 days at 70% of single cycle burst strength, then pressurize to burst point	-	BB-5, BB-6	-	-
Sustained loading for 90 days at 70% of single cycle burst strength, then pressurize to burst point	-	BB-3, BB-4	-	-
Subtotals	5	11	3	5

No. of Design A Vessels = 13

No. of Design B Vessels = 11

Total No. of Vessels = 24

TABLE 8

SINGLE CYCLE BURST TEST DATA

Pressure(1) Vessel	Test Temperature		Ultimate Strain		Burst Pressure		Fiber Stress (2)				Composite Stress (2)				Location of Failure	Remarks
	°F	°K	Hoop, %	Long, %	psig	N/cm ²	ksi	MN/m ²	Hoop, ksi	MN/m ²	ksi	MN/m ²	Hoop, ksi	Long, MN/m ²		
B-1	75	297	0.261	0.326	1669	1151	200	1380	190	1310	89	610	80	550	Longitudinal filaments at head-to-cylinder junction and head	
B-3	75	297	0.414	0.370	1994	1375	240	1650	230	1590	143	990	130	900	Longitudinal filaments of head at boss and hoop filaments of cylinder	
B-7	75	297	0.201	0.277	1111	766	130	900	182	1250	78	540	104	720	Longitudinal filaments of head at boss extending to head-to-cylinder junction.	Failure occurred in knuckle area where specimen was deformed during cure, and must be considered premature failure. Fabrication records indicate that one revolution (2 layers) of longitudinal winding inadvertently not included in the chamber. Longitudinal stresses based on 4 layers rather than 6 prescribed layers.

(1) "B" series pressure vessels were metal lined. "BB" series were tested using an elastomeric bladder.

(2) See Appendix D for equations and sample calculations.

TABLE 8 (cont.)

Pressure(1) Vessel	Test Temperature		Ultimate Strain		Burst Pressure		Fiber Stress (2)		Composite Stress (2)		Location of Failure	Remarks
	°F	°K	Hoop, %	Long, %	psig	N/cm ²	ksi	MN/m ²	ksi	MN/m ²		
BB-1	75	297	0.253	0.287	1825	1258	276	1900	127	880	Hoop filament fracture extending into head	
BB-2	75	297	0.320	0.324	1668	1150	252	1740	126	870	Hoop filament fracture extending into head	
BB-11	75	297	0.479	0.438	2342	1615	354	2440	176	1210	Hoop filament fracture extending into head	
B-2	-320	77	0.305	0.332	1760	1214	202	1390	183	1260	General failure in longitudinal filaments of head.	
B-6	-423	20	0.455	0.420	2305	1565	263	1810	151	1040	Longitudinal filaments of head. One head blown off, and other head crushed.	
B-13	-423	20	0.395	0.300	2175	1500	251	1730	119	820	Longitudinal filaments of head. One head blown off and other head crushed.	

(1) "B" series pressure vessels were metal lined. "BB" series were tested using an elastomeric bladder.

(2) See Appendix D for equations and sample calculations.

TABLE 9

CYCLIC FATIGUE LOADING TEST DATA

Pressure(1) Vessel	Test Temperature °F °K	Load Level			Fiber Stress (2)				Composite Stress (2)				Cycles to Failure	Location of Failure	Remarks
		% Ult. Burst Pressure	Pressure Level		Hoop,		@ Cyclic Load Level		Hoop,		Long,				
			psi	N/cm ²	ksi	MN/m ²	ksi	MN/m ²	ksi	MN/m ²	ksi	MN/m ²			
B-12	75 297	~ 87	1600 1100	191	1320	182	1250	102	700	92	630	9	Longitudinal filaments of head at boss extend- ing to head-to-cylinder junction.	Tank inadvertently subjected to 1850 psig (1280 N/cm ²) over- pressurization on second pressure cycle.	
BB-7	75 297	~ 70	1225 845	185	1280	151	1040	93	640	72	500	111	Longitudinal filaments at knuckle of head.	Failed at 1198 psig (826 N/cm ²) on 111th cycle.	
BB-8	75 297	~ 70	1225 845	185	1280	151	1040	87	600	68	470	46	Longitudinal filaments at knuckle of head.	Failed at 1208 psig (833 N/cm ²) on 46th cycle.	
B-4	75 297	~ 63	1200 830	181	1250	133	920	93	640	65	450	430	Longitudinal filaments of head at boss extend- ing to head-to-cylinder junction.		
BB-9	75 297	~ 63	1100 760	166	1140	135	930	72	500	56	390	6659	Longitudinal filaments at head-to-cylinder junction.		
BB-10	75 297	~ 63	1100 760	166	1140	135	930	77	530	59	410	4901	Longitudinal filaments at knuckle of head.		

(1) "B" series pressure vessels were metal lined. "BB" series were tested using an elastomeric bladder.

(2) See Appendix D for equations and sample calculations.

TABLE 9 (cont.)

Pressure(1) Vessel	Test Temperature		Load Level			Fiber Stress (2)				Composite Stress (2)				Cycles to Failure	Location of Failure	Remarks
			% Ult. Burst Pressure	Pressure psig	Pressure N/cm ²	Hoop,		@ Cyclic Load Level		Hoop,		Long				
						ksi	MN/m ²	ksi	MN/m ²	ksi	MN/m ²	ksi	MN/m ²			
B-9	-320	77	~ 75	1550	1070	176	1210	157	1080	100	690	85	590	28	General failure in longitudinal filaments of head.	
B-5	-320	77	~ 60	1250	860	139	960	120	830	70	480	57	390	611	Longitudinal filaments at head-to-cylinder juncture.	
B-10	-423	20	~ 85	1880	1300	215	1480	194	1340	124	850	106	730	41	Longitudinal filaments of head. One head blown off.	Some necking and splitting of tape during winding.
B-11	-423	20	~ 71	1580	1090	178	1230	157	1080	99	680	83	570	50	Longitudinal filaments of head. One head blown off.	Poor prepreg hoop layer.

(1) "B" series pressure vessels were metal lined. "BB" series were tested using an elastomeric bladder.

(2) See Appendix D for equations and sample calculations.

TABLE 10

STRENGTH RETAINED AFTER SUSTAINED LOADING TEST DATA

Pressure(1) Vessel	Test Temperature		Prior Loading					Burst Pressure		(2) Fiber Stress @ Failure				(2) Composite Stress				Location of Failure	Remarks
			% Ult. Burst Pressure	Pressure Mode	Pressure Level		Hoop, ksi			Long, ksi	Hoop, MN/m ²	Long, MN/m ²	Hoop, ksi	Long, ksi	Hoop, MN/m ²	Long, MN/m ²			
					psig	N/cm ²											psig		
B-8	-423	20	~ 61	100 pressure cycles to 55% of ultimate longitudinal filament strength	1360	938	1920	1320	220	1520	199	1370	118	810	101	700	Longitudinal filaments of head.	Fiber stress @ cyclic load level; Hoop 150 ksi (1030 MN/m ²) Long. 130 ksi (900 MN/m ²)	
BB-5	75	297	~ 70	30 days sustained pressure loading at 70% of ultimate strength	1225	845	1825	1258	276	1900	224	1540	124	850	96	660	Hoop filament of cylinder.	Fiber stress @ sustained load level; Hoop 185 ksi (1280 MN/m ²) Long 150 ksi (1030 MN/m ²)	
BB-6	75	297	~ 70	30 days sustained pressure loading at 70% of ultimate strength	1225	845	2005	1382	303	2090	247	1700	161	1110	125	860	Hoop filaments of cylinder.	Fiber stress @ sustained load level; Hoop 185 ksi (1280 MN/m ²) Long 150 ksi (1030 MN/m ²)	

(1) "B" series pressure vessels were metal lined. "BB" series was tested using an elastomeric bladder.

(2) See Appendix D for equations and sample calculations.

TABLE 10 (cont.)

Pressure(1) Vessel	Test Temperature °F °K		Prior Loading			Burst Pressure psig N/cm ²			(2) Fiber Stress @ Failure				(2) Composite Stress				Location of Failure	Remarks		
									Pressure Level psig N/cm ²		Hoop, ksi MN/m ²		Long, ksi MN/m ²		Hoop, ksi MN/m ²				Long, ksi MN/m ²	
BB-3	75	297	~ 70	90 days sustained pressure loading at 70% of ultimate strength	1225	845	214	1480	175	1210	105	720	81	560	Knuckle of head.	Fiber stress @ sustained load level: Hoop 185 ksi (1280 MN/m ²) Long 150 ksi (1030 MN/m ²)				
BB-4	75	297	~ 70	90 days sustained pressure loading at 70% of ultimate strength	1225	845	283	1950	231	1590	128	880	99	680	Hoop fila- ments of cylinder	Fiber stress @ sustained load level: Hoop 185 ksi (1280 MN/m ²) Long 150 ksi (1030 MN/m ²)				

(1) "B" series pressure vessels were metal lined. "BB" series was tested using an elastomeric bladder.

(2) See Appendix D for equations and sample calculations.

TABLE 11

PRESSURE VESSEL PERFORMANCE FACTORS(1)

Test Temperature	S/N	Burst Pressure, P_b (psi)		Composite Weight, W_c (grams)		Performance, PbV_o/W_c			
						Specific Vessel		Average for Series	
						in-lbf/lbm $\times 10^{-6}$	J/g	in-lbf/lbm $\times 10^{-6}$	J/g
75°F (297°K)	B-1	1669	1151	797	1.76	0.485	121		
	B-3	1994	1375	784	1.73	0.589	147		
	B-7(2)	1111	766	621	1.37	0.414	103		
	Average							0.496	124
	BB-1	1825	1258	912	2.01	0.464	116		
-320°F (77°K)	BB-2	1668	1150	786	1.73	0.493	123		
	BB-11(3)	2342	1615	755	1.66	0.721	180		
	Average							0.559	139
	B-2	1760	1214	864	1.90	0.473	118	0.473	118
	B-6	2270	1565	779	1.72	0.674	168		
-423°F (20°K)	B-13	2175	1500	861	1.90	0.585	146		
	Average							0.630	157

Notes:

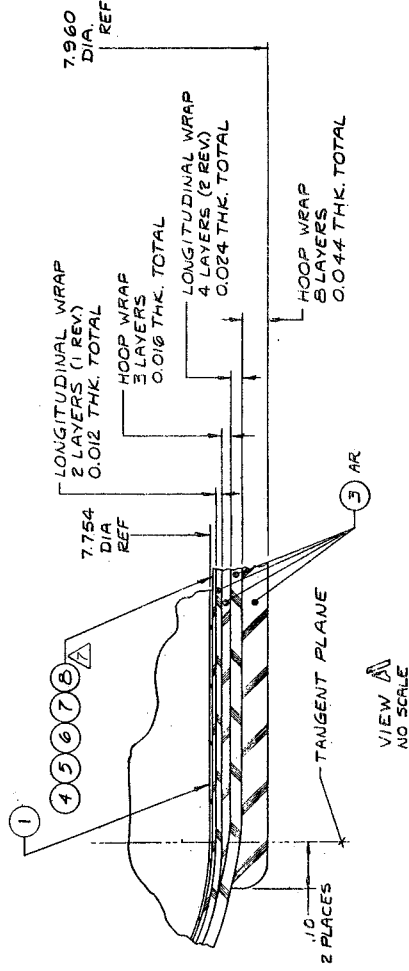
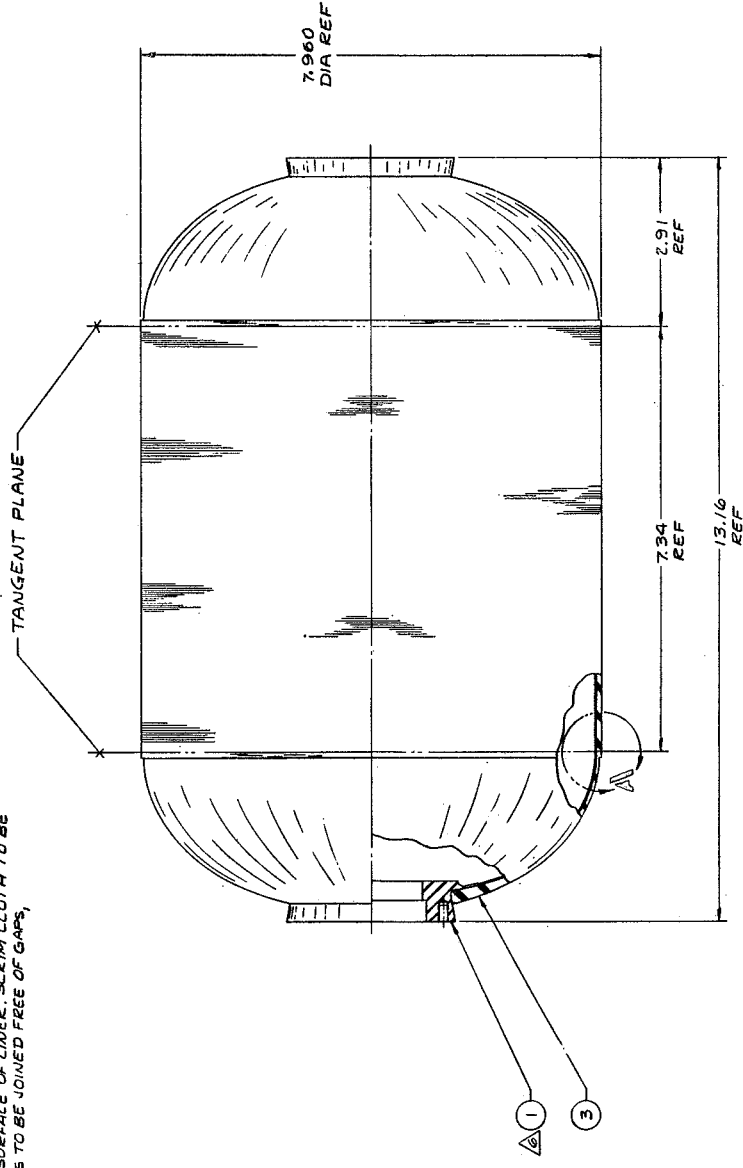
- (1) Internal volume, $V_o = 511 \text{ in.}^3$ (8380 cm^3)
- (2) Vessel missing one longo rev
- (3) Fabricated from different lot of prepreg material

FOLDOUT FRAME

FOLDOUT FRAME 2:

NOTES:

1. FABRICATE PRESSURE VESSEL IN ACCORDANCE WITH FABRICATION PROCEDURE PROVIDED BY ENGINEERING
2. WINDING TENSION: 5 LBS PER 0.125 IN-WIDE TAPE
3. WINDING PATTERN: LONGITUDINAL: 3 REVOLUTIONS 153 TURNS + 1 TURN FOR "16-OFF" ; 0.125-IN-WIDE TAPE GO TURNS PER LAYER IN 7.54-IN LENGTH ; 0.125-IN-WIDE TAPE CIRCUMFERENTIAL: 11 LAYERS
4. CURE CYCLE: 2 HRS AT 200° F, 2 HRS AT 250° F, 12 HRS AT 300° F.
5. IN LIST OF MATERIALS, B IN SYMBOL COLUMN DENOTES BULK MATERIAL.
6. ACID ETCH LINER AND RINSE WITH TAP WATER TO WATER BREAK-FREE SURFACE. DRY IN OVEN AT 160° F, PRIME WITH ITEM 5 AND AIR DRY FOR 30 MINUTES.
7. APPLY ONE LAYER OF ITEM 4, SCREAM CLOTH (SCOURED & HEAT SET) SATURATED WITH ITEM 6, 7 & 8, ADHESIVE MIXED IN RATIO OF 80/10/10 PARTS BY WEIGHT ON OUTSIDE SURFACE OF LINER. SCREAM CLOTH TO BE FREE OF WRINKLES, AND EDGES TO BE JOINED FREE OF GAPS, OVERLAP, OR WRINKLES.

[illegible]

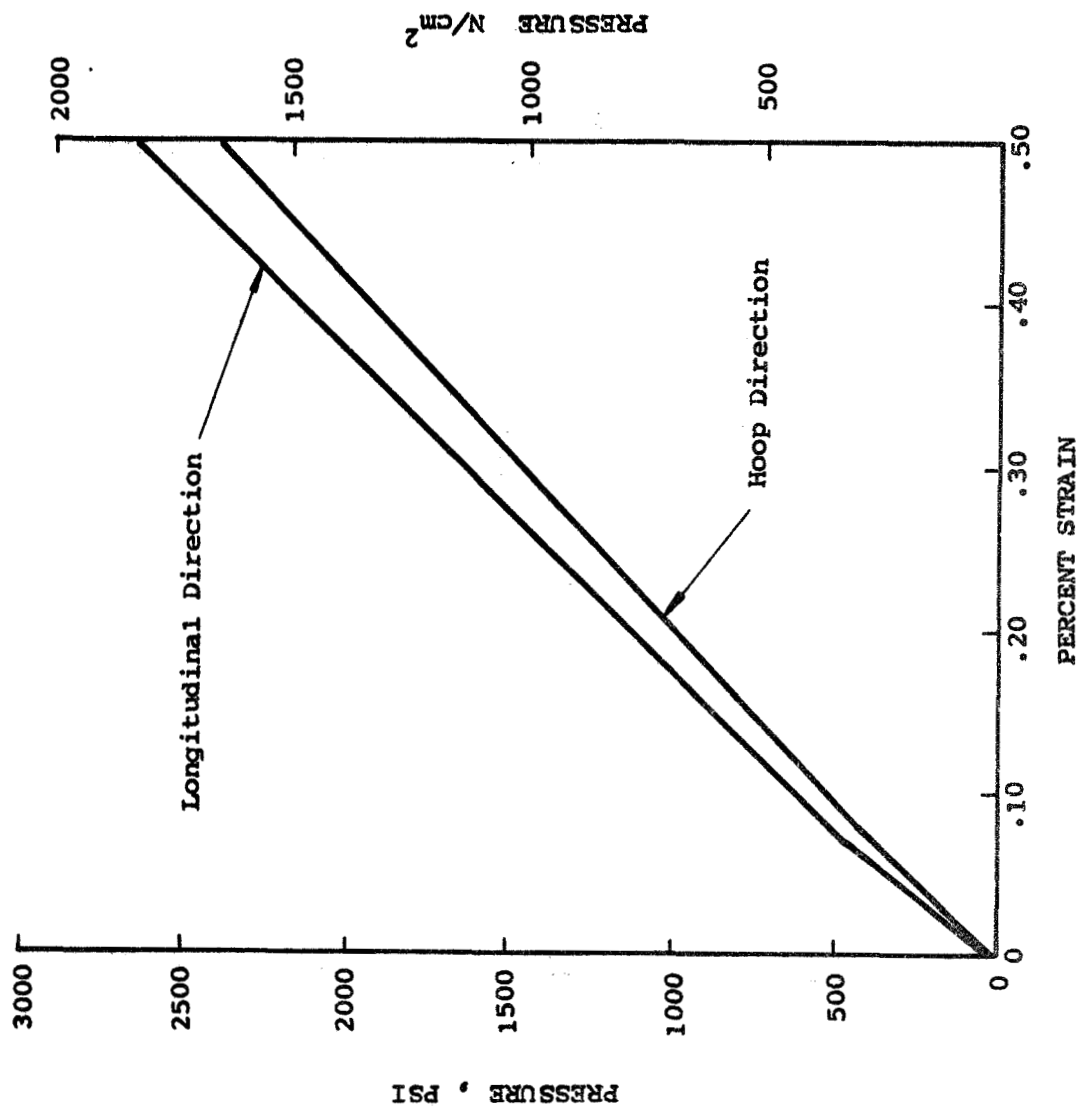


Fig. 2 Vessel Pressure vs. Strain Relationships at Ambient Temperature

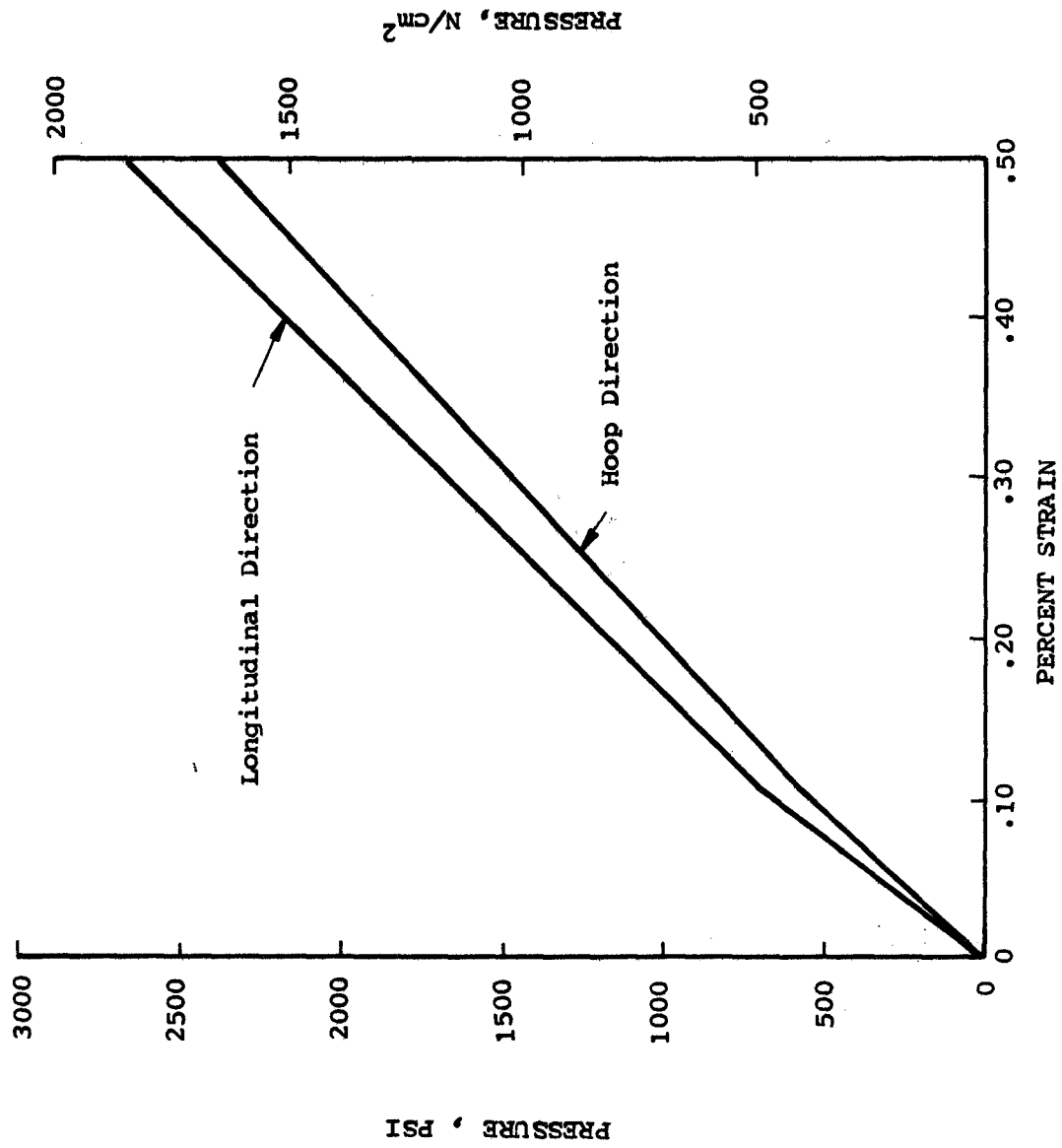


Fig. 3 Vessel Pressure vs. Strain Relationships at Liquid Nitrogen Temperature

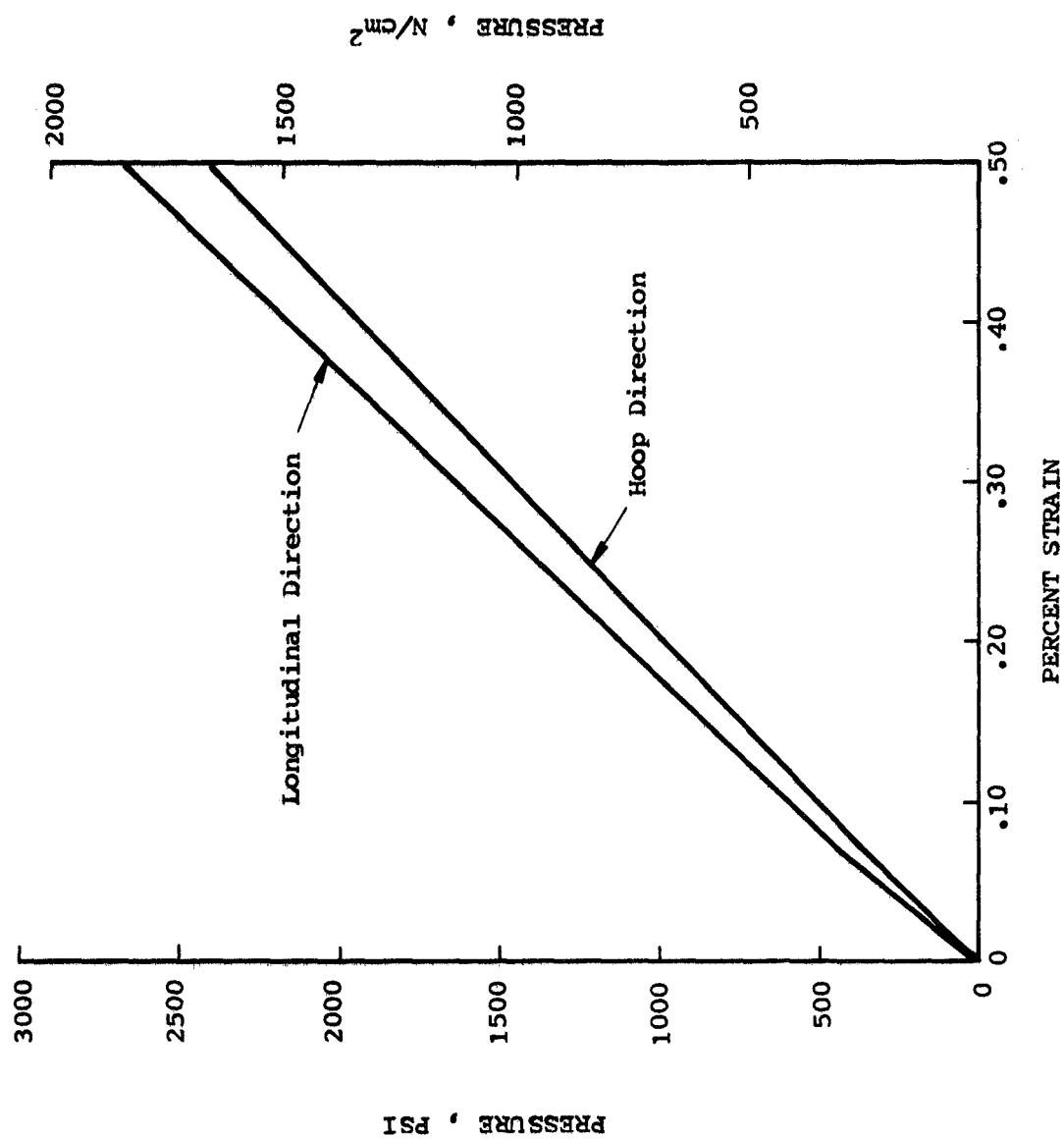


Fig. 4 Vessel Pressure vs. Strain Relationships at Liquid Hydrogen Temperature

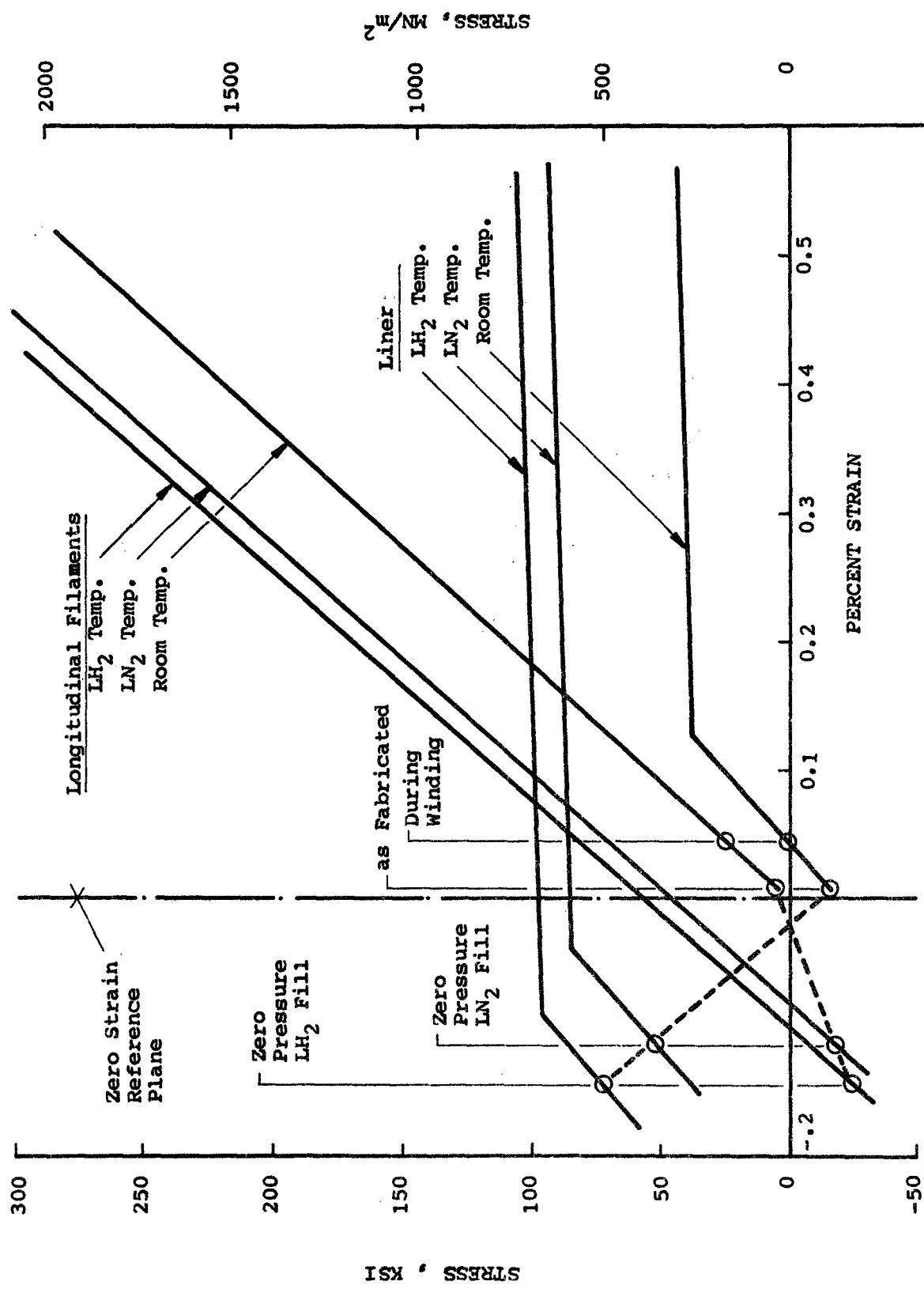


Fig. 5 Pressure Vessel Stress — Strain Relationships, Longitudinal Direction of Cylinder

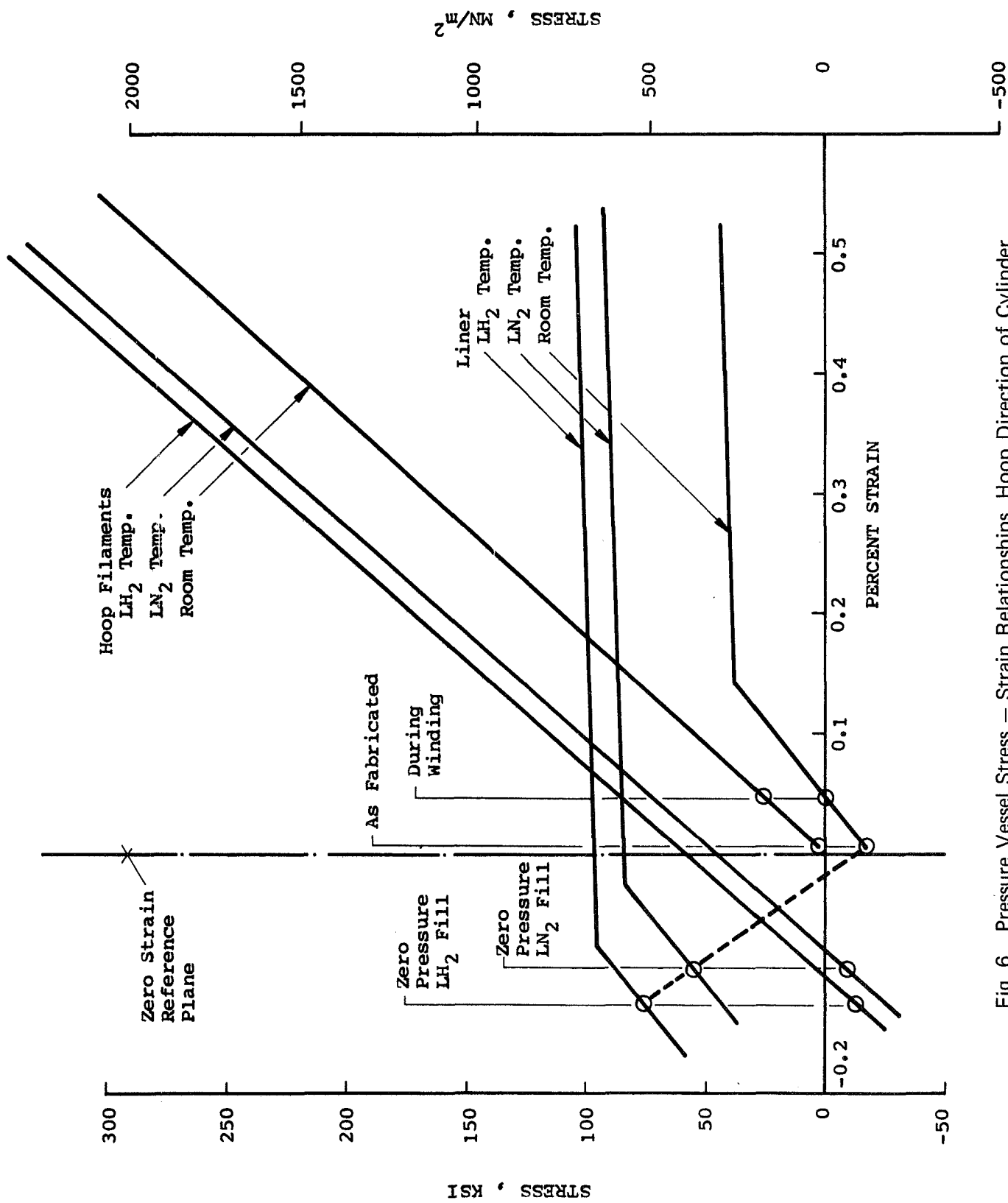
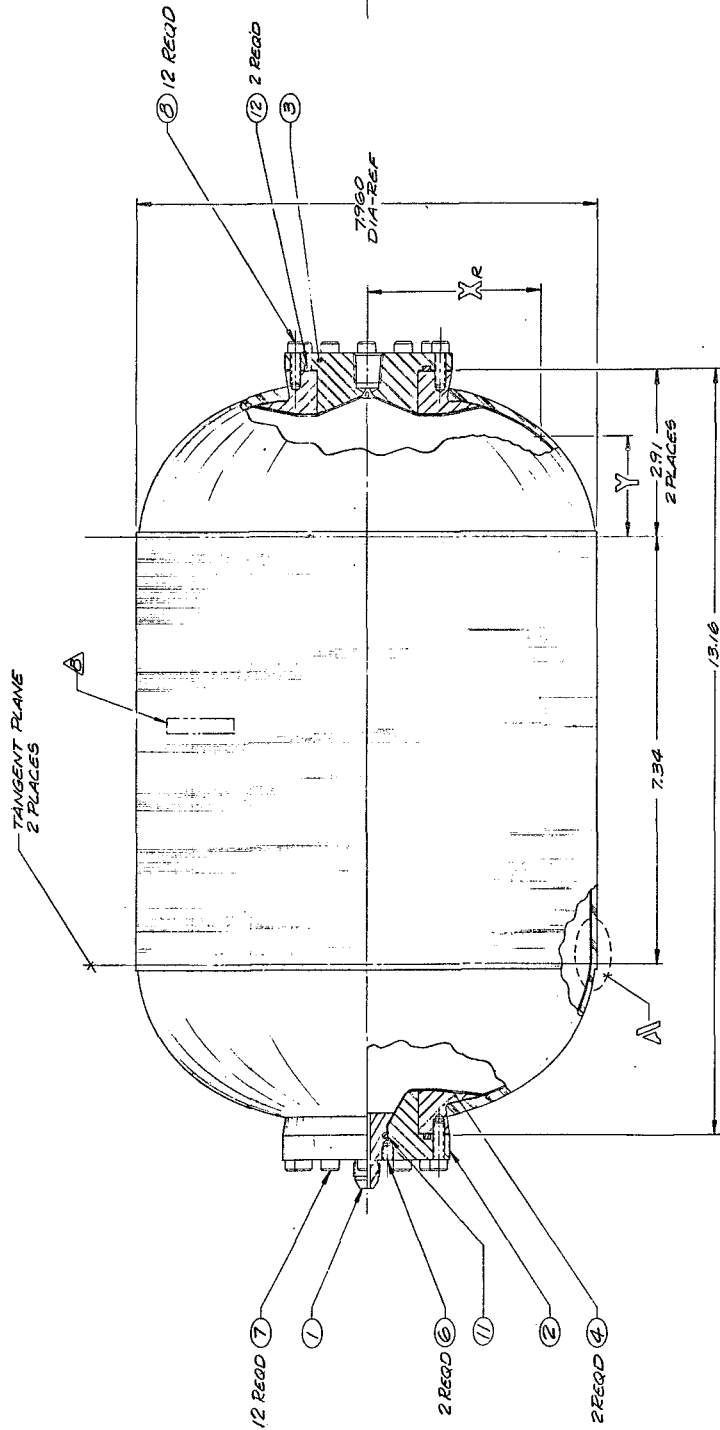
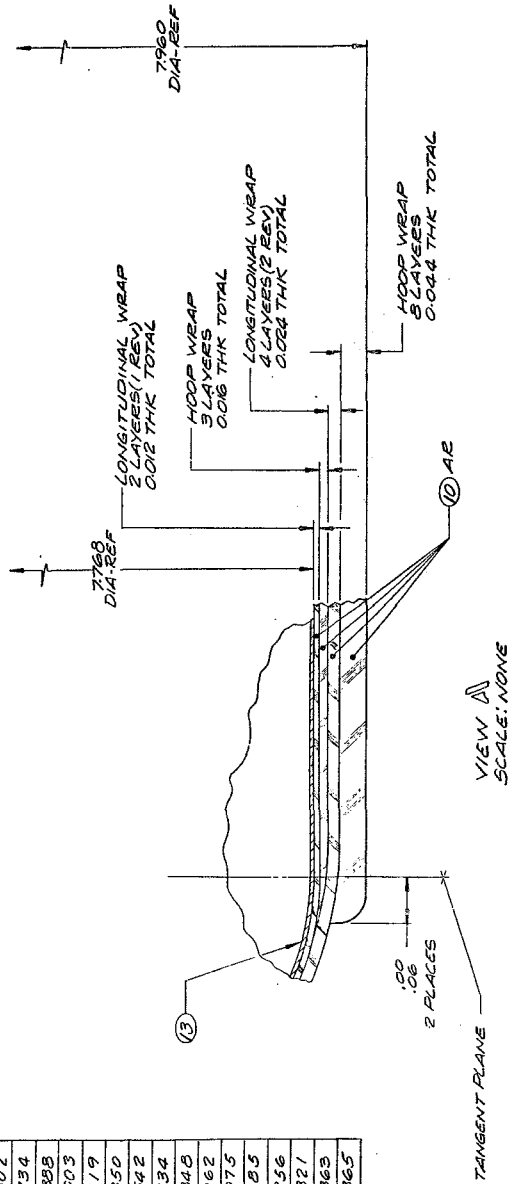


Fig. 6 Pressure Vessel Stress — Strain Relationships, Hoop Direction of Cylinder

- NOTES:
1. REMOVE ALL BURRS AND SHARP EDGES
 2. INTERPRET DRAWING PER MIL-D-1000.
 3. WINDING TENSION: 9 LBS. PER 0.125 IN WIDE TAPE
 4. WINDING PATTERN:
LONGITUDINAL: 3 REVOLUTIONS
93 TURNS ± 1 TURN FOR TIE-OFF, 0.125 IN WIDE TAPE.
CIRCUMFERENTIAL: 11 LAYERS
60 TURNS PER LAYER IN 7.46 IN LENGTH, 0.125 IN WIDE TAPE.
5. CURE CYCLE: 2 HRS AT 300°F; 2 HRS AT 250°F; 12 HRS AT 300°F.
6. IN LIST OF MATERIALS, 8 IN SYMBOL COLUMN, DENOTES
BULK MATERIAL.
 7. FABRICATE PRESSURE VESSEL IN ACCORDANCE WITH
FABRICATION PROCEDURES PROVIDED BY ENGINEERING.
8. MARK PER AS00215H WITH PART NO. 1269187-1.



INSIDE HEAD CONTOUR	
X	Y
3.883	0.000
3.870	0.232
3.820	0.502
3.747	0.734
3.682	0.888
3.624	1.003
3.556	1.119
3.492	1.350
3.219	1.542
3.006	1.734
2.854	1.848
2.677	1.962
2.472	2.075
2.227	2.185
2.037	2.256
1.823	2.321
1.621	2.363
1.556	2.365



LIST OF MATERIALS	
QTY	SYMBOL
1	1
2	2
3	3
4	4
5	5
6	6
7	7
8	8
9	9
10	10
11	11
12	12
13	13

TITLE	
TEST ASSEMBLY -	
BORED FILAMENT WOUND	
PRESSURE VESSEL, 800 DIA	
1269187	

SPECIFICATION	
70143	
1269187	

FOLDOUT FRAME

4

3

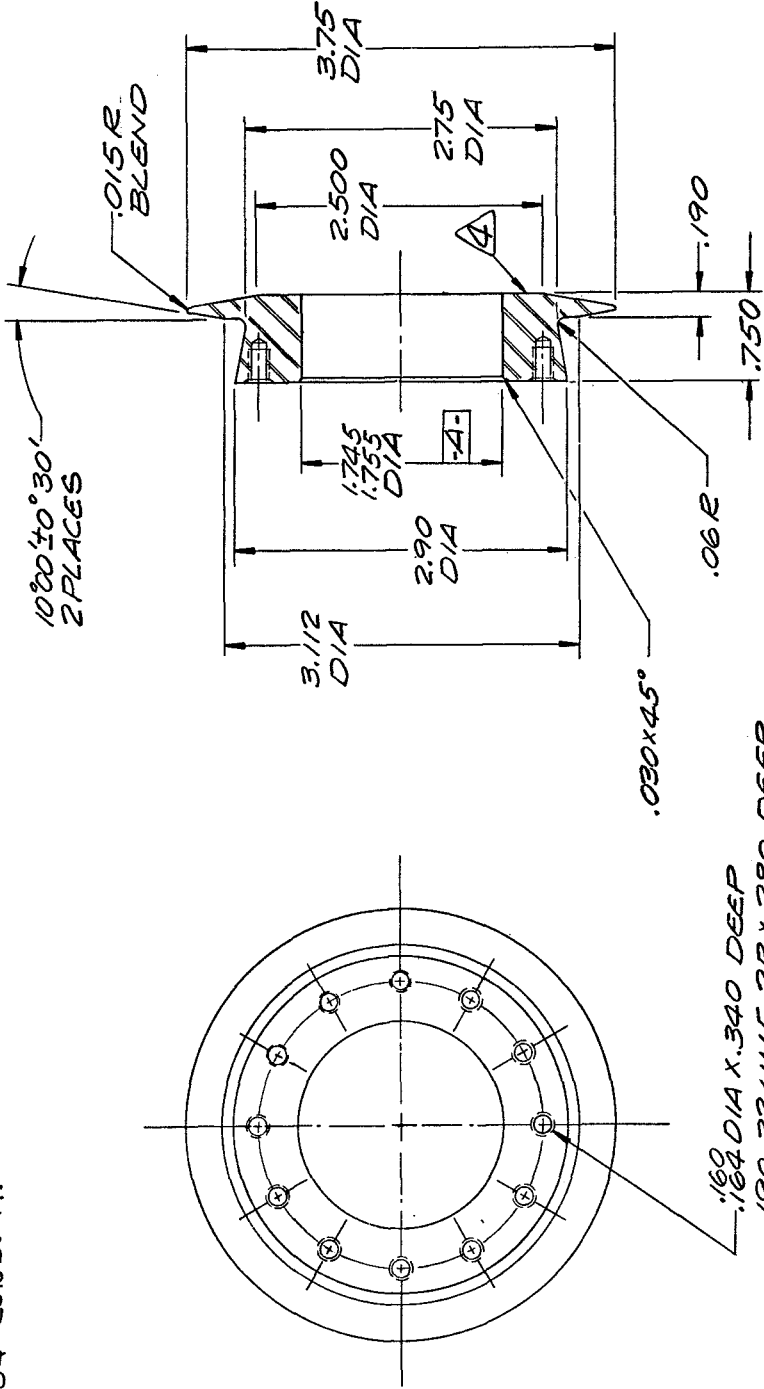
2

FOLDOUT FRAME 2

1

NOTES:

1. REMOVE ALL BURRS & SHARP EDGES.
2. INTERPRET DRAWING PER MIL-D-1000.
3. ALL MACHINED SURFACES TO BE 125/ UNLESS OTHERWISE SPECIFIED.
4. MARK PER ASD5215D WITH PART NO. 1269186-1.
5. ALTERNATE MATERIAL: 4.00 BAR CRES PER QQ-S-763 CLASS 304 COND. A.



.160 DIA X .340 DEEP
.190-32 UNF-28 X .280 DEEP
12 HOLES EQUALLY
SPACED ON A 2.500 DIA
BSC \varnothing 1.010 DIA

QTY REQD	SYM	CODE IDENT	PART OR IDENTIFYING NO.	NOMENCLATURE OR DESCRIPTION	MATERIAL	SPECIFICATION	UNIT WT.	ZONE	ITEM NO.
			-1		100 PLATE A	QQ-S-763			
CRES TYPE 304 COND A									

UNLESS OTHERWISE SPECIFIED		CONTRACT NO.		AEROJET-GENERAL CORPORATION	
DIMENSIONS ARE IN INCHES		DRAWN H.Q.C.H.O.A.		AZUSA, CALIFORNIA	
TOLERANCE ON DECIMALS		CHECK 8-25-69			
XX ± .03		DESIGN 8-11-69			
XXX ± .010		STRESS/STRUCTURE 8-18-67			
DO NOT SCALE DRAWING		MATERIALS			
TREATMENT		PRODUCTION 8-11-69			
FINISH		DESIGN ACTIVITY APPD			
SIMILAR TO		CUSTOMER			
ACT. WT/CALC WT					

ON	THRU	EFFECTIVE SERIAL NO.	USAGE DATA	ON	THRU	EFFECTIVE SERIAL NO.	USAGE DATA

PART DASH QTY REQD NO. PER ASSY	NEXT ASSY	USED ON	APPLICATION	DRAWING LEVEL
-1	1	2	1269186-1	1

TITLE		BOSS -	
BORON FILAMENT WOUND			
PRESSURE VESSEL, 8000 DIA			
DWG SIZE	CODE IDENT NO.	DWG NO.	RELEASE DATE
C	70143	1269186	8/25/69
SCALE: 1/1		SHEET	

FOLDOUT FRAME

4

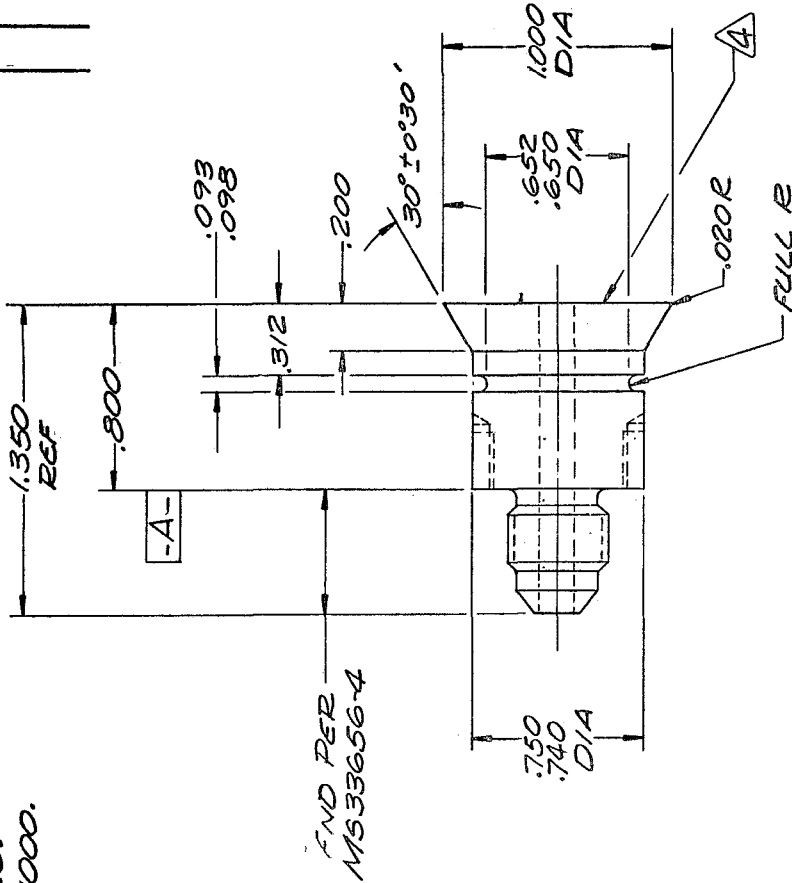
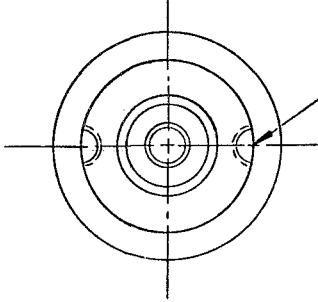
3

2

FOLDOUT FRAME 2

NOTES:

1. REMOVE ALL BURRS & SHARP EDGES.
2. INTERPRET DRAWING PER MIL-D-1000.
3. ALL SURFACES TO BE 125 UNLESS OTHERWISE SPECIFIED.
4. MARK PER ASD52150 WITH PART NO. 1269183-1.



FND PER
MS33856-4

.160 DIA X .310 DP
.190-32NF-38 X.250 DP
2 PLACES
EQUALLY SPACED
ON A .750 DIA BSC

Ø .160 DIA

1269183

COPY

QTY REQD	SYM	CODE IDENT	PART OR IDENTIFYING NO.	NOMENCLATURE OR DESCRIPTION	MATERIAL	SPECIFICATION	UNIT WT.	ZONE	ITEM NO.
			-1		1/2 DIA BAR	605-5763 CLASS 304 COND A			

UNLESS OTHERWISE SPECIFIED DIMENSIONS ARE IN INCHES TOLERANCE ON DECIMALS ANGULAR ± 2°		CONTRACT NO.	
XX ± .03	XXX ± .010	DRAWN	DATE
DO NOT SCALE DRAWING		00412A	22-1-69
TREATMENT		CHECK	
		DESIGN	8-25-69
		STRESS/STRUCTURE	8-11-69
		MATERIALS	8-18-69
FINISH		PRODUCTION	8-11-69
		HHNS PER 602	
		DESIGN ACTIVITY APPD	
		EE MORRIS	
SIMILAR TO		CUSTOMER	

ON	THRU	EFFECTIVE SERIAL NO.	USAGE DATA

PART	NEXT FINAL	NEXT ASSY	USED ON
DASH QTY REQD NO. PER ASSY	1	1	1269187-1
DRAWING LEVEL		APPLICATION	
1			

AEROJET GENERAL CORPORATION	
AZUSA, CALIFORNIA	
TITLE	
TEST PLUG -	
BOEON FILAMENT WOUND	
PRESSURE VESSEL-8.00 DIA	
DWG NO.	70143
CODE IDENT NO.	1269183
SCALE: 2/1	RELEASE DATE: 8/25/69
SHEET	

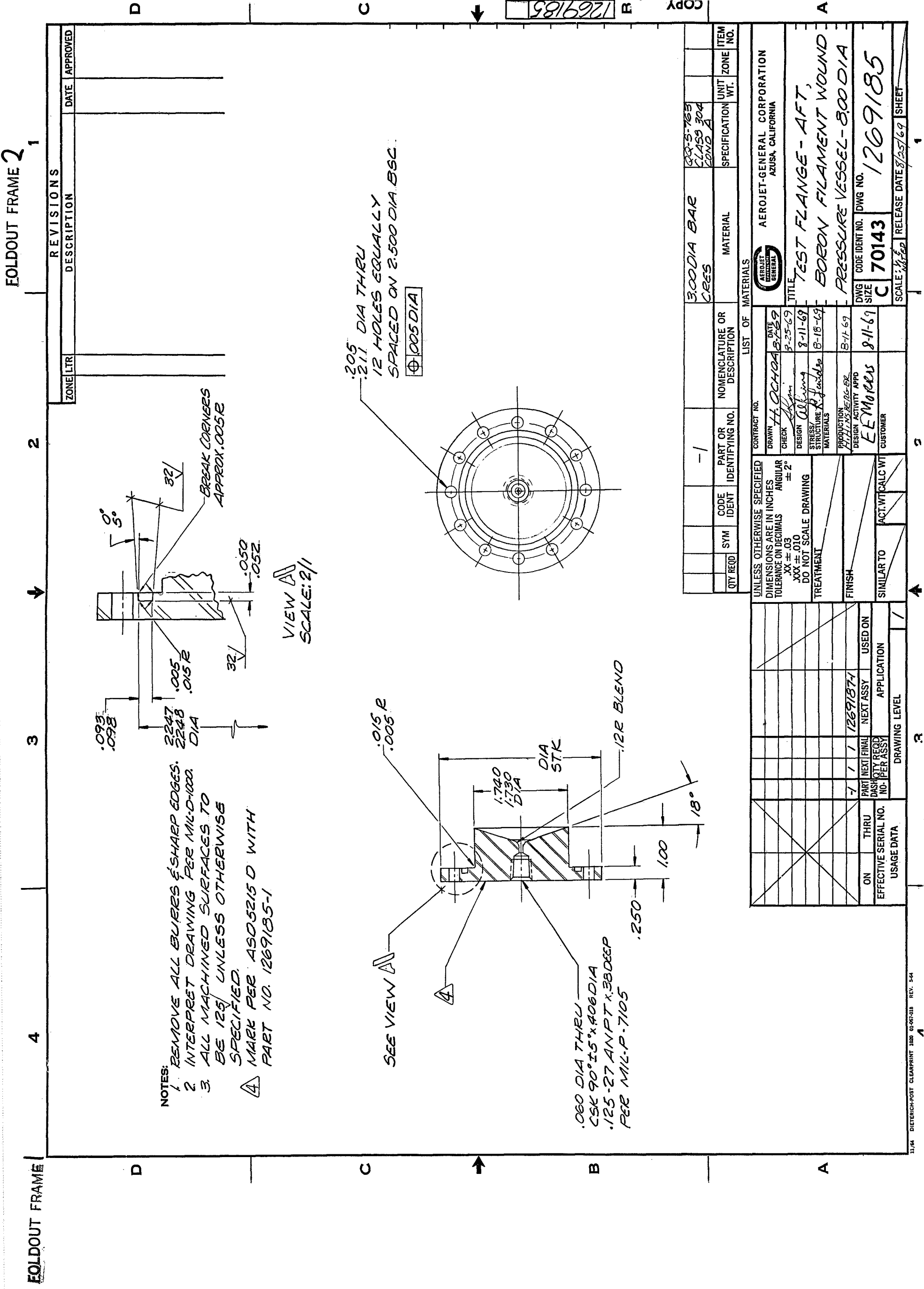
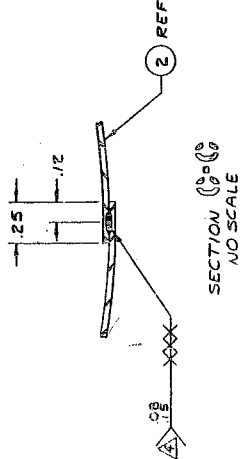
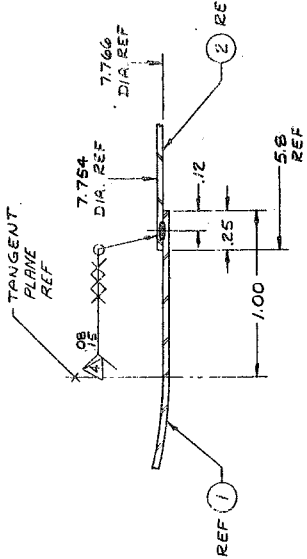
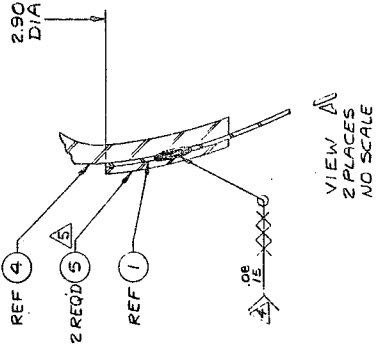
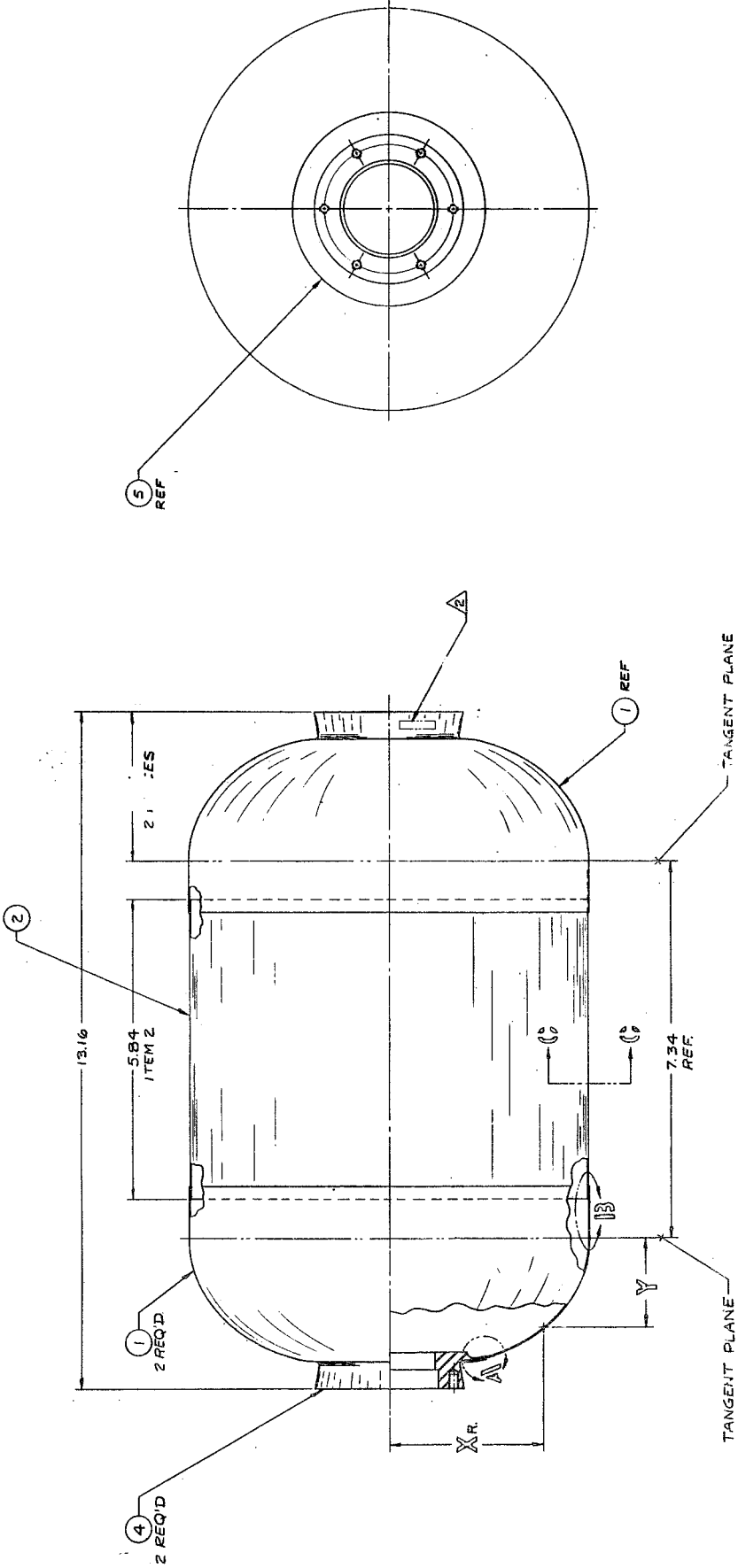


Fig. 12 Pressure Vessel Test Flange (Engineering Drawing) Pg. 76

NOTES:
1. REMOVE ALL BURRS AND SHARP EDGES.
2. MARK PER ASD2215H WITH 1269205-1
3. LEAK TEST LINER BY PRESSURIZING WITH FREON GAS, TYPE F-12 TO 7 ± 1 PSIG AND EXAMINING ALL WELDED AREAS WITH G.E. HALOGEN LEAK DETECTOR, MODEL H-2. AN ACCEPTABLE ALTERNATE TEST IS TO APPLY SOAP SOLUTION OVER ENTIRE EXTERIOR SURFACE, HOLDING AT 7 ± 1 PSIG FOR 15 MINUTES. MINIMUM ALL LEAKS WILL BE NOTED, REPAIRED AND TEST REPEATED.
4. RESISTANCE SPAM WELD PER MIL-N-6858, CLASS A
5. ITEM 5, RING, MAY BE SPOT WELDED PRIOR TO SEAM WELDING.

INSIDE HEAD CONTOUR	
X _R	Y
3.883	0.000
3.870	0.232
3.820	0.502
3.747	0.734
3.682	0.888
3.624	1.003
3.556	1.119
3.392	1.350
3.219	1.542
3.006	1.734
2.854	1.848
2.677	1.962
2.472	2.075
2.227	2.185
2.037	2.256
1.823	2.321
1.621	2.363
1.556	2.365



REVISIONS		DATE		APPROVED	
NO.	DESCRIPTION	DATE	APPROVED	DATE	APPROVED
1					
2					
3					
4					
5					

TITLE		DATE		APPROVED	
NO.	DESCRIPTION	DATE	APPROVED	DATE	APPROVED
1					
2					
3					
4					
5					

MATERIAL		SPECIFICATION		UNIT		ITEM	
NO.	DESCRIPTION	DATE	APPROVED	DATE	APPROVED	DATE	APPROVED
1							
2							
3							
4							
5							

LIST OF MATERIALS		CONTRACT NO.		PROJECT NO.	
NO.	DESCRIPTION	DATE	APPROVED	DATE	APPROVED
1					
2					
3					
4					
5					

AEROMET-GENERAL CORPORATION		TITLE		DATE		APPROVED	
NO.	DESCRIPTION	DATE	APPROVED	DATE	APPROVED	DATE	APPROVED
1							
2							
3							
4							
5							

LINER WELDED		DATE		APPROVED	
NO.	DESCRIPTION	DATE	APPROVED	DATE	APPROVED
1					
2					
3					
4					
5					

PRESSURE VESSEL		DATE		APPROVED	
NO.	DESCRIPTION	DATE	APPROVED	DATE	APPROVED
1					
2					
3					
4					
5					

BIN. DIA.		DATE		APPROVED	
NO.	DESCRIPTION	DATE	APPROVED	DATE	APPROVED
1					
2					
3					
4					
5					

70143		DATE		APPROVED	
NO.	DESCRIPTION	DATE	APPROVED	DATE	APPROVED
1					
2					
3					
4					
5					

1269205		DATE		APPROVED	
NO.	DESCRIPTION	DATE	APPROVED	DATE	APPROVED
1					
2					
3					
4					
5					

11/54 DIETRICH-POST CLEARPRINT 1000-10 41-987-998 NOV. 3-64

FOLDOUT FRAME

FOLDOUT FRAME 2

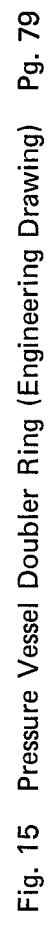


Fig. 15 Pressure Vessel Doubler Ring (Engineering Drawing) Pg. 79

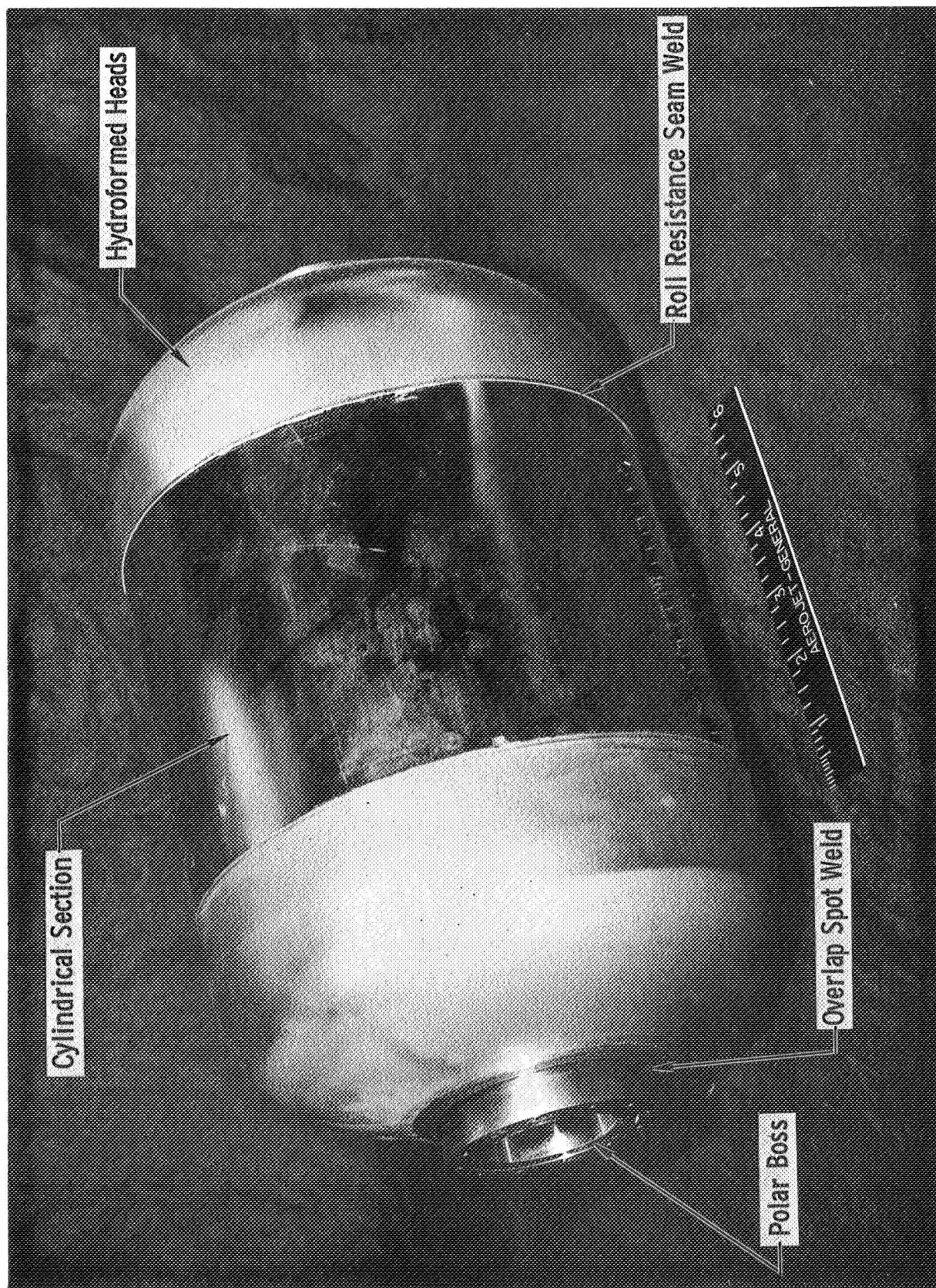


Fig. 16 Metal Liner for Design A Vessels Pg. 80

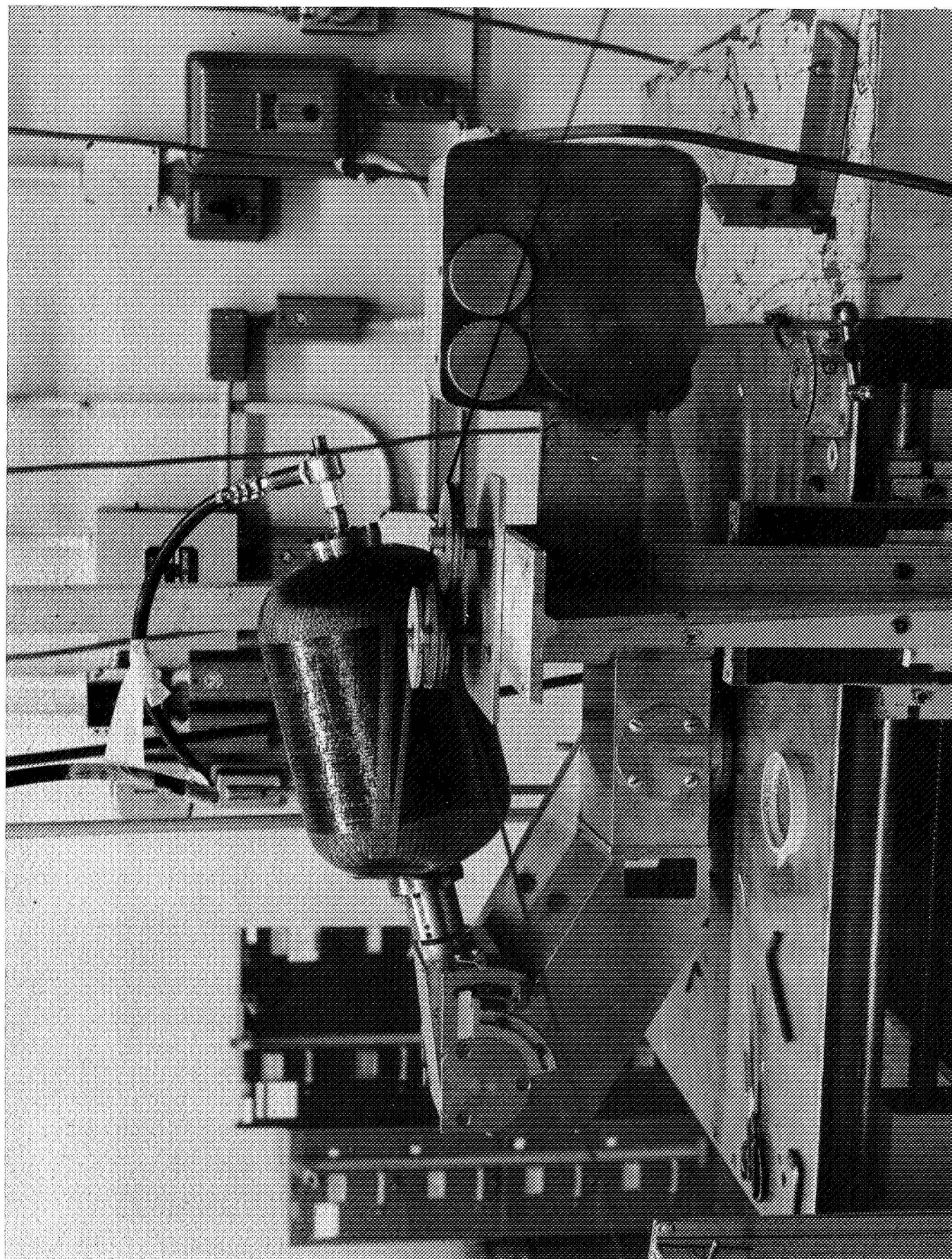


Fig. 17 Longitudinal Winding Boron Filament-Wound Vessel Pg. 81

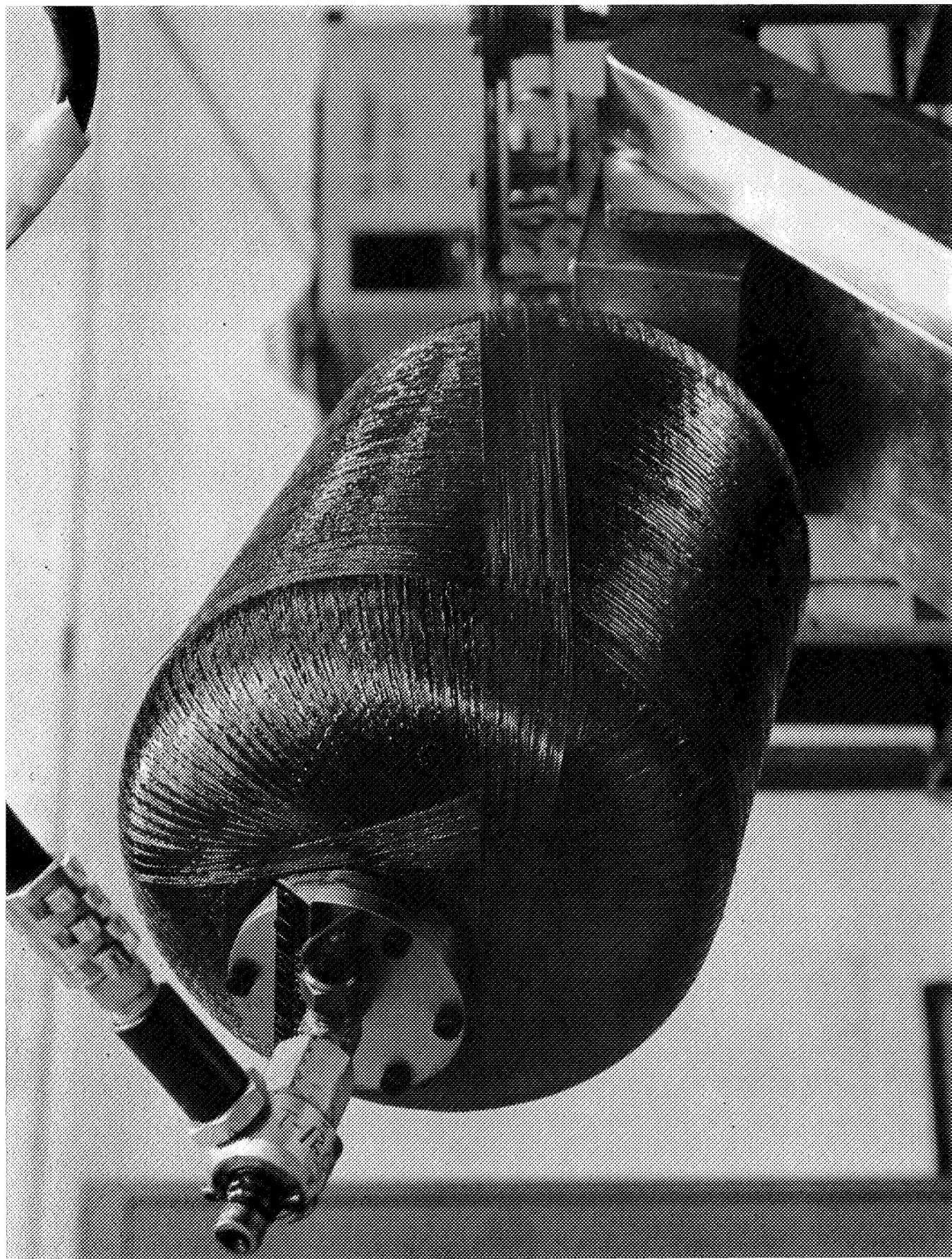


Fig. 18 Intersperced Longitudinal and Hoop Patterns, Boron Filament-Wound Vessel Pg. 82

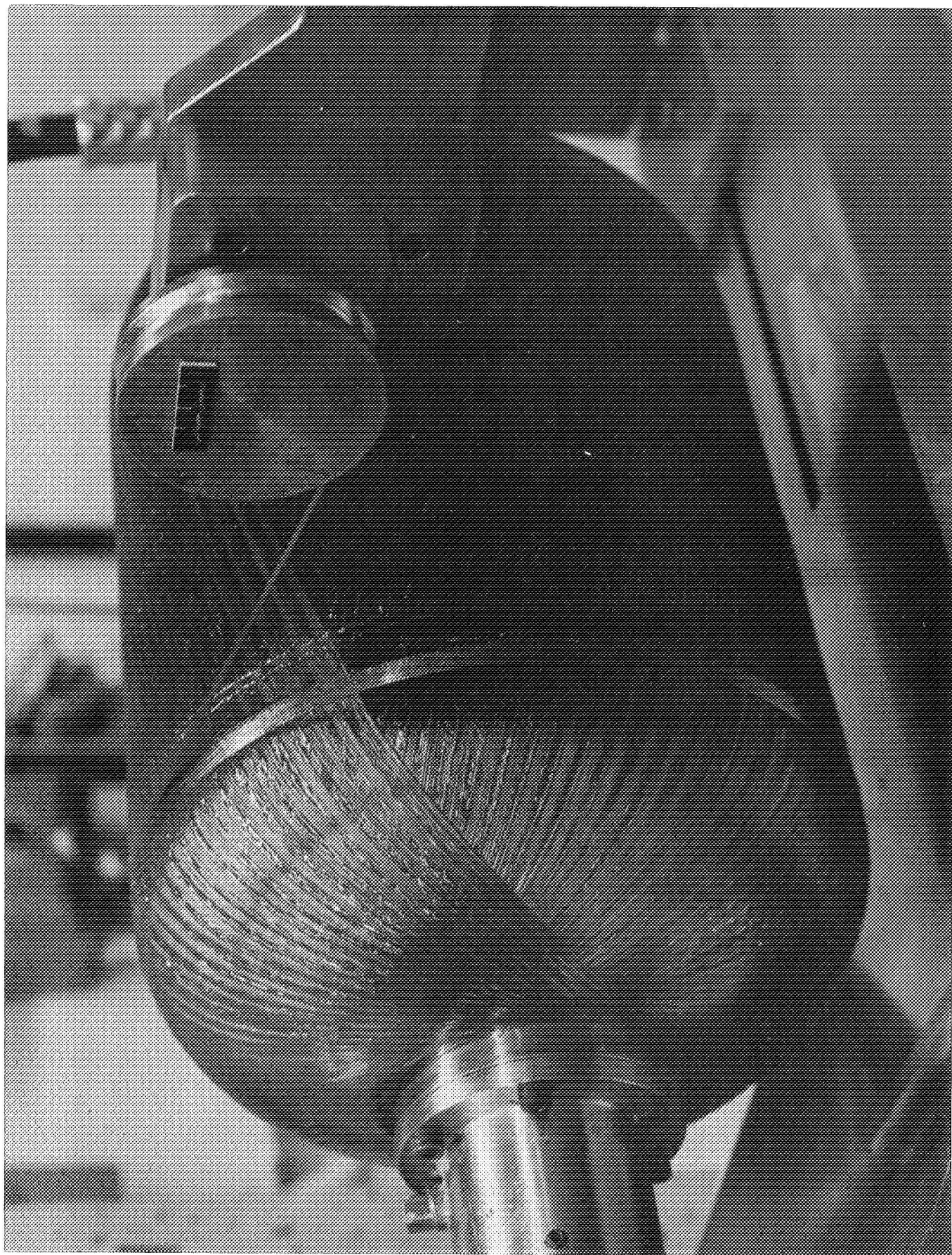


Fig. 19 Circumferential Winding Boron Vessel Pg. 83

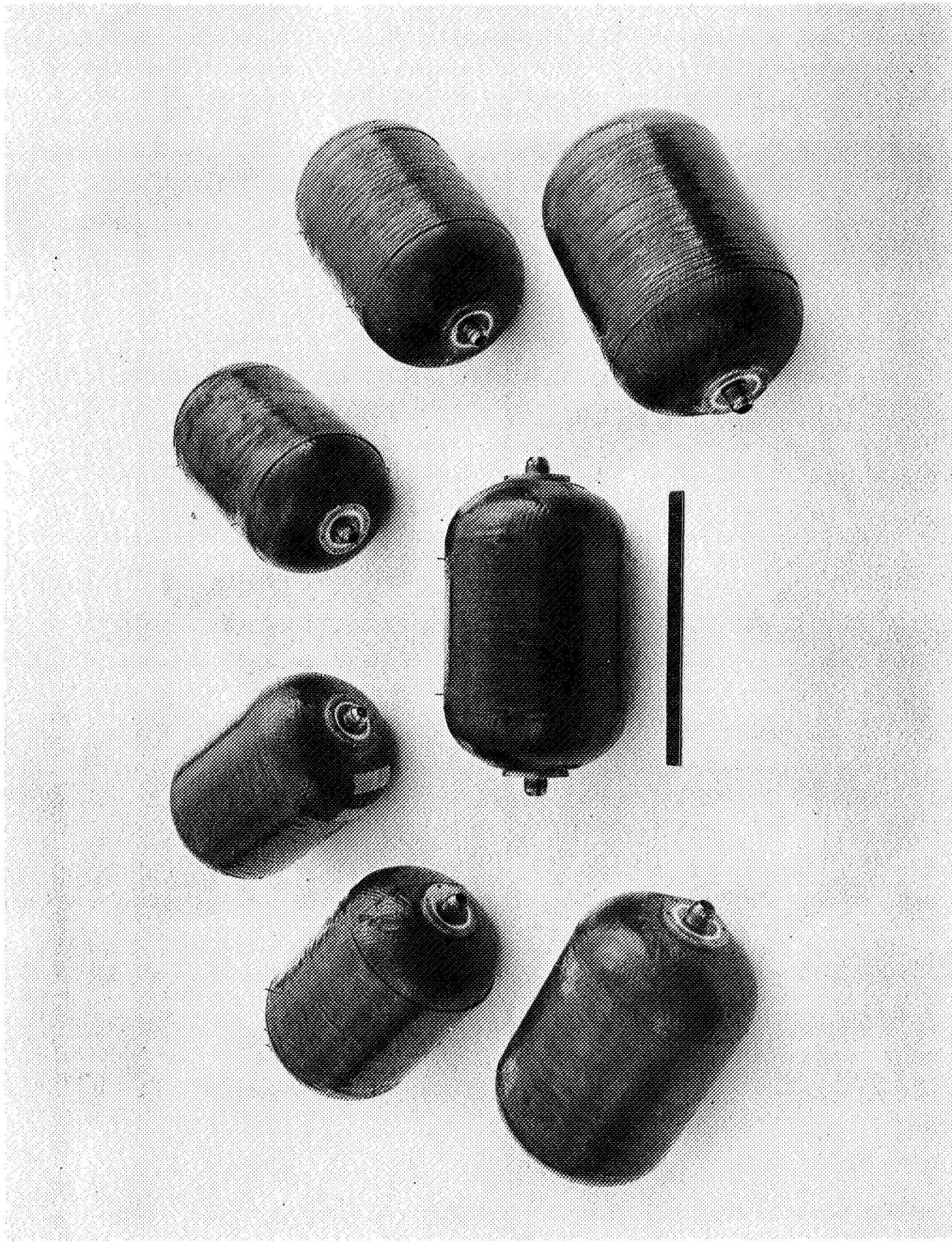


Fig. 20 Group of Completed Boron Filament-Wound Vessels Pg. 84

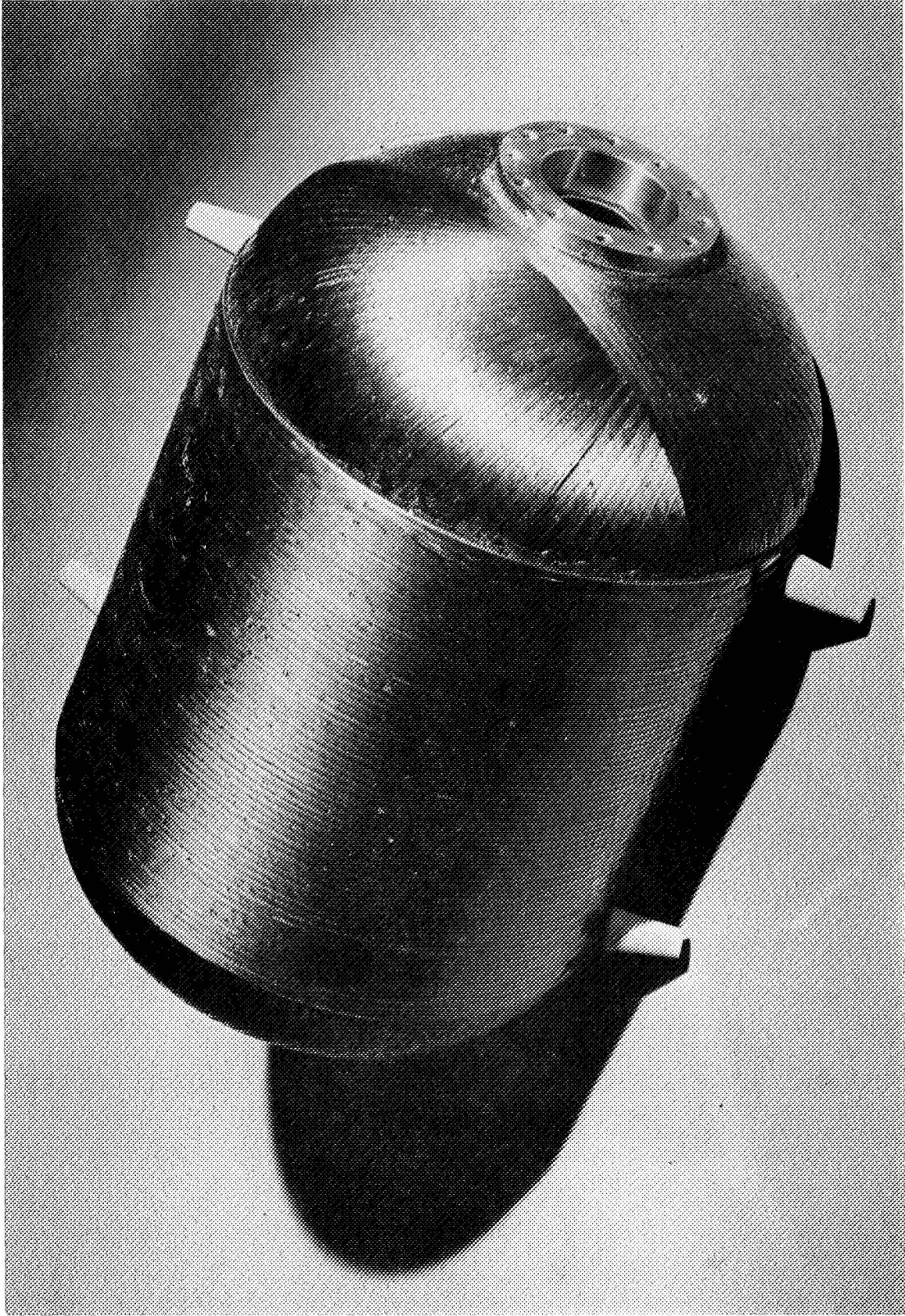


Fig. 21 Design B Boron Filament-Wound Vessel Pg. 85

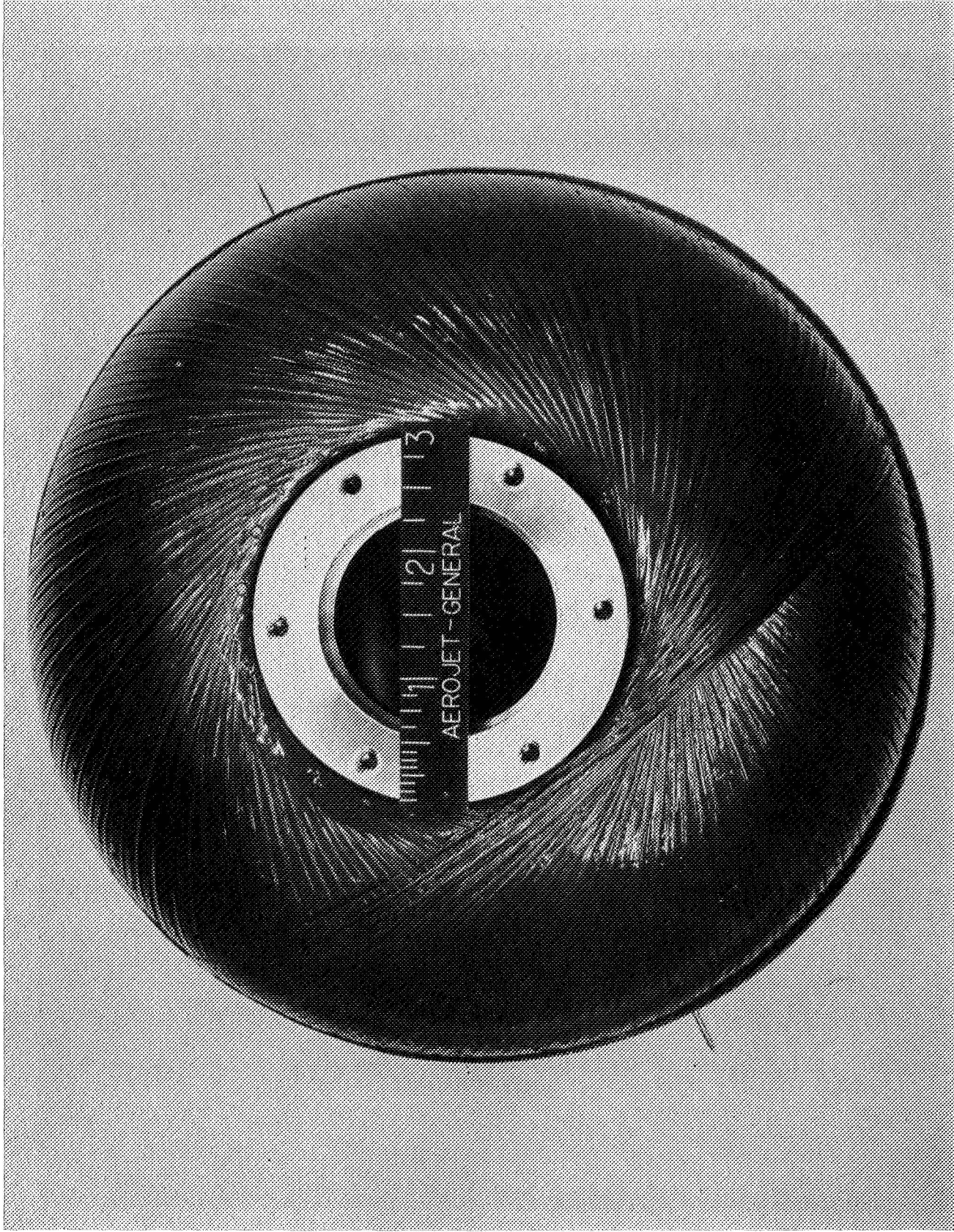


Fig. 22 View of Head of Vessel B-1 Pg. 86



Fig. 23 Boron Prepreg Tape Spool, Showing Poor Packaging Pg. 87

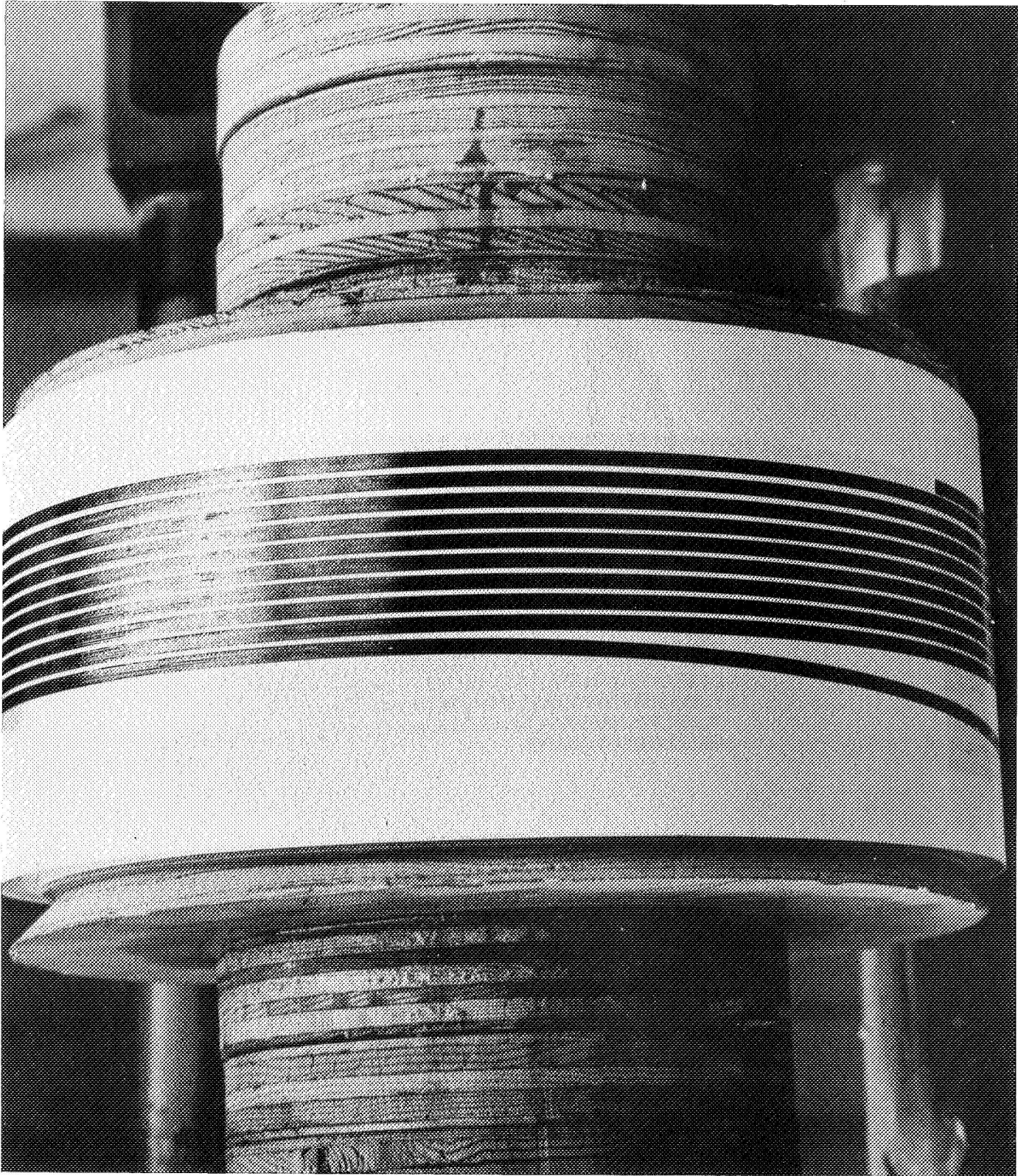


Fig. 24 Boron Prepreg Tape Spool, Showing Typical Packaging Pg. 88

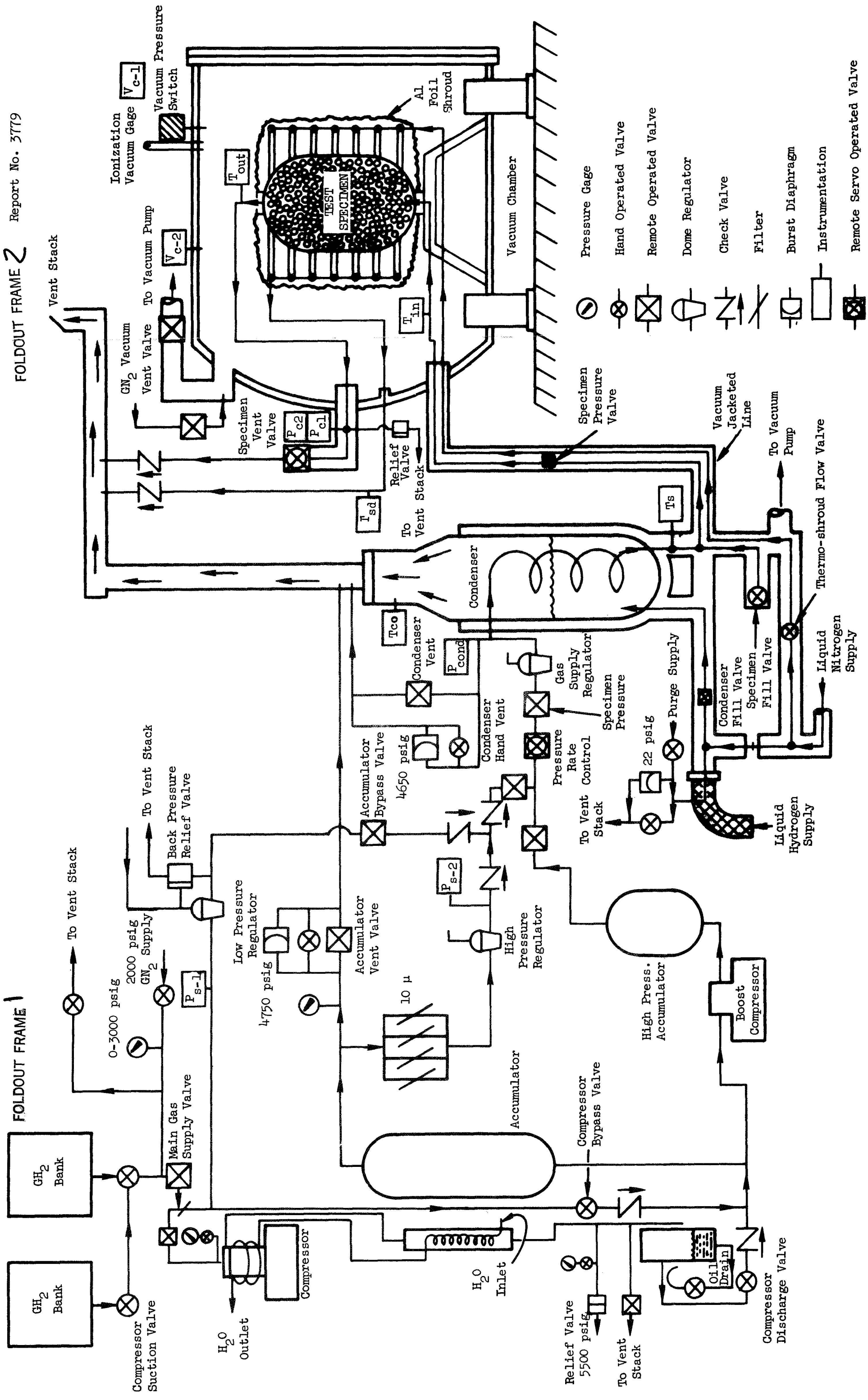


Fig. 25 Liquid Cryogen Test Facility Pg. 89

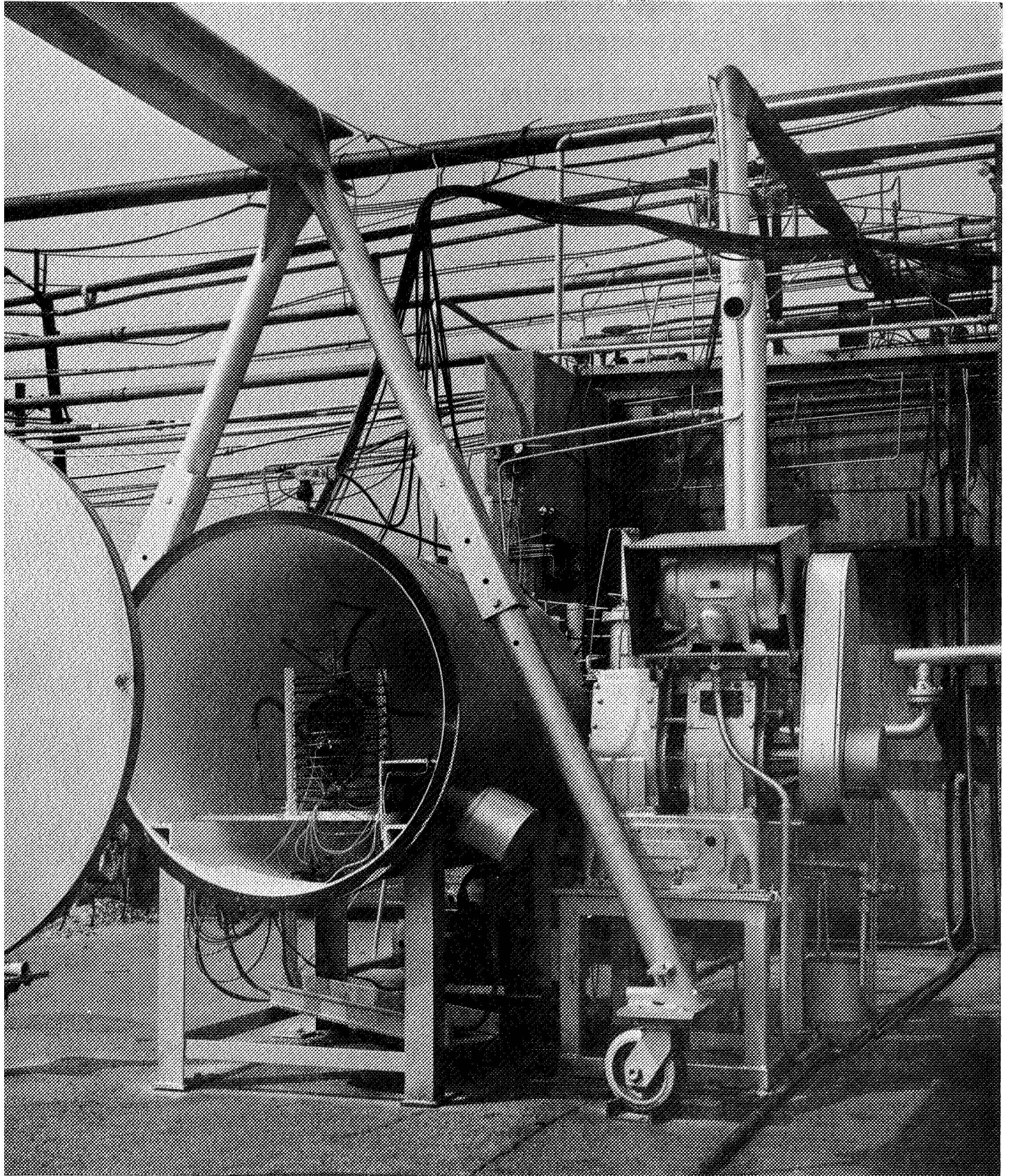


Fig. 26 Cryogenic Pressure-Test Facility Pg. 90

Symbol	Measurement
P_s	Supply Pressure
P_c	Specimen Pressure
T_s	Supply Temperature
T_o	Specimen Temperature
SG_1	Specimen Deflection, Hoop
$SG_{2, 3}$	Specimen Deflections, Longitudinal
$TSG_{1, 2, 3}$	Deflection Beam Temperatures
$TC_{1, 2}$	Specimen (Skin) Temperatures

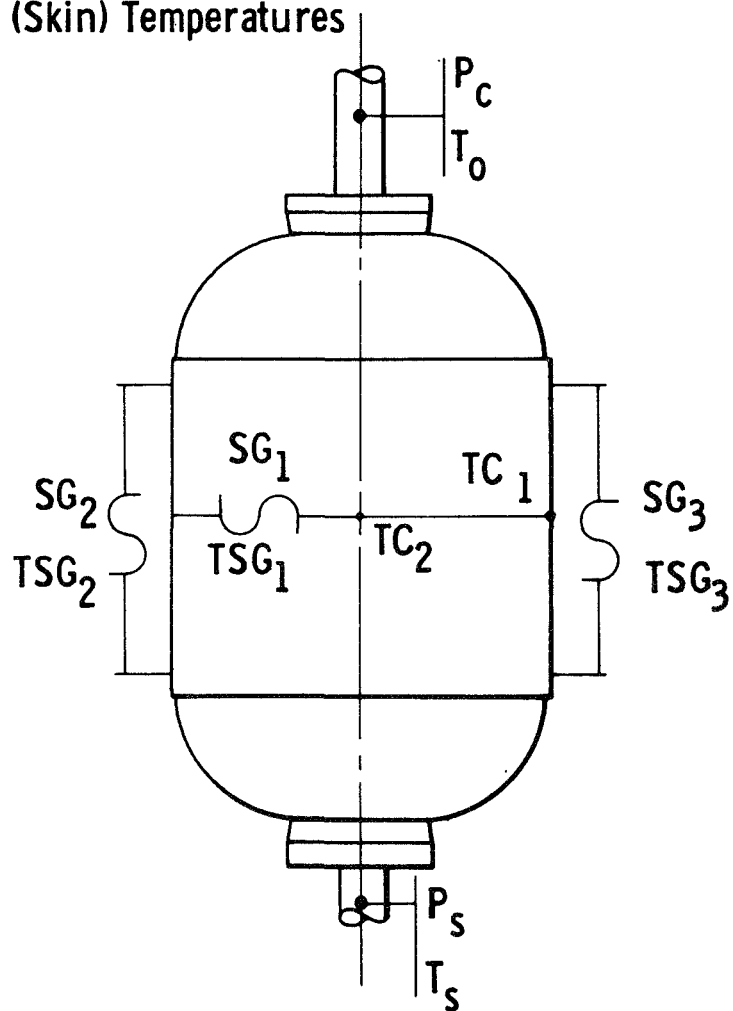


Fig. 27 Location of Instruments on Test Vessels Pg. 91

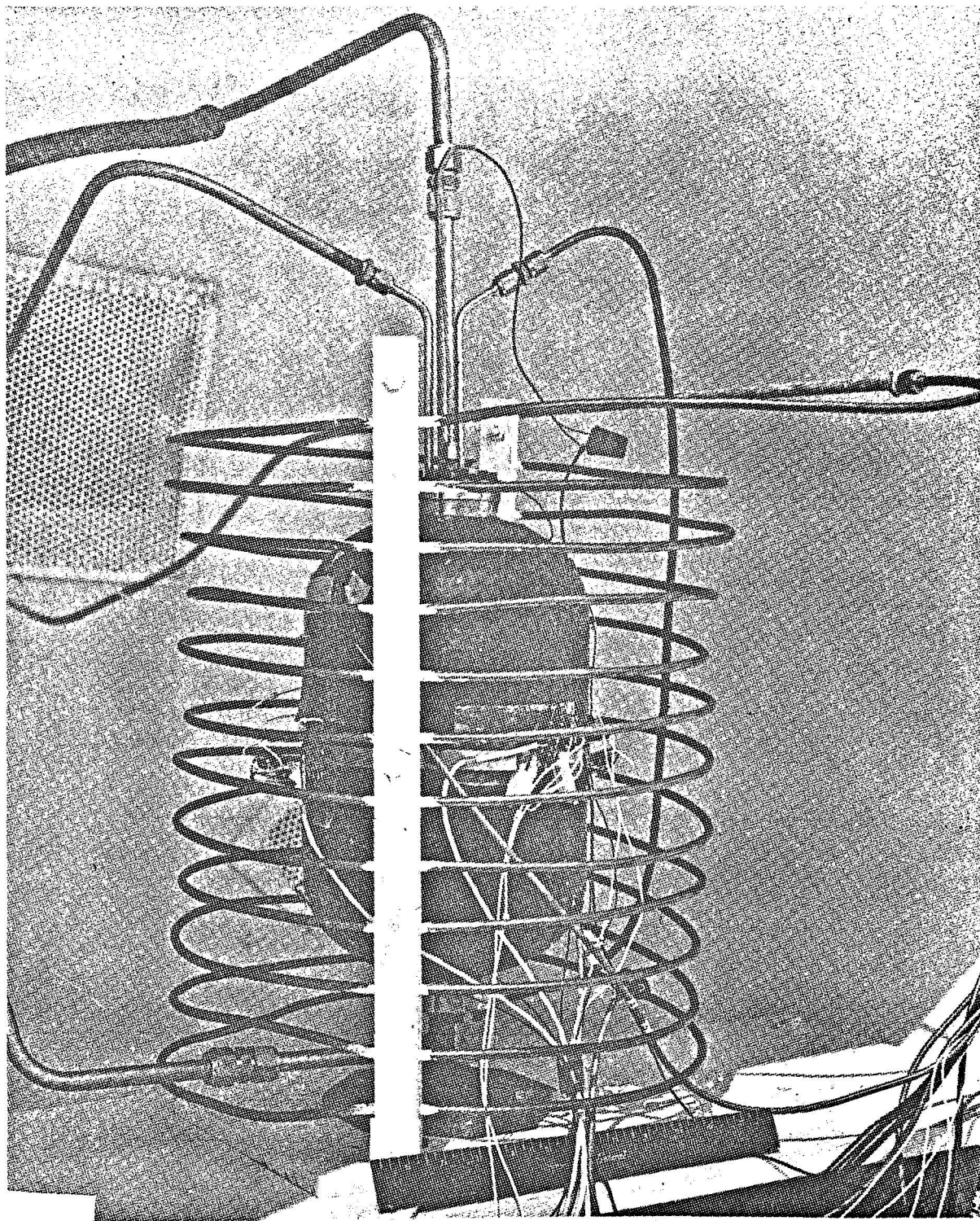
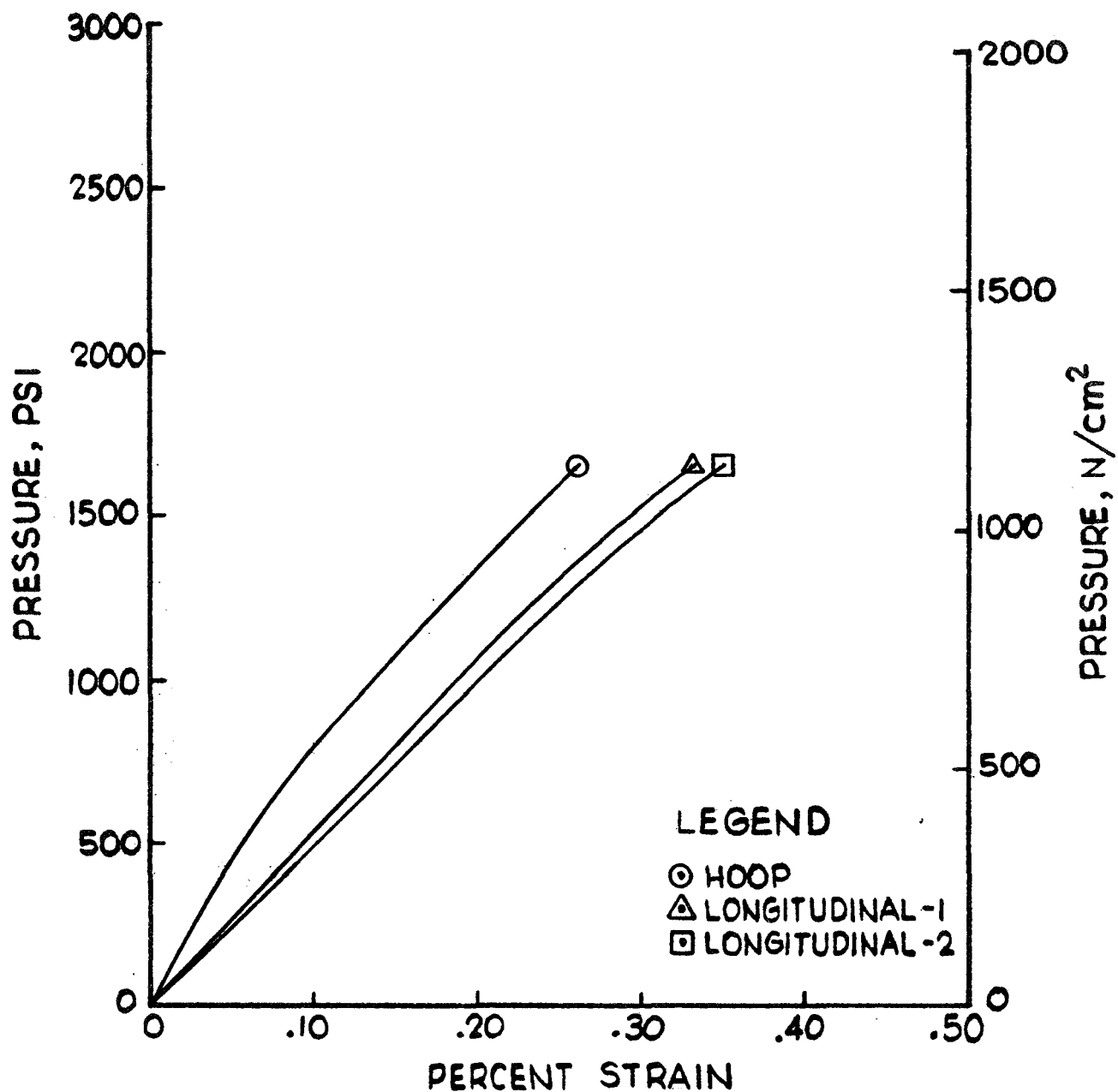


Fig. 28 Instrumentation and Cooling Coil on Pressure Vessel Pg. 92



Fig. 29 Post Test Photograph of Tank B-1 Pg. 93



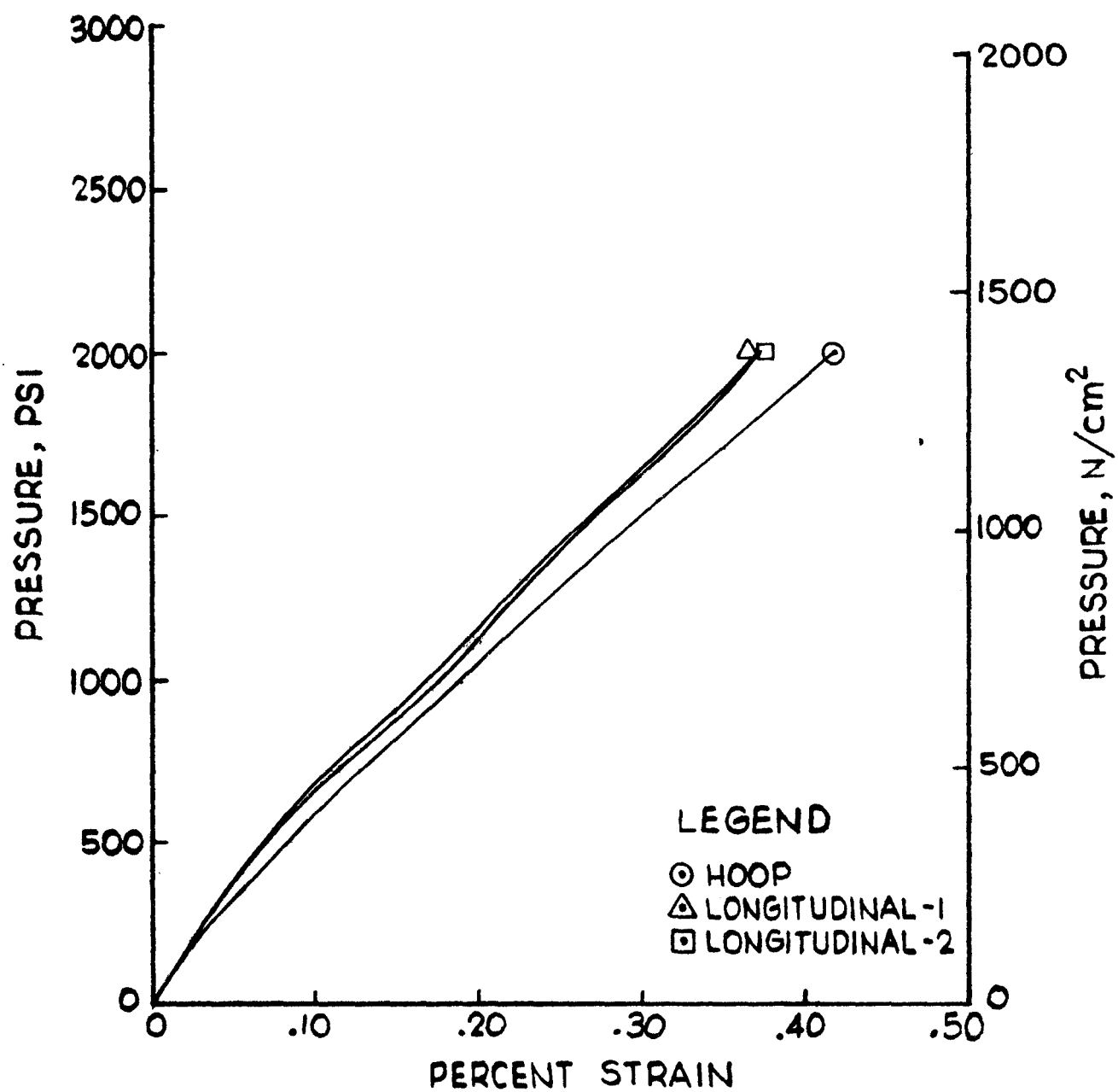
TANK S/N B-1

PRESSURE VS STRAIN FOR BURST TEST AT 75°F (297°K)

Figure 30



Fig. 31 Post Test Photograph of Tank B-3 Pg. 95



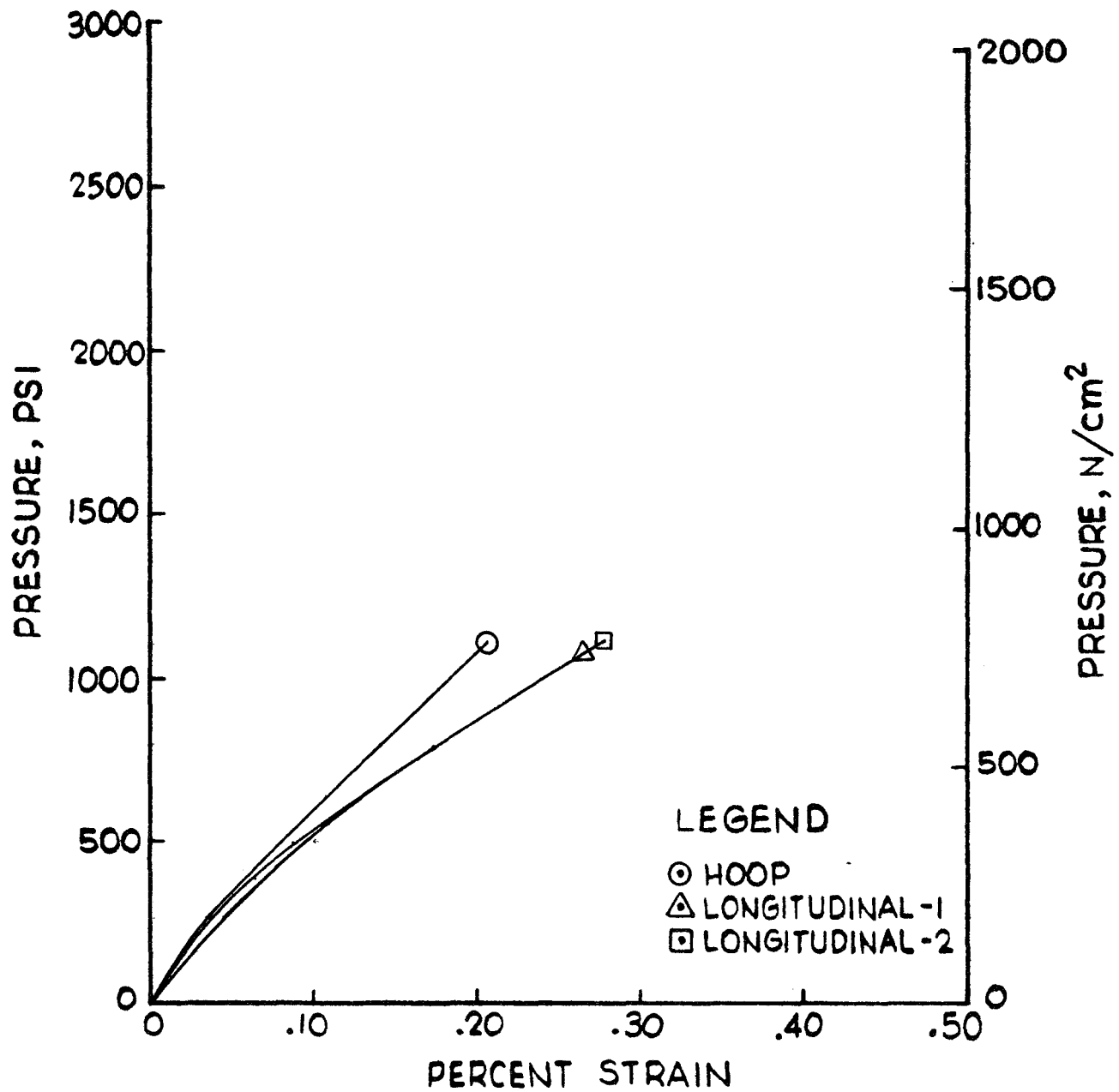
TANK S/N B-3

PRESSURE VS STRAIN FOR BURST TEST AT 75°F (297°K)

Figure 32



Fig. 33 Post Test Photograph of Tank B-7 Pg. 97



TANK S/N B-7

PRESSURE VS STRAIN FOR BURST TEST AT 75°F (297°K)

Figure 34

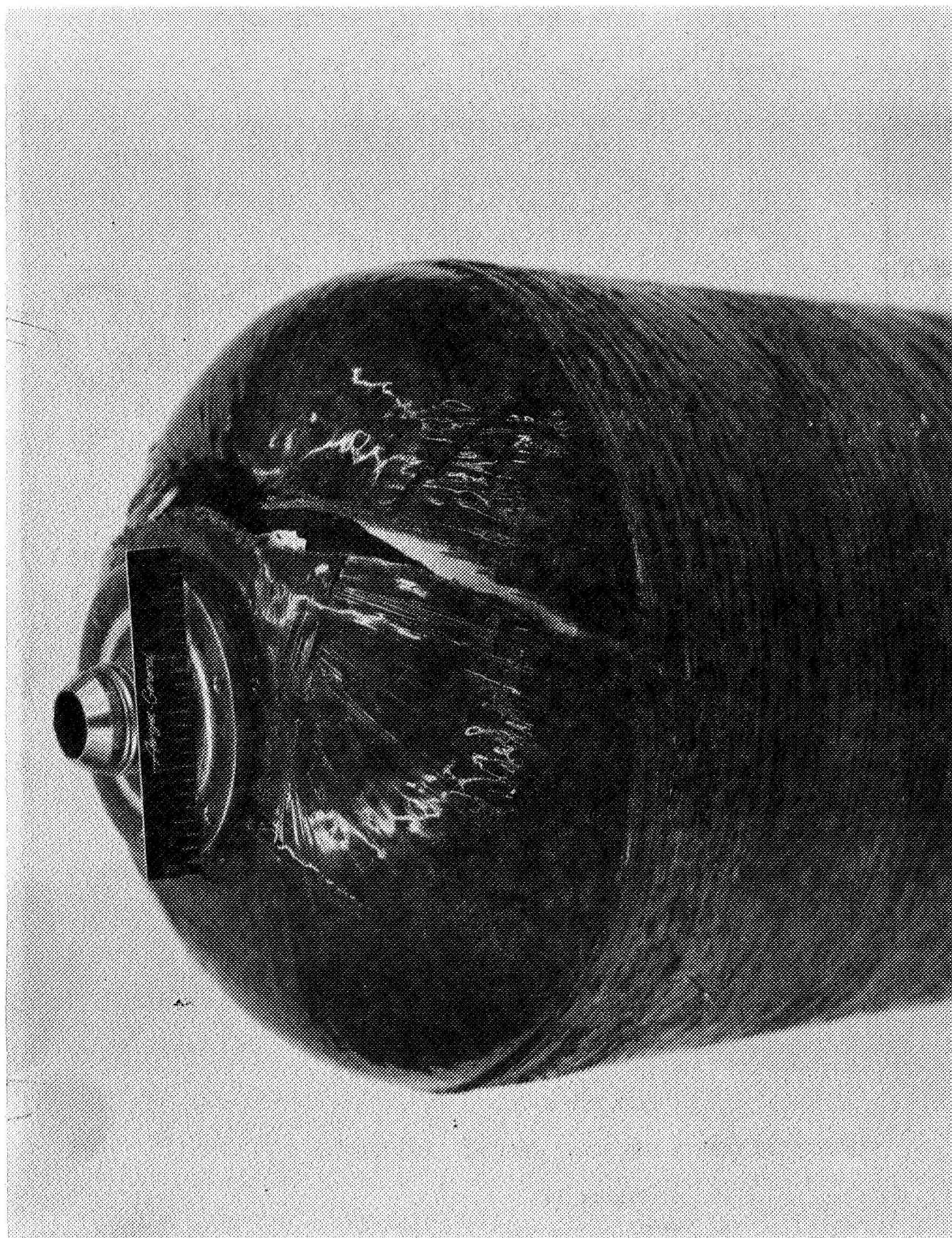
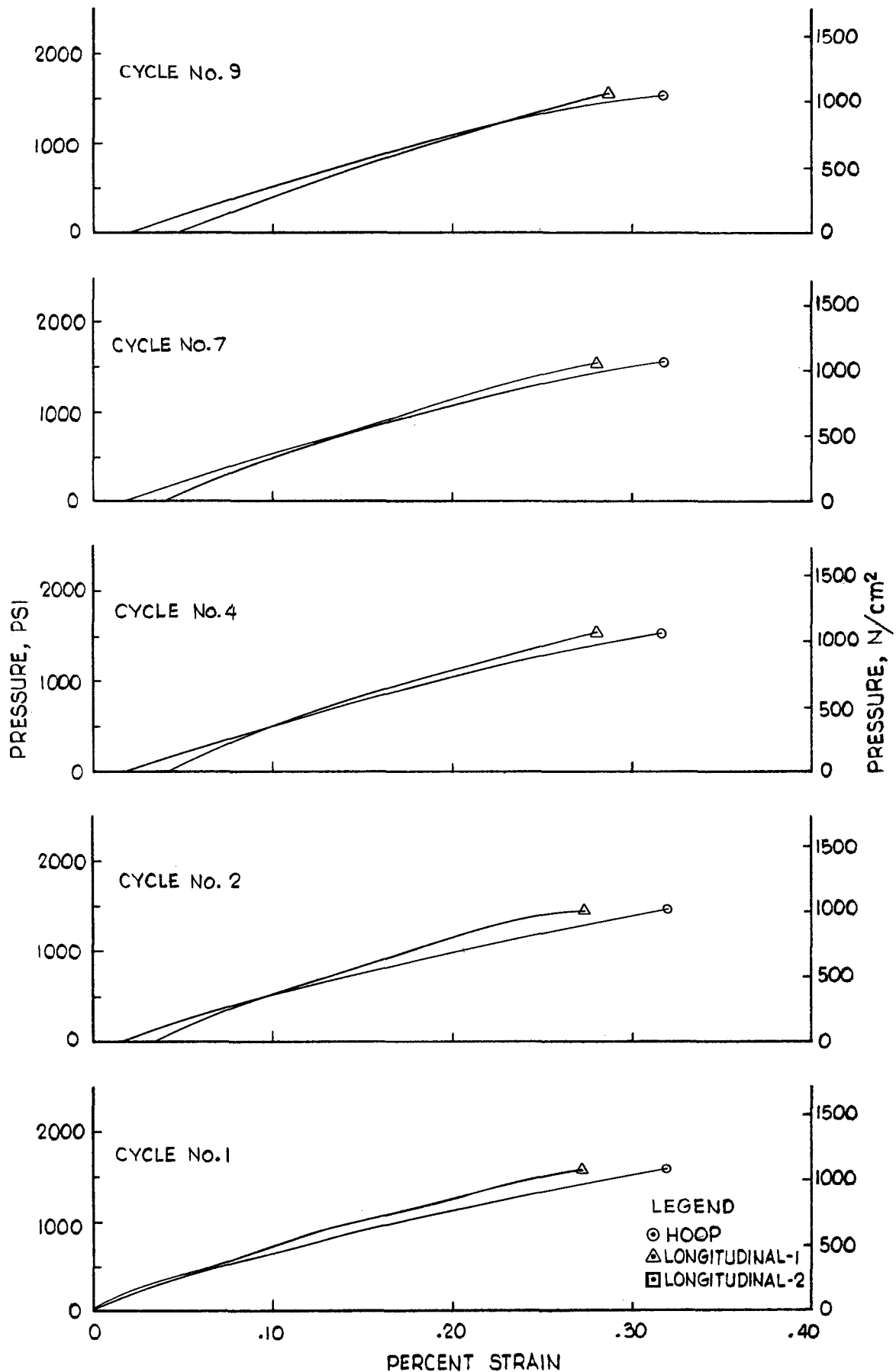


Fig. 35 Post Test Photograph of Tank B-12 Pg. 99



TANK S/N B-12

Page 100

PRESSURE VS STRAIN FOR CYCLE TEST AT 75°F(297°K)

Figure 36

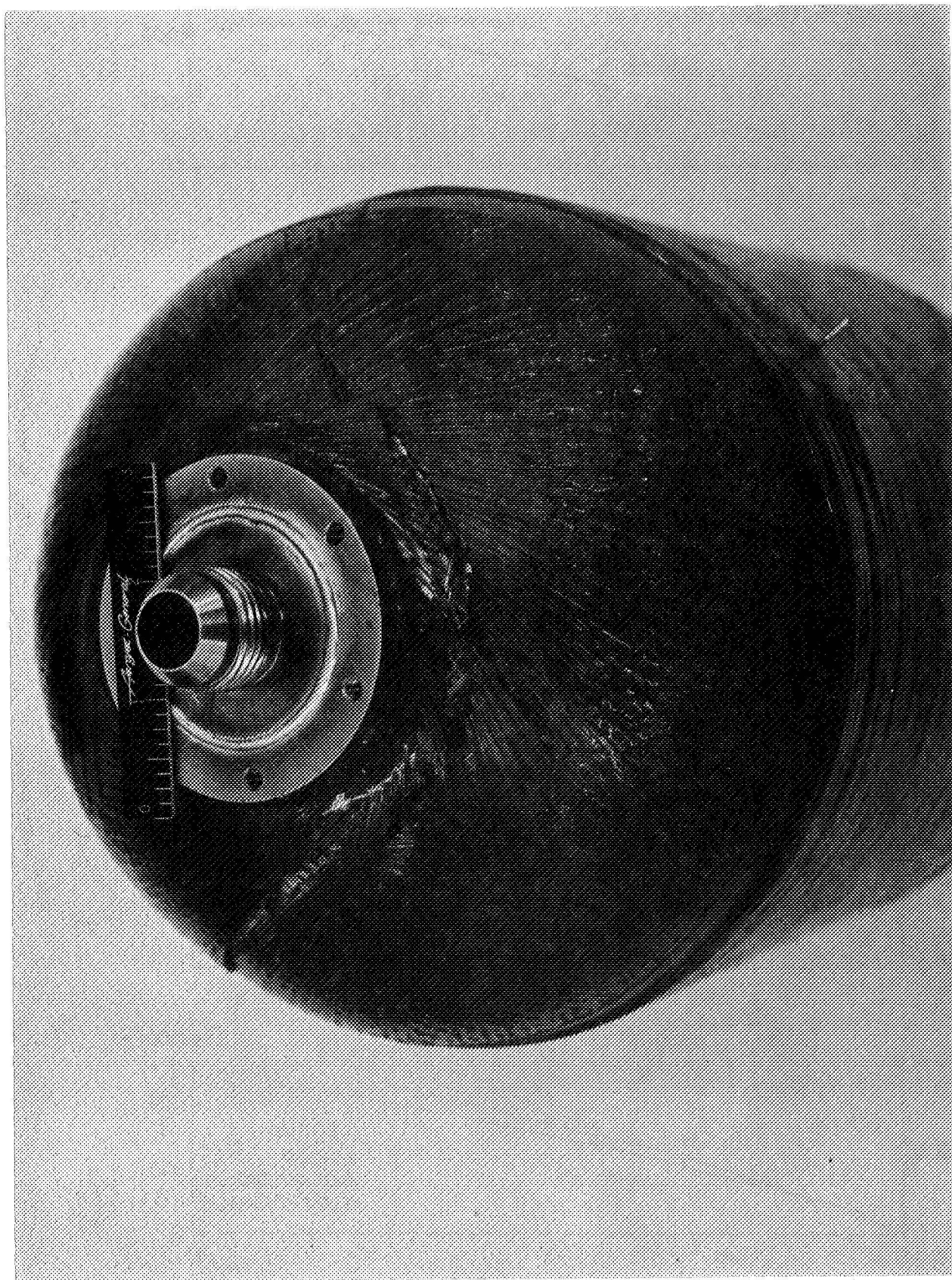
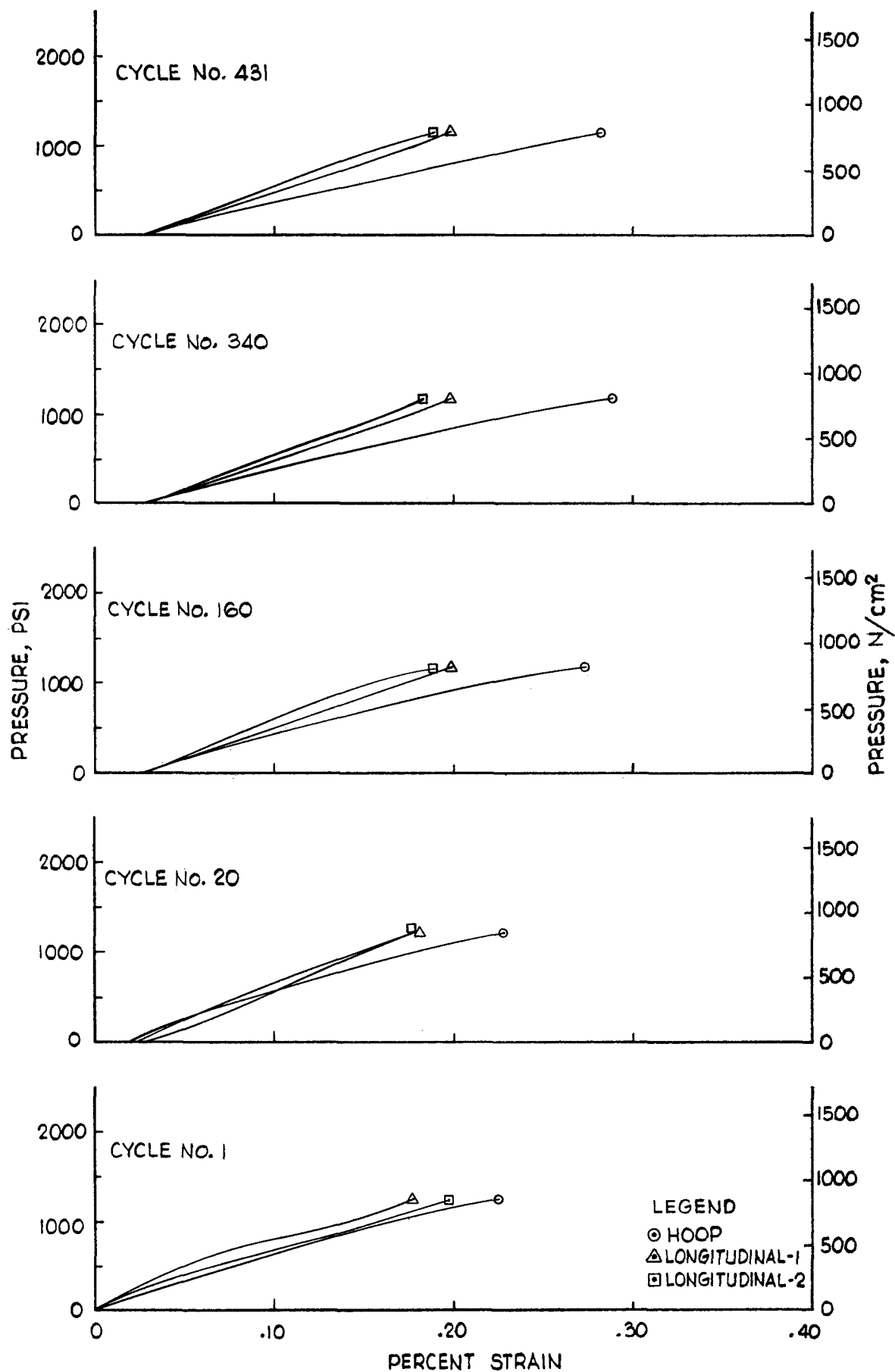


Fig. 37 Post Test Photograph of Tank B-4 Pg. 101



TANK S/N B-4
 PRESSURE VS STRAIN FOR CYCLE TEST AT 75°F(297°K)
 Figure 38

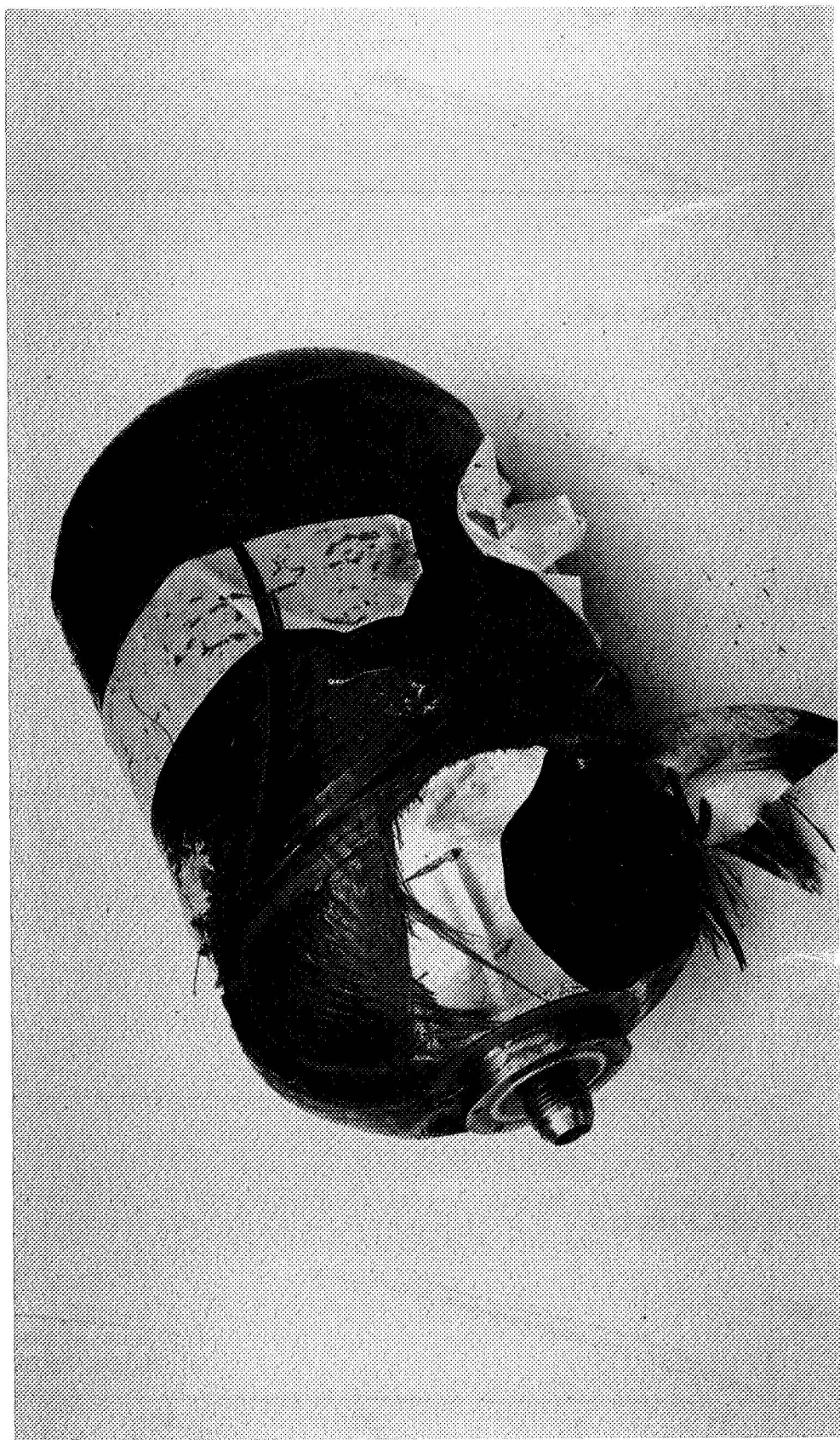
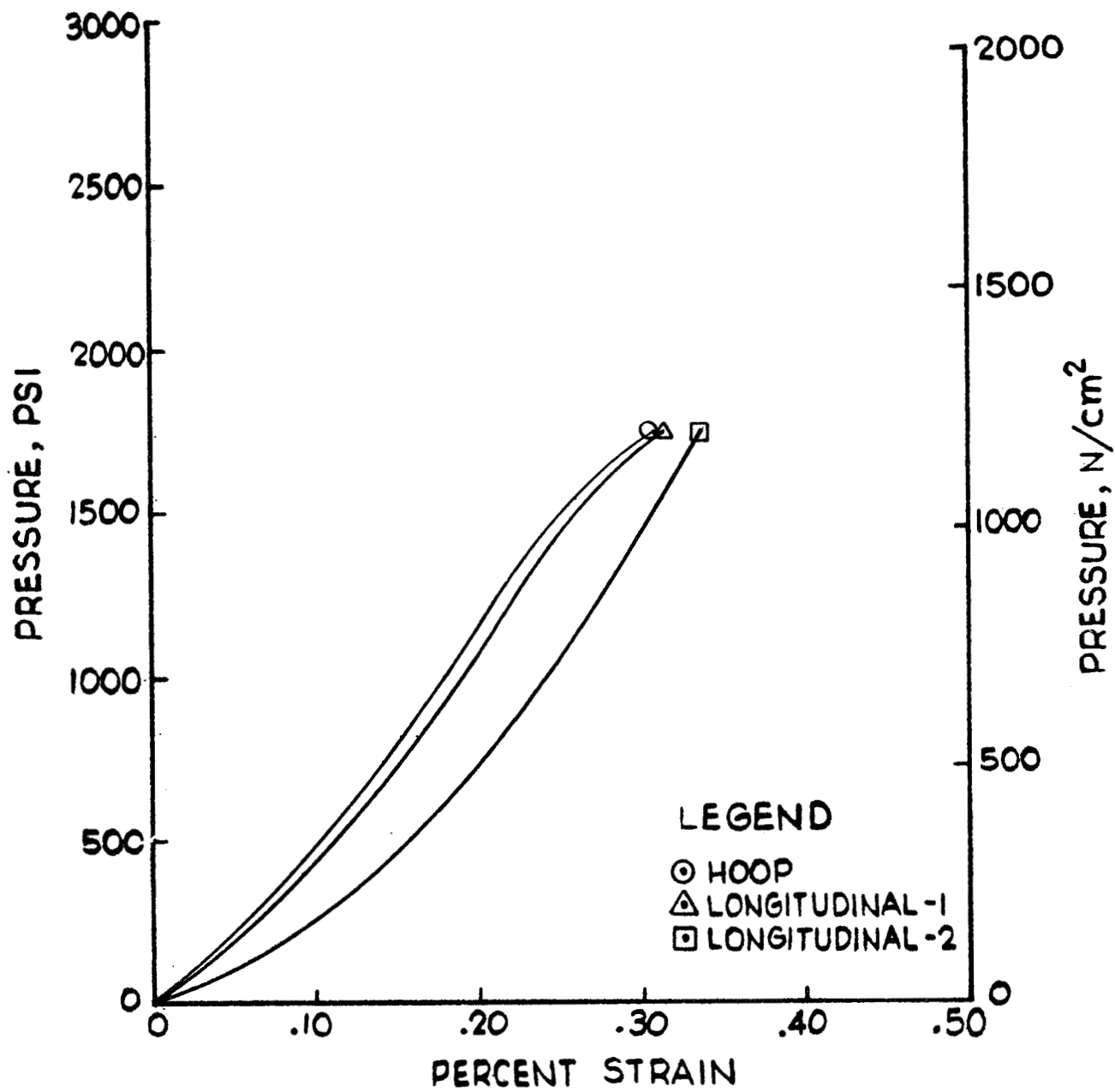


Fig. 39 Post Test Photograph of Tank B-2 Pg. 103



TANK S/N B-2

PRESSURE VS STRAIN FOR BURST TEST AT -320°F (77°K)

Figure 40

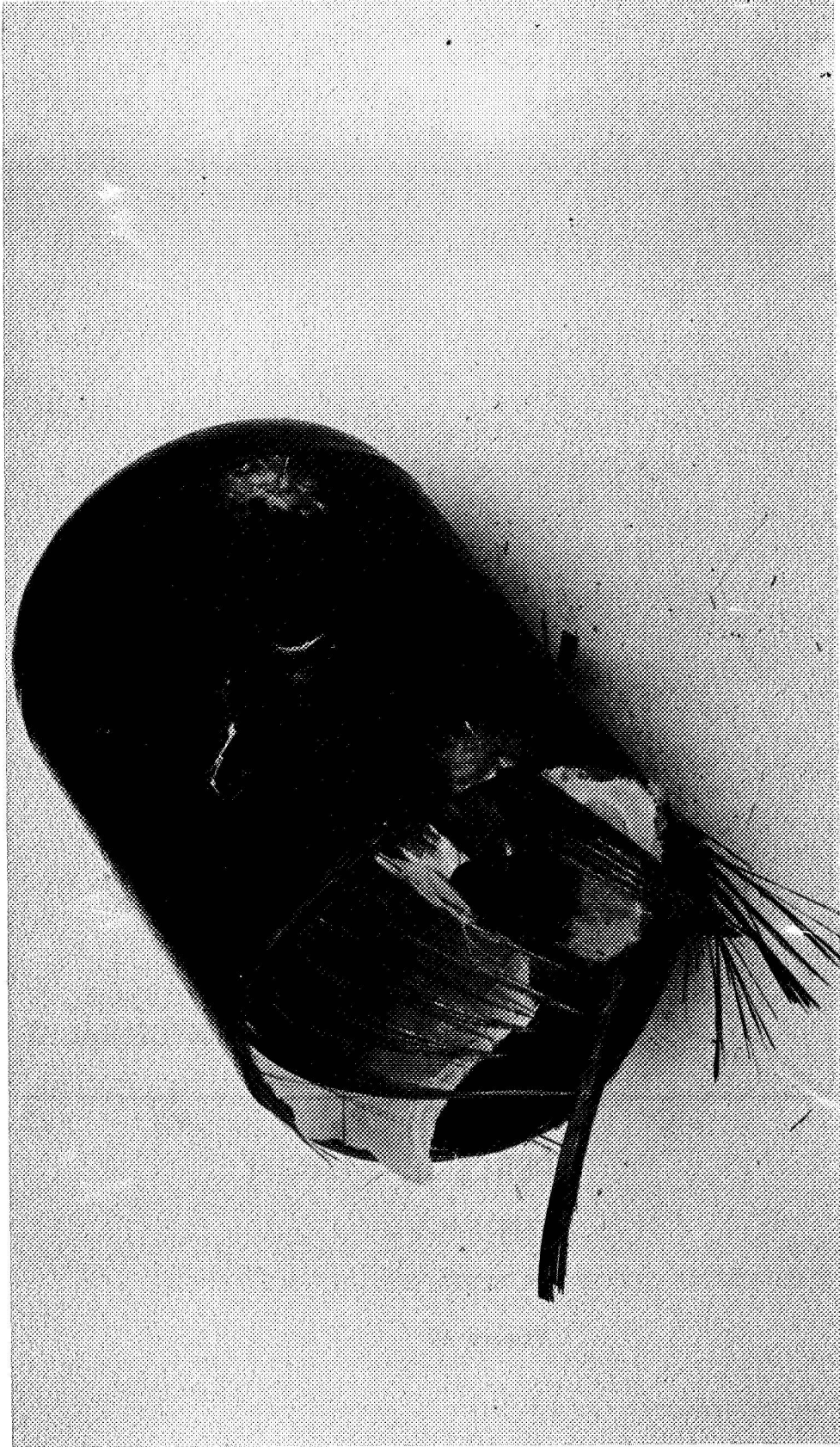
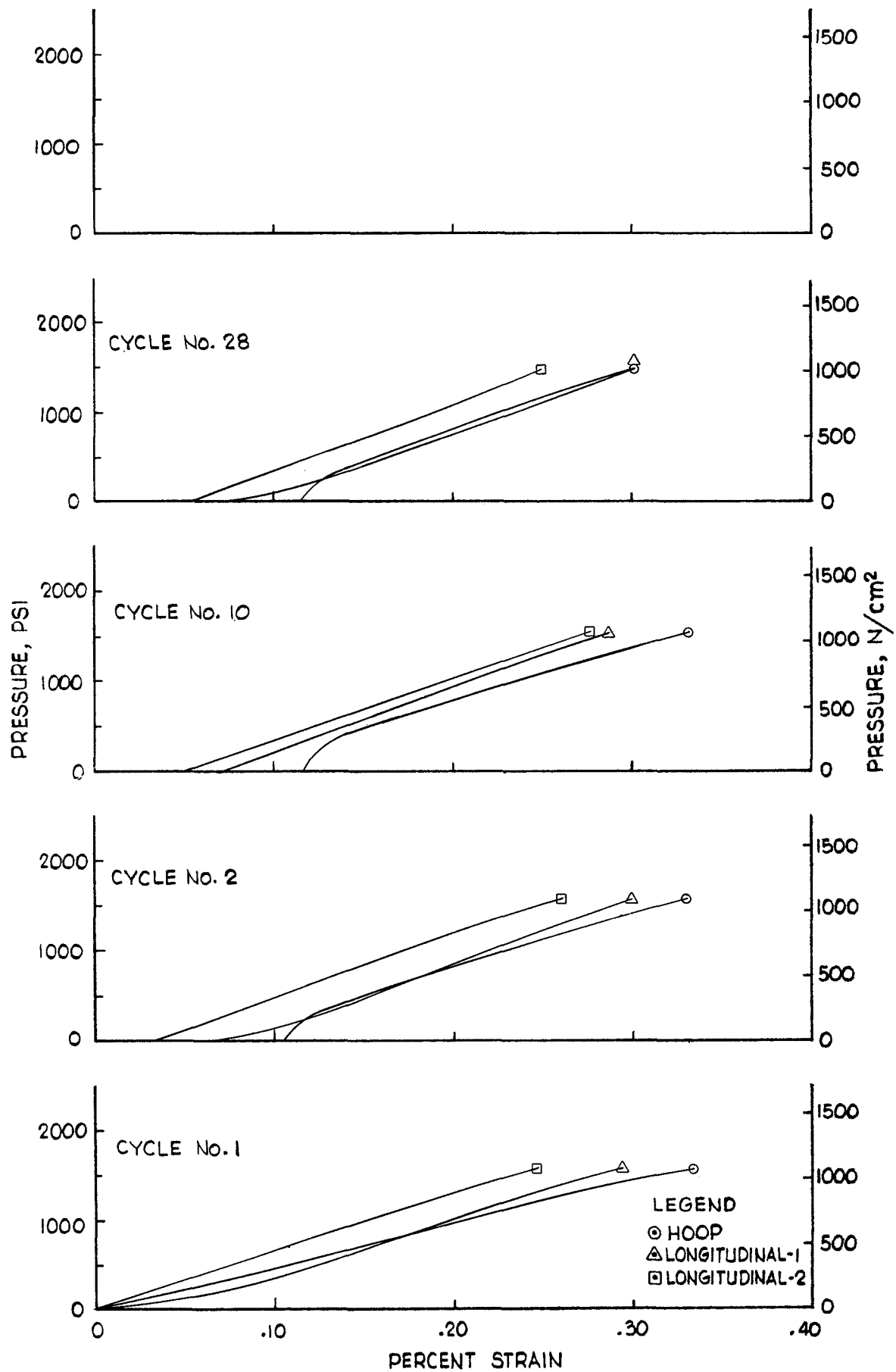


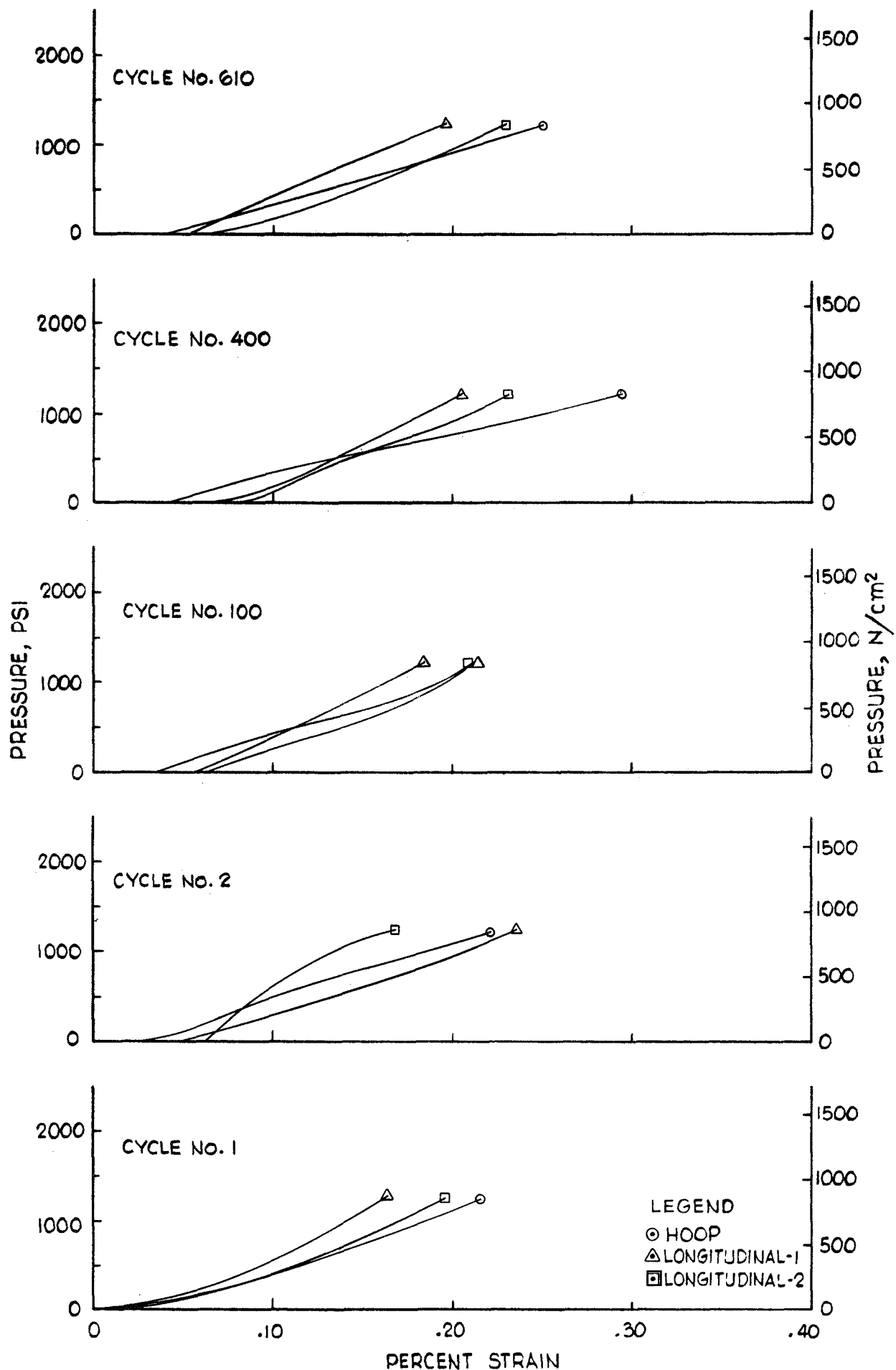
Fig. 41 Post Test Photograph of Tank B-9 Pg. 105



TANK S/N B-9
 PRESSURE VS STRAIN FOR CYCLE TEST AT $-320^{\circ}F (77^{\circ}K)$
 Figure 42



Fig. 43 Post Test Photograph of Tank B-5 Pg. 107



TANK S/N B-5
PRESSURE VS STRAIN FOR CYCLE TEST AT -320°F (77°K)

Figure 44

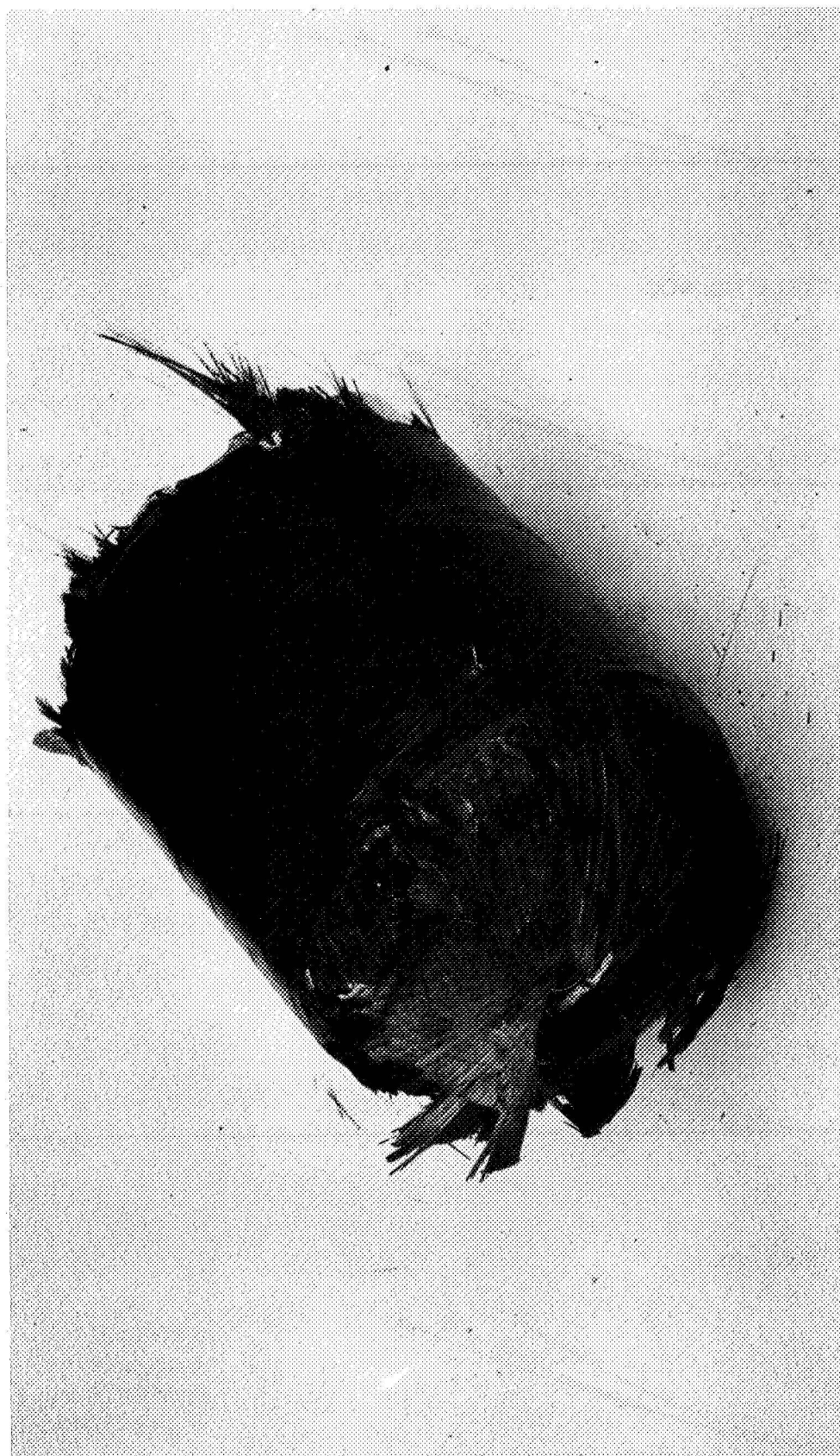


Fig. 45 Post Test Photograph of Tank B-6 Pg. 109

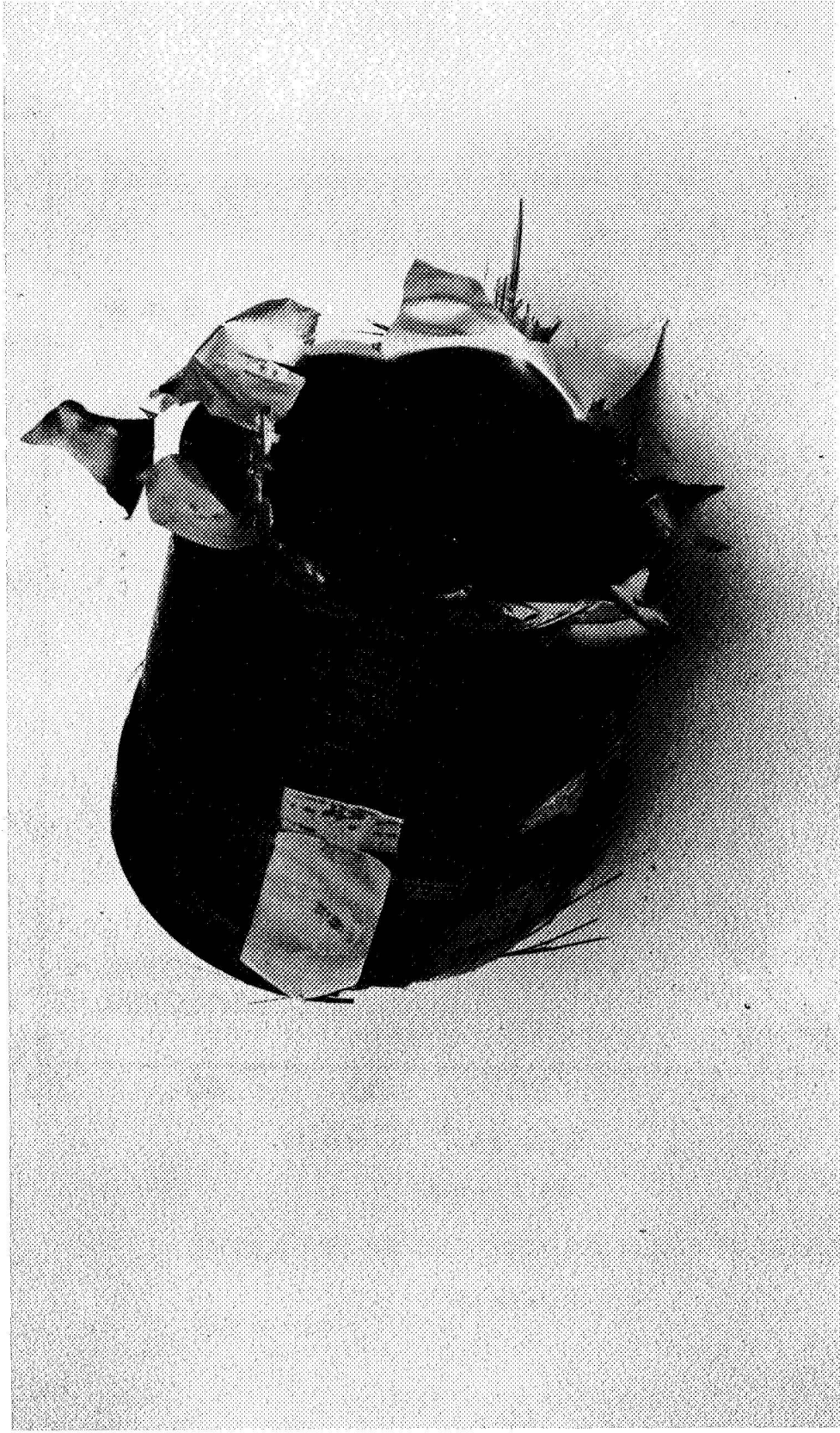
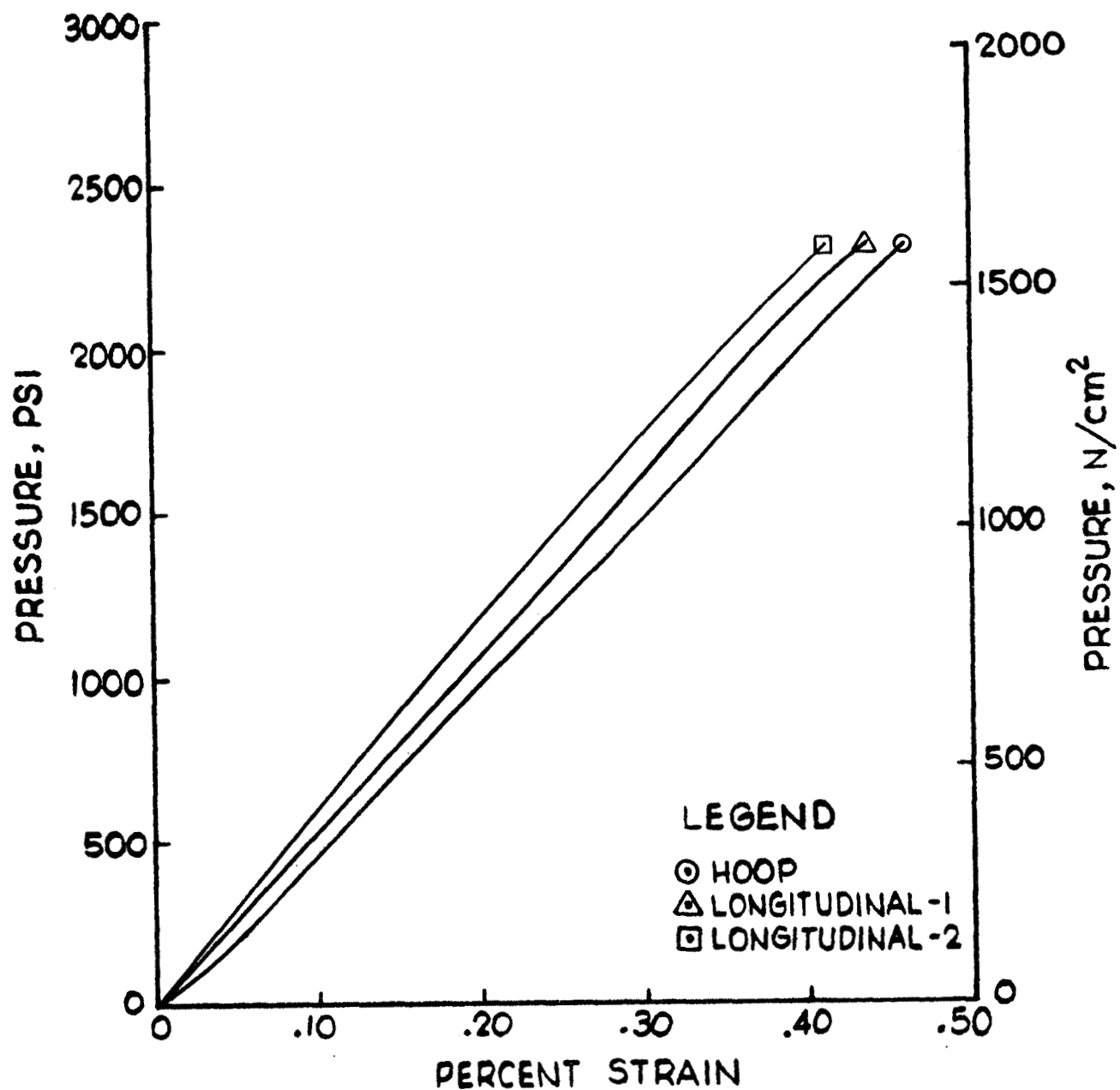


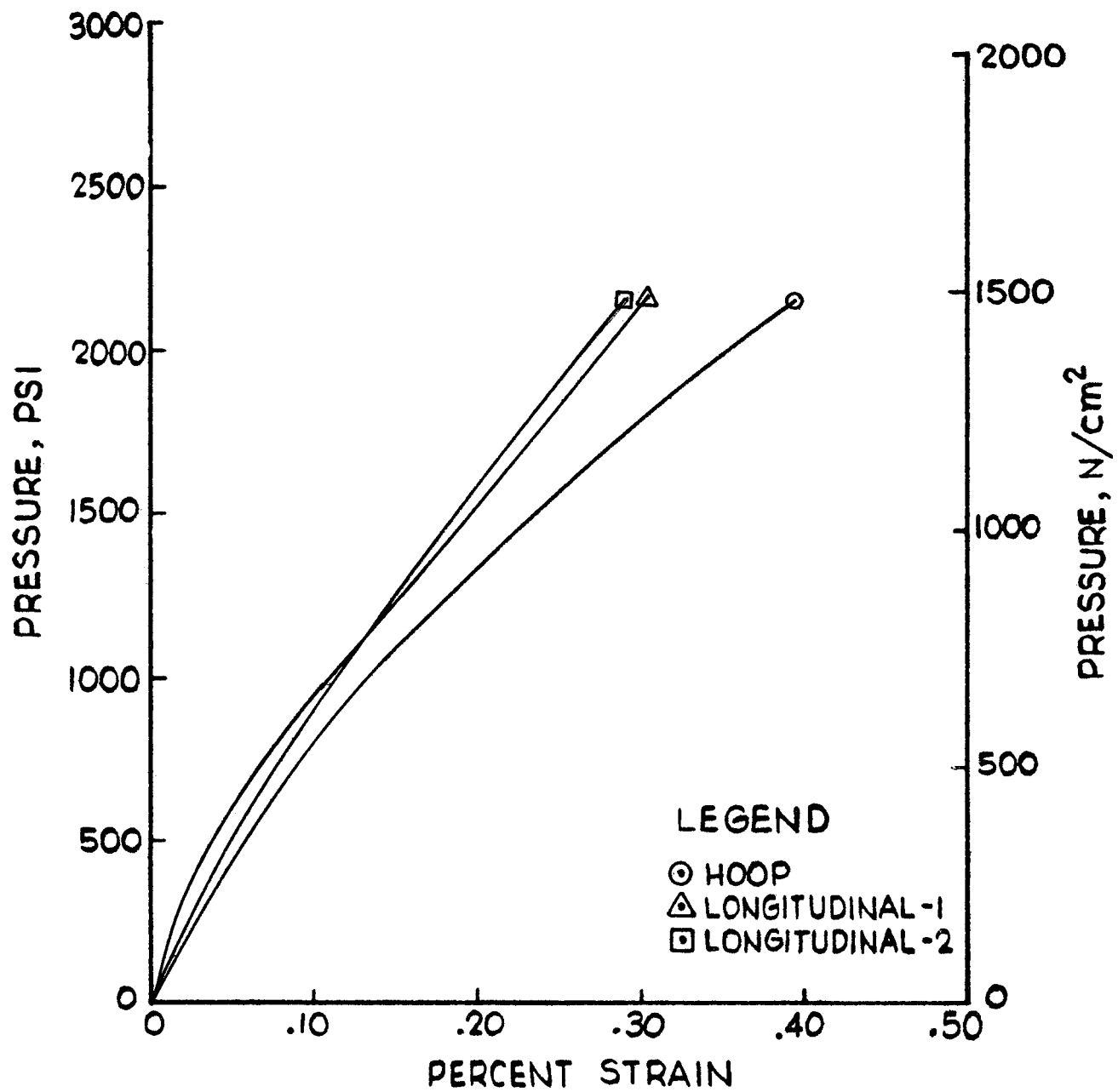
Fig. 46 Post Test Photograph of Tank B-13 Pg. 110



TANK S/N B-6

PRESSURE VS STRAIN FOR BURST TEST AT -423°F (20°K)

Figure 47



TANK S/N B-13

PRESSURE VS STRAIN FOR BURST TEST AT -423°F (20°K)

Figure 48

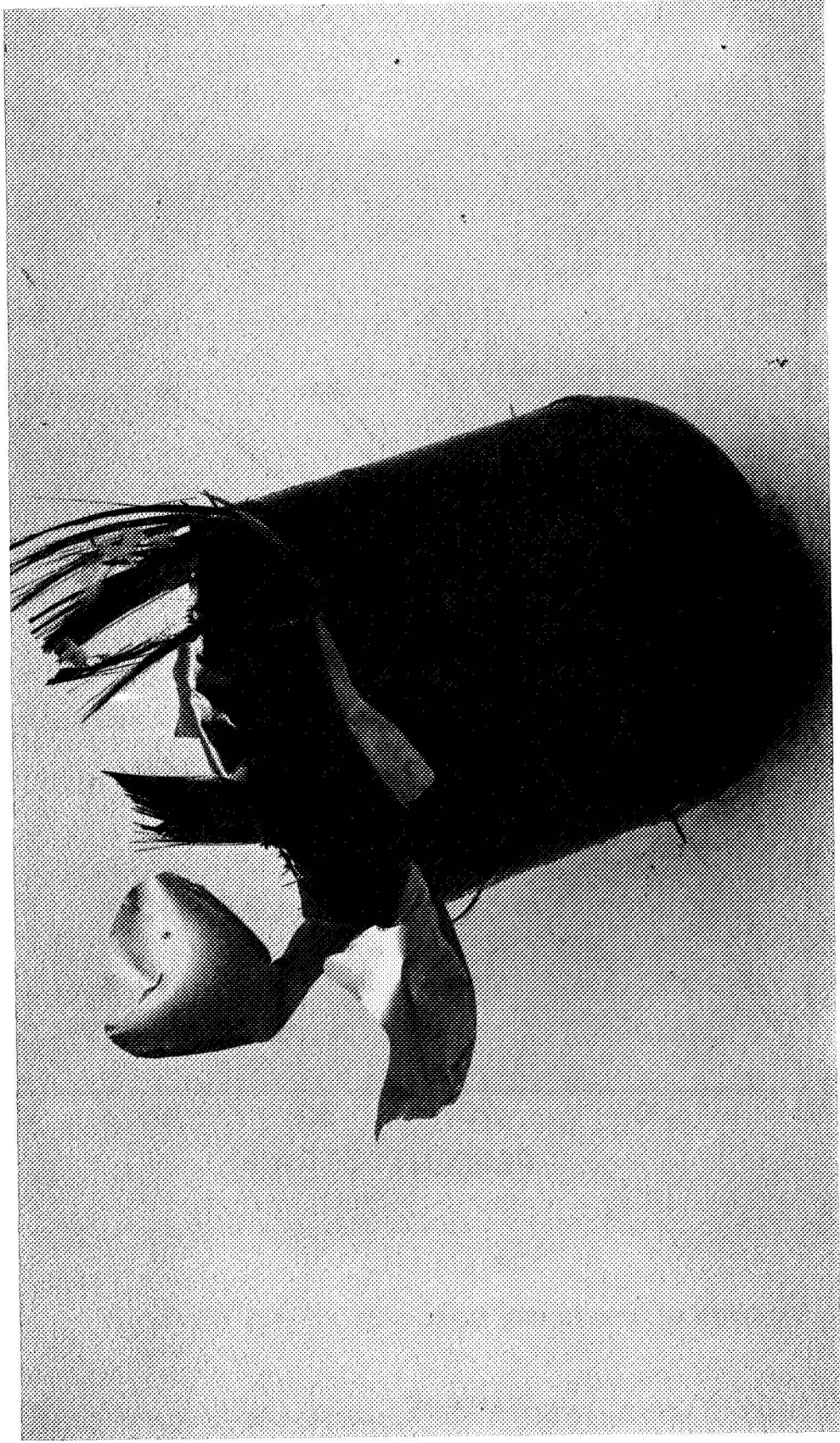


Fig. 49 Post Test Photograph of Tank B-10 Pg. 113

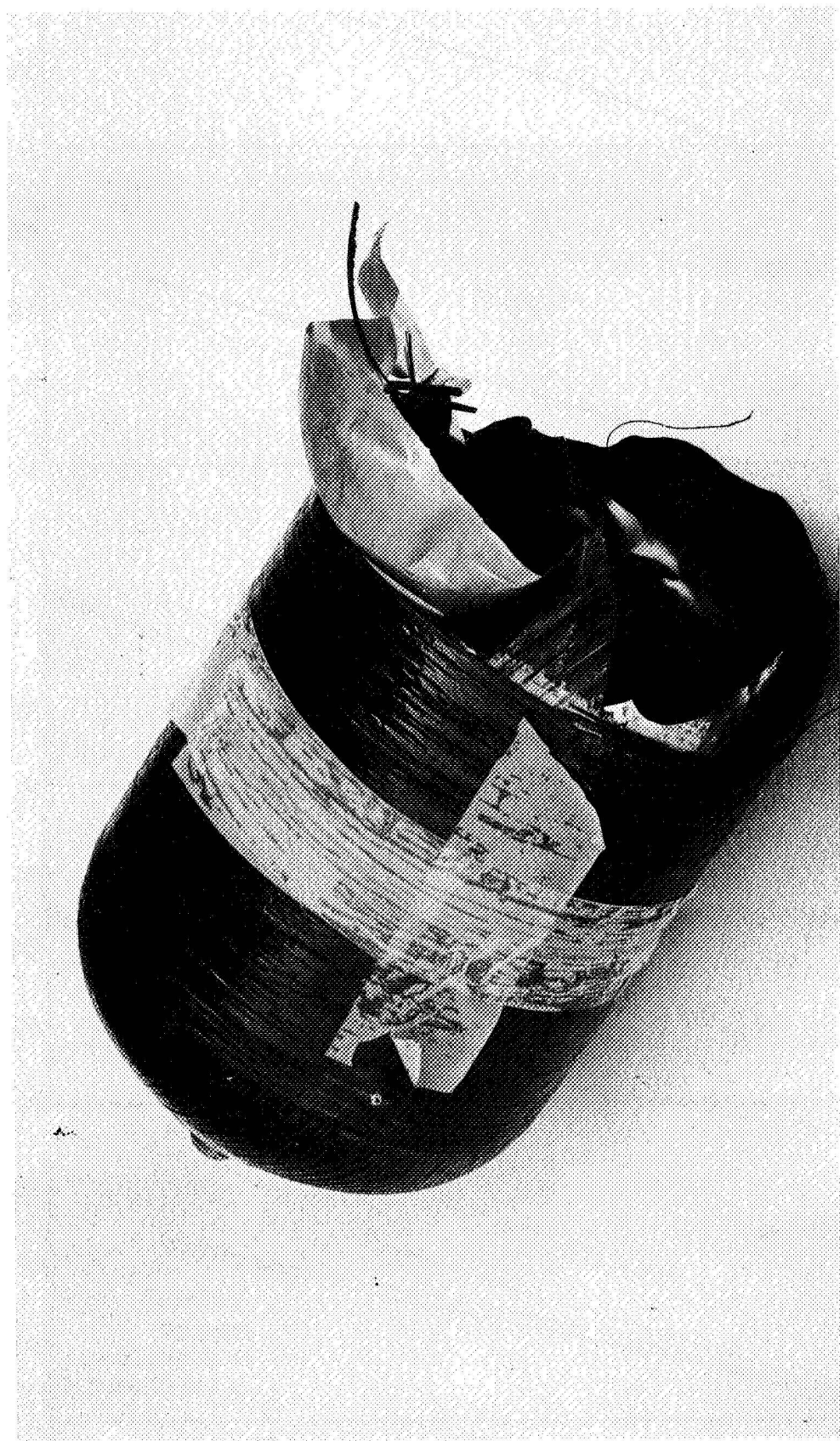
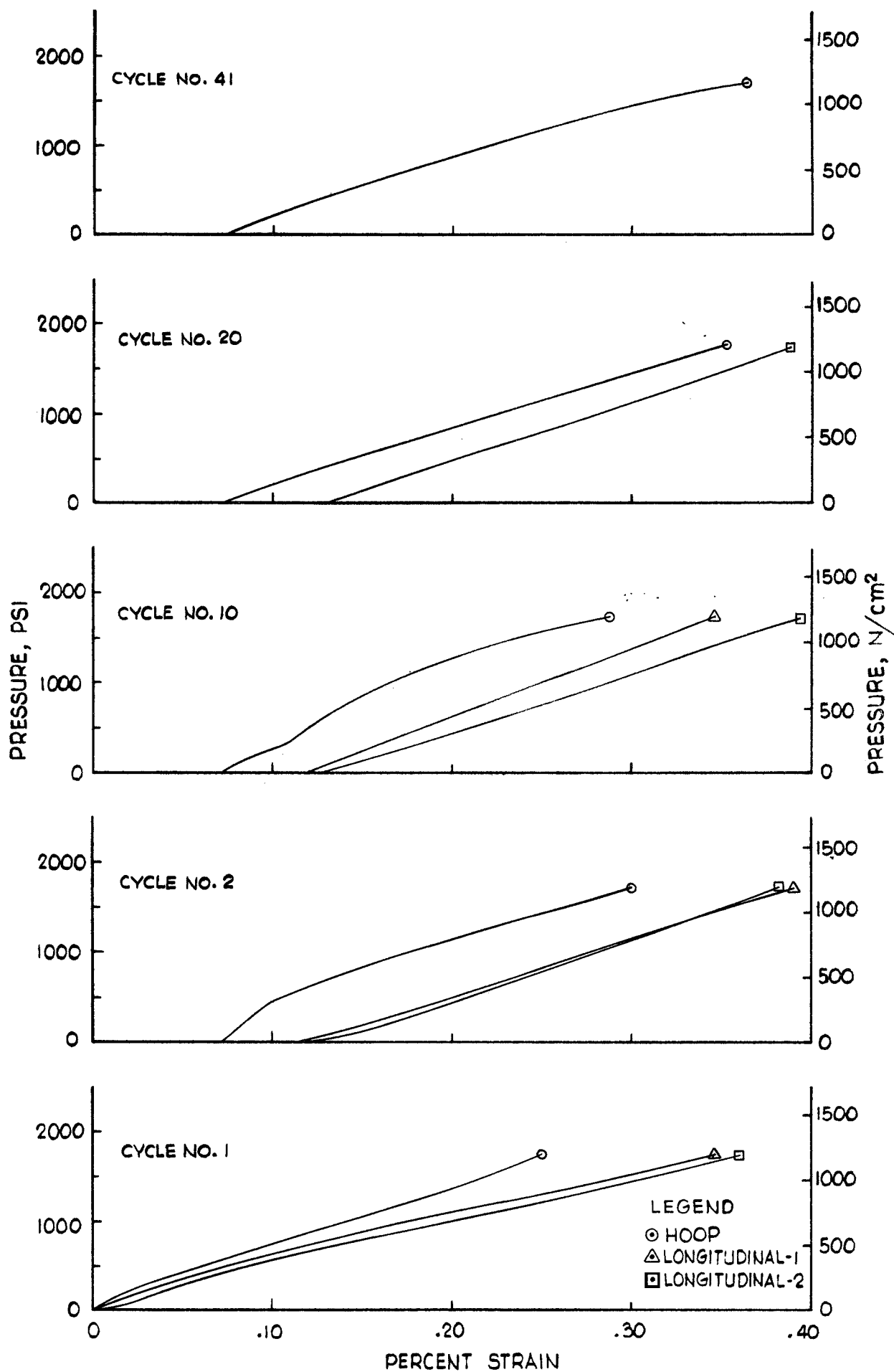
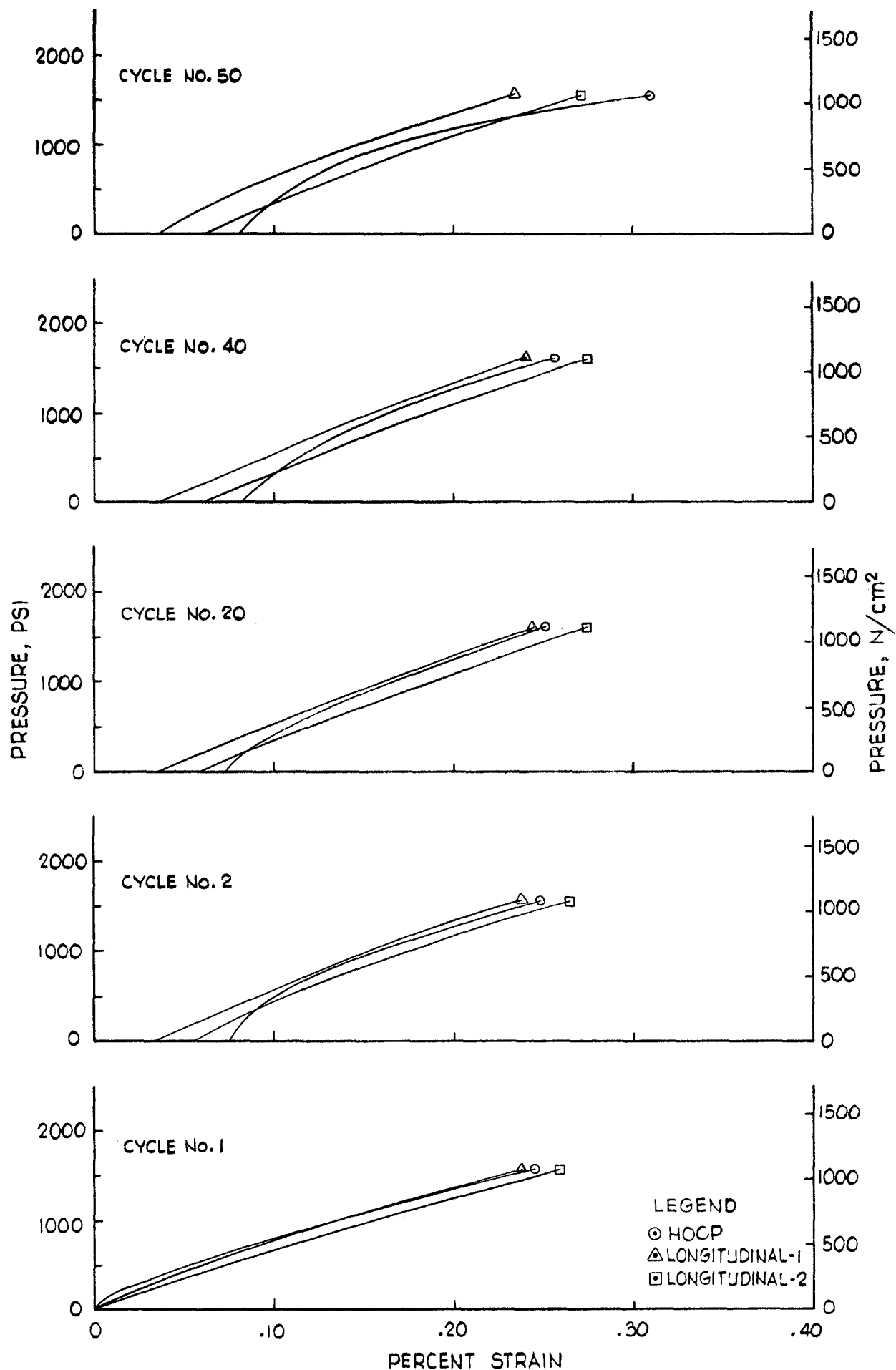


Fig. 50 Post Test Photograph of Tank B-11 Pg. 114



TANK S/N B-10
 PRESSURE VS STRAIN FOR CYCLE TEST AT -423°F (20°K)
 Figure 51



TANK S/N B-11
PRESSURE VS STRAIN FOR CYCLE TEST AT -423°F (20°K)

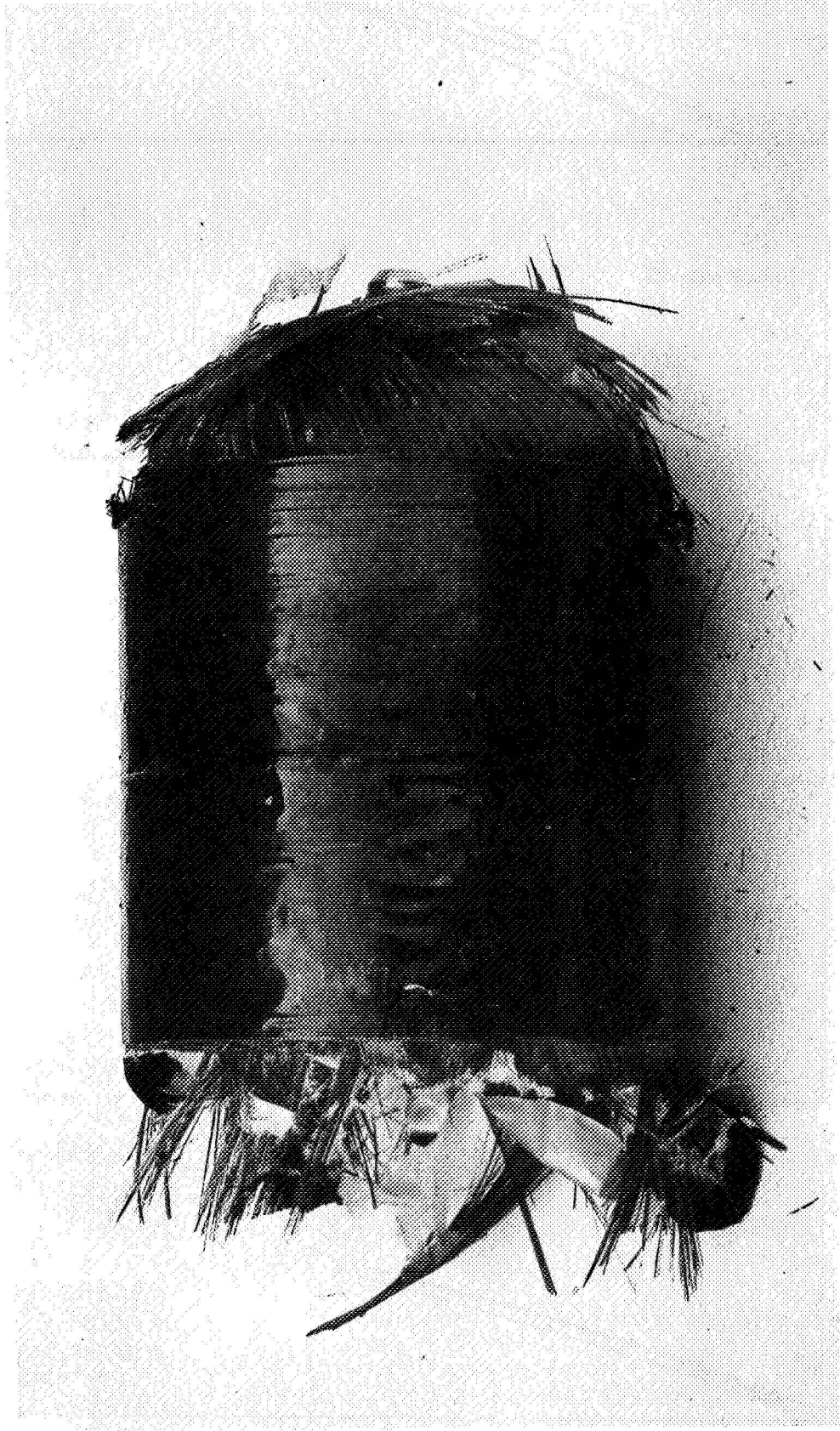
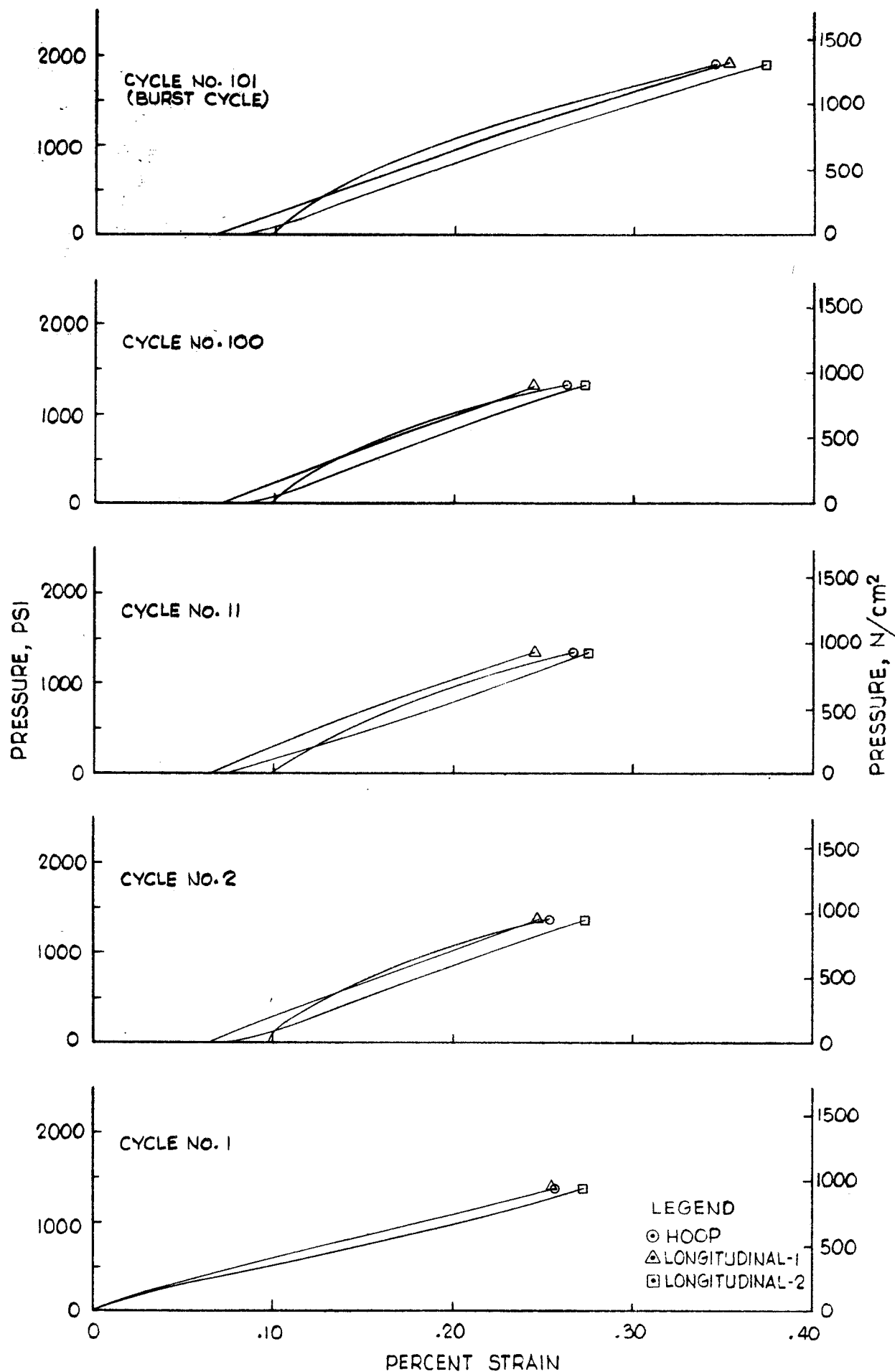


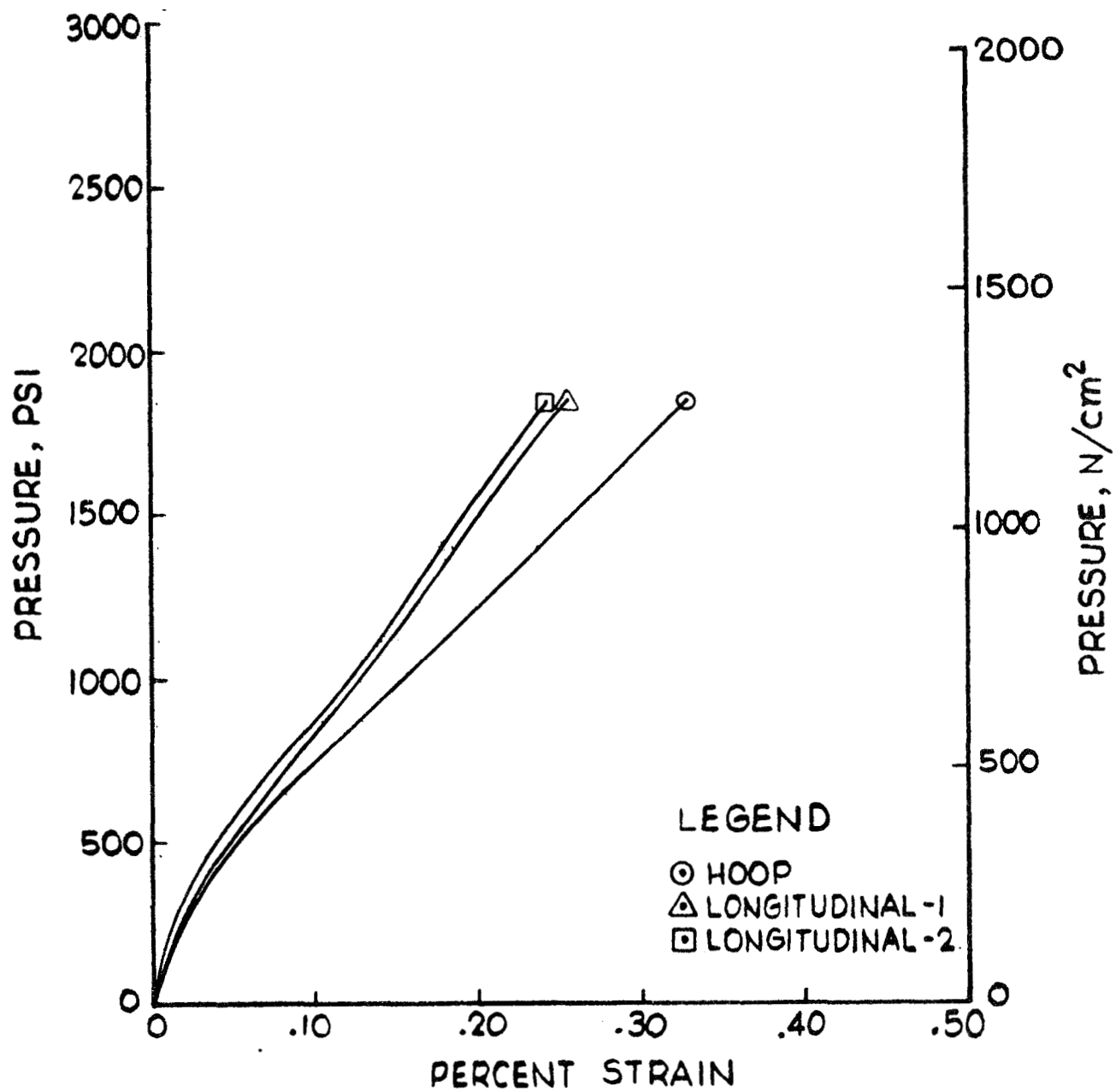
Fig. 53 Post Test Photograph of Tank B-8 Pg. 117



TANK S/N B-8
 PRESSURE VS STRAIN FOR CYCLE TEST AT -423°F (20°K)
 Figure 54



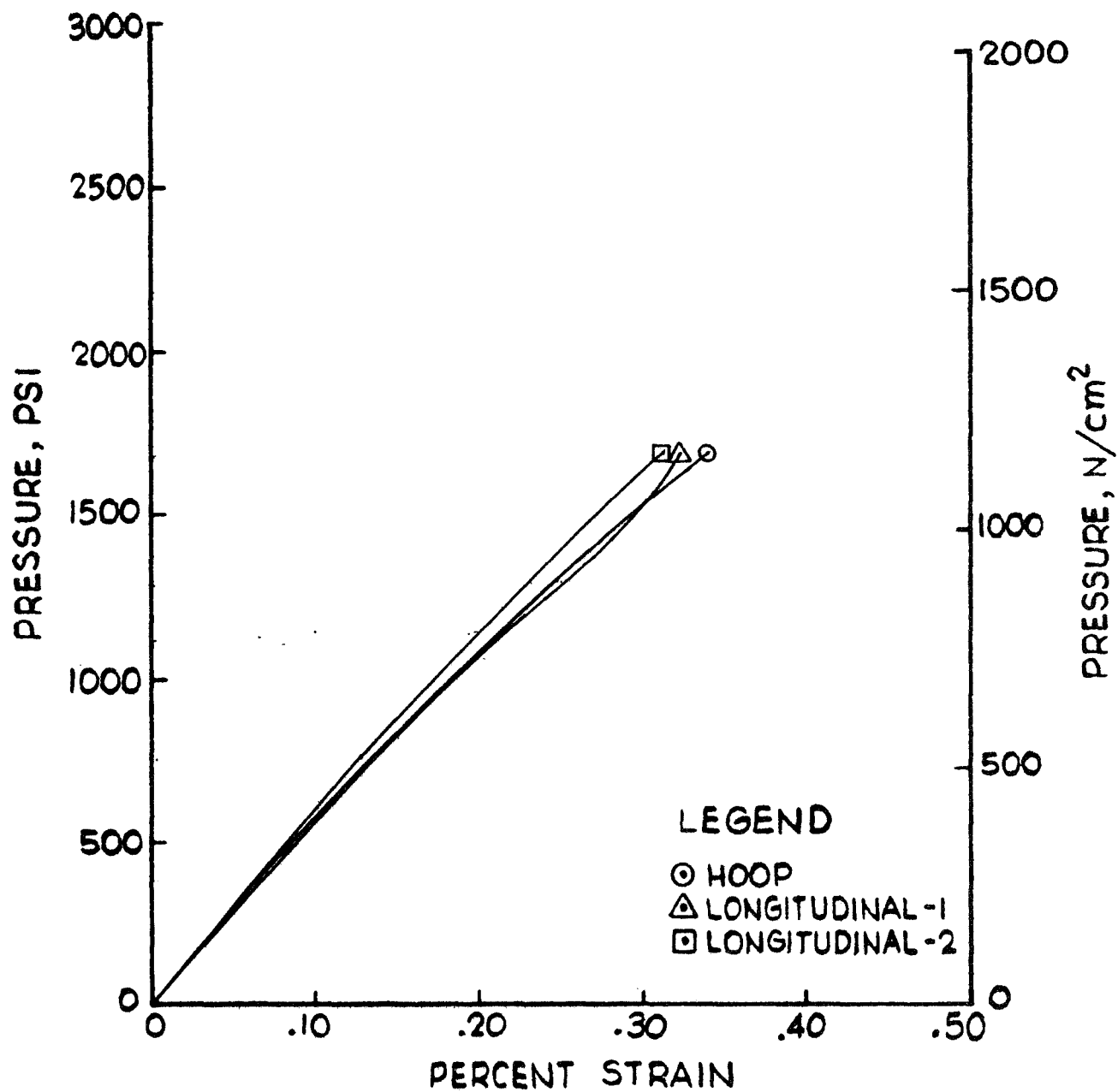
Fig. 55 Post Test Photograph of Tank BB-1 Pg. 119



TANK S/N BB-1

PRESSURE VS STRAIN FOR BURST TEST AT 75°F(297°K)

Figure 56



TANK S/N BB-2

PRESSURE VS STRAIN FOR BURST TEST AT 75°F (297°K)

Figure 57

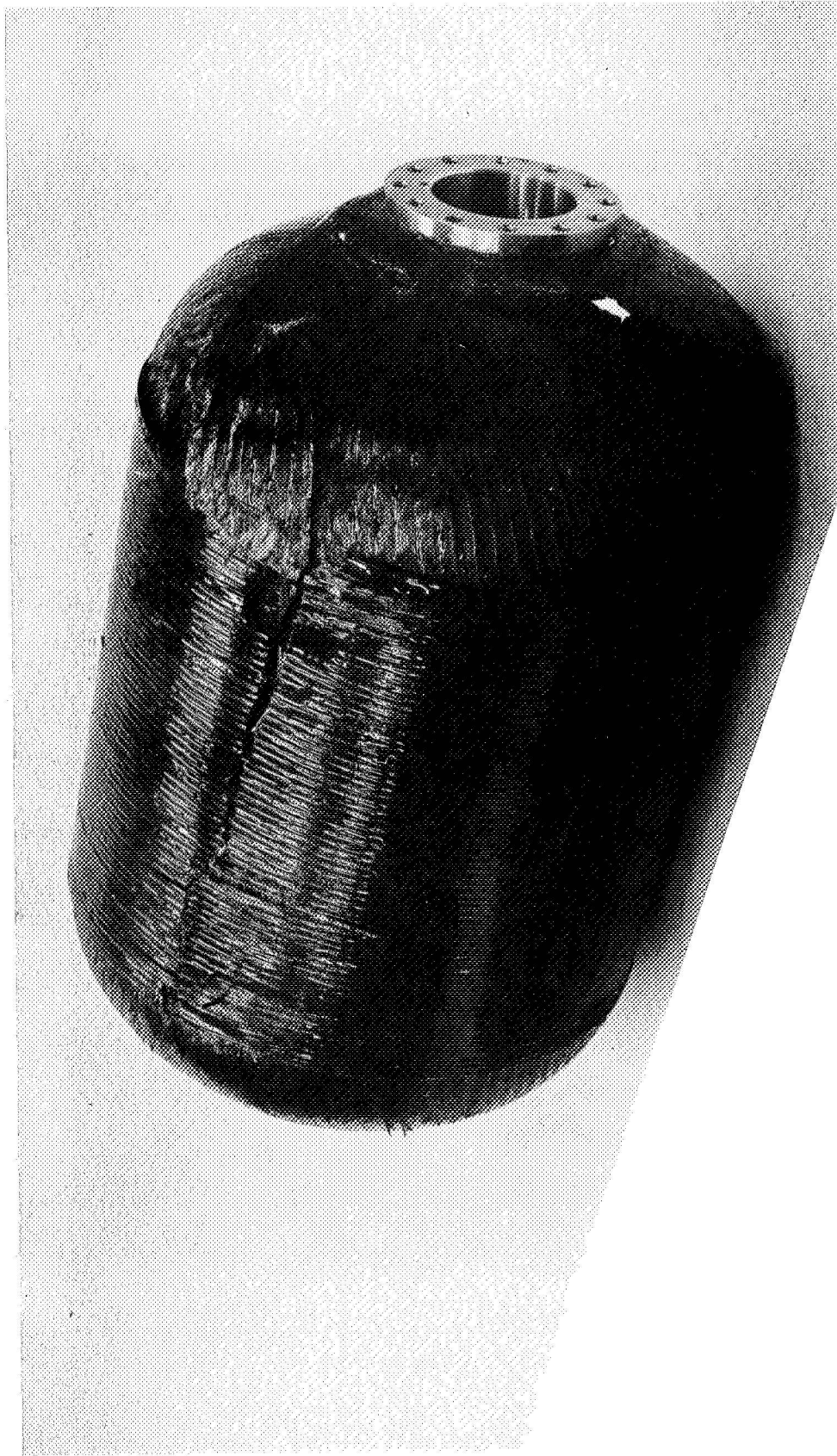


Fig. 58 Post Test Photograph of Tank BB-2 Pg. 122

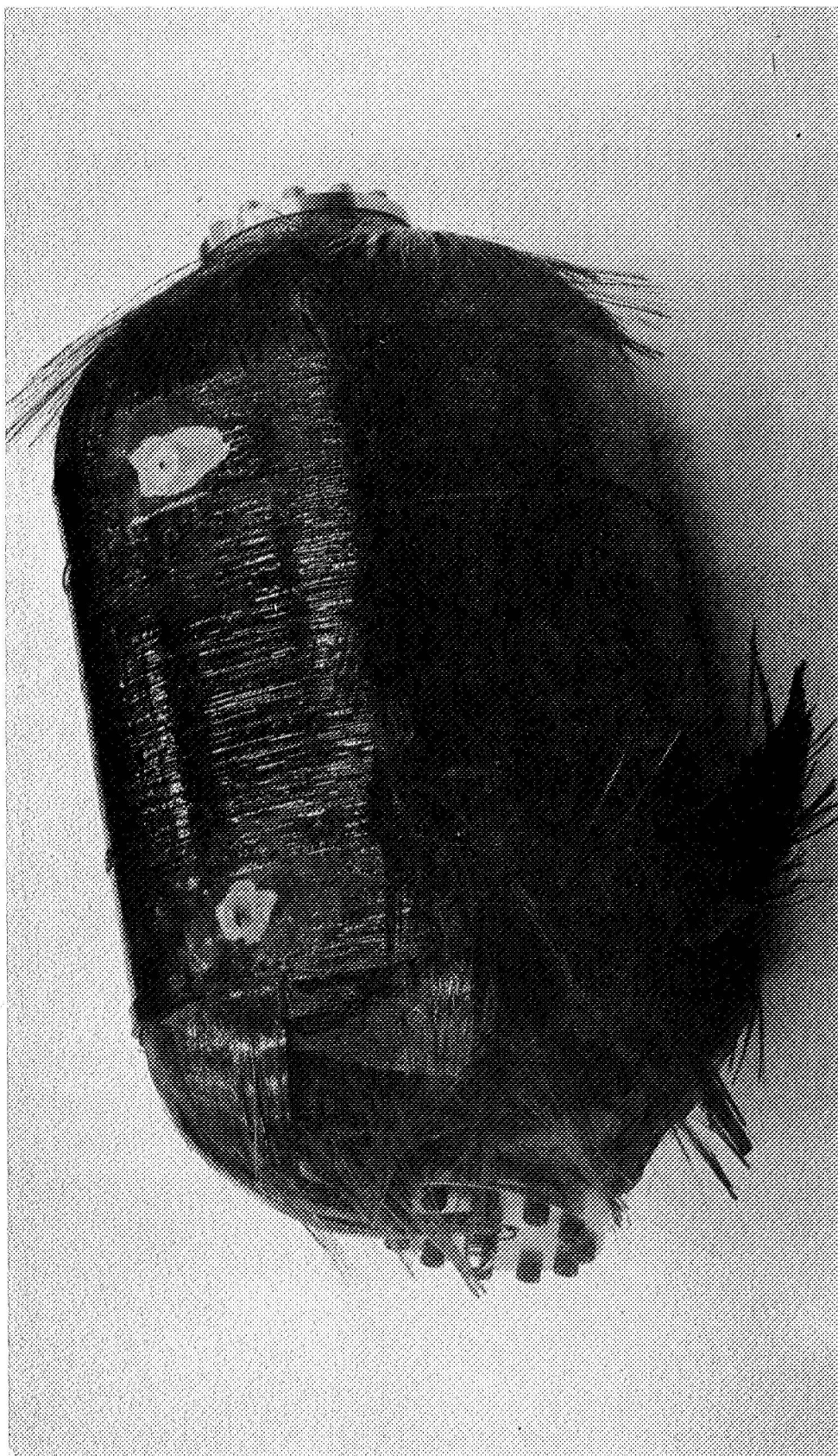
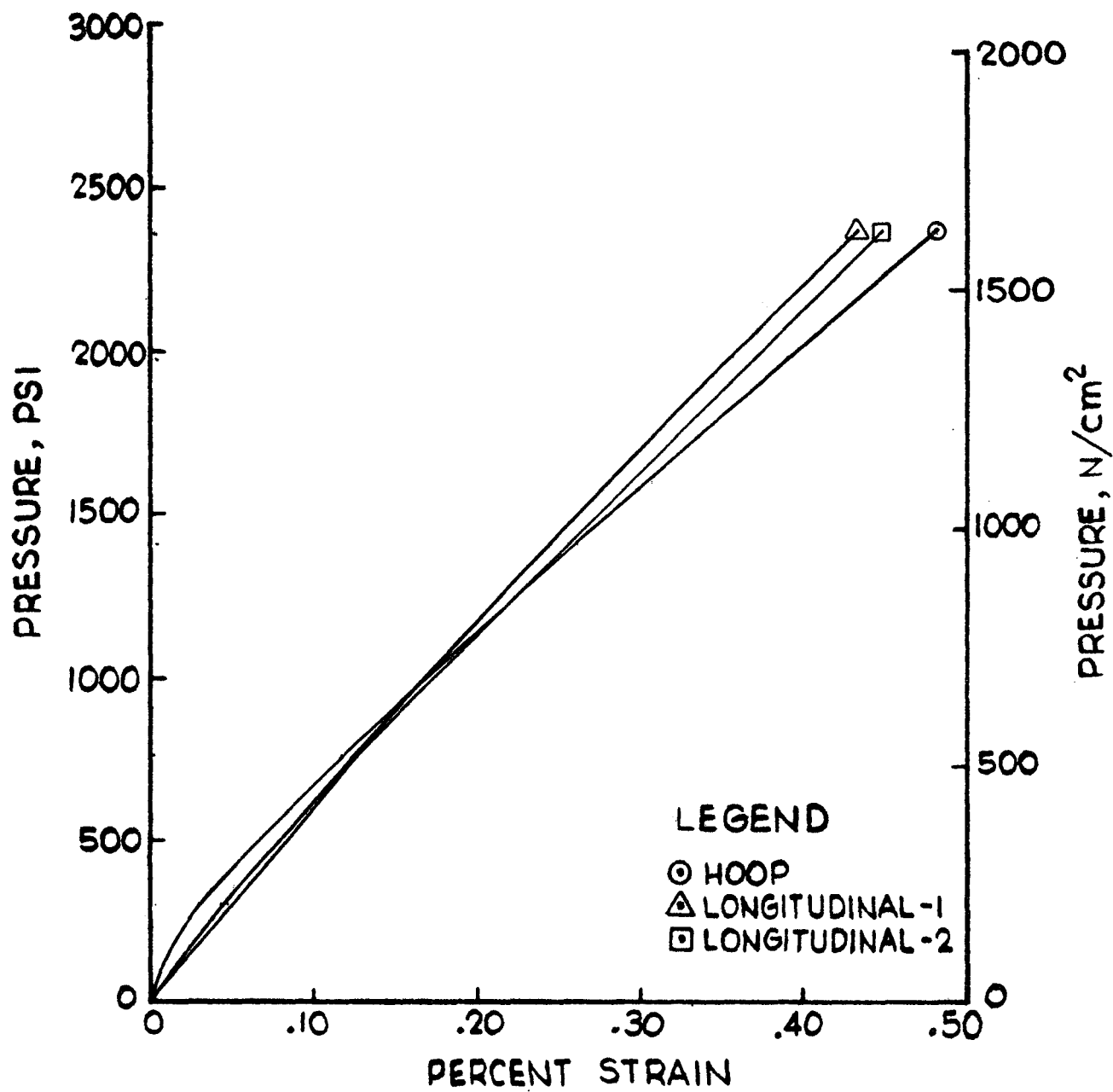


Fig. 59 Post Test Photograph of Tank BB-11 Pg. 123



TANK S/N BB-11

PRESSURE VS STRAIN FOR BURST TEST AT 75°F (297°K)

Figure 60

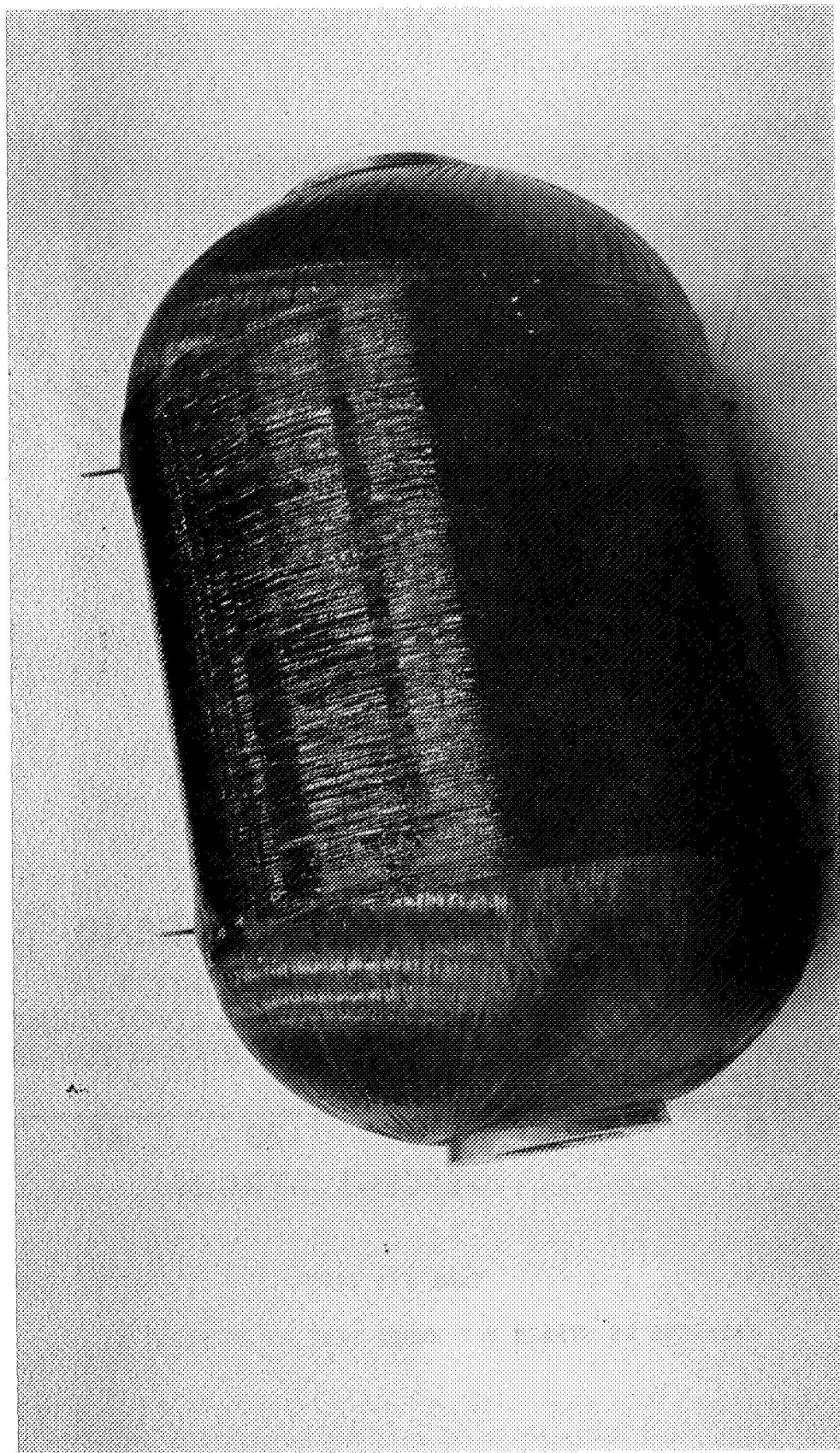


Fig. 61 Post Test Photograph of Tank BB-7 Pg. 125

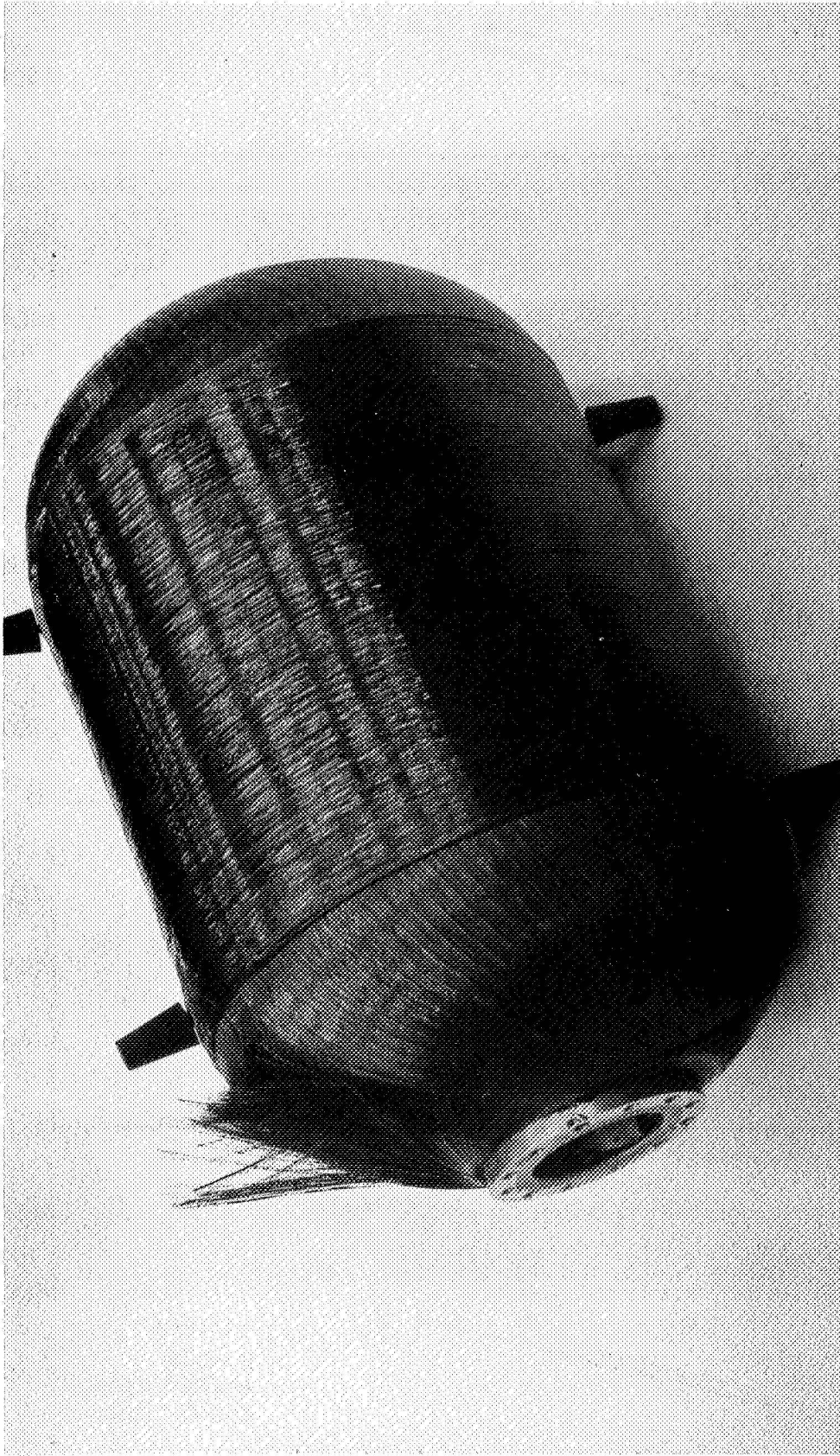
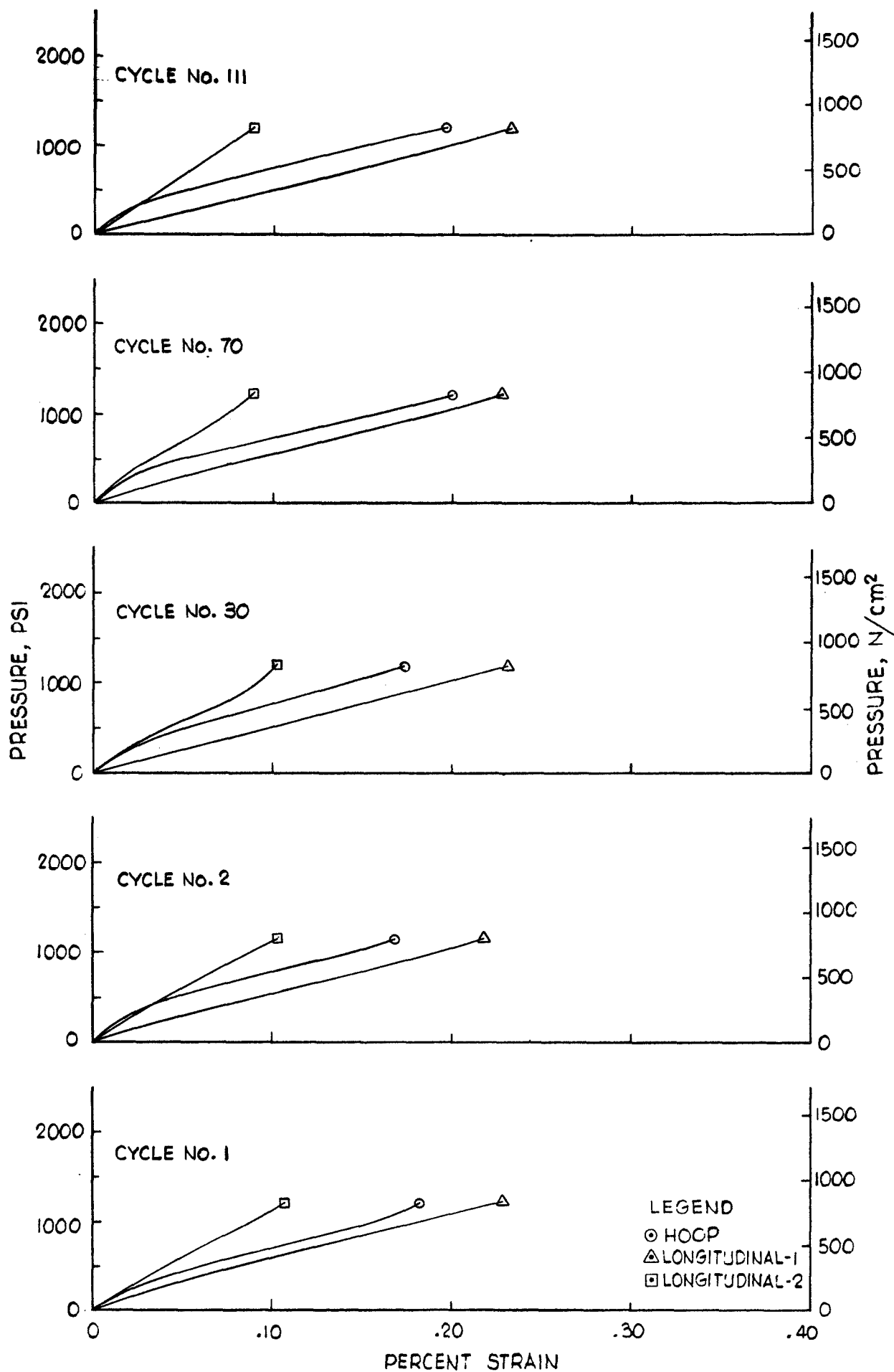
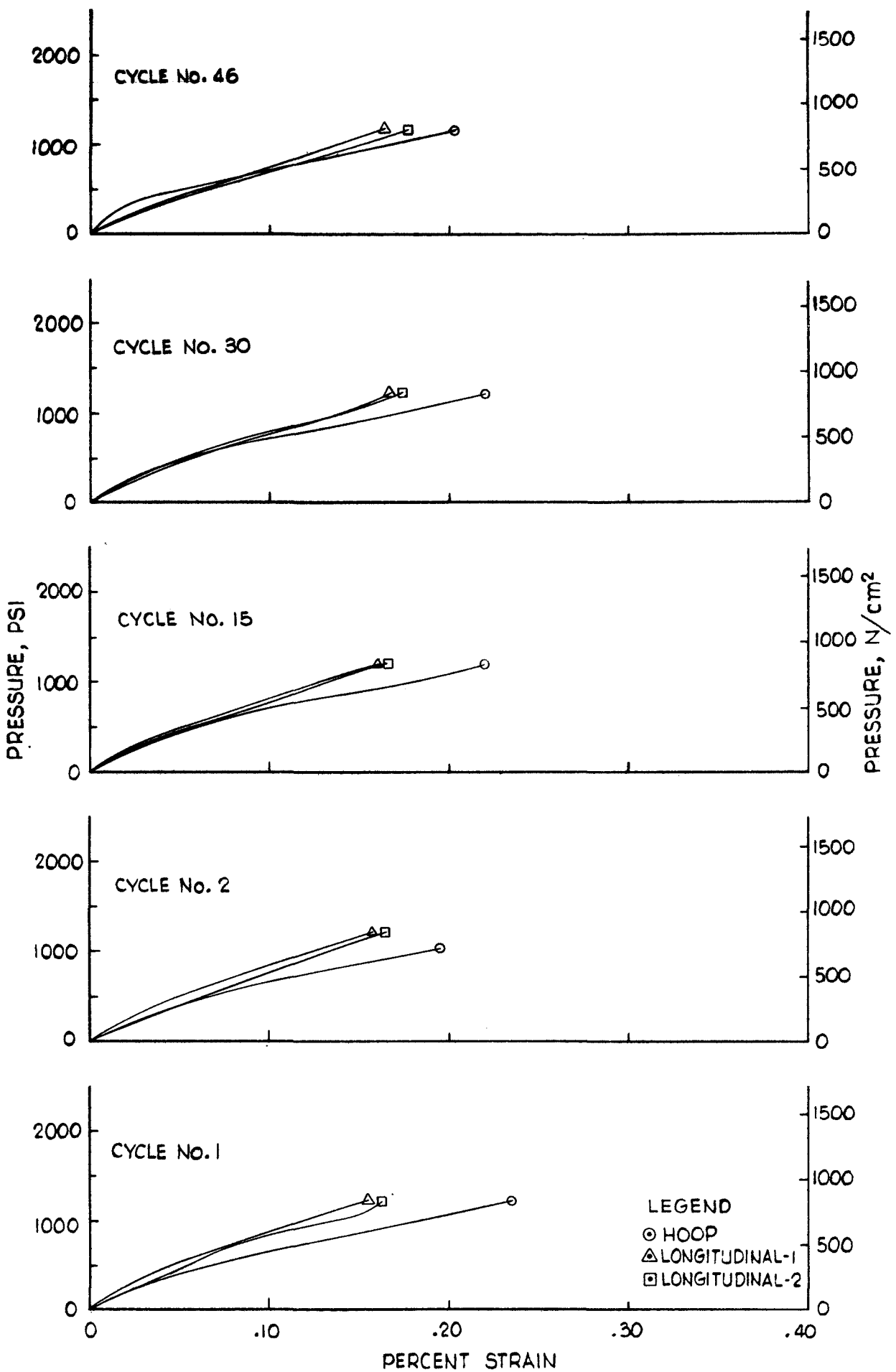


Fig. 62 Post Test Photograph of Tank BB-8 Pg. 126



TANK S/N BB-7
 PRESSURE VS STRAIN FOR CYCLE TEST AT 75°F(297°K)
 Figure 63



TANK S/N BB-8
 PRESSURE VS STRAIN FOR CYCLE TEST AT 75°F(297°K)

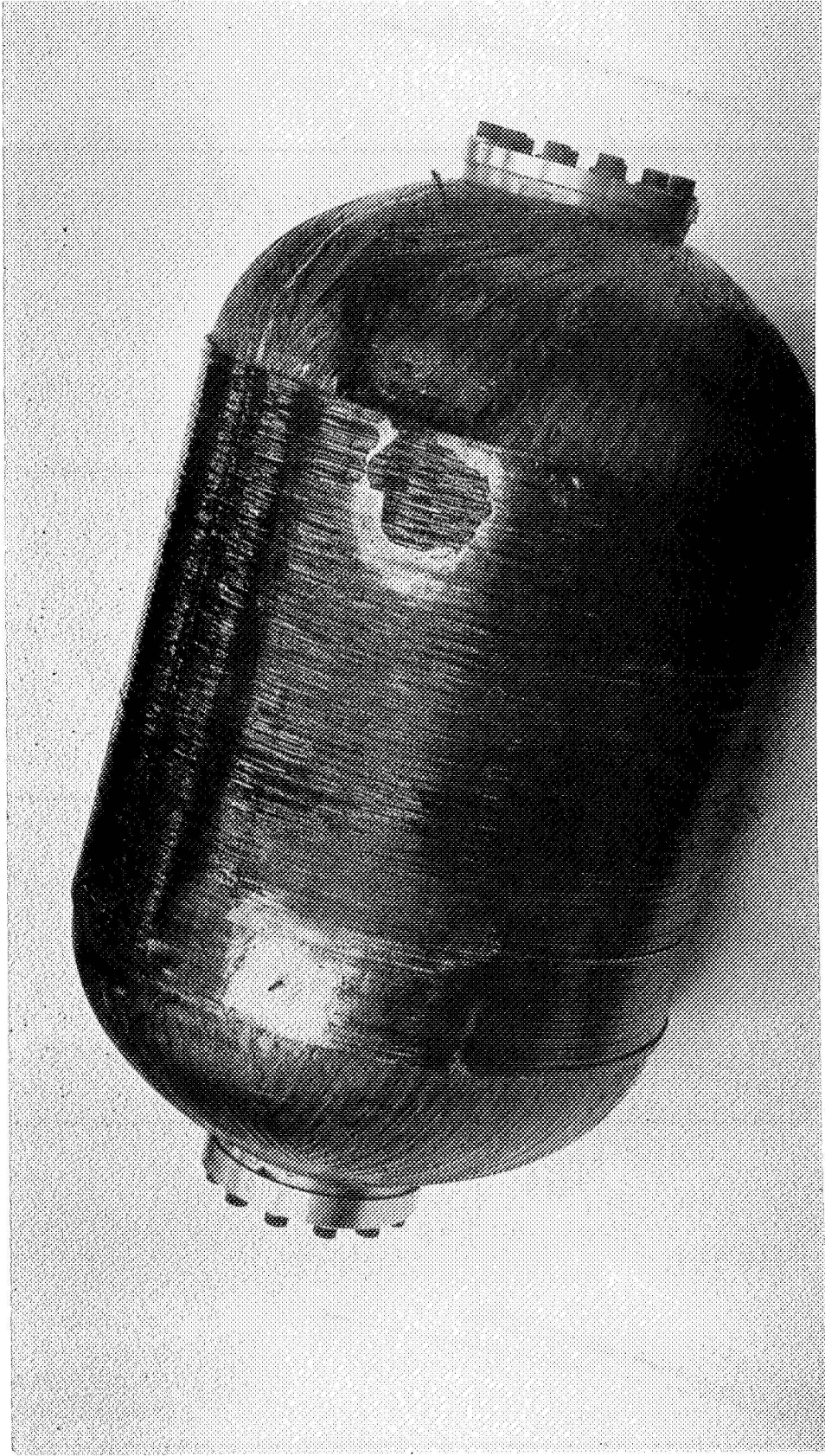


Fig. 65 Post Test Photograph of Tank BB-9 Pg. 129

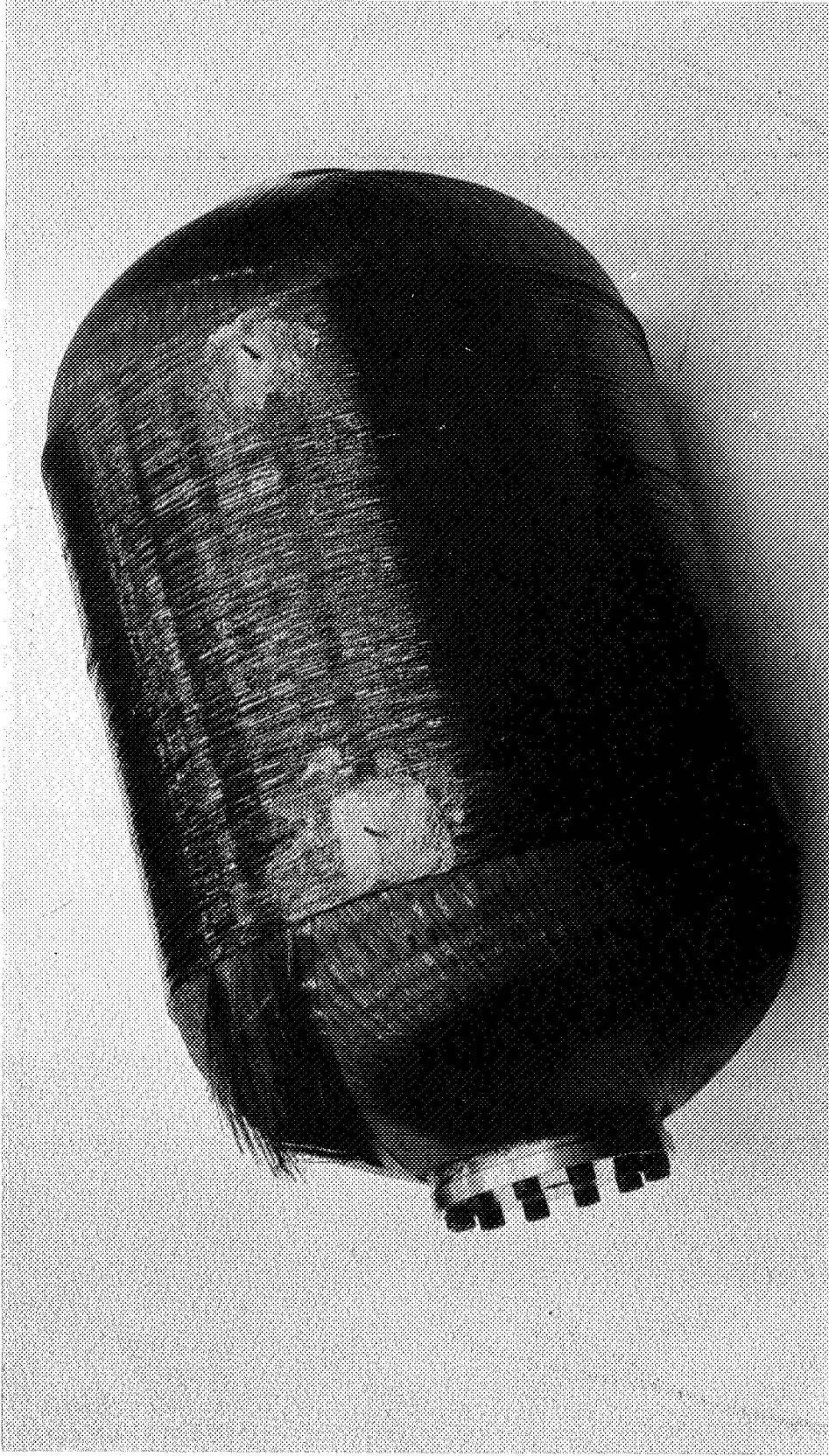
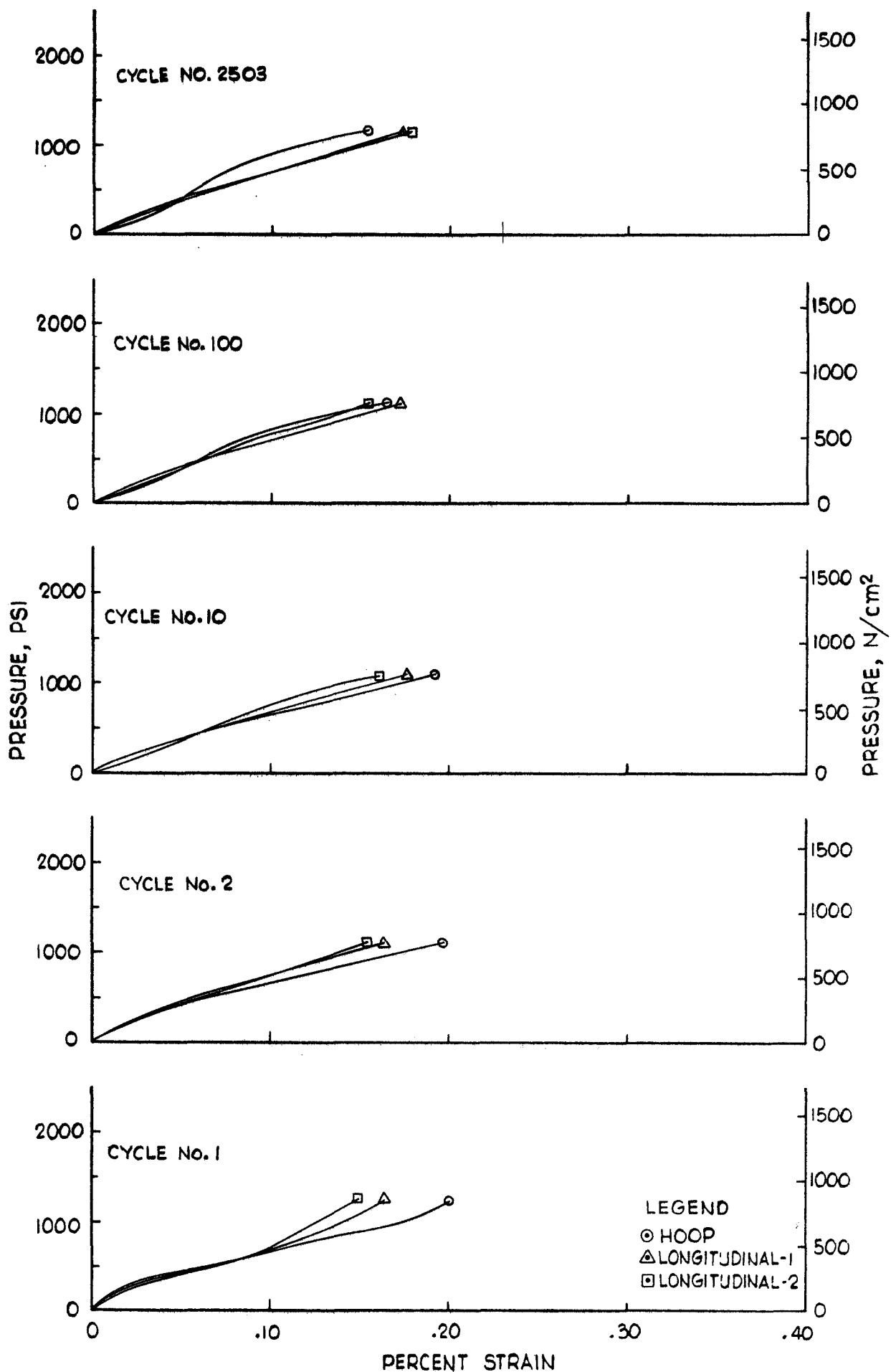
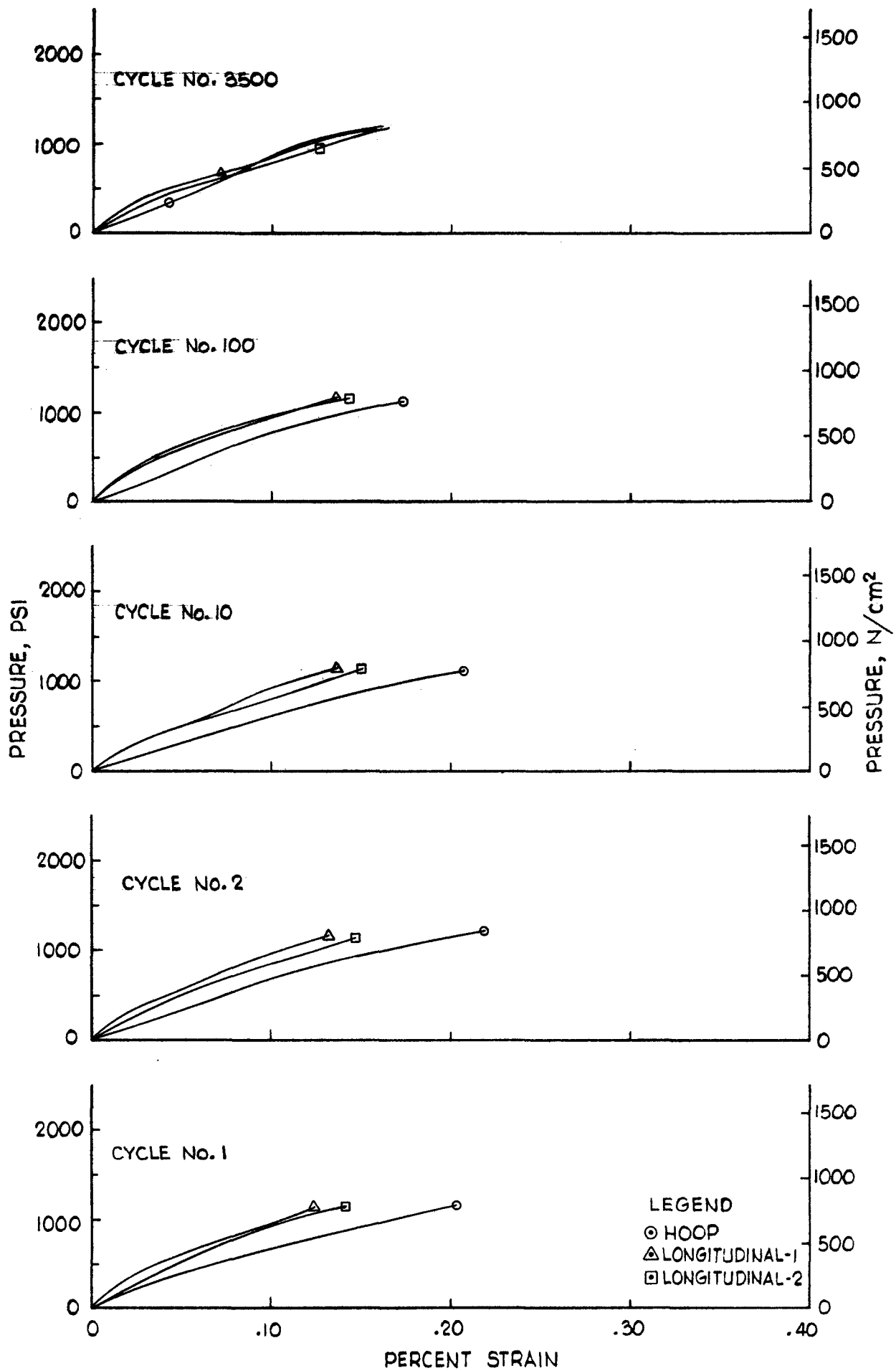


Fig. 66 Post Test Photograph of Tank BB-10 Pg. 130



TANK S/N BB-9
 PRESSURE VS STRAIN FOR CYCLE TEST AT 75°F(297°K)
 Figure 67



TANK S/N BB-10
 PRESSURE VS STRAIN FOR CYCLE TEST AT 75°F(297°K)

Figure 68

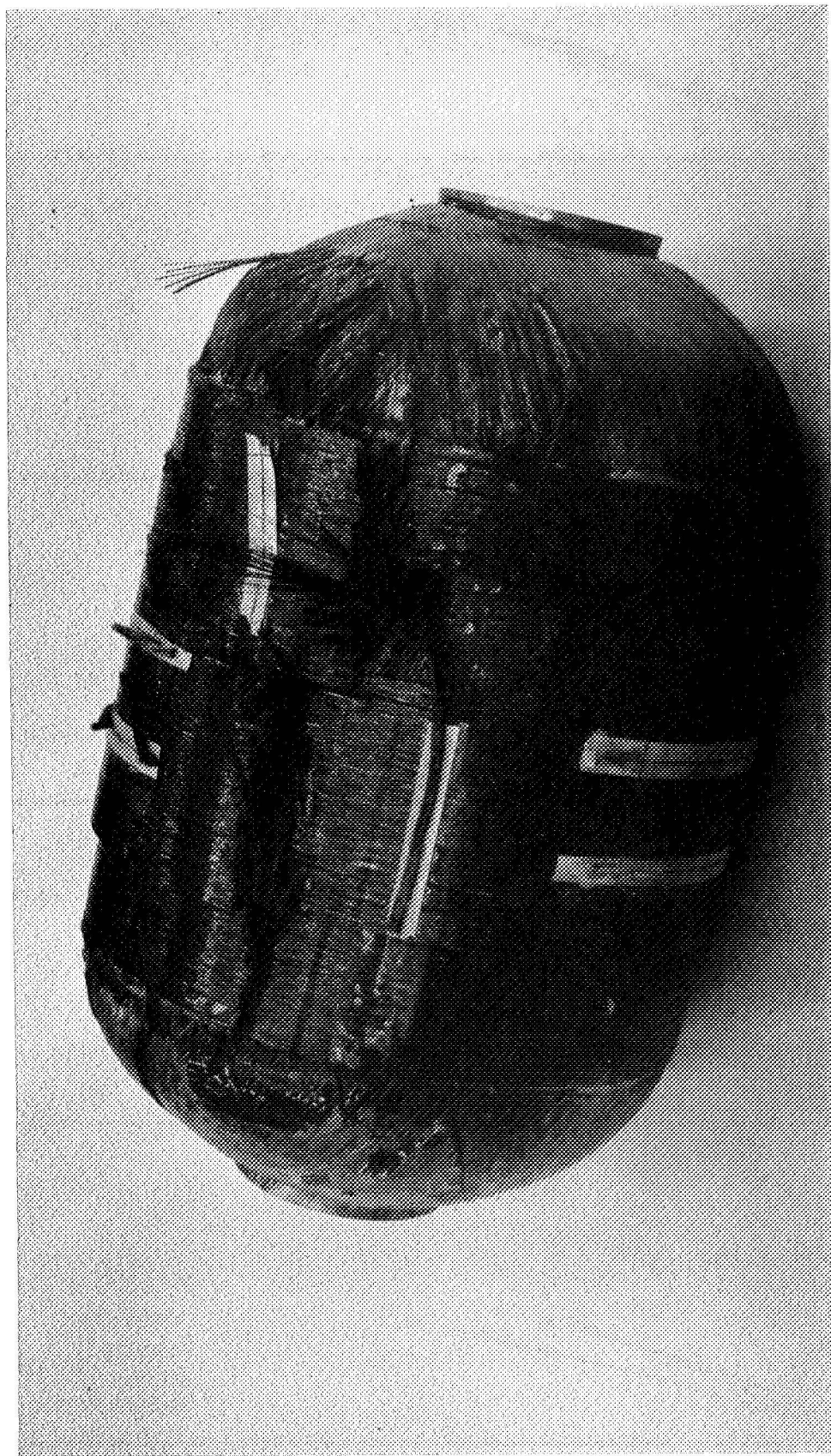


Fig. 69 Post Test Photograph of Tank BB-5 Pg. 133

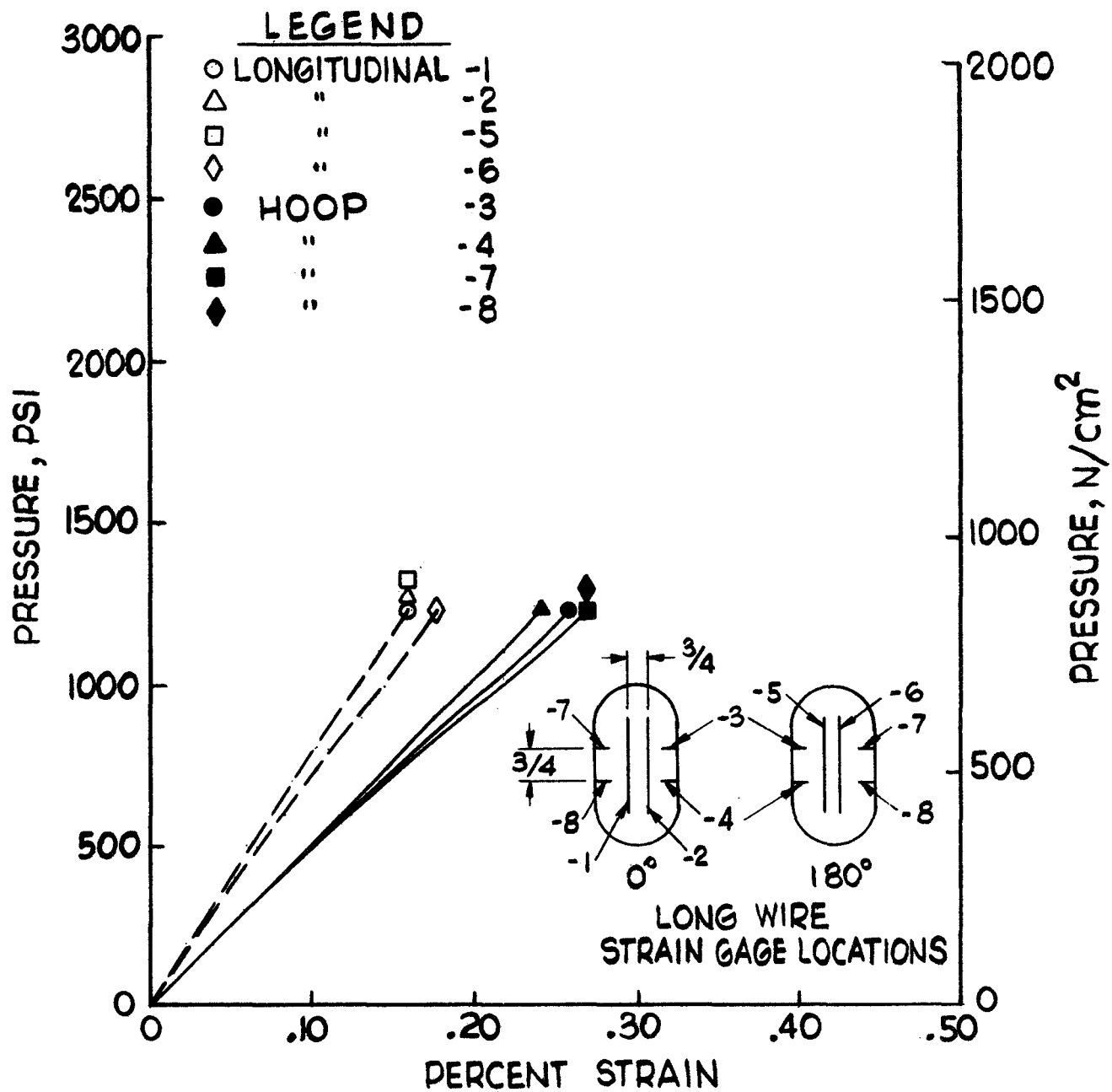


FIGURE 70
PRESSURE VS STRAIN FOR TANK BB-5
PRESSURIZATION TO SUSTAINED LOAD LEVEL

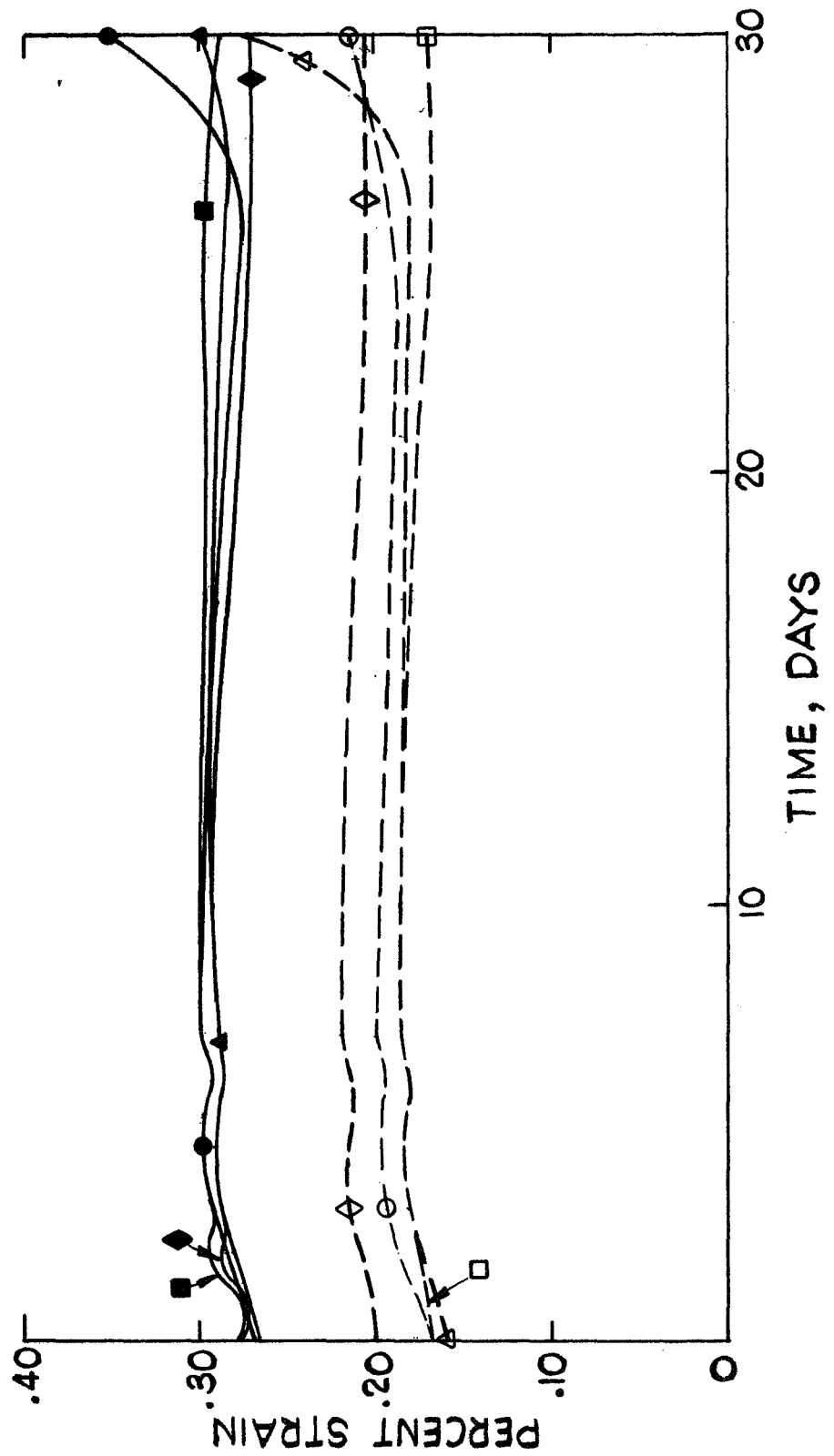


FIGURE 70

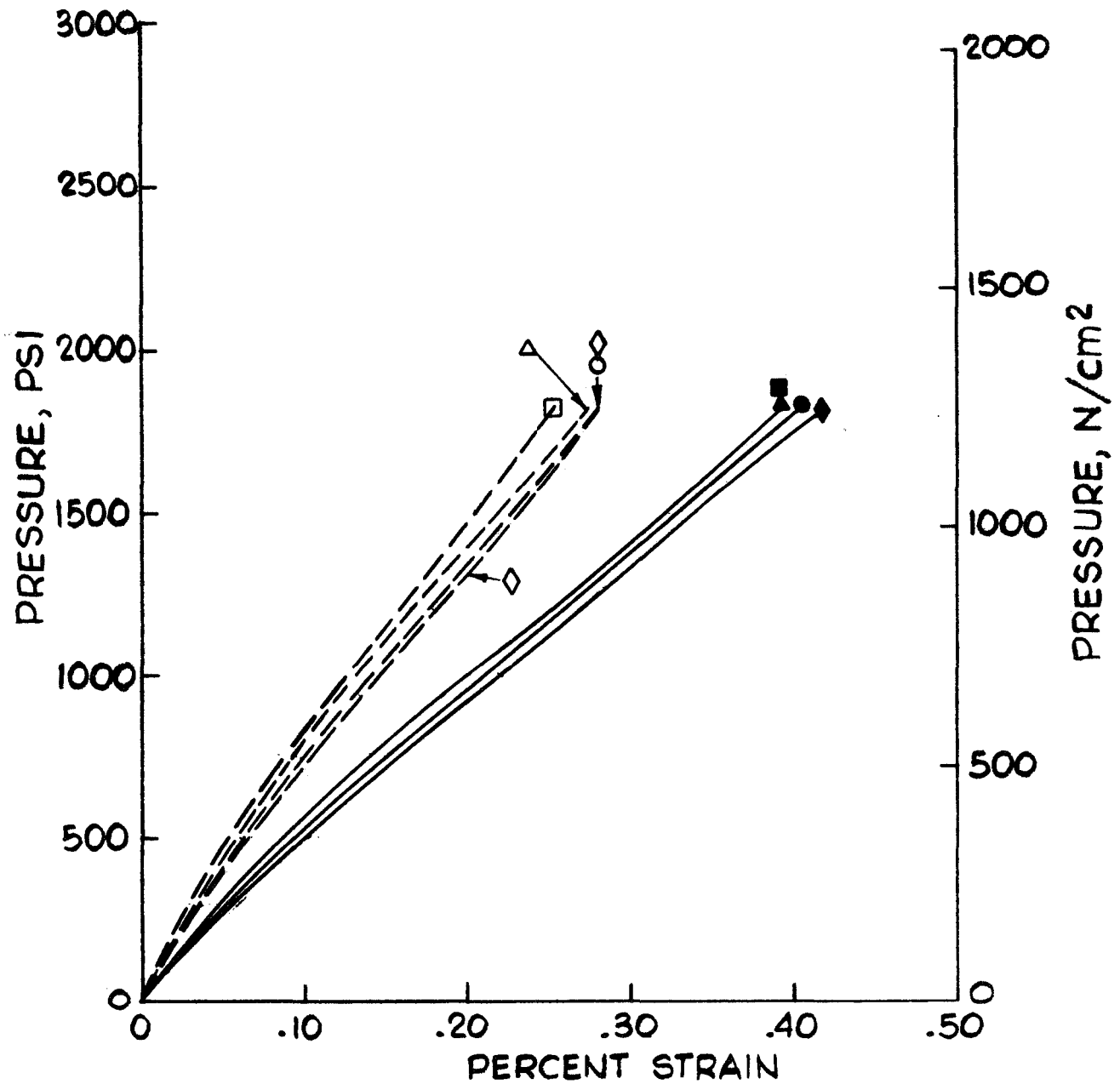


FIGURE 70

PRESSURE VS STRAIN FOR TANK 1B-5

PRESSURIZATION TO FAILURE AFTER SUSTAINED LOADING

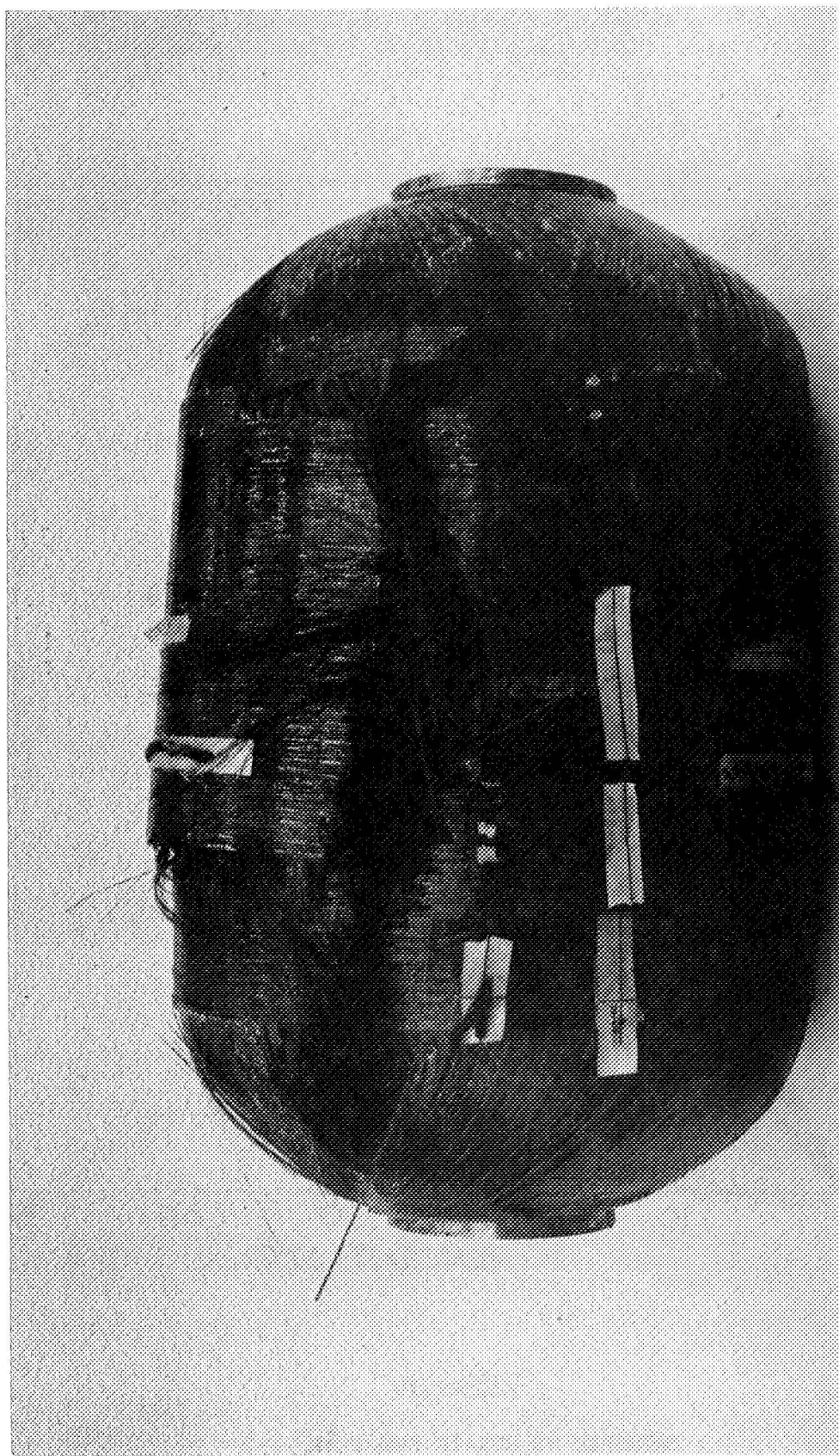


Fig. 71 Post Test Photograph of Tank BB-6 Pg. 137

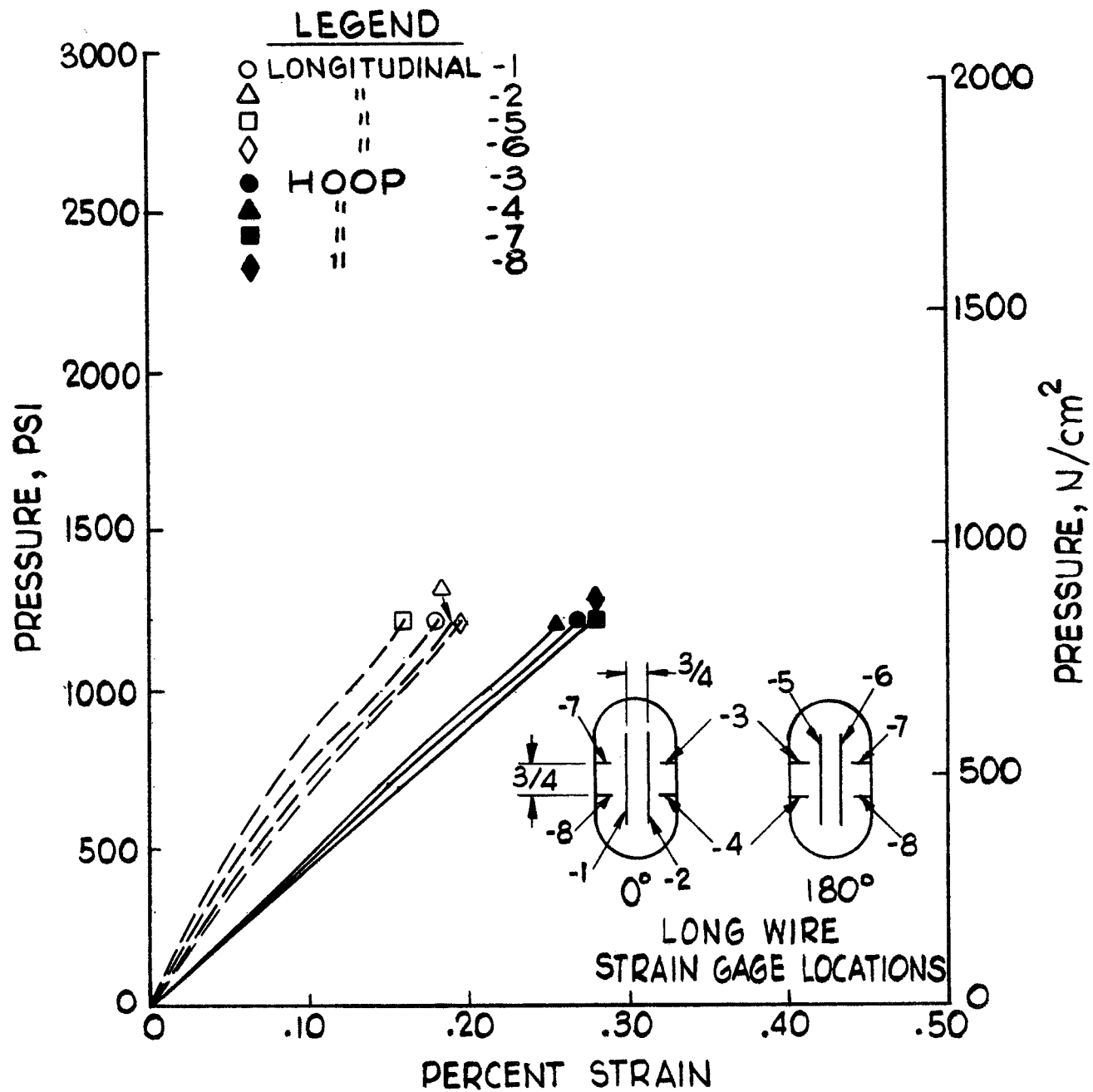


FIGURE 72
 PRESSURE VS STRAIN FOR TANK BB-6
 PRESSURIZATION TO SUSTAINED LOAD LEVEL

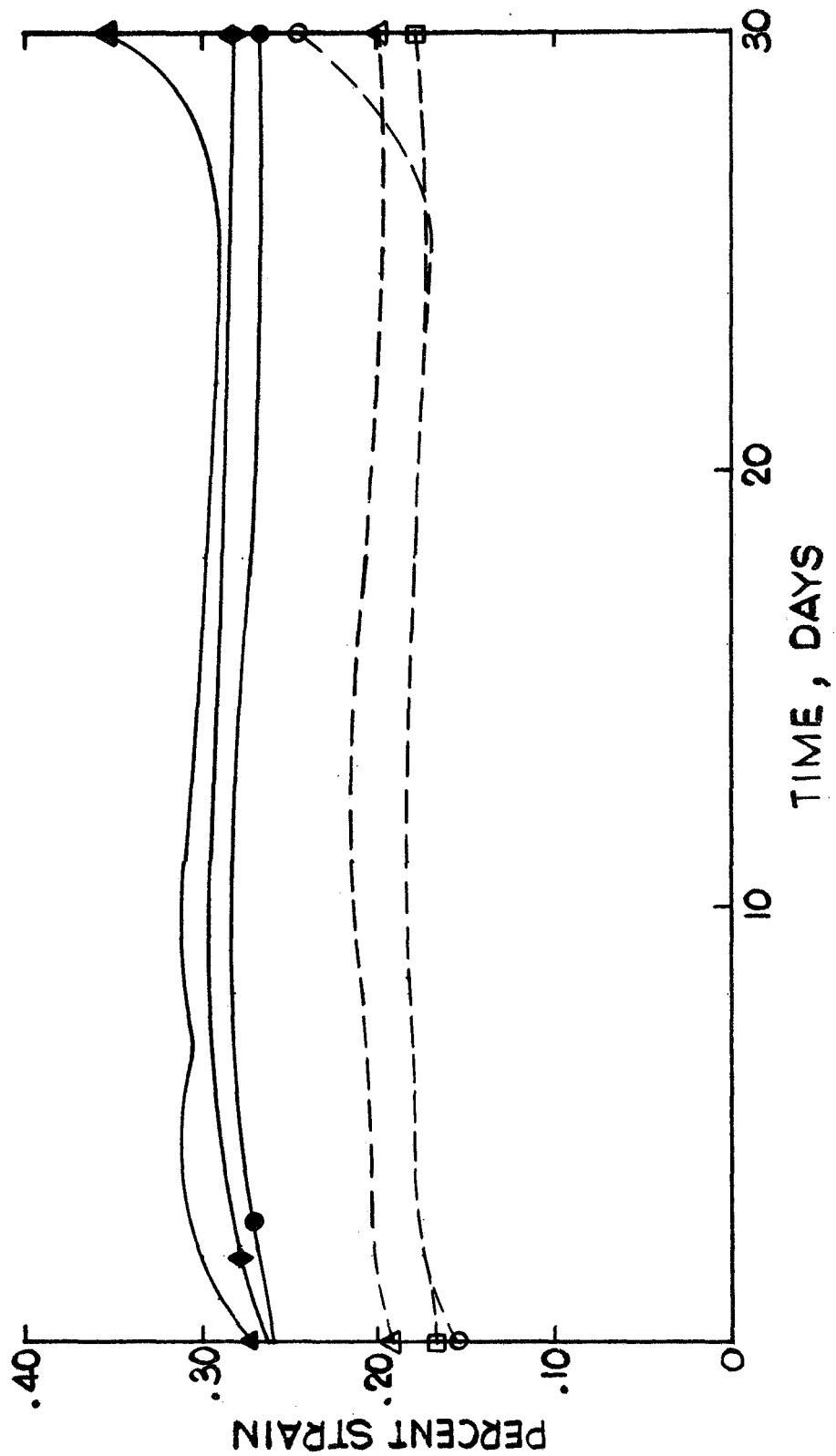


FIGURE 72
PRESSURE VS STRAIN FOR TANK BB-6
DURING SUSTAINED LOADING

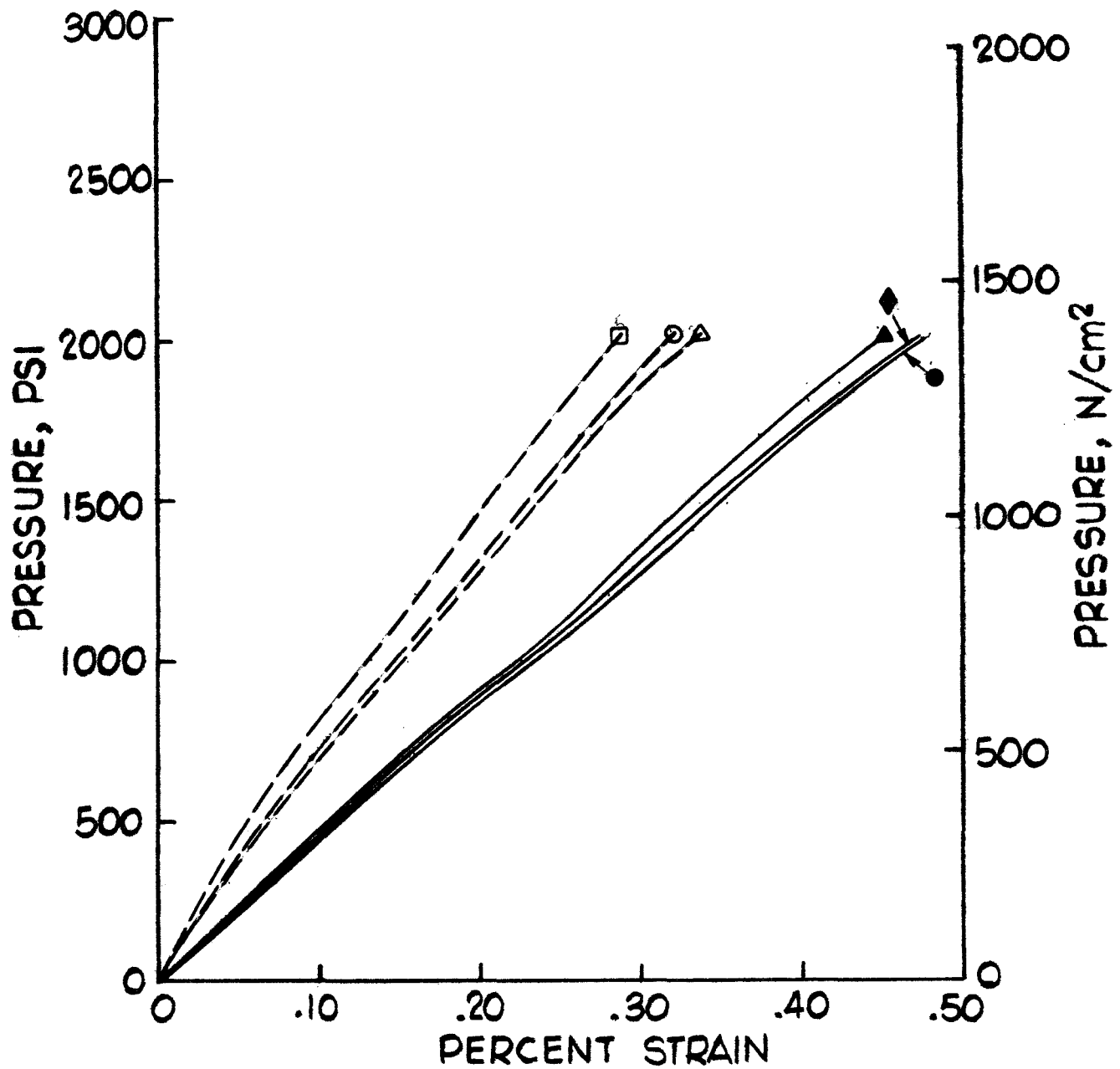


FIGURE 72

PRESSURE VS STRAIN FOR TANK BB-6
PRESSURIZATION TO FAILURE AFTER SUSTAINED LOADING

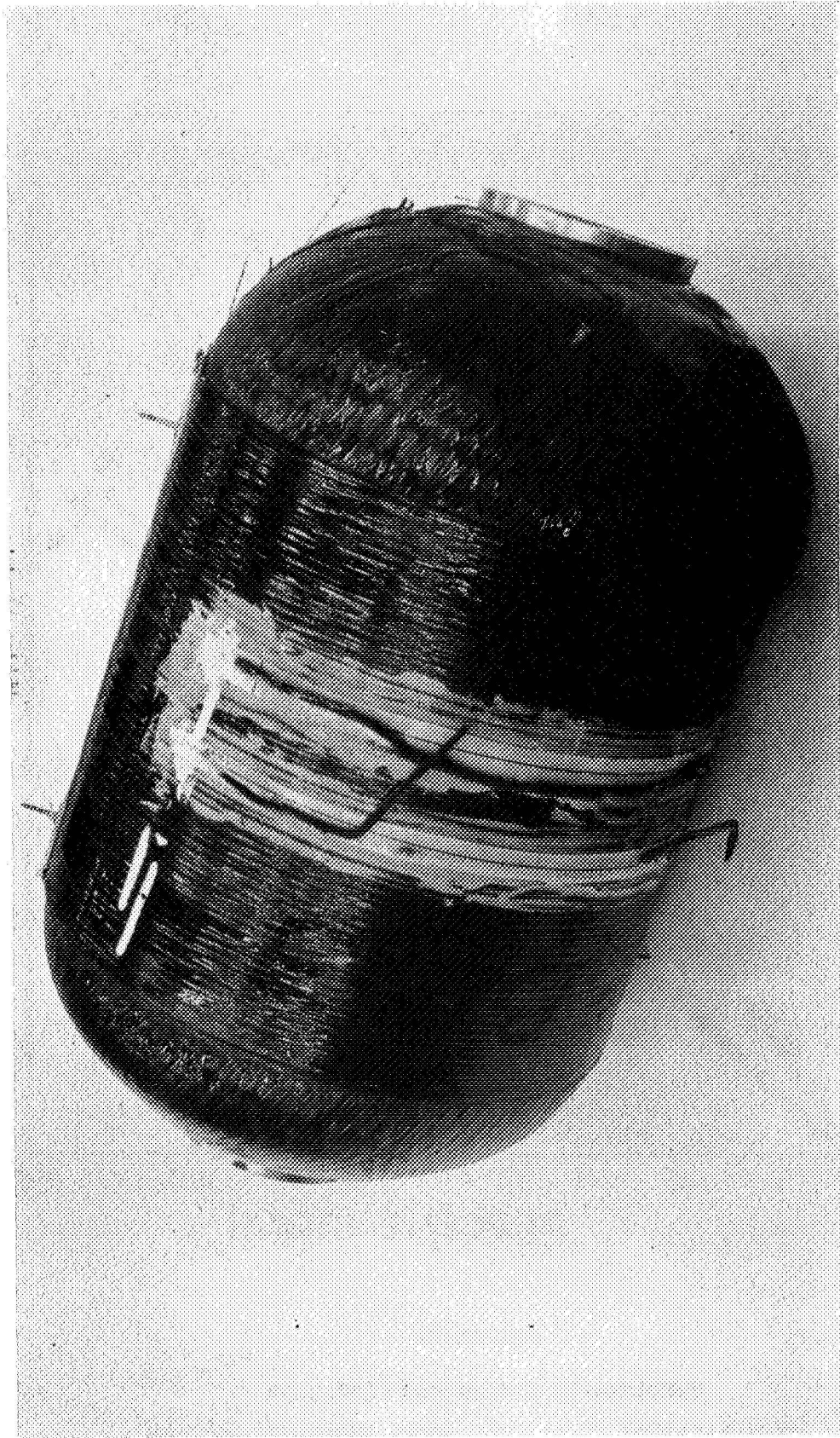


Fig. 73 Post Test Photograph of Tank BB-3 Pg. 141

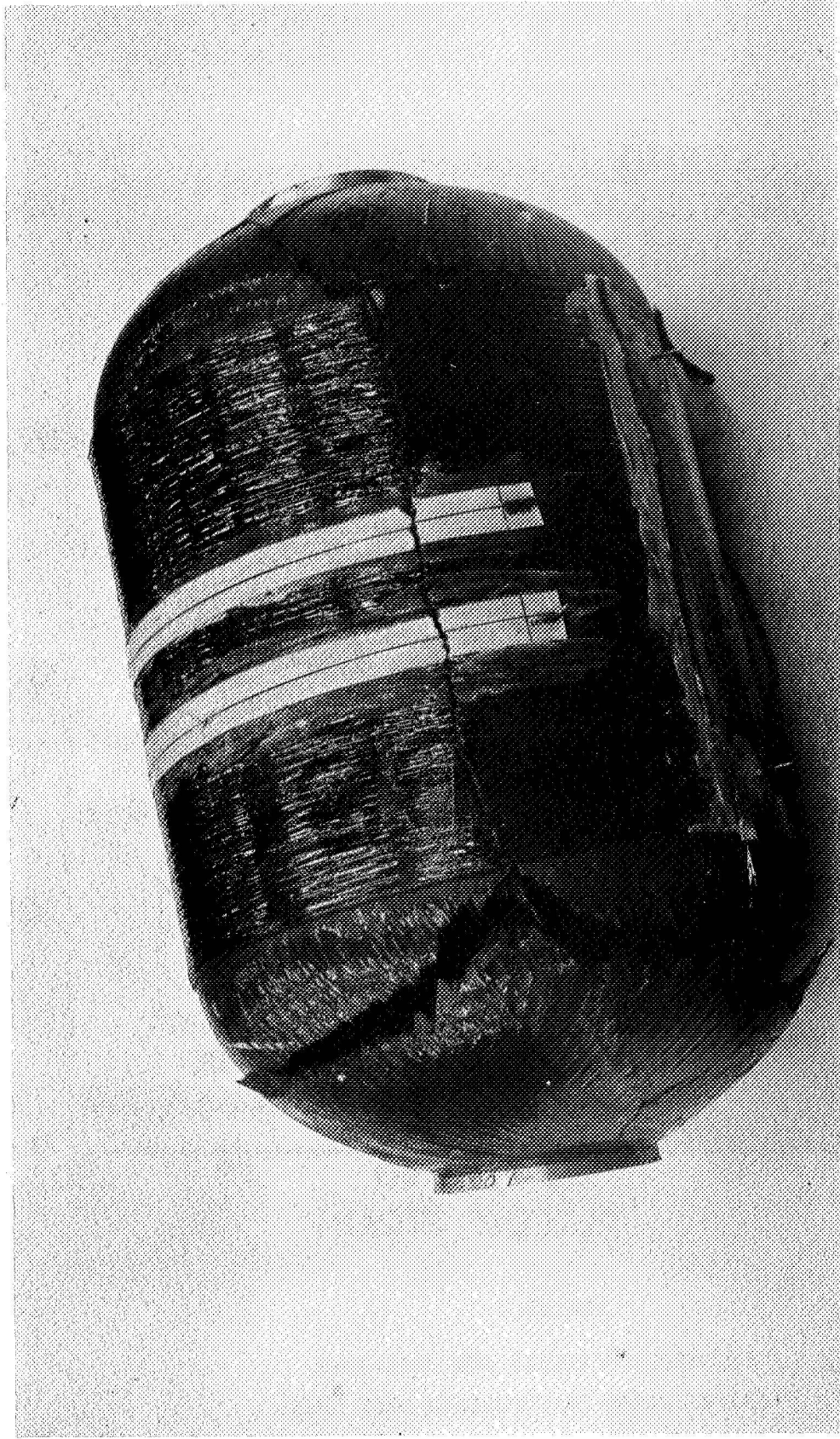


Fig. 74 Post Test Photograph of Tank BB-4 Pg. 142

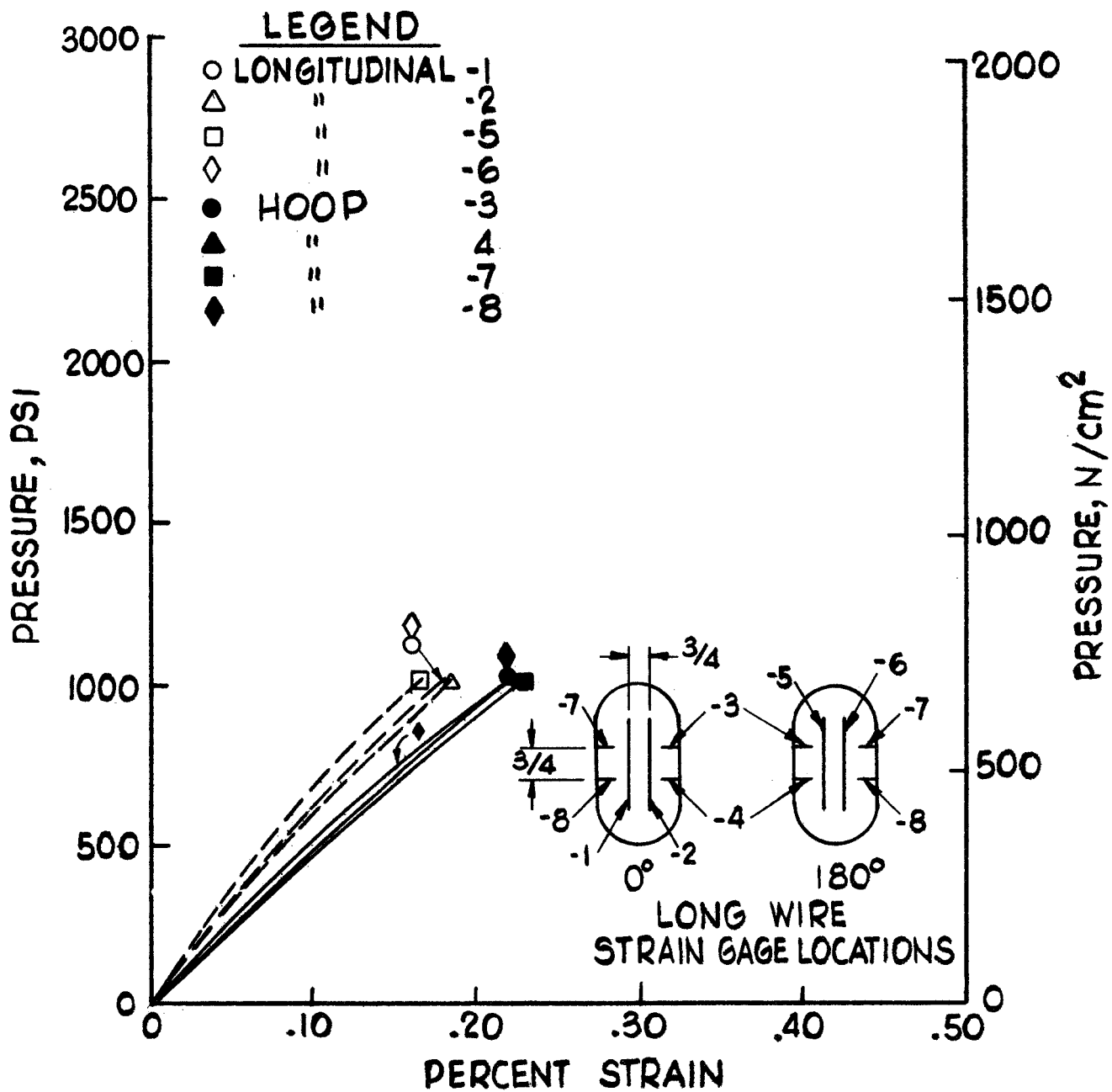


FIGURE 75

PRESSURE VS STRAIN FOR TANK BB-3
PRESSURIZATION TO SUSTAINED LOAD LEVEL

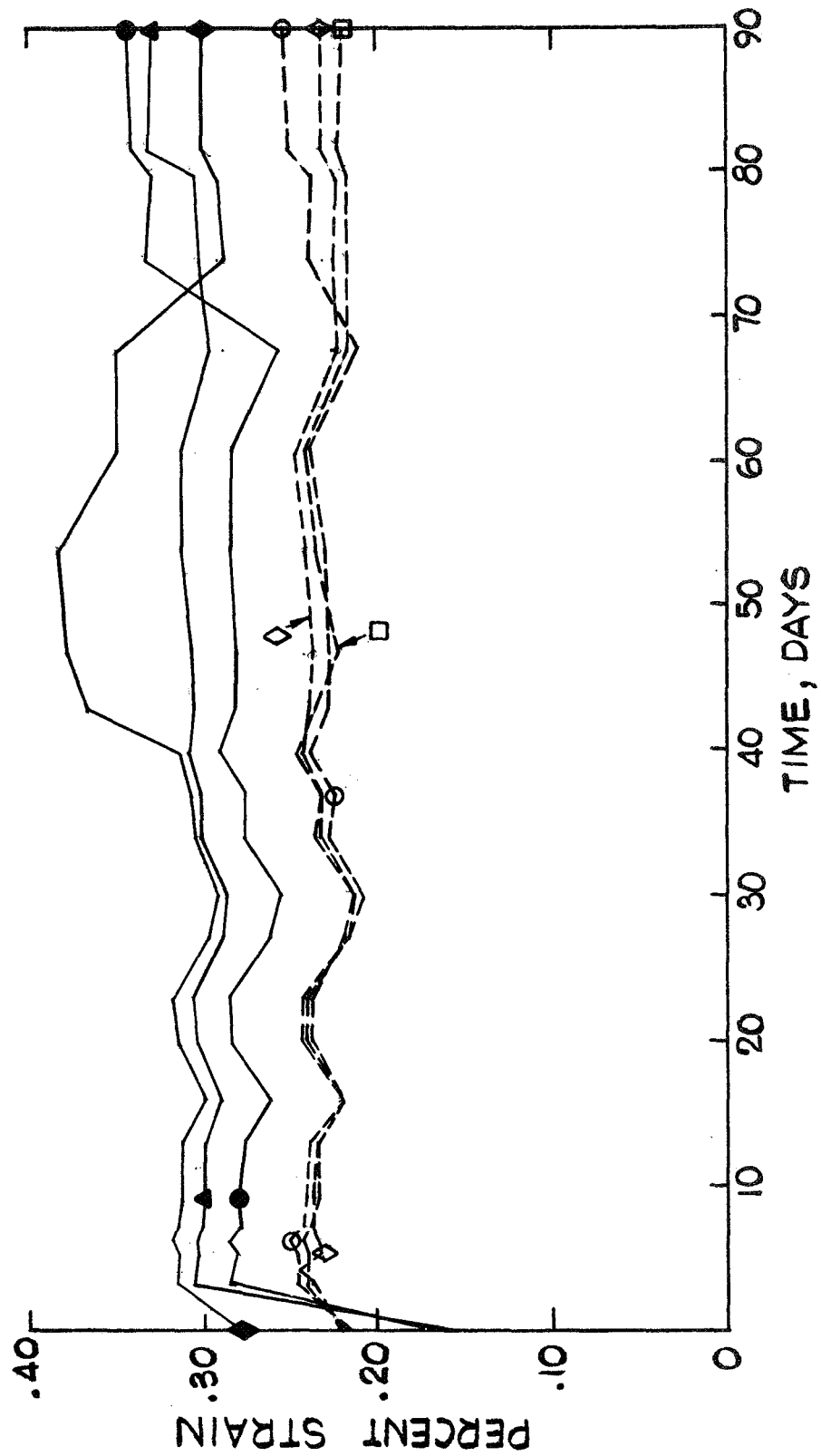


FIGURE 75
PRESSURE VS STRAIN FOR TANK BB-3
DURING SUSTAINED LOADING

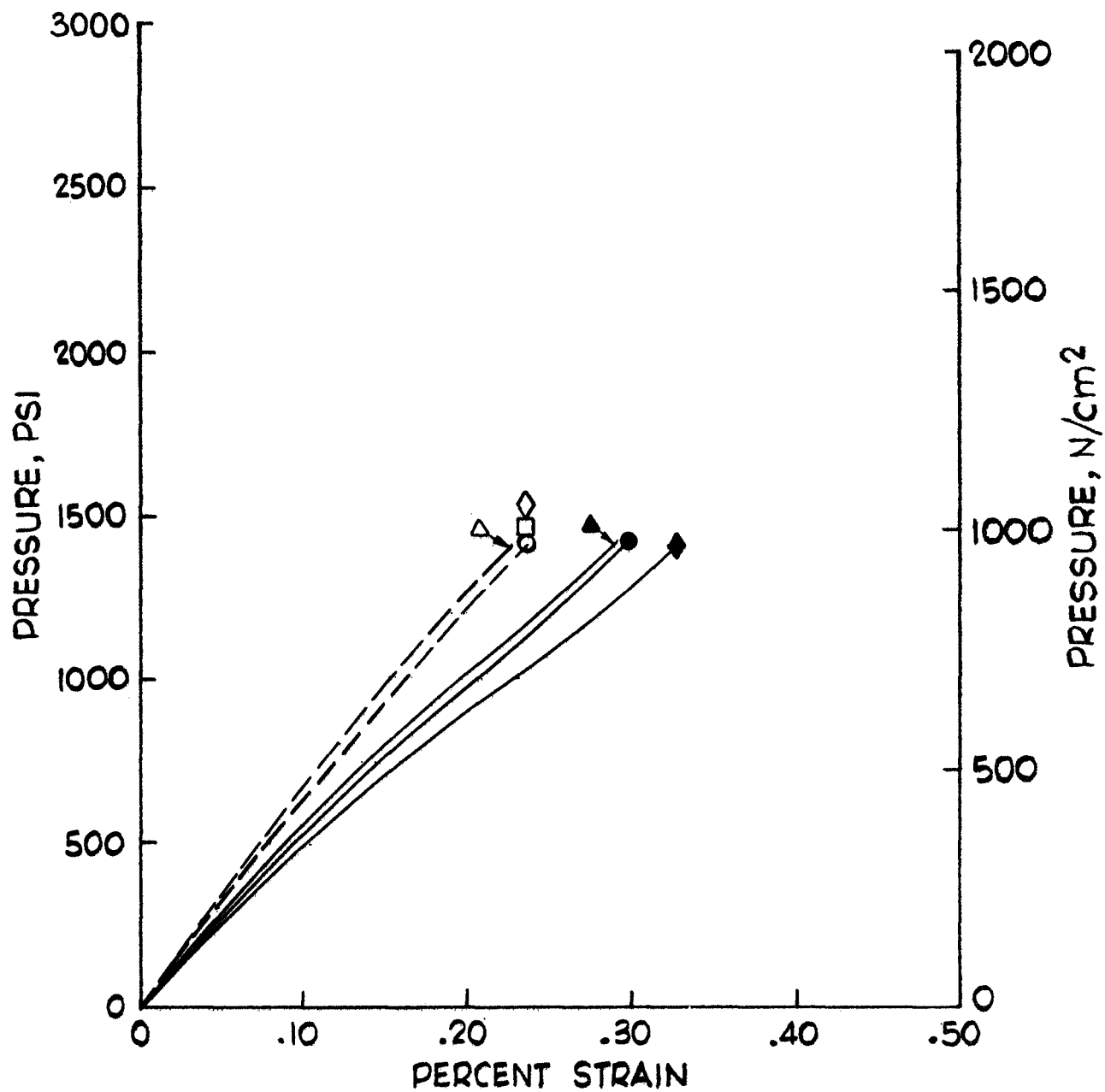


FIGURE 75

PRESSURE VS STRAIN FOR TANK BB-3

PRESSURIZATION TO FAILURE AFTER SUSTAINED LOADING

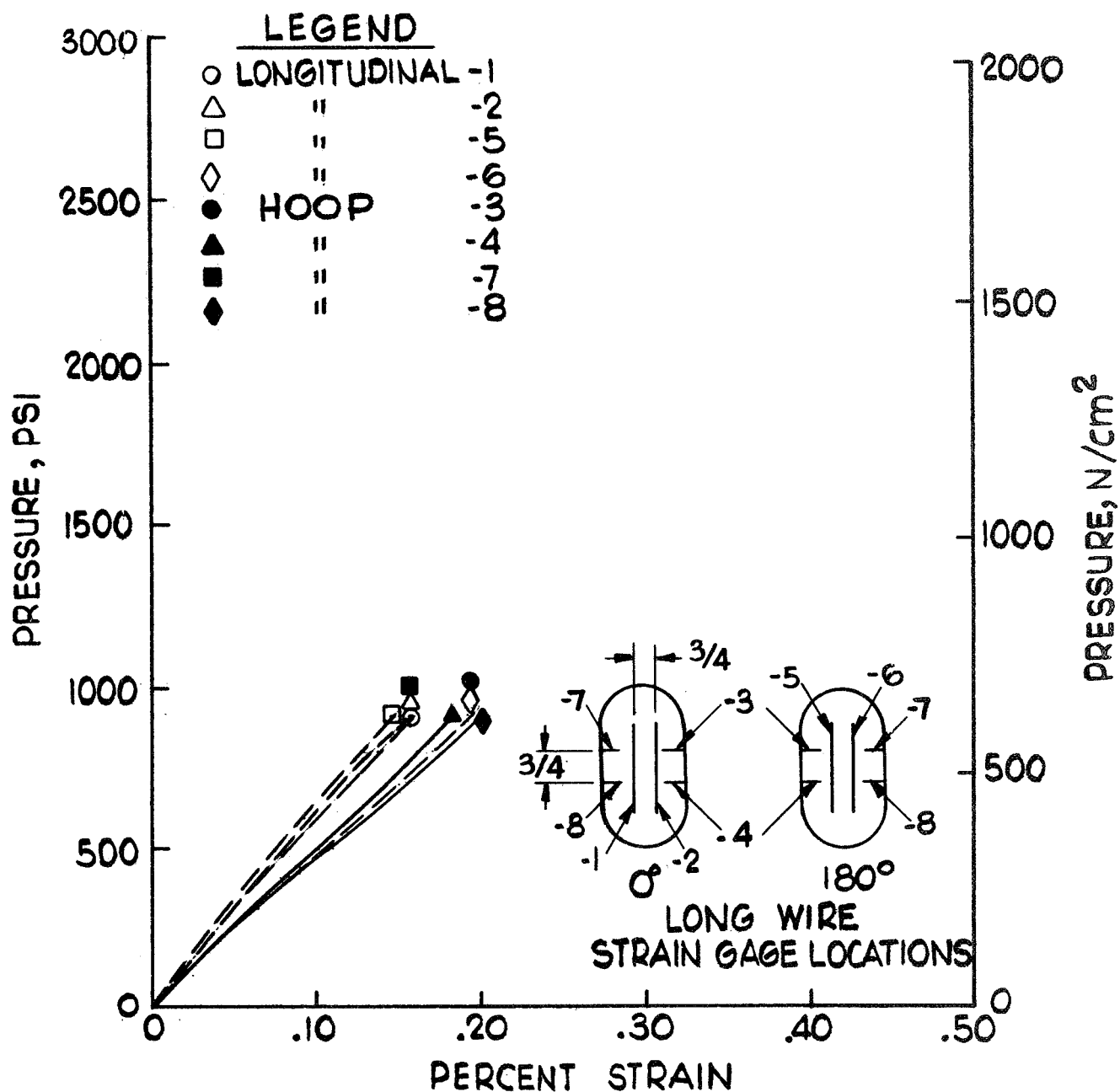


FIGURE 76

PRESSURE VS STRAIN FOR TANK BB-4
PRESSURIZATION TO SUSTAINED LOAD LEVEL

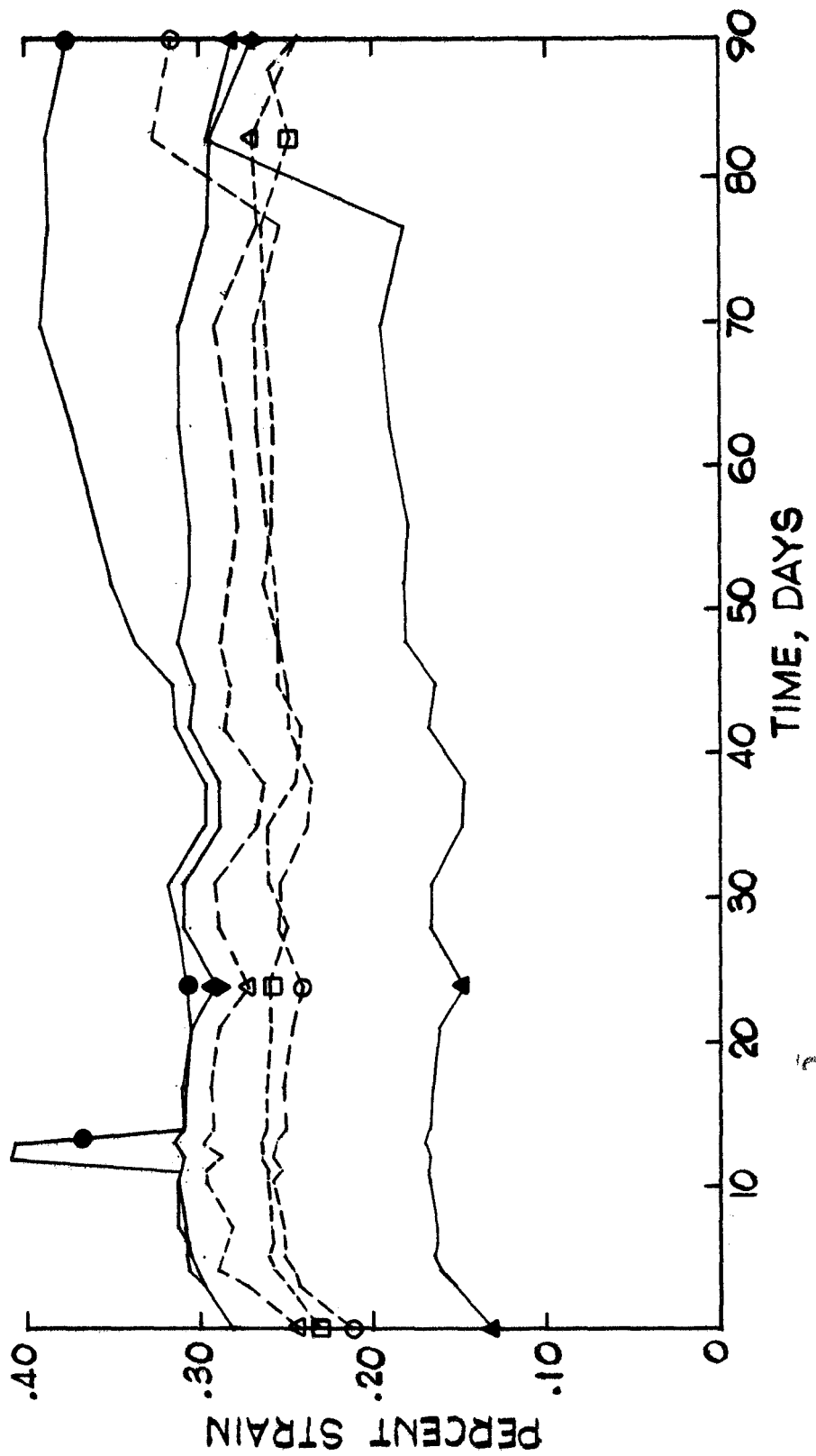


FIGURE 76
 PRESSURE VS STRAIN FOR TANK BB-4
 DURING SUSTAINED LOADING

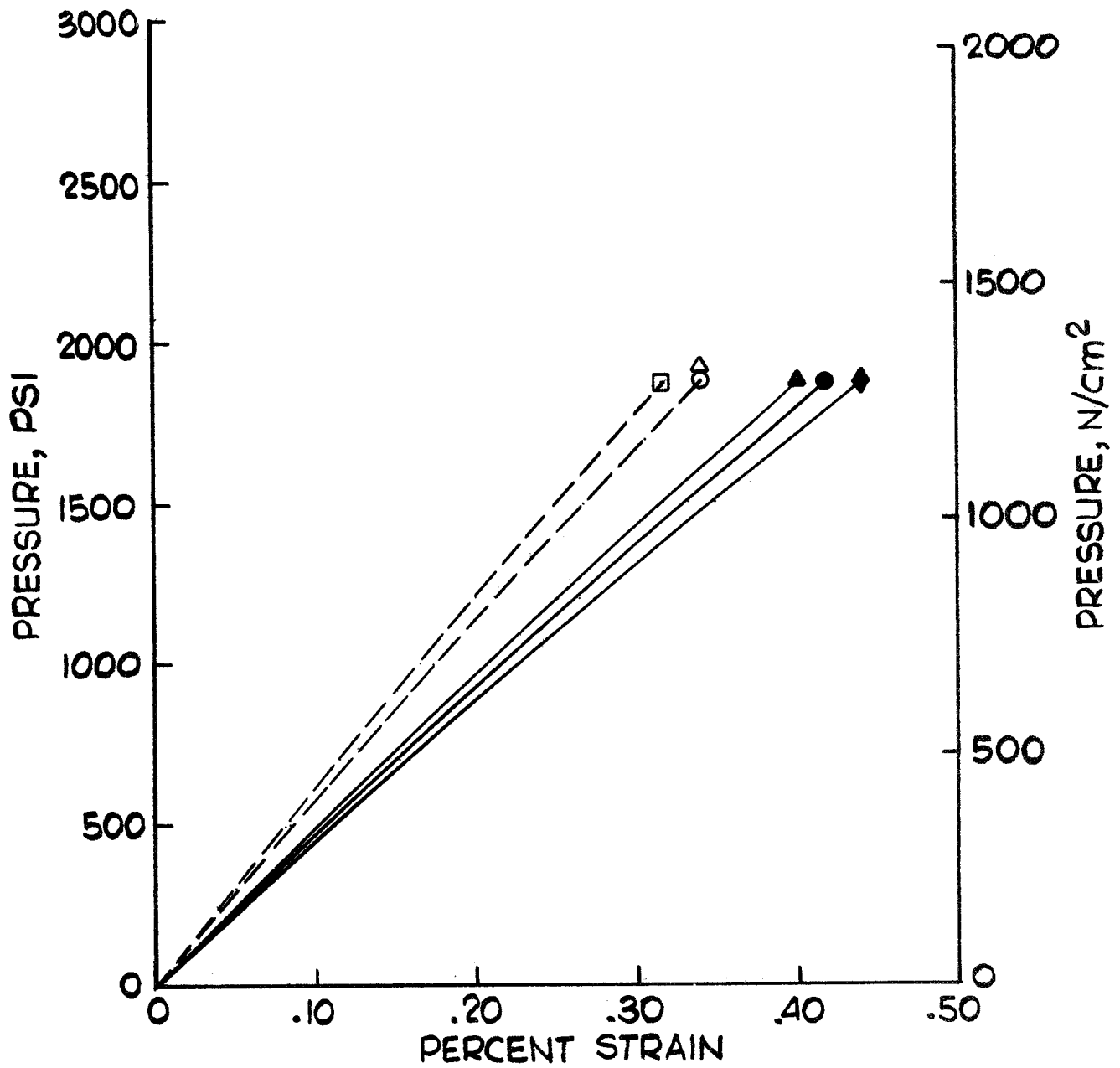


FIGURE 76
PRESSURE VS STRAIN FOR TANK BS-4
PRESSURIZATION TO FAILURE AFTER SUSTAINED LOADING

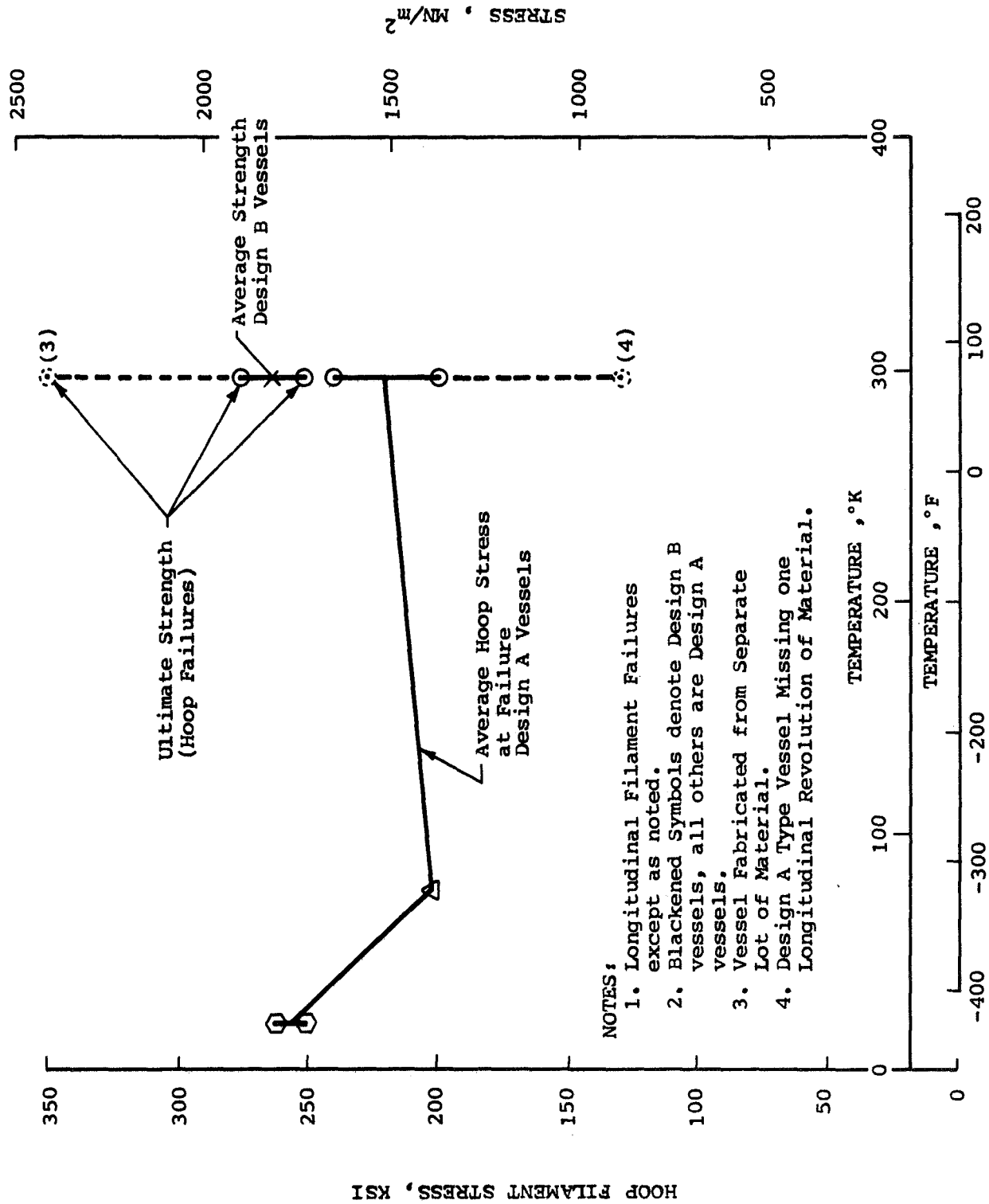


Fig. 77 Boron Hoop Filament Stress at Filament-Wound Vessel Failure in Single Cycle Burst Tests vs. Temperature

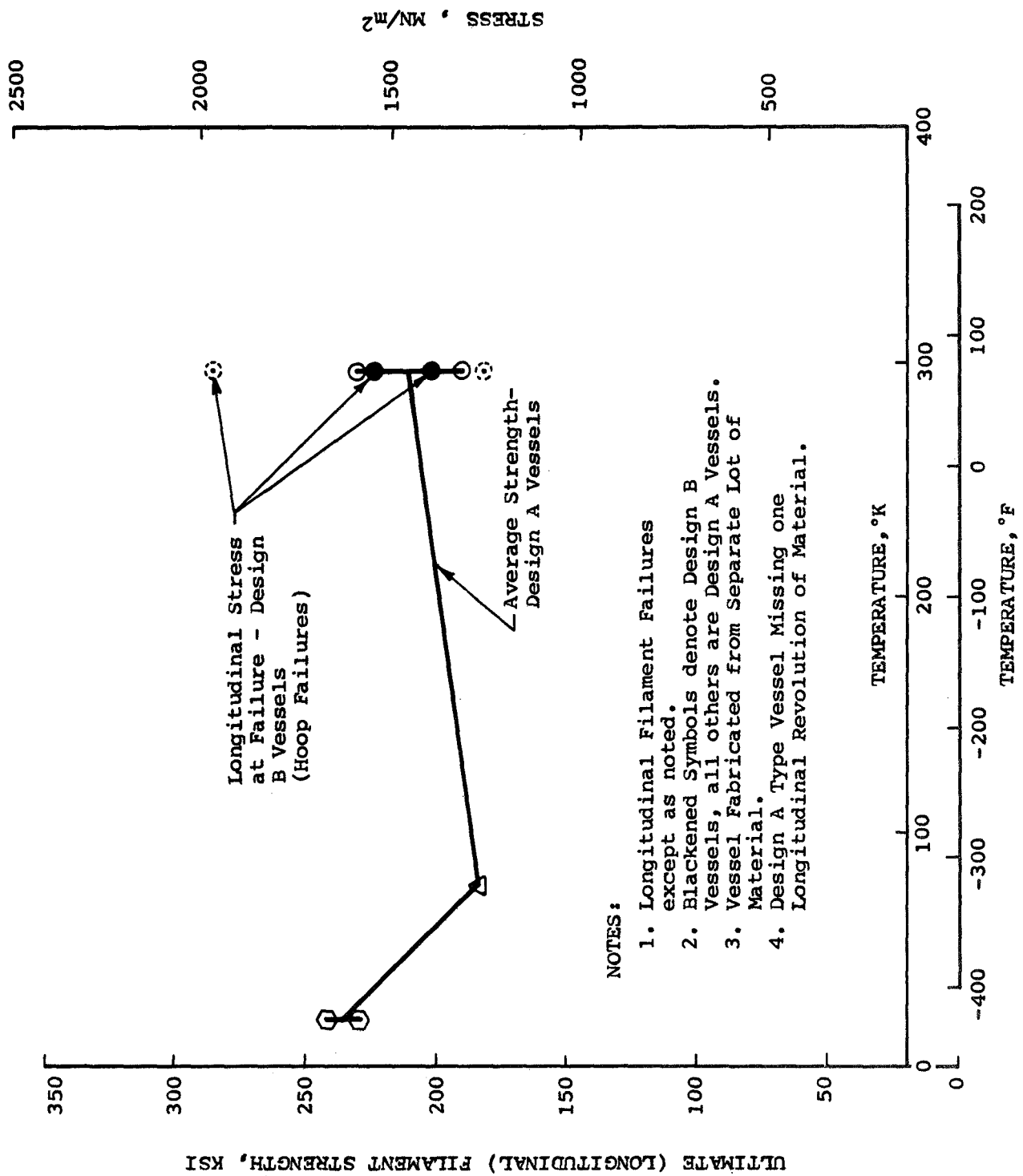


Fig. 78 Boron Longitudinal Filament Stress at Filament-Wound Vessel Failure in Single Cycle Burst Tests vs. Temperature

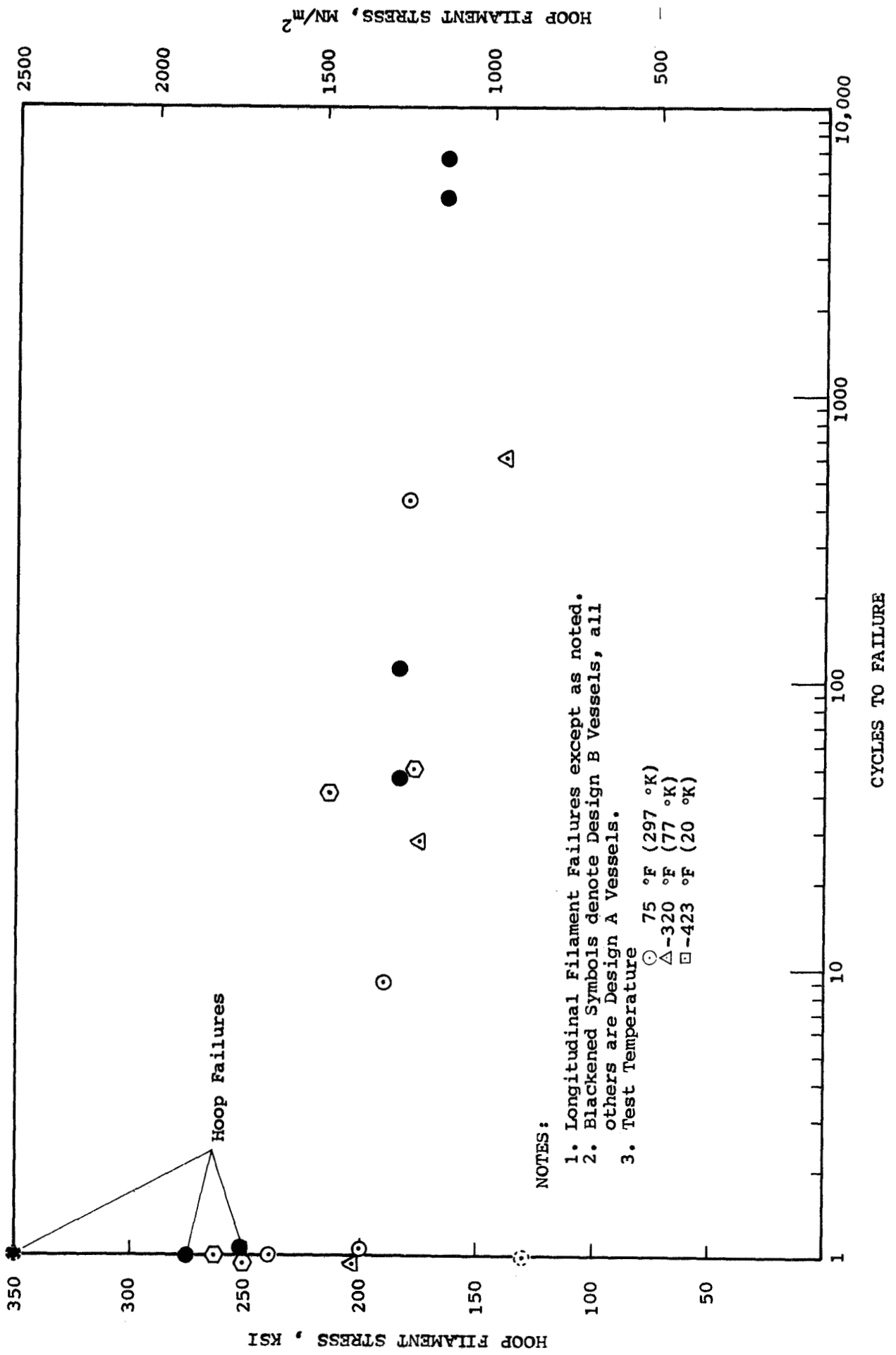


Fig. 79 Hoop Filament Stress During Cycling vs. Cycles to Boron Filament-Wound Vessel Failure

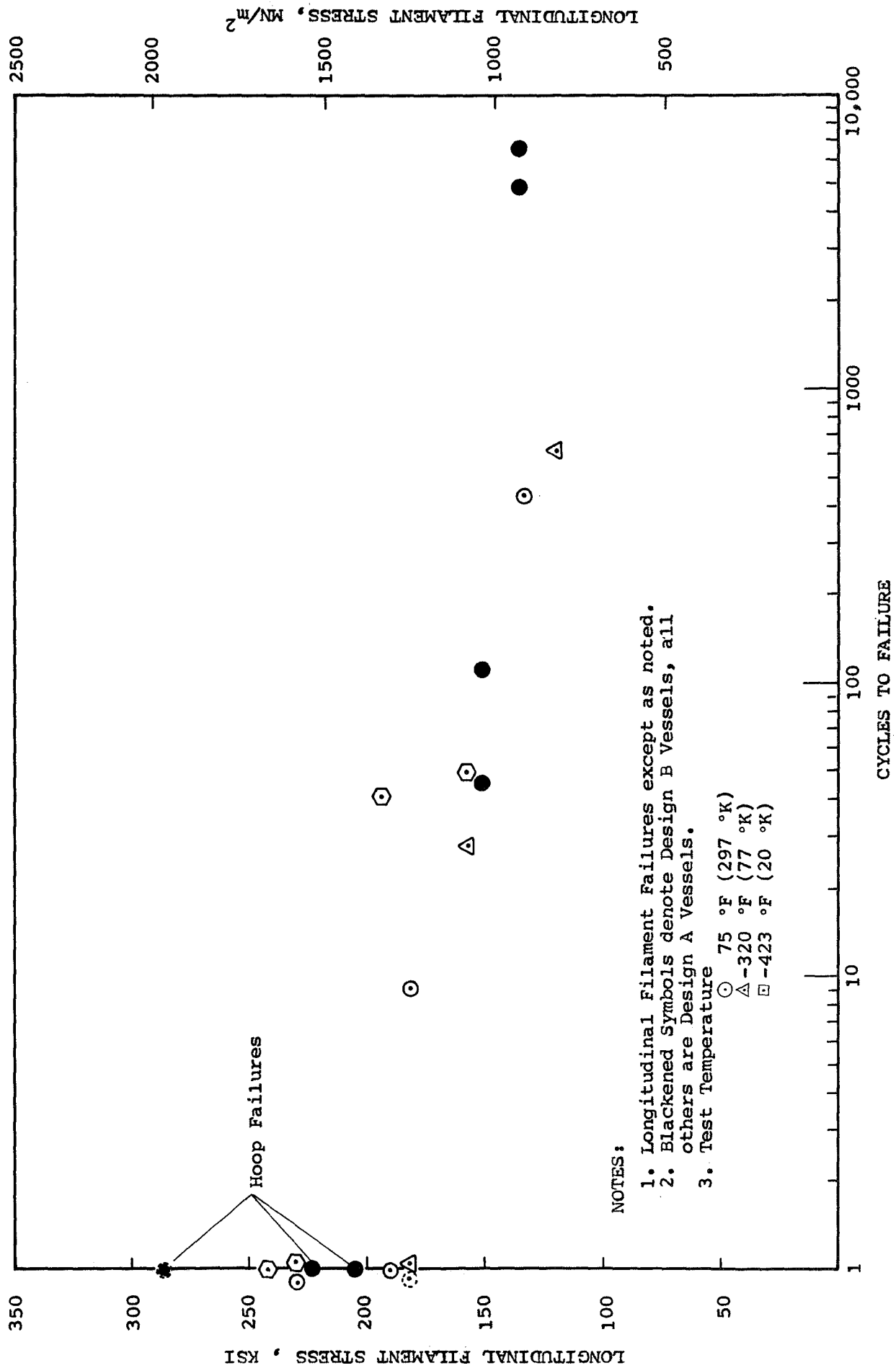


Fig. 80 Longitudinal Filament Stress During Cycling vs. Cycles to Boron Filament-Wound Vessel Failure

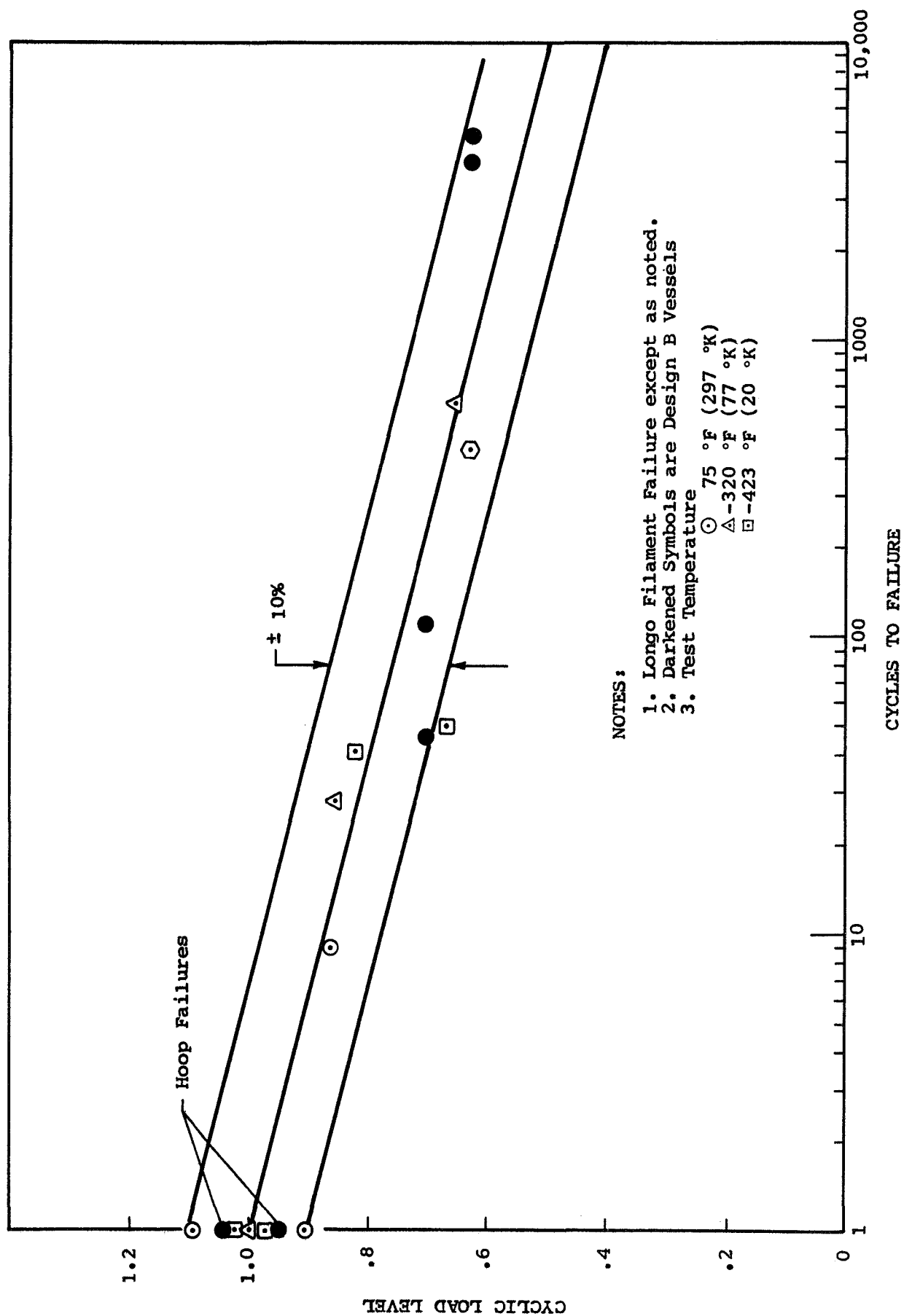


Fig. 81 Cyclic Load Level vs. Cycles to Failure for Boron Filament-Wound Vessel Failure

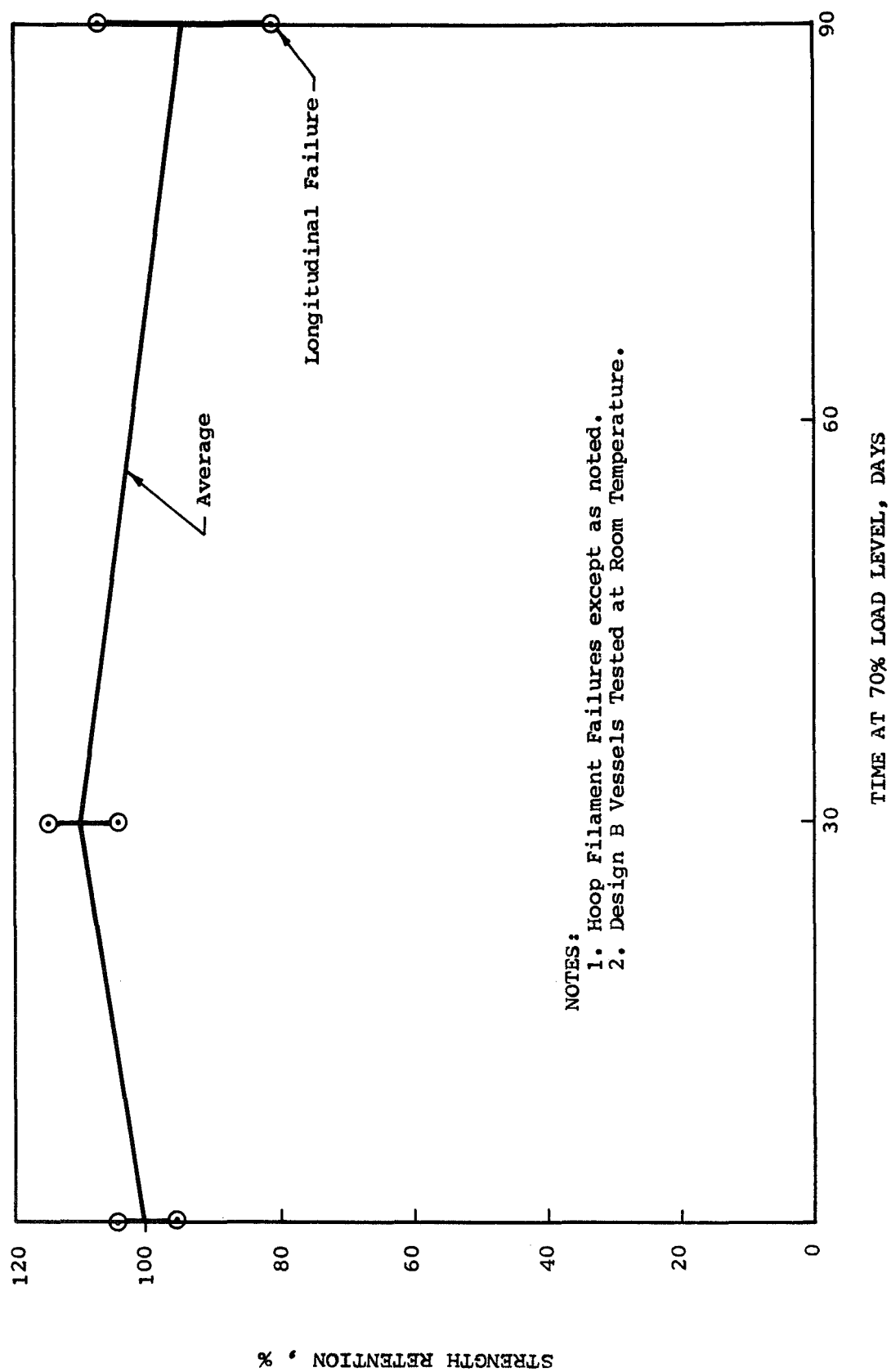


Fig. 82 Strength Retention for Boron Filament-Wound Vessels under Sustained Pressurization at 70% of Original Strength vs. Time at Load

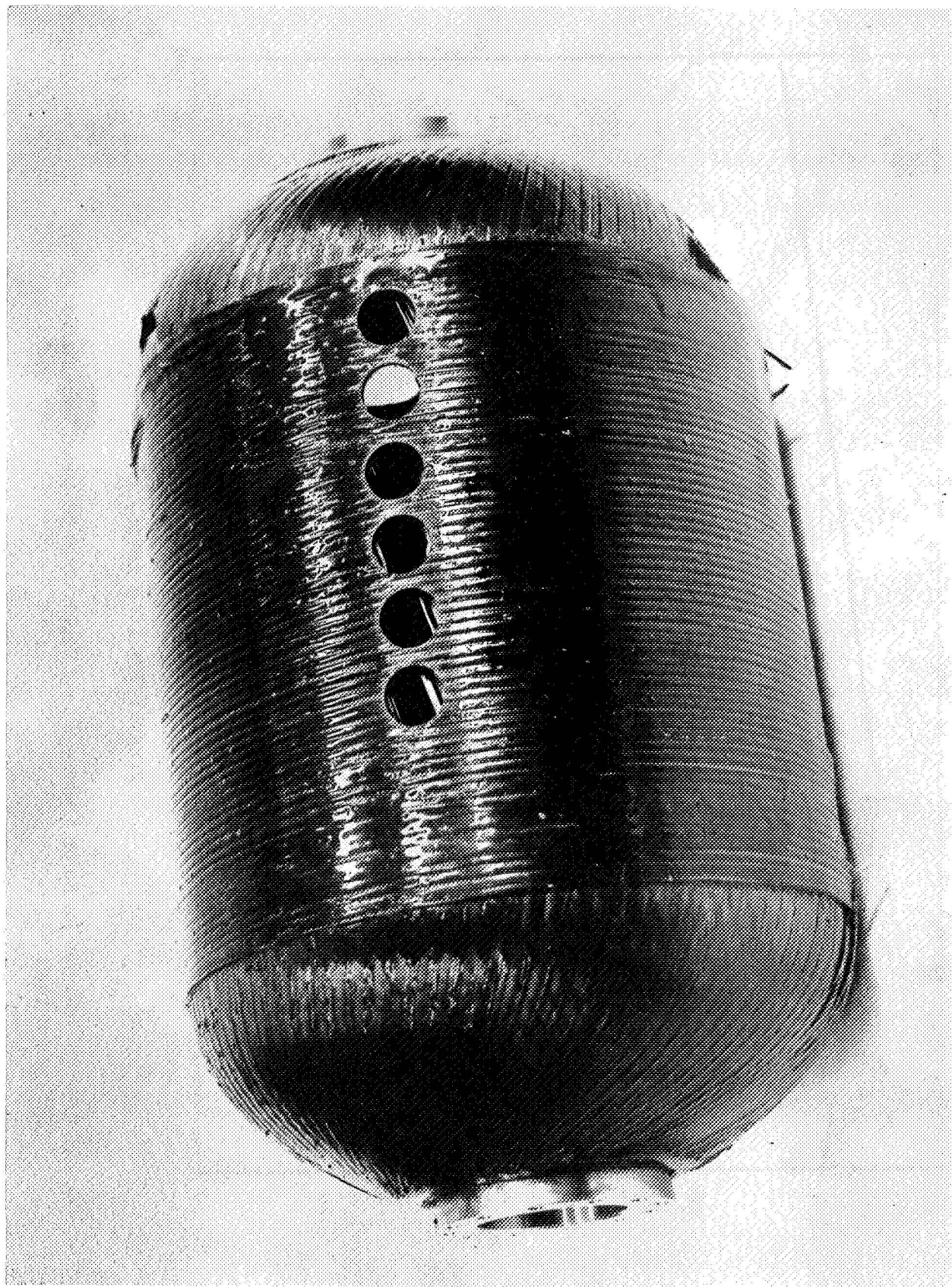


Fig. 83 Post Test Vessel Showing Boron and Void Content Specimen Locations Pg. 155

APPENDIX A

SPECIFICATION FOR ORGANIC-RESIN-PREIMPREGNATED TAPE WITH CONTINUOUS BORON-FIBER BASE FOR USE IN FILAMENT WINDING

1. Raw Materials

a. Resin

The resin material used in the manufacture of this pre-impregnated product shall be epoxy resin consisting of

<u>Component</u>	<u>Parts by Weight</u>	<u>Applicable Specification*</u>
Epon 828	50 \pm 3	WS 1068
Epon 1031	50 \pm 3	WS 1004
Nadic methyl anhydride	90 \pm 3	OS 10818
Benzyl dimethylamine	0.3 \pm 0.5	OS 10785

b. Boron Fibers

The boron fibers used in the manufacture of the preimpregnated goods shall be of high quality and unetched, and shall have no crossovers or broken ends. The fiber diameter, determined optically, shall be 0.0040 ± 0.0002 (0.102 ± 0.005 mm)₂. The fiber tensile strength shall be a minimum of 400,000 psi ($276,000$ N/cm²), based on five tensile pulls at a 1-in. (2.54-cm) gage length from each end of the filament roll.

Fiber splices shall be kept to a minimum (see paragraph 2.c. below).

2. Preimpregnated Goods

The preimpregnated tape shall consist of parallel, in-plane, boron fibers impregnated with the resin binder and suitable for use in filament winding.

a. Dimensions and Number of Filaments in Tape

The preimpregnated boron tape shall be 0.125 ± 0.003 in. (0.318 ± 0.008 cm) wide and consist of 29 single filaments collimated in a side-by-side orientation.

* Latest issue of Weapons Specification (WS) or Ordnance Specification (OS) prepared by Aerojet-General Corporation, Sacramento, California, for Department of the Navy, Bureau of Naval Weapons, in the Polaris Fleet Ballistic Missile program.

b. Resin Content

The resin content shall be 29 ± 2 wt%.

c. Splices

The tape supplier shall attempt to control splices so that no more than three shall occur in any 25-ft. (7.62-m) length of tape, and that two splices shall occur no closer than 2-ft. (0.60-m) of each other. All spliced fibers shall be flat in the plane of the tape.

d. Uniformity

The tape shall be of uniform quality.

e. Degree of Resin Advancement

The resin matrix shall be green, but not to the point it would transfer to a finger when touched at room temperature. It should not be so dry that tape integrity is affected (e.g., when tape is bent to a 1-in. (2.54-cm) radius, the resin should not shatter or fracture). The tape shall adhere to a vertical surface.

f. Workmanship

The impregnated tape shall be of the highest quality of workmanship and shall be free of major defects or contaminants detrimental to fabrication or to the performance of the finished, filament-wound parts.

g. Defects

Any defects that were not detectable during lot acceptance and become apparent during subsequent use shall be cause for rejection of the unused portion of the roll, provided that these defects are cause for rejection under the requirements of this document and do not result from mishandling, improper storage, or expiration of shelf life.

h. Packaging

The tape shall be level-wound in rolls on tubes, using non-adhering paper sheets to separate each layer. Adjacent winds within each layer shall not touch or lap. Each roll shall be individually sealed in a moisture-proof plastic bag.

i. Packing

Materials shall be packed in clean, dry containers so

constructed as to ensure acceptance by common carriers or others for safe transportation at the lowest rate to the delivery point specified by the purchase order or contract. Cartons shall be so constructed and insulated that solid carbon dioxide can be packed in sufficient quantities to maintain the material at a temperature not in excess of 0°F (256°K).

Immediately upon completion of packaging, the materials shall be refrigerated to 0°F (256°K) or less, and shall be maintained at that temperature until packed with solid carbon dioxide for shipment.

j. Data

Each roll of preimpregnated tape shall be identified with the original boron-monofilament roll numbers and source, and data provided on filament strength, modulus, and diameter, as well as number of lineal feet wound on each spool. A summary sheet showing the number of feet stored on each spool shall be provided with each shipment.

APPENDIX B

FABRICATION PROCEDURE FOR DESIGN A METAL-LINED, BORON FILAMENT-WOUND PRESSURE VESSEL

Part Name: Pressure vessel, metal-lined, boron-filament-wound, 8-in.-dia.

Part No.: 1269206

1. GENERAL INSTRUCTIONS

a. This procedure describes the fabrication sequence and methods and provides a permanent record for the data generated. Its purpose is to ensure that optimum results are obtained. Deviations in parts, materials, processes, etc. shall be recorded. Comments and suggestions should also be noted.

b. A total of thirteen pressure vessels shall be filament-wound with 0.125-in.-(0.318-cm-) wide boron-filament tape preimpregnated with Shell 58-68R epoxy resin.

c. Extreme care shall be exercised in the handling of the metal liner throughout fabrication because of its thin wall (0.006 in. or 0.152 mm).

d. Clean, white, cotton gloves shall be worn when the liner is handled after its outer surfaces have been chemically cleaned.

2. INSPECTION OF STAINLESS STEEL LINER

a. Wear clean, white cotton gloves while handling stainless steel liner.

b. Remove liner from container and record any defects below under notes. Record acceptance tag number of liner and record serial number on data sheet.

c. Measure liner length and weight and record on data sheet.

d. Replace liner in container.

Notes _____

3. PREPARATION OF SCRIM CLOTH TO COVER LINER HEADS

a. Obtain roll of J. P. Stevens Style 34168-2 nylon cloth, 36 in. (0.91 m) wide, scoured and heat set, natural color.

b. Cut two flat patterns suitable for forming over each liner head past head-to-cylinder tangency point.

c. Cut hole in center of each pattern to permit positioning over metal boss of liner.

d. Cut a rectangular piece of scrim cloth to cover the cylindrical length of the liner assembly.

e. If scrim cloth is not to be used immediately, store in a plastic bag.

4. ASSEMBLY OF TOOLING

The liner and winding-shaft components shall be assembled as directed by the cognizant engineer.

5. CLEANING AND PRIMING OF LINER

a. Apply .005 to .007 in. (0.127 to 0.178 mm) thick layer of Hughson EXB727-6 paste cleaner to outside surface of liner.

b. Allow coating to air dry until it becomes powdery, which will require approximately 90 minutes.

c. Remove paste cleaner coating by washing with tap water. Continue washing and rinsing until a continuous film of water (water breakfree surface) is maintained for 15 seconds.

d. Wash with acetone to remove water and air dry for a minimum of 30 minutes.

e. Apply a thin coating of Minnesota Mining and Manufacturing Company EC-3901 primer to bonding surface and air dry 30 minutes. Record the net weight of paste cleaner on the fabrication record sheet.

f. Force dry for approximately 30 minutes at 190°F (361°K) with heat gun, infra-red lamps or quartz strip heaters.

NOTE: After application of the primer, the liner may be stored at room temperature, if necessary, prior to subsequent operations. Protect primed liner with plastic sheet.

6. APPLICATION OF ADHESIVE COATING AND SCRIM CLOTH TO LINER, AND BLENDING OF WELD JOINTS

a. Prepare small batches of adhesive according to following proportions and method of mixing:

<u>Composition</u>	<u>Parts by Weight</u>
Adiprene L-100	80.0
Epirez 5101	20.0
MOCA	17.0
	<hr/>
	117.0

Mixing Method:

1. Blend Adiprene L-100 and Epirez 5101 resins thoroughly.
2. Melt MOCA at 200°F (367°K) and thoroughly mix into resin blend.
3. Degas under vacuum until bubbling ceases.
- b. Record gross weight of all materials, containers, and tools.
- c. Brush coat adhesive on liner to a thickness of approximately 0.003 in. (0.076 mm).
- d. Pull scrim cloth over shoulder of head section and stretch in place. Be sure opening in scrim cloth is centered over boss.
- e. Work scrim cloth into adhesive-coated surface with clean brush until all air pockets and wrinkles in fabric disappear.
- f. Apply more adhesive over scrim cloth and brush carefully.
- g. Repeat Steps d, e, and f for other head section.
- h. Apply approximately .003 in. (0.076 mm) thickness of adhesive over cylindrical section of liner. Avoid any movement of edges of scrim cloth head sections already in place.
- i. Apply scrim cloth to cylindrical section. Work edges of cylindrical section scrim cloth with brush to insure joints with no gaps between head sections and cylindrical section.
- j. Cut small pieces of No. 112 glass cloth for the blending of weld joints. Brush coat an additional thin coat of adhesive on the scrim-cloth-covered liner in the area of the boss welds, the girth welds and the longitudinal welds. Use care to prevent applying adhesive to areas which will not

be covered by the pieces of glass cloth.

k. Apply a single thickness of the No. 112 glass cloth over the weld joints.

l. Coat the single thickness of glass cloth with additional adhesive, working out all wrinkles and bubbles, but avoiding movement of the scrim cloth or glass cloth.

m. Cover the prepared liner with a plastic sheet until ready to start filament winding.

7. WINDING MACHINE SETUP

a. Set the winding machine gear trains to give 96 turns per revolution of longitudinal winding and 0.125 in. (0.318 cm) lead per turn of hoop winding (60 turns in 7.54 in. or 19.15 cm).

b. Install the prepared liner and shaft assembly in the winding machine.

c. For longitudinal winding, set payoff rollers to give a tape width of 0.250 in. (0.635 cm) from two strands of 0.125-in.-(0.318-cm-) wide boron prepreg tape.

d. For hoop winding, set payoff rollers to give a tape width of 0.125 in. (0.318 cm) from one strand of boron prepreg tape.

8. FILAMENT WINDING THE BORON/EPOXY PREPREG TAPE

a. Weigh each spool of boron prepreg tape before starting or changing from longitudinal to hoop mode or vice-versa. Provide a plastic scrap bag to allow retention and a subsequent weighing of scrapped yarn and paper inter-leafing.

b. Install two spools of boron tape on the tensioning device for longitudinal winding or one spool for hoop winding. Set the static tension of each strand at 6.5 lbf (28.9 N) tension for longitudinal winding and at 10 lbf (44.5 N) for hoop winding. Set tensioning device in the position which has been experimentally determined and marked on the floor of the winding laboratory.

c. Proceed to wind 96 turns of two-strand tape in longitudinal orientation. After winding the first several turns, position an iron-constantan thermocouple next to one of the bosses so that the junction will record temperature during curing at the bottom of the thickest portion of the composite. Apply a small piece of No. 112 glass cloth over the thermocouple

to protect the subsequent winding.

d. Select winding speeds so as to minimize filament breakage. Record net weights of windings and number of turns of windings for each winding pass. A winding pass is defined as any group of consecutive longitudinal or hoop layers.

e. Change the machine setup to hoop mode and wind three layers of prepreg tape. Step back from the end approximately 0.12 in. (0.30 cm) for each layer of the interspersed winding pattern.

f. After weighing and recording of tape spools and waste, wind two more longitudinal revolutions and the second group of eight hoop layers.

g. During the winding of the last eight hoop layers, fill out the ends of the cylindrical section as required to give an even hoop layer over the entire 7.54 in. (19.15 cm) length. Bury test temperature sensors under the last two hoop layers and four extensometer pins under the last hoop layer, using small pieces of No. 112 glass cloth on each side of each item for protection of the adjacent windings.

h. Package spools of prepreg tape in plastic bags and store at 0°F (256°K) when not in use.

9. CURING OF COMPOSITE STRUCTURE

a. Transfer filament-wound tank to the cure oven.

b. Place the unit and the support stand inside the oven.

c. Cure the tank with oven temperatures of 150°F (340°K) for 4 hours, 200°F (370°K) for 4 hours, 250°F (390°K) for 2 hours, and 300°F (420°K) for 6 hours. A record of the oven and composite cure temperatures must be kept with a continuous temperature recording chart.

d. After cure, reduce oven temperature to 150°F (340°K) at approximately 100°F/hour (56°K/hour).

e. Disconnect thermocouple leads and place unit on a stand outside the oven.

10. CLEANING, DIMENSION CHECKING, AND WEIGHING

a. Clean the inside of the vessel with solvent, until all foreign matter has been removed. Air dry at room temperature.

b. Record the finished weight, length, and diameter of the filament-

wound tank on the data sheet.

c. Route the tank to Test Operations for de-gassing prior to EB-welding of the boss pressure fittings.

Curing Notes: _____

BORON FILAMENT-WOUND TANK

FABRICATION DATA SHEET NO. 1

- A. Tank Serial No. _____ Liner Serial No. _____
Liner Acceptance Tag No. _____ Liner Weight _____ grams
Liner Overall Length _____ inches
- B. Gross Weight of Paste Cleaner, Adhesive, Scrim Cloth, and No. 112 Glass
Cloth Before Application _____ grams.
Residual Weight After Application _____ grams.
Net Weight of Bonding Materials _____ grams.
- C. Weight of Extensometer Pins, Temperature Sensors, and No. 112 Glass
Cloth _____ grams.
- D. Total Weight of Longitudinal Tape _____ grams.*
Total Weight of Hoop Tape _____ grams.*
Total Weight of Tape _____ grams.*
- E. Total Ancillary Materials Weight _____ grams (A+B+C).
- F. Final Weight of Cured Tank _____ grams.
- G. Final Weight of Cured Composite _____ grams (F-E).
- H. Weight of Lost Resin _____ grams (D-G).
- I. Cured Tank Overall Length _____ in., Diameter _____ in.
Date _____ Time _____ Signature _____

*From Sheet 2

BORON FILAMENT-WOUND TANK

FABRICATION DATA SHEET NO. 2

	Winding Pass							
	Longi- tudinal 1		Hoop 1-3	Longi- tudinal 2&3		Hoop 4 - 11	Total Longi- tudinal Deposited	Total Hoop Deposited
Winding Tension (lbs)								
No. of Turns								
Spool Numbers								
Spool Weight Before Winding, Grams								
Spool Weight After Winding, Grams								
Grams of Prepreg Tape and Paper Consumed								
Grams of Waste Paper								
Grams of Waste Tape								
Grams of Tape Deposited								
Feet of Tape Consumed (Deposited Plus Waste)								

APPENDIX C

FABRICATION PROCEDURE FOR DESIGN B BORON FILAMENT-WOUND PRESSURE VESSEL

Part Name: Pressure vessel, boron-filament-wound, 8-in.-dia.

Part No.: 1269187

1. GENERAL INSTRUCTIONS

a. This procedure describes the fabrication sequence and methods and provides a permanent record for the data generated. Its purpose is to ensure that optimum results are obtained. Deviations in parts, materials, processes, etc. shall be recorded. Comments and suggestions should also be noted.

b. A total of eleven pressure vessels shall be filament-wound with 0.125-in.-(0.318-cm-) wide boron-filament tape preimpregnated with Shell 58-68R epoxy resin.

2. APPLICATION OF RUBBER LINER TO POLAR BOSSES

a. Mask inside, outside, and top faces of boss hub and powder blast both sides of the flange surface.

b. Clean the flange with acetone and apply Chemlock 203 primer in a thin layer with a brush and air dry.

c. Apply Chemlock 220 adhesive in a thin layer with a brush and air dry.

d. Cut two (2) pieces of GenGard V-45 rubber stock in accordance with the dimensions on Drawing 1269188 and apply to the adhesive surface. Vacuum bag the assembly and cure for one (1) hour at 325°F (436°K). After cooling, strip the vacuum bag and cleanup the rubber edges as required.

e. Weigh two (2) lined bosses and package together with weight noted for data sheet. Package twelve (12) pairs of bosses, marking serial numbers (BB-1 through BB-12) and weight of each pair on the package.

3. ASSEMBLY OF TOOLING TO MANDREL

a. Inspect the plaster mandrel for smooth surface.

b. Coat the plaster with two (2) applications of Rezolin 833A mandrel sealant.

c. Assemble a rubber-coated boss to the shaft flanges with six socket-head cap screws. Assemble to the winding shaft and mandrel.

d. Store the assembly in a plastic bag and a protective box or

install directly in the winding machine.

4. WINDING MACHINE SETUP

a. Set the winding machine gear trains to give 96 turns per revolution of longitudinal winding and 0.125 in. (0.318 cm) lead per turn of hoop winding (59 turns in 7.34 in. or 18.64 cm).

b. Install the prepared mandrel and shaft assembly in the winding machine.

c. For longitudinal winding, set payoff rollers to give a tape width of 0.250 in. (0.635 cm) from two strands of 0.125-in.-(0.318-cm-) wide boron prepreg tape.

d. For hoop winding, set payoff rollers to give a tape width of 0.125 in. (0.318 cm) from one strand of boron prepreg tape.

5. FILAMENT WINDING THE BORON/EPOXY PREPREG TAPE

a. Weigh each spool of boron prepreg tape before starting or changing from longitudinal to hoop mode or vice-versa. Record the starting weight and the starting remaining footage for each roll on the record sheets. Provide a plastic scrap bag to allow retention and a subsequent weight of scrapped yarn and paper inter-leafing.

b. Install two spools of boron tape on the tensioning device for longitudinal winding or one spool for hoop winding. Set the static tension of each strand at 6.5 lbf (28.9N) tension for longitudinal winding and 6.5 lbf (28.9N) for hoop winding.

c. Proceed to wind 96 turns of two-strand tape in longitudinal orientation.

d. Select winding speeds so as to minimize filament breakage. Record net weights of windings and number of turns of windings for each winding pass. A winding pass is defined as any group of consecutive longitudinal or hoop layers.

e. Change the machine setup to hoop mode and wind two layers of prepreg tape. Step back from the end approximately 0.12 in. (0.30 cm) for each for the interspersed winding pattern.

f. After weighing and recording of tape spools and waste from hoop winding, wind one more longitudinal pass, two more hoop layers, and another longitudinal pass. Record the ending and beginning weights and footages for each winding pass. Wind the third group of five hoop layers and again record

the spool data. Fill out the ends of the cylinder section as required to give an even hoop layer over the entire 7.34 in. (18.64 cm) length. During the hoop winding allow the carriage travel to dwell at each end for one full turn in order to insure the full thickness before engaging the feed.

g. Package spools of prepreg tape in plastic bags and store at 0°F when not in use.

6. STAGING AND CURING OF COMPOSITE STRUCTURE

a. Using heat lamps and the hoop rotary drive of the winding machine, or rotisserie drive in an oven, stage the resin system overnight at approximately 135°F (330°K) to firm up the first longitudinal revolution before winding the first two hoop layers.

b. After completion of vessel winding, place the unit and the support stand inside the oven on the rotisserie drive.

c. Cure the tank with oven temperatures of 150°F (340°K) for 4 hours, 200°F (370°K) for 4 hours, 250°F (390°K) for 2 hours, and 300°F (420°K) for 6 hours. A record of the oven and composite cure temperatures must be kept with a continuous temperature recording chart.

d. After cure, reduce oven temperature to 150°F (340°K) at approximately 100°F/hour (56°K/hour).

e. Record the finished weight, length, and diameter of the filament-wound tank on the data sheet.

Curing Notes: _____

7. MANDREL REMOVAL, CLEANING, DIMENSION CHECKING, AND WEIGHING

a. Wash out plaster mandrel by circulating warm acetic acid through vessel interior.

b. Clean the inside of the tank with solvent until all foreign material has been removed. Air dry at room temperature.

c. Record the finished weight, length, and diameter of the filament-wound tank on the data sheet.

d. Route the tank to test operations.

BORON FILAMENT-WOUND TANK

FABRICATION DATA SHEET NO. 1

- A. Tank Serial No. _____
- B. Weight of Lined Boss Pair _____ grams
- C. Weight of Extensometer Pins and
No. 112 Glass Cloth _____ grams
- D. Total Weight of Longitudinal Tape _____ grams.*
Total Weight of Hoop Tape _____ grams.*
Total Weight of Tape _____ grams.*
- E. Total Boss and Ancillary Materials Weight _____ grams (B+C)
- F. Final Weight of Cured Tank _____ grams
- G. Final Weight of Cured Composite _____ grams (F-E)
- H. Cured Tank Overall Length _____ in., Diameter _____ in.
Date _____ Time _____ Signature _____

*From Sheet 2

BORON FILAMENT-WOUND TANK

FABRICATION DATA SHEET NO. 2

	Winding Pass									
	Longitudinal 1		Hoop 1 & 2		Longitudinal 2 & 3		Hoop 3 Thru 9			
	Roll No.	Roll No.	Roll No.	Roll No.	Roll No.	Roll No.	Roll No.	Roll No.	Roll No.	Roll No.
No. of Turns										
Spool Weight Before Winding, Grams										
Spool Weight After Winding, Grams										
Grams Consumed Including Paper										
Grams Of Waste Paper										
Grams Of Waste Tape										
Grams Of Tape Deposited										

APPENDIX D

CALCULATED DATA - METHODS AND PROCEDURES

1. EQUIVALENT FILAMENT THICKNESS

An equivalent filament thickness per layer of the boron/epoxy tape is determined from the expression

$$t_e = A_f N_1 N_2 / w \quad (D1)$$

where

$$A_f = \text{area of single filament} = \pi D_f^2 / 4 \text{ in.}^2 (\text{cm}^2)$$

$$D_f = \text{diameter of single filament} = 0.00393 \text{ in. (0.0998 mm)}$$

$$N_1 = \text{number of filaments per tape} = 29$$

$$N_2 = \text{number of tapes per layer} = 1$$

$$w = \text{width of tape} = 0.125 \text{ in. (0.318 cm)}$$

Therefore,

$$t_e = \frac{\pi (.00393)^2 (29) (1)}{4 (.125)}$$

$$t_e = 0.00281 \text{ in. (0.0714 mm)}$$

2. FILAMENT STRESSES

In order to calculate vessel filament stresses at the pressures of interest, load balance relations are required which take into account loads carried by the metal liner and oriented filaments in both directions.

a. Longitudinal Direction

Assuming the loads carried by the matrix material are insignificant, the load balance in the longitudinal direction of the cylinder is

$$\sigma_{f,l} (N_3 t_e) \cos^2 \alpha_o + \sigma_{\phi L} t_L = p \bar{R} / 2$$

where

$\sigma_{f,l}$ = longitudinal filament stress, psi (N/cm²)

N_3 = number of longitudinally oriented layers

α_o = orientation of longitudinal filaments with respect to axis of rotation, 13 degrees (0.227 rad)

$\sigma_{\phi L}$ = longitudinal stress in liner, psi (N/cm²)

t_L = thickness of liner, in (mm)

p = internal pressure, psi (N/cm²)

\bar{R} = average radius of cylinder wall, in. (cm)

Rearrangement of the load balance relation results in the following equation for calculation of longitudinal filament stress

$$\sigma_{f,l} = \frac{p \bar{R}/2 - \sigma_{\phi L} t_L}{N_3 t_e \cos^2 \alpha_o} \quad (D2)$$

b. Hoop Direction

The load balance in the hoop direction of the cylinder is

$$\sigma_{f,h} (N_4 t_e) + \sigma_{f,l} (N_3 t_e) \sin^2 \alpha_o + \sigma_{\theta L} t_L = p \bar{R}$$

where

$\sigma_{f,h}$ = hoop filament stress, psi (N/cm²)

N_4 = number of hoop oriented layers

$\sigma_{\theta L}$ = hoop stress in liner, psi (N/cm²)

Rearrangement of the load balance relation, with the assumption of a 1:1 stress field in the liner ($\sigma_{\theta L} = \sigma_{\phi L}$), results in the following equation for calculation of hoop filament stress

$$\sigma_{f,h} = \frac{p \bar{R} (1 - .5 \tan^2 \alpha_o) - \sigma_{\phi L} t_L (1 - \tan^2 \alpha_o)}{N_4 t_e} \quad (D3)$$

c. Sample Calculations

The room temperature single cycle burst data from vessel S/N B-1 are used to provide a sample calculation. Output from the computer indicates the 0.006-inch (0.152 mm) thick metal liner is just above its yield stress at the burst pressure of 1669 psi (1151 N/cm²). Thus, the longitudinal filament stress is

$$\sigma_{f,l} = \frac{1669(3.929)/2 - 40,000(.006)}{6(.00281)(.97437)^2}$$

$$\sigma_{f,l} = 190,000 \text{ psi } (131,000 \text{ N/cm}^2)$$

The hoop filament stress at the burst pressure is

$$\sigma_{f,h} = \frac{1669(3.929)(1 - .5(.23087)^2) - 40,000(.006)(1 - (.23087)^2)}{11(.00281)}$$

$$\sigma_{f,h} = 200,000 \text{ psi } (138,000 \text{ N/cm}^2)$$

3. BORON AND VOID CONTENTS IN COMPOSITE

a. Weight Fraction Boron

The following laboratory procedure is used to determine the weight fraction of reinforcement in a boron/epoxy composite by the sulfuric acid strip method.

(1) Specimen

The specimen is to contain at least 10 mg of resin.

(2) Procedure

(a) Weigh the sample to the nearest 0.1 mg in a 200 ml (cm³) beaker, add 50 ml (cm³) of concentrated sulfuric acid, and place the beaker and its contents (covered with a watch glass) on a hot plate.

- (b) Heat the beaker for 2-hrs at 400°F (478°K)
- (c) Allow the beaker to cool to room temperature.
- (d) Carefully decant sulfuric acid and wash the beaker and fibers twice with distilled water, decanting carefully after each rinse.
- (e) If residual resin is observed after the water rinse, add 50 ml (cm³) concentrated sulfuric acid return the sample to the hot plate for 1 hour at 400°F (478°K). Repeat if necessary until no more resin remains.
- (f) Rinse the beaker and fibers with acetone, decant, and dry in an oven at 176°F (353°K) for 1 hour.
- (g) Allow the beaker and fibers to cool to room temperature and weigh the fibers.

(3) Calculation

Calculate the boron content by weight (P_{wf}) from the expression

$$P_{wf} = \frac{W_r}{W_1} \quad (D4)$$

where

W_1 = initial weight of sample, g.

W_r = weight of reinforcement after acid stripping, g.

b. Volume Fraction Boron

The volume fraction of reinforcement in the composite is calculated from the expression

$$P_{vf} = P_{wf} \left[\frac{SG_c}{SG_b} \right] \quad (D5)$$

where

SG_b = specific gravity of boron fibers, 2.63 g/cm^3

SG_c = specific gravity of composite specimen, g/cm^3

c. Void Content

The fraction of voids (P_{vv}) in a composite is established by balancing the volumetric constituents according to the expression

$$P_{vv} = 1.0 - P_{vf} - P_{vr} \quad (D6)$$

where

P_{vr} = volume fraction resin

$$P_{vr} = (1 - P_{wf}) \left[\frac{SG_c}{SG_r} \right] \quad (D7)$$

SG_r = specific gravity of 5868R resin, 1.25 g/cm^3

d. Sample Calculation

The following raw data obtained from specimens cut from the composite of vessel S/N B-1 was used in conjunction with equation (D4) to arrive at boron content by weight.

<u>Specimen No.</u>	<u>SG_c</u>	<u>$W_l(g)$</u>	<u>$W_r(g)$</u>	<u>P_{wf}</u>
1.	1.74	1.3186	0.8690	0.6590
2.	1.79	1.3038	0.8752	0.6713
3.	1.78	1.2924	0.8438	0.6502
Ave.	1.77	N.A.	N.A.	0.660

The average values for volumetric fractions of boron and resin are

$$P_{vf} = 0.660(1.77)/2.63 = 0.444$$

$$P_{vr} = (1-0.660)(1.77)/1.25 = 0.481$$

and, the average void content is

$$P_{vv} = 1.00-0.444-0.481 = 0.075$$

4. COMPOSITE THICKNESS

Composite thickness may be calculated by dividing the total equivalent thickness of boron by the volume fraction obtained from laboratory analysis. Thickness of the longitudinal composite is

$$t_l = \frac{N_3 t_e}{P_{vf}} \quad (D8)$$

and, for the hoop composite

$$t_h = \frac{N_4 t_e}{P_{vf}} \quad (D9)$$

Application of these expressions to the sample vessel, S/N B-1, yields the values

$$t_l = 6(.00281)/0.444 = 0.038 \text{ in. (0.097 cm)}$$

$$t_h = 11(.00281)/0.444 = 0.070 \text{ in. (0.178 cm)}$$

5. COMPOSITE STRESSES

Since neither the hoop nor longitudinal composites resist the entire applied loads (for the general case of a metal lined vessel), composite stresses are based on previously determined filament stresses and the volume fraction of filaments in the composite. For the hoop composite the stress is

$$\sigma_h = P_{vf} \sigma_{f,h} \quad (D10)$$

and, for the longitudinal composite

$$\sigma_l = P_{vf} \sigma_{f,l} \cos^2 \alpha_o \quad (D11)$$

where the cosine function accounts for both area and force vector rotation effects.

The required data associated with vessel S/N B-1 are used to provide a sample calculation. The hoop composite stress is

$$\sigma_h = 0.444(200,000) = 89,000 \text{ psi } (61,000 \text{ N/cm}^2)$$

and, the longitudinal composite stress is

$$\begin{aligned} \sigma_l &= 0.444(190,000)(.97437)^2 \\ &= 80,000 \text{ psi } (55,000 \text{ N/cm}^2) \end{aligned}$$

DISTRIBUTION LIST

	<u>Copies</u>		<u>Copies</u>
Natl. Aeronautics & Space Admin. Lewis Research Center 21000 Brookpark Road Cleveland, OH 44135		Natl. Aeronautics & Space Admin. George C. Marshall Space Flight Ctr. Huntsville, AL 35812	
Attn: Contracting Officer, MS 77-3	1	Attn: Library	1
Tech. Rpt. Control Off. MS 5-5	1	John T. Schell, S&E-ASTN-MNR	1
Tech. Utilization Off, MS 3-16	1	James M. Stuckey, S&E-ASTN-MNM	1
AFSC Liaison Off, MS 4-1	1	Don D. Thompson, S&E-ASTN-PPA	1
Library	2		
Off. Reliability & Quality Assurance, MS 500-11	1	Natl. Aeronautics & Space Admin. Manned Spacecraft Center Houston, Texas 77001	
R. H. Kemp, MS 49-1	1	Attn: Library	1
T. T. Serafini, MS 49-1	1	L. G. St. Leger, SMD-Structures	1
R. F. Lark, Project Manager MS 49-1	10	R. E. Johnson, SMD-Materials Tech.	1
J. R. Barber, MS 500-209	1		
D. L. Nored, MS 500-209	1		
Liquid Rocket Tech. Branch MS 500-209	1	Natl. Aeronautics & Space Admin. Office of Tech. Utilization Washington, D. C. 20546	1
G. M. Ault, MS 3-13	1		
Natl. Aeronautics & Space Admin Office of Advanced Res. & Tech. Washington, D. C. 20546		Natl. Aeronautics & Space Admin. Ames Research Center Moffett Field, CA 94035	
Attn: G. C. Deutsch, Director Materials & Structures Div, Code RW	1	Attn: Library	1
J. J. Gangler, Code RW	1		
B. Achhammer, Code RW	1	Natl. Aeronautics & Space Admin. Flight Research Center P. O. Box 273 Edwards, CA 93523	
N. Mayer, Code RW	1	Attn: Library	1
Natl. Aeronautics & Space Admin Langley Research Center Hampton, Virginia 23365			
Attn: E. E. Mathauser, MS 188A	1	Natl. Aeronautics & Space Admin. Goddard Space Flight Center Greenbelt, MD 20771	
R. A. Pride, MS 188A	1	Attn: Library	1

	<u>Copies</u>	<u>Copies</u>
Natl. Aeronautics & Space Admin. Langley Research Center Langley Station Hampton, VA 23365 Attn: Library	1	Air Force Materials Laboratory Wright-Patterson Air Force Base, OH 45433 Attn: MAA A. Olevitch (MAEE) T. Reinhart (MAAE)
Natl. Tech. Information Service Springfield, VA 22151	6	
Jet Propulsion Laboratory 4800 Oak Grove Drive Pasadena, CA 91103 Attn: Library	1	Air Force Office of Scientific Research 1400 Wilson Boulevard Arlington, VA 22209 Attn: SIGL
Warren Jensen	1	Air Force Rocket Propulsion Lab. Edwards, California 93523 Attn: J. Branigan
Air Force Materials Laboratory Wright-Patterson Air Force Base, OH 45433 Attn: J. D. Ray (MANC)	1	Air Force Office of Scientific Research Washington, DC 20333 Attn: SREP, Dr. J. F. Masi
W. H. Gloor (MANF)	1	
H. S. Schwartz (MAN)	1	
R. T. Schwartz (MAN)	1	
Air Force Materials Laboratory Wright-Patterson Air Force Base, OH 45433 Attn: G. P. Peterson (MAC)	1	Space and Missile Systems Organization Air Force Unit Post Office Los Angeles, CA 90045 Attn: Technical Data Center
Wm. J. Schulz (MAC)	1	
E. Jaffe (MAC)	1	U. S. Air Force Washington, D. C. Attn: Library Col. C. K. Stambaugh, Code AFRST
Air Force Materials Laboratory Wright-Patterson Air Force Base, OH 45433 Attn: MAT	1	
S. Litvak (MATC)	1	
NASA Scientific & Tech. Infor. Facility, Attn: NASA Representative Box 33 College Park, MD 20740	2	

	<u>Copies</u>		<u>Copies</u>
U. S. Army Missile Command Redstone Scientific Information Center Redstone Arsenal, AL 35808 Attn: Document Section	1	Commander Natick Laboratories U. S. Army Natick, MA 01762 Attn: T. Ciavarini	1
Advanced Research Projects Agency Washington, DC 20525 Attn: Library	1	Commander Naval Air Systems Command U. S. Navy Department Washington, DC 20360 Attn: AIR-5203 (P. Goodwin)	1
Department of the Army U. S. Army Material Command Washington, DC 20315 Attn: AMCRD-RC	1	AIR-52032 (P. Stone)	1
		AIR-52032A (C. Bersch)	1
		AIR-52032C (J. Gurtowski)	1
		AIR-52032D (M. Stander)	1
		AIR-320A (T. Kearns)	1
Department of the Army U. S. Army Aviation Matl. Lab. Fort Eustis, VA 23604 Attn: A. J. Gustafson	1	Commander Naval Ordnance Systems Command U. S. Navy Department Washington, DC 20360 Attn: ORD-033 (B. Drimmer)	1
R. Berrisford	1	ORD-0333 (S. Matesky)	1
Department of the Army U. S. Army Aviation Systems Command P. O. Box 209 St. Louis, MO 63166 Attn: R. Vollmer, AMSAV-A-UE	1	ORD-0333A (M. Kinna)	1
Department of the Army Watertown Arsenal Watertown, MA 02172 Attn: A. Thomas	1	Director Deep Submergence Systems Project 6900 Wisconsin Avenue Washington, DC 20015 Attn: DSSP-221 (H. Bernstein)	1
Department of the Army Watervliet Arsenal Watervliet, NY 12189 Attn: F. W. Schmiedershoff	1	Commander Naval Ship Engineering Center Center Building Prince Georges Center Hyattsville, MD 20792	
		Code 6101E03 (W. Graner)	1
		Code 6101E (J. Alfors)	1
Department of the Army Plastics Technical Evaluation Cr. Picatinny Arsenal Dover, NY 07801 Attn: H. E. Pebly, Jr.	1		

	<u>Copies</u>	<u>Copies</u>
Director Naval Research Laboratory Washington, DC 20390 Attn: Code 8430	1	Aeronutronic Division of Philco Ford Corporation Ford Road Newport Beach, CA 92663 Attn: Technical Information Dept.
Dr. W. Zisman, Code 6050	1	
Dr. R. Kagarise, Code 6100	1	
Dr. I. Wolock, Code 8433	1	
 Department of the Navy Office of Naval Research Washington, DC 20360 Attn: J. H. Shenk	1	Bell Aerospace Company Box 1 Buffalo, NY 14205 Attn: S. Cross
 Director Strategic Systems Projects Office Department of the Navy Washington, DC 20360	1	Bell Helicopter Company P. O. Box 482 Fort Worth, Texas, 76101 Attn: H. Zinberg
 Commander U. S. Naval Missile Center Point Mugu, CA 93041 Attn: Technical Library	1	Brunswick Corporation Defense Products Division P. O. Box 4594 43000 Industrial Avenue Lincoln, NB Attn: J. Carter
 Commander U. S. Naval Weapons Center China Lake, CA 93557 Attn: Library	1	The Boeing Company P. O. Box 3999 Seattle, WA 98124 Attn: J. T. Hoggatt P. Kennedy
 AVCO Corporation Applied Technology Division Lowell Industrial Park Lowell, MA 01851 Attn: Mr. Allan S. Bufferd	1	The Boeing Company Vertrol Division Morton, PA 19070 Attn: W. D. Harris R. Pickney

	<u>Copies</u>		<u>Copies</u>
Case-Western Reserve Univ. University Circle Cleveland, OH 44106 Attn: Prof. T. P. Kicher	1	General Electric Company Flight Propulsion Lab. Dept. Cincinnati, OH 45201 Attn: Library	1
Chemical Propulsion Information Agency Applied Physics Laboratory 8621 Georgia Avenue Silver Spring, MD 20910	1	General Electric Company Valley Forge Space Technology Ctr. P. O. Box 8555 Philadelphia, PA 19101 Attn: J. Anthony	1
Esso Research and Engineering Co. P. O. Box 45 Linden, NJ 07036 Attn: D. J. Angier	1	Grumman Aircraft Engineering Corp. Bethpage, Long Island, NY 11714 Attn: Library	1
Fairchild Hiller Corporation Republic Aviation Division Farmingdale, NY 11735 Attn: J. Clark F. Damasco	1 1	Goodyear Aerospace Corporation 1210 Massillon Road Akron, OH 44315 Attn: L. W. Toth E. Rottmayer	1 1
The Fiberite Corporation 512 W. Fourth Street Winona, MN 55987 Attn: S. P. Prosen	1	General Dynamics P. O. Box 748 Fort Worth, TX 76100 Attn: W. S. Hay T. P. Airhart	1 1
FMC Corporation Chemical Research & Development Ctr. P. O. Box 8 Princeton, NJ 08540 Attn: Security Officer	1	Hercules Corporation Allegheny Ballistics Laboratory P. O. Box 210 Cumberland, MD 21052 Attn: E. Crossland T. C. White	1 1
General Dynamics/Convair P. O. Box 1128 San Diego, CA 92112 Attn: J. L. Christian	1	Hercules, Inc. Wilmington, DE 19899 Attn: G. McHugh G. Kuebeler	1 1
General Electric Company 1 Campbell Rd. Schenectady, NY 12306 Attn: J. Wetzel	1	IIT Research Institute Technology Center Chicago, Illinois 60616 Attn: Library	1

	<u>Copies</u>	<u>Copies</u>
Ling-Temco-Vought Corporation P. O. Box 5003 Dallas, TX 75222 Attn: M. Pollos	1	Massachusetts Institute of Tech. Cambridge, MA Attn: Prof. F. J. McGarry
Lockheed Missiles and Space Co. P. O. Box 504 Sunnyvale, CA 94087 Attn: R. W. Fenn	1	McDonnell Douglas Aircraft Corporation 3855 Lakewood Blvd. Long Beach, CA 90810 Attn: H. C. Schjeiderup
Lockheed/California Corp. Burbank, CA 91503 Attn: M. G. Childers	1	McDonnell Douglas Aircraft Corp. P. O. Box 516 Lambert Field, MS 63166 Attn: J. C. Watson
Lockheed/George Corporation Marietta, GA 30060 Attn: W. S. Cremens	1	North American Rockwell, Inc. 4300 E. Fifth Street Columbus, OH 43219 Attn: R. L. Foye
Lawrence Radiation Laboratory P. O. Box 808 Livermore, California 94550 Attn: Library T. T. Chiao	1 1	Northrop Space Laboratories 3401 West Broadway Hawthorne, CA 90250 Attn: D. Stanbarger
Lockheed-Georgia Company Advanced Composites Information Ctr. Dept. 72-14, Zone 402 Marietta, GA 30060		North American Rockwell Corporation Space Division 12214 Lakewood Blvd. Downey, CA 90241 Attn: Max Nadler
Martin-Marietta Corporation P. O. Box 179 Denver, CO 80201 Attn: A. Feldman	1	Sandia Corporation P. O. Box 969 Livermore, CA 94550 Attn: Technical Library H. Lucas
Marquardt Corporation 16555 Saticoy Street Van Nuys, CA 91406 Attn: J. F. Dolowy	1	TRW Equipment Group 23555 Euclid Avenue Euclid, OH 44111 Attn: W. E. Winters

	<u>Copies</u>	<u>Copies</u>
United Aircraft Corporation Corporation Library 400 Main Street East Hartford, CT 06108	1	
United Aircraft Corporation Research Laboratories East Hartford, CT 06108 Attn: K. Kreider	1	
Whittaker Corporation 3640 Aero Court San Diego, CA 92123 Attn: V. Chase	1	